NASA CONTRACTOR REPORT

KINETIC DESCRIPTION OF IONOSPHERIC DYNAMICS IN THE THREE-FLUID APPROXIMATION

R. H. Comfort

Prepared by
NORTHROP SERVICES, INC.
Huntsville, Ala. 35807
for George C. Marshall Space Flight Center

NATIONAL AERONAUTICS AND SPACE ADMINISTRATION • WASHINGTON, D.C. JULY 1975

TECHNICAL REPO

1. REPORT NO.	2. GOVERNMENT ACCESSION NO.	3. REC
NASA CR-2572		

4. TITLE AND SUBTITLE	5. REPORT DATE
Kinetic Description of Ionospheric Dynamics in the Three-Fluid Approximation	JULY 1975
	6. PERFORMING ORGANIZATION CODE M146
7. AUTHOR(S) R. H. Comfort	8. PERFORMING ORGANIZATION REPORT #
9. PERFORMING ORGANIZATION NAME AND ADDRESS Northrop Services, Inc. P. O. Box 1484 Huntsville, Alabama 35807	10. WORK UNIT NO. 11. CONTRACT OR GRANT NO. NAS8-21810
12. SPONSORING AGENCY NAME AND ADDRESS National Aeronautics and Space Administration Washington, D. C. 20546	13. TYPE OF REPORT & PERIOD COVERED Contractor Topical 14. SPONSORING AGENCY CODE

15. SUPPLEMENTARY NOTES
This report prepared under the technical monitorship of the Aerospace Environment Division, Space Sciences Laboratory, NASA-Marshall Space Flight Center.

16. ABSTRACT

This work is composed of two basic parts. In the first, conservation equations are developed in the three-fluid approximation for general application to problems of ionospheric dynamics in the altitude region 90 km to 800 km for all geographic locations. In the second part, these equations are applied to a detailed study of auroral E region neutral winds and their relationship to ionospheric plasma motions.

17. KEY WORDS	18. DISTRIBUTION STATEMENT
Ionosphere Three-fluid model Auroral zone Neutral winds	UNCLASSIFIED–UNLIMITED STAR CATEGORY 46

19. SECURITY CLASSIF. (of this report)	20. SECURITY CLASSIF. (of this page)	21. NO. OF PAGES	22. PRICE
Unclassified	Unclassified	251	$8.50

FOREWORD

This report presents the results of research performed by Northrop Services, Inc., Huntsville, Alabama for the National Aeronautics and Space Administration, George C. Marshall Space Flight Center, under Contract NAS8-21810. This research was performed for the Science and Engineering Directorate in response to the requirements of Appendix A, Schedule Order Number A02Z, Paragraph III, Task 3.1. Dr. Robert E. Smith was the Technical Coordinator for this task.

ACKNOWLEDGEMENTS

The author is grateful to Prof. S. T. Wu, University of Alabama in Huntsville, for reviewing the manuscript and providing valuable comments. Special thanks go to Prof. Peter M. Banks and Dr. Joe R. Doupnik, University of California, San Diego, for making available unpublished ion velocity and electron number density data from observations made by the incoherent scatter radar facility at Chatanika, Alaska, and for providing background information on the experimental techniques. Computer calculations were greatly aided by the programming of Mrs. Marion Bishop.

SUMMARY

Development of the conservation equations in the first part starts from the Boltzmann equation. A general transport equation for an arbitrary particle property is derived; from this the species mass, momentum, and energy conservation equations are obtained. Collision terms are treated in detail in the approximation of two independent, displaced Maxwellian distribution functions, which takes into account the effects of different flow velocities and temperatures. A new formalism is developed for these terms, simplifying analytic evaluation; this is illustrated by analytic evaluation for a sufficient variety of interaction potentials to meet most ionospheric requirements. The three-fluid approximation is applied to the species conservation equations, resulting in separate sets of equations for electrons, ions, and neutral particles. Order-of-magnitude estimates, based on extreme values for ionospheric properties in the altitude region 90 km to 800 km, are used to delete terms which are not important for the specified ionospheric conditions. Closure of the conservation equations is accomplished through transport tensors and coefficients. A condensation of Shkarofsky's method for calculating electron transport tensors is presented. Use of this technique is facilitated by the derivation of a new method for representing the electron-neutral collision frequency velocity dependence as a power law. Transport coefficients for ions and neutral particles are also presented. The resulting set of conservation equations should provide appropriate starting points for a wide variety of studies, both theoretical calculations and data analysis.

In the second part, these conservation equations are applied to the detailed examination of auroral E region neutral winds observed by the incoherent scatter radar at Chatanika, Alaska, during geomagnetic disturbances (15 May 1974). Two primary objectives of this study are: (1) to determine the effects of altitude structure in ion and neutral velocity fields on neutral velocities derived from the radar observations; and (2) to determine the relative importance of ion drag and auroral heating in generating these winds. Ion and neutral momentum equations for the ion drag model are solved numerically, using observed electric fields and electron number densities. The coriolis force is included; its importance is demonstrated in model calculations.

The following results are obtained from these velocity calculations. Large vertical gradients are found in the calculated velocities for altitudes below about 130 km. As a consequence of this structure and fluctuations in the electron density profiles, the data analysis procedure of Brekke, et al. (1973) for obtaining neutral winds from radar data are found to underestimate the wind speed by up to 40 percent, but it represents the direction and temporal structure reasonably well. Comparison of observed neutral velocities with calculated values shows that ion drag alone cannot account for the observations. An equation is derived to estimate the pressure gradients required to resolve the discrepancy between calculated and observed neutral winds. Accelerations due to these pressure gradients are of the same order as those due to ion drag, but at least an order of magnitude larger than those due to solar heating. Directions of the pressure gradients are consistent with expected locations of auroral heating. During geomagnetic disturbances, ion drag and auroral heating both appear to play important roles in the generation and modification of neutral winds.

TABLE OF CONTENTS

TABLE OF CONTENTS (Concluded)

LIST OF ILLUSTRATIONS

LIST OF ILLUSTRATIONS (Continued)

LIST OF ILLUSTRATIONS (Concluded)

LIST OF TABLES

Section I

INTRODUCTION

Recent interest in upper atmospheric dynamics has been directed toward high latitudes, both because of increased observations in this region and because of increased awareness and understanding of the importance of the coupling between the magnetosphere and ionosphere (Folkestad, 1972; Chappel, 1974), which is most prominently displayed in the vicinity of the auroral oval (Akasofu, 1968). Observations of ionospheric properties in auroral latitudes (~60° to 80° geomagnetic latitude), made by a variety of remote and *in situ* techniques, have found electric fields, ionization number densities, flow velocities, and temperatures to be highly variable in space and time relative to conditions at lower latitudes. Time scales for significant variations of these properties are typically on the order of minutes at high latitudes (e.g., Banks, et al., 1974), compared with hours at middle and low latitudes (cf. Rishbeth and Garriott, 1969). Similarly, spatial scales for significant variations, on the order of several thousand kilometers at low and middle latitudes, are an order of magnitude smaller at high latitudes and even smaller near auroral arcs (e.g., Chan and Colin, 1969; Jelly and Petrie, 1969). These relatively small spatial and temporal scales complicate the comparison and interpretation of observational data (Maynard, 1972). They also increase the difficulties of theoretical studies because appropriate boundary conditions are uncertain, and approximations which permit physical insight and mathematical tractability in lower latitude problems are not valid for high latitude conditions. In addition, the magnitudes of electric fields and associated plasma drift velocities are an order of magnitude larger at high latitudes (Maynard, 1972; Banks, et al., 1974). As a consequence, different and sometimes new physical considerations enter into the formulation of the governing equations. The primary objectives of this study are to develop a theoretical framework adequate for treating problems of the dynamics of magnetosphere-ionosphere interactions at high latitudes, and to use this framework in the investigation of such a problem.

Two approaches, continuum and particle, may be taken in formulating the governing equations for upper atmospheric gases. The goal of both approaches is to determine the relations among and the behavior of the macroscopic observables, those measured by experiments which detect the average properties of a small but finite volume of the gas, specifically: number density n, flow velocity $\vec{v}$, and translational temperature T. In the continuum approach, equations governing the macroscopic observables are formulated directly from physical considerations of the bulk behavior of the gases. This involves the introduction of transport coefficients, which indicate how readily spatial inhomogeneities in the density, momentum, and energy of the gas approach a homogeneous state. These coefficients must be determined experimentally in the continuum approach. Proceeding from a particle viewpoint involves formulating equations which incorporate interactions of individual particles with fields and other particles, using statistical methods to determine the macroscopic behavior of the aggregate. To the order of approximation appropriate to the upper atmosphere, both methods lead to essentially the same macroscopic equations. Important advantages of the particle formulation are (1) the enhanced insight gained into the physical processes which affect the macroscopic observables, (2) the possibility of direct calculation of the transport coefficients, and (3) the assurance of a consistent treatment, especially when new physical processes must be considered. In addition, the particle approach is particularly flexible in treating multicomponent gases, which recommends its use in upper atmospheric problems. This, then, is the approach to be used in this study.

Relating the macroscopic behavior of a nonuniform, multicomponent gas to the microscopic interactions of its constituent particles is the task of kinetic theory. Methods used for accomplishing this end are discussed in detail by Chapman and Cowling (1970). The basic procedure begins with a Boltzmann equation for each particle species (e.g., N_2, O_2, e, O_2^+, O^+, etc.); this equation governs the velocity distribution of each species. A general transport equation is obtained by multiplying both sides of the Boltzmann equation by an arbitrary function of particle velocity, and integrating over velocity space. When those particular particle properties which are conserved in (elastic) collisions (mass, momentum, energy) are used in this transport

equation, the conservation equations for number density, momentum, and energy result. In general, a set of conservation equations for each particle species is required to determine properly the aggregate behavior of the system. However, if several species have in common those properties which are of primary interest (e.g., temperature and flow velocity), the appropriate equations can be easily combined, resulting in a considerable reduction in computational effort when the system of equations must be solved. This is the basis of the three-fluid approximation.

As applied to a partially ionized plasma, such as the ionosphere, the three-fluid approximation implies that electrons, ions, and neutral particles have distinct properties, but that these properties are undifferentiated by species within these gases. Applicability to problems of ionospheric dynamics can be better understood from a brief review of typical ionospheric conditions which affect the dynamics. Basically, four factors play primary roles in determining and differentiating the motions of upper atmospheric gases: (1) relative number densities of different gases, (2) types of interaction between particles, (3) relative masses of particles, and (4) forces which act differently on different gases. These are examined in turn below.

Although particle populations vary considerably in both space and time, Figures 1-1a and 1-1b show typical daytime, midlatitude altitude profiles of constituent number densities. Both neutral and ion compositions are seen to shift from diatomic to monatomic species and toward the lighter species with increasing altitude. This is due to diffusive separation in the Earth's gravitational field and results in a decreasing mean mass per particle with increasing altitude. Ions are only singly ionized (negative ions are negligible above 90 km (Banks and Kockarts, 1973)), and charge neutrality (electron number density is equal to total ion number density) is assumed to hold everywhere on the macroscopic scale of interest here.

Strictly in terms of numbers, the upper atmosphere is seen to be a weakly ionized plasma at all altitudes shown. However, the collisional coupling between the gases also depends on the interactions between the particles and

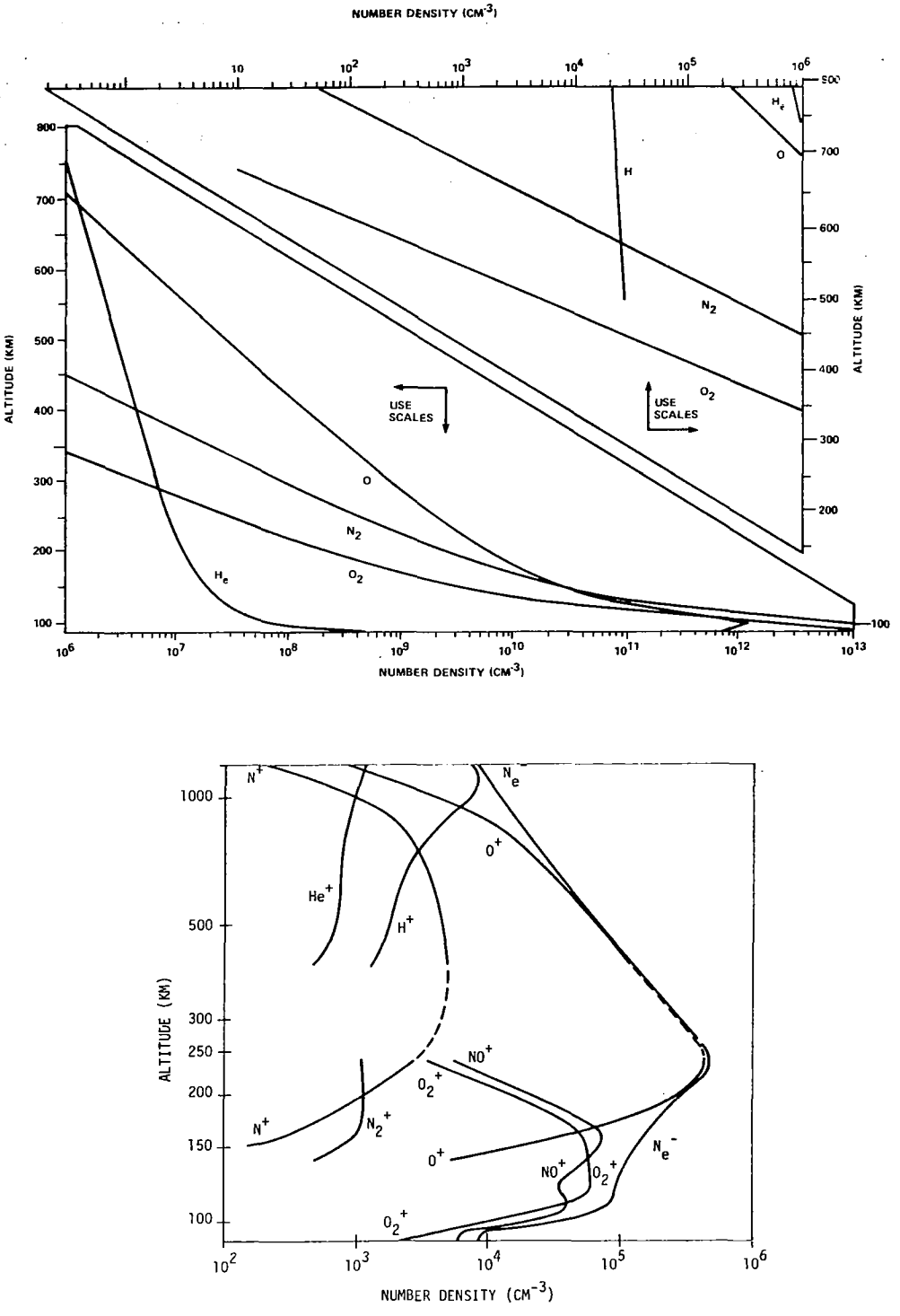

Figure 1-1. REPRESENTATIVE NUMBER DENSITIES OF UPPER ATMOSPHERIC GASES BY SPECIES FOR DAYTIME, MIDLATITUDE CONDITIONS: (a) NEUTRAL SPECIES (JACCHIA, 1971); (b) CHARGED SPECIES (JOHNSON, 1966)

on their relative masses. These considerations are taken into account to some extent in the momentum transfer collision frequencies, ν_{ij}, which indicate the degree of momentum coupling among the gases. Altitude profiles of collision frequencies, based on the number densities in Figure 1-1, are shown in Figure 1-2. Most of the altitude variation in Figure 1-2 is due to variation in total number densities, and to a lesser extent to the changing compositions (hence changing interactions) and changing temperatures. Temperature profiles used in computing these collision frequencies are shown in Figure 1-3; these profiles are representative of daytime midlatitude conditions.

In addition to collisional coupling among the species, electromagnetic forces, which selectively affect only charged particles, have a pronounced effect in differentiating the motions of ionospheric gases. For purposes of this study, detailed consideration is limited to the effects of the static geomagnetic field and electrostatic (curl free) fields, in addition to the Coulomb interaction between charged particles. The intensity of the geomagnetic field varies geographically, ranging from about 0.2 gauss to about 0.6 gauss at ionospheric altitudes (Matsushita and Campbell, 1967). Since this range of values is relatively small, the more important variation is in the geometry. A somewhat schematic view of the magnetosphere is presented in Figure 1-4, showing the dipolar configuration of the geomagnetic field at ionospheric altitudes. Not indicated in this diagram is the fact that the dipole axis is tilted about 11 degrees with respect to the Earth's rotational axis.

The significance of this geometry derives from the Lorentz force $(q\vec{v} \times \vec{B}/c)$ which causes charged particles moving in a magnetic field to spiral about the field lines. This inhibits motion transverse to the field, so that charged particles are, to some extent, tied to the field lines. The strength of this coupling is indicated by the particle gyrofrequency,

$$\omega_s = |q_s| B/m_s c \qquad \text{(Gaussian Units)} \qquad (1\text{-}1)$$

where q_s is the particle charge, B is the magnetic field strength, m_s is the mass, and c the speed of light. For a magnetic field strength of 0.5 gauss

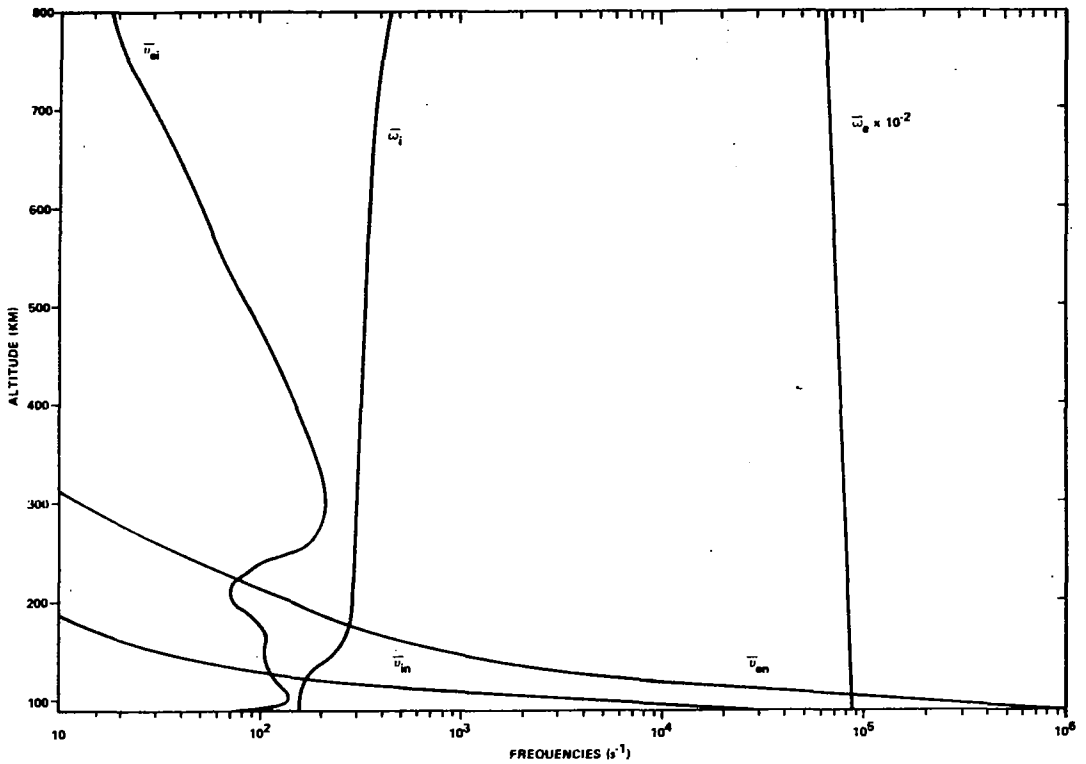

Figure 1-2. REPRESENTATIVE COLLISION FREQUENCIES (υ) AND GYROFREQUENCIES (ω) OF UPPER ATMOSPHERIC GASES FOR DAYTIME, MIDLATITUDE CONDITIONS

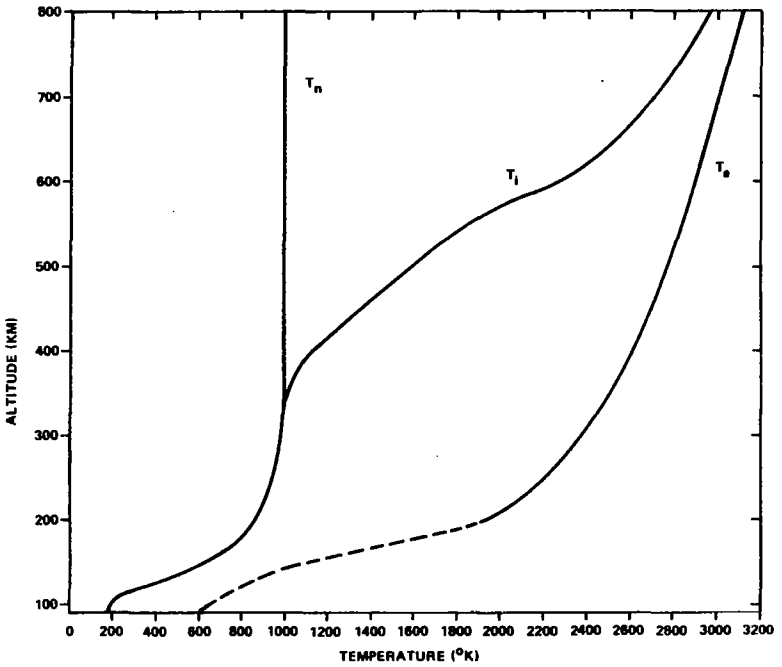

Figure 1-3. THERMAL STRUCTURE OF THE UPPER ATMOSPHERE, REPRESENTATIVE OF DAYTIME, MIDLATITUDE CONDITIONS (JACCHIA, 1971; NASA, 1971)

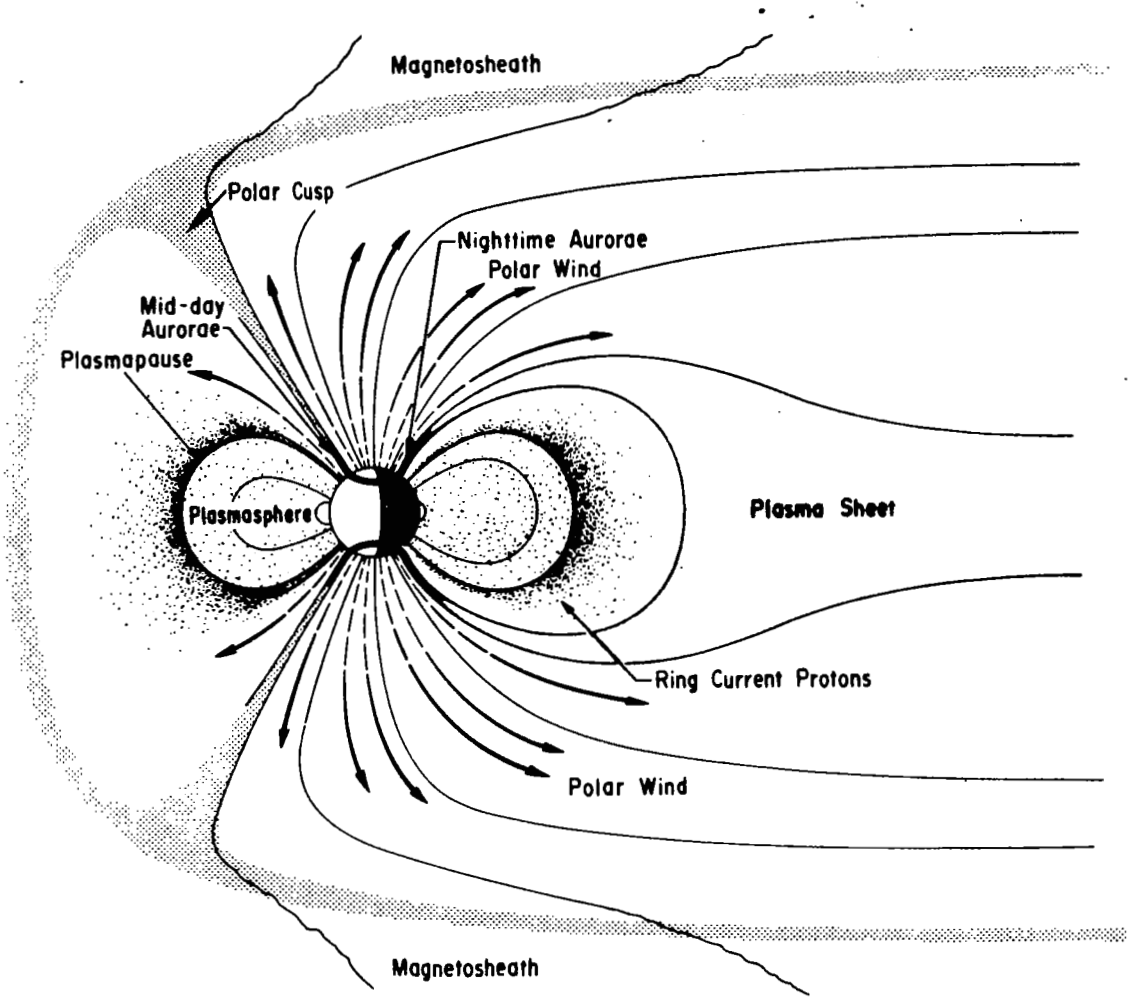

Figure 1-4. SCHEMATIC STRUCTURE OF THE EARTH'S MAGNETOSPHERE (BANKS AND KOCKARTS, 1973, p. B-305)

(representative of the continental United States), electron and mass-averaged ion gyrofrequencies are shown along with the collision frequencies in Figure 1-2. Since collision frequencies and gyrofrequencies play similar roles in the charged particle equations of motion, they may be compared directly to determine whether the magnetic field or the other gases will dominate the motion of a given gas.

From Figure 1-2 it is evident that the electrons are firmly coupled to the geomagnetic field at all altitudes shown, since they gyrate about a field line many times between collisions with either ions or neutrals. Ions, however, undergo a transition from strong coupling to neutral particles at low altitudes to strong coupling to the geomagnetic field at high altitudes. The characteristic distance associated with coupling to a magnetic field is the gyroradius, given by

$$r_s = \frac{w_\perp}{\omega_s} \tag{1-2}$$

where $w_\perp$ is the particle velocity component perpendicular to the magnetic field. If thermal velocities are used for order-of-magnitude estimates, representative gyroradii are about 3 cm for electrons and 4 m for ions, corresponding to $T_e = 2400°K$ ($\bar{w}_e \simeq 3 \times 10^7$ cm s^{-1}) and $T_i = 1200°K$ ($\bar{w}_i \simeq 8 \times 10^4$ cm s^{-1}). As a result of this restriction in the transverse direction, charged particles move most freely parallel to the geomagnetic field lines, that is, in a north-south direction over the magnetic equator and vertically over the magnetic poles.

At this point, several questions can be examined with respect to applicability of the three-fluid approximation in studies of ionosphere dynamics, particularly at high latitudes where magnetosphere-ionosphere interactions are so important. Is a three-fluid approximation necessary, or would a two-fluid or even a single fluid approximation be sufficient? Is a three-fluid approximation adequate, or must the different species of the ion and neutral gases be treated separately? If the answers to these are affirmative, are present three-fluid formulations adequate, or are further developments required? The answers to these questions essentially determine the scope of the theoretical framework developed in this study.

The first question inquires whether the macroscopic properties n, $\vec{v}$, and T of the electrons, ions, and neutrals are sufficiently different to warrant consideration of three separate gases. Experimental and theoretical work on ionospheric temperatures have been reviewed by Banks (1969) and Willmore (1970). The prevalence of nonthermal equilibrium among the gases of at least the ionospheric F region is well established observationally and reasonably well explained theoretically. The basic mechanism for this condition is preferential heating of thermal electrons (energies $\lesssim$ 0.3e V) by photoelectrons in the process of being collisionally thermalized. Preferential heating of electrons results from their small masses and long-range Coulomb interaction. In turn, electrons transfer energy collisionally to ions and neutrals, but preferentially to ions, again because of the long-range Coulomb interaction. At higher altitudes (above ~300 km), ions lose close thermal contact with the neutrals and, through a balance of energy gained from electrons and loss to neutrals, attain a temperature intermediate to those of the electrons and neutrals (e.g., see Figure 1-3). Theoretical calculations (Rees and Walker, 1968) have suggested that heating due to large auroral electric fields may cause ion temperatures to exceed electron temperatures, although no direct observation verifying this is presently known. Thermal nonequilibrium in the E region has been a subject of some controversy for several years because of apparently conflicting results from different observational techniques (D'Arcy and Sayers, 1974). However, this is immaterial to the present question since conditions in the F Region clearly require consideration of distinct electron, ion, and neutral temperatures.

For flow velocities, fewer observational data are available for several reasons. Flow velocity measurements are more difficult, particularly those which measure velocities for different gases simultaneously. Also, conditions in which substantial differences in flow velocities of the different gases are likely to occur are less prevalent in space and time than for thermal nonequilibrium. Nevertheless, there is sufficient evidence to establish that large differences in flow velocity, on the order of hundreds of meters per second, can and do occur at high latitudes. In this region, large electric fields, sometimes in excess of 100 mV m^{-1}, can occur due to sources far out in the magnetosphere (Maynard, 1972). These fields are mapped from the magnetosphere into

the ionosphere along geomagnetic field lines (see Figure 1-4), which act approximately as equipotentials (Farley, 1959; Reid, 1965). This results from the high conductivity along field lines relative to that transverse to field lines. (A qualitative grasp of this idea may be gained from the comparison of collision frequencies and gyrofrequencies in Figure 1-2, recognizing that for $\omega_s > \nu_{ij}$, collisions inhibit motion along the field line while gyrations inhibit motion transverse to the field line.) Implicit in this conception is that electrostatic fields are transverse to magnetic field lines. The degree to which parallel electric fields are actually negligible in the ionsophere is presently the subject of considerable controversy (Maynard, 1972; Zmuda, et al., 1974). However, the existence of large transverse ionospheric electric fields at auroral latitudes is an observational fact (Maynard, 1972; Banks, et al., 1974); and for present purposes that is sufficient.

Large transverse electric fields cause large electron and ion flow velocities of several hundred meters per second. In the absence of collisions, this velocity is given by

$$\vec{V} = \frac{\vec{E} \times \vec{B}}{B^2} c \qquad \text{(Hall Drift).} \qquad (1\text{-}3)$$

For B = 0.5 gauss, an electric field of 30 mV m^{-1} results in a drift velocity of about 600 m s^{-1}. At high altitudes where ion-neutral collision frequencies are much smaller than ion gyrofrequencies (Figure 1-2), electrons and ions drift with the same velocity, given by equation (1-3) (which is independent of charge sign). Thus, when an electric field suddenly becomes large, the charged particles respond rapidly, resulting in a large velocity difference between the charged and the neutral particles at high altitudes. Under the same circumstances at low altitudes, where the ions are collisionally coupled to the motion of the neutrals, the electrons will again respond rapidly to the electric field (since $\omega_s >> \nu_e$) while ions are constrained to move with the neutrals. So at low altitudes the large velocity difference is between the electrons and the heavy particles. Numerical calculations, by Fedder and Banks (1972), among others, demonstrate these effects theoretically. Barium cloud release experiments, for example, those analyzed by Meriwether, et al. (1973), provide direct observational evidence of ion-neutral velocity differences of several hundred meters per second. Comparison of high altitude and

low altitude incoherent scatter radar observations allows similar inferences to be drawn with respect to electrons and ions, if transverse electric fields are assumed to be mapped along magnetic field lines unchanged from F region to E region altitudes (Brekke et al., 1973, 1974a). From these considerations, it is concluded that different flow velocities for electrons, ions, and neutrals must be taken into account in any theoretical framework used for treating problems of dynamics at high latitudes.

For the final macroscopic observable, number densities, different reasoning must be used. If composition of either the ion or neutral gas is required as part of the solution to a problem under study, then a continuity equation for every particle species is required. If composition can be assumed and only total numbers of particles of each gas (electrons, ions, and neutrals) are of interest, as in some dynamical problems, then only a two-fluid approximation is required, since the charge neutrality assumption eliminates one charged particle continuity equation. For present purposes, consideration will be restricted to the latter case, that in which composition is not required.

With the necessity of considering separate properties of at least three gases established, the next question must be examined: Are three gases enough? For number densities, this question has been somewhat sidestepped by limiting the scope of applications to problems in which more than three gases need not be treated. For temperatures and flow velocities the question reduces to asking whether or not all ion species share a common temperature and flow velocity, and likewise for neutrals. Experimental techniques are not sufficiently selective to be able to measure the flow velocity or temperature of a single species of ion or neutral gas. However, theoretical calculations indicate that temperature differences between O^+ and H^+ in excess of 100°K could be expected to occur (Banks, 1967). Since H^+ is a minor ion below about 800 km (see Figure 1-1b), this will cause no difficulty for studies below that altitude; and even above that altitude it may be of little consequence. Since O^+ is predominant between 200 km and 800 km, and below 200 km the ion temperature is equal to the neutral temperature, thermal nonequilibrium among ion species is negligible for altitudes below about 800 km (and perhaps above).

No theoretical work has suggested that neutral species in the ionosphere may have differing temperatures. Similarly, no information is available to indicate that flow velocities of either ion or neutral gases might be significantly differentiated by species. Therefore, it appears that the three-fluid approximation is adequate for a wide variety of problems in the altitude range 90 km to 800 km for all geographic locations.

Finally, the question of the present state of development of multifluid formalism must be considered. Since gases interact by collisions (leaving aside collective phenomena of plasmas for the present), the important multifluid effects are contained in the collision terms. Different temperatures mean different thermal velocities; and since collision cross sections are functions of the relative speed of the colliding particles in general, average collision frequencies depend on the temperatures of both gases. Intuitively, it is apparent that if the relative flow velocities are comparable to or larger than the thermal velocities, the collision frequencies will also be affected. In the ionosphere, ion thermal velocities are of the order of 10^2 to 10^3 meters per second. Ion drift velocities of this order occur frequently at high latitudes due to relatively large electrostatic fields, as discussed previously. This is why proper treatment of flow velocities in the collision terms is important in problems of high latitude ionospheric dynamics.

In the context of these ideas, various multifluid formalisms can be considered briefly; a more detailed examination is deferred to Section III. Chapman and Cowling (1970) present an extensive treatment of the kinetic theory approach to gas dynamics in the single-fluid approximation. Their treatment of gas mixtures is based on deviations of the individual species properties from the (global) properties of the mixture as a whole. S. T. Wu (1969, 1970) treats gas mixtures in a similar manner, but includes detailed consideration of inelastic interactions between the gases and with the radiation field; however, he includes no external forces (e.g., electrostatic and magnetostatic fields). Because of the relatively loose coupling of the three ionospheric gases, more physical insight is to be gained by treating these gases individually, rather than in terms of global mixture properties. Moreover, since deviations of the properties of the electron and ion gases from

those of the neutral gas (which dominates the mixture, due to much larger number densities) may be quite large, the global approach is likely to be either inefficient or mathematically troublesome.

More appropriate for the ionosphere is the work by Burgers (1969). He considers explicitly mixtures of gases with arbitrarily different temperatures and flow velocities. However, his treatment of collision terms for the case of arbitrary flow velocities is limited to a few examples (hard sphere, Coulomb, and Maxwellian-molecule interactions) which only partially satisfy the requirements of ionosphere studies. Moreover, since Burgers' (1969) study treats higher order approximations extensively, his framework (and notation) is more general and complicated than is necessary for ionospheric applications. This makes it cumbersome to use and difficult to extend to other interactions of interest. This latter objection has been remedied somewhat by Banks and Kockarts (1973), who take appropriate results (conservation equations) from Burgers (1969) and present them in a more transparent notation. The difficulty here is that only the results are presented, so that the mathematical origin of parts of the equations remains somewhat obscure. In particular, the collision terms are presented with insufficient formalism to permit extension of the results to other interactions of ionospheric interest. In addition to these, separate treatments of the collision terms alone have appeared in the literature, to be discussed in detail in Section III; but none have extended results beyond those presented by Burgers (1969). Thus, there appears to be a need for a more thorough development of the collision terms for the multifluid case, with extension to additional interactions of ionospheric interest.

Conclusions which may be drawn from the considerations above are as follows: the three-fluid approximation is needed for and applicable to ionospheric problems, particularly at high latitudes; and present formulations need further work on the collision terms. The first objective of this study is then to develop the formal framework of the conservation equations in the three-fluid approximation, suitable for application to ionospheric problems at all latitudes and 90 km to 800 km in altitude (E region and lower and middle F region). The second objective is to use this framework in the investigation

of a problem of current interest in ionospheric dynamics at high latitudes. In the formal development of the conservation equations the treatment is necessarily uneven, since parts are covered in many texts, while others have been little discussed. To ensure completeness and consistency, steps of the more familiar parts are at least outlined; detailed mathematics is reserved for those areas involving original formulations or results.

The approach taken is to start with the Boltzmann equation for each species and, following procedures noted previously, to develop the general transport equation. This is then used to obtain species conservation equations for number density, flow velocity, and energy. These steps are presented briefly in Section II, along with an introduction of the notation and physical ideas associated with the mathematics.

Detailed treatment of the collision terms is reserved for Section III. Emphasis is placed on this treatment because an original formalism is developed which allows more physical insight into the energy transfer process when gases move through one another with a large relative velocity, a condition frequently occurring at high latitudes. The Appendix is a logical extension of Section III. Included there are proofs that the collision terms reduce to accepted expressions in the limit of zero relative flow velocity, and analytic calculations of collision frequencies for a sufficient variety of interactions that most ionospheric requirements should be met. Because these calculations are detailed, extensive, and tend to divert attention from the principal objective (formulation of the conservation equations), they are relegated to the Appendix.

Formal development of the species conservation equations is completed with the collision term treatment in Section III. It is the task of Section IV to turn these formal equations into working equations, applicable to the E and F regions of the ionosphere. Here the three-fluid approximation is applied to obtain three sets of conservation equations. Through conservative order-of-magnitude estimates, a system of working equations of general applicability to ionospheric problems is obtained. Nonelastic and external source-loss processes, which are excluded from the formalism, but which nevertheless

significantly affect the conservation equations, are also examined briefly. The results of Section IV represent the starting points for practical problems in the sense that all approximations of general validity have been made. Further modifications will depend on the conditions of any particular problem.

In Section V, transport properties of the gases in the ionosphere are discussed briefly in order to provide a means for remedying the closure problem of the set of conservation equations. It is characteristic of any set of equations formed by taking velocity moments of the Boltzmann equation that a higher velocity moment is introduced that is not determined by the (finite) set of equations (T.-Y. Wu, 1966). Through the use of transport coefficients (calculated or experimental), these higher order moments can be related to lower order moments, permitting closure of the set of equations. They can also be used in simplified model studies to examine some effects of transport without solving the entire set of velocity moment equations (e.g., Schunk and Walker, 1971). Emphasis here is placed on electron transport properties, both because electrons are much more mobile than other gas particles due to their small mass and because an adequate treatment is readily available. Mathematical detail is restricted primarily to that necessary to use results from the literature. The main exception is the derivation of an original method for approximating the energy dependence of collision frequencies by a power law in velocity, thus making available for arbitrary velocity dependence the relatively simple transport coefficient results of the power law case. Explicit analytic expressions for collision frequencies, some obtained from the literature and some from the present investigation, are introduced at this point since they are basic to the transport properties.

A problem of contemporary interest is examined in Section VI, making partial use of the mathematical apparatus developed in earlier sections. This is an investigation of the altitude structure of auroral E region neutral winds and some of the consequences of this structure for incoherent scatter radar observations. Since the primary calculation is based on observational data at a single location as a function of time, severe limitations are placed on the spatial information available. This results in a considerably simplified calculation for a problem which is not necessarily susceptible to such

simplification. The use of theory, observation, and calculation together, however, makes it possible to obtain estimates of some elements left out of the calculation by necessity. A summation is presented in Section VII.

Section II

KINETIC DESCRIPTION OF GOVERNING EQUATIONS

2.1 GENERAL FORM OF THE TRANSPORT EQUATION

Investigations of transport phenomena based on a particle description of gases generally begin with the Boltzmann equation. Since the derivation of the Boltzmann equation is discussed in detail in many texts on kinetic theory, it is sketched only briefly here. At time t, the number of particles in a volume element $d\vec{r}d\vec{w}$ of six dimensional phase space located at $\vec{r}$, $\vec{w}$ is given by $f(\vec{r}, \vec{w}, t)d\vec{r}d\vec{w}$, where $f(\vec{r}, \vec{w}, t)$ is the distribution function of the gas. Suppose each gas particle is subject to an external force $\vec{F}$ and no collisions between particles occur. Then at time $t + \delta t$, particles previously at $\vec{r}$, $\vec{w}$ at time t will be located at $\vec{r} + \vec{w}\,\delta t$, $\vec{w} + (\vec{F}/m)\,\delta t$, where m is the particle mass. Due to collisions, however, not all particles at $\vec{r}$, $\vec{w}$ at time t will arrive at $\vec{r} + \vec{w}\,\delta t$, $\vec{w} + (\vec{F}/m)\,\delta t$ at time $t + \delta t$. Likewise, due to collisions, not all particles at $\vec{r} + \vec{w}\,\delta t$, and $\vec{w} + (\vec{F}/m)\,\delta t$ at time $t + \delta t$ originated at $\vec{r}$, $\vec{w}$ at time t. This collisional effect is expressed in the following equation:

$$[f(\vec{r} + \vec{w}\,\delta t, \vec{w} + \frac{\vec{F}}{m}\,\delta t, t + \delta t) - f(\vec{r}, \vec{w}, t)]d\vec{r}d\vec{w}$$

$$= \left(\frac{\partial f}{\partial t}\right)_c d\vec{r}d\vec{w}\,\delta t. \qquad (2\text{-}1)$$

Dividing through by $d\vec{r}d\vec{w}\,\delta t$, expanding the first term to first order in δt, and taking the limit as $\delta t \to 0$ results in the Boltzmann equation:

$$\frac{\partial f}{\partial t} + \vec{w} \cdot \nabla f + \frac{\vec{F}}{m} \cdot \nabla_w f = \left(\frac{\partial f}{\partial t}\right)_c \qquad (2\text{-}2)$$

The right side will be treated explicitly later; for the present it simply denotes the time rate of change of the distribution function due to collisions.

If there is a mixture of gases, each species has a distribution function governed by equation (2-2). For the species r this is written

$$\frac{\partial f_r}{\partial t} + \vec{w}_r \cdot \nabla f_r + \frac{\vec{F}_r}{m_r} \cdot \nabla_w f_r = \left(\frac{\partial f_r}{\partial t}\right)_c \quad , \tag{2-3}$$

where the collision term now includes collisions with other species in addition to self collisions. The distribution function is taken to be normalized such that the number density of species r at the location $\vec{r}$ is given by

$$n_r(\vec{r}, t) \equiv \int f_r(\vec{r}, \vec{w}, t) d\vec{w}_r, \tag{2-4}$$

where the integration extends over all velocity space. In this definition, it is assumed that f_r vanishes for infinite velocities. Conventionally, equation (2-4) is called the zeroth (velocity) moment of the distribution function.

The velocity $\vec{w}_r$ denotes the total velocity of an r-particle with respect to some fixed (laboratory) reference frame. It is convenient to define also the species random (thermal) velocity by

$$\vec{c}_r \equiv \vec{w}_r - \vec{v}_r, \tag{2-5}$$

where $\vec{v}_r$ is the average velocity (also referred to as the drift or flow velocity) of species r. In the literature random or thermal velocities are frequently defined with respect to the mass average velocity of the entire fluid. That is convenient when the species flow velocities of all species are close to one another. However, in the ionosphere species flow velocities may differ significantly from one another. A more consistent and physically more transparent treatment is possible if the parameters for each species are defined in their own reference frames.

The species average value of some particle property θ_r is defined to be

$$\langle\theta\rangle_r \equiv \frac{1}{n_r} \int \theta_r f_r \, d\vec{w}_r \quad . \tag{2-6}$$

In particular

$$\vec{v}_r \equiv \langle\vec{w}\rangle_r = \frac{1}{n_r} \int \vec{w}_r f_r \, d\vec{w}_r \quad . \tag{2-7}$$

It then follows from equations (2-5) and (2-7) that

$$\langle c \rangle_r = \langle \vec{w} \rangle_r - \vec{v}_r = 0 \quad . \tag{2-8}$$

A transport equation for the property θ_r is obtained by multiplying both sides of equation (2-3) by θ_r and integrating over all velocity space:

$$\int \theta_r \frac{\partial f_r}{\partial t} d\vec{w}_r + \int \theta_r \vec{w}_r \cdot \nabla f_r \, d\vec{w}_r + \int \theta_r \frac{\vec{F}_r}{m_r} \cdot \nabla_w f_r \, d\vec{w}_r$$
$$= \int \theta_r \left(\frac{\partial f_r}{\partial t} \right)_c d\vec{w}_r \quad . \tag{2-9}$$

It is assumed that the integrands are well-behaved and vanish as velocities become infinite.

For macroscopic analysis, a more convenient form for equation (2-9) can be obtained by considering each term individually. If θ_r is assumed to have no explicit dependence on position or time, then since time and velocity are independent coordinates, the first term in equation (2-9) may be written

$$\int \theta_r \frac{\partial f_r}{\partial t} d\vec{w}_r = \frac{\partial}{\partial t} \int \theta_r f_r \, d\vec{w}_r \equiv \frac{\partial}{\partial t} (n_r \langle \theta \rangle_r) \tag{2-10}$$

from equation (2-6). The second term can be treated in a similar manner:

$$\int \theta_r \vec{w}_r \cdot \nabla f_r \, d\vec{w}_r = \nabla \cdot \int \theta_r \vec{w}_r f_r \, d\vec{w}_r \equiv \nabla \cdot (n_r \langle \vec{w} \theta \rangle_r) \quad . \tag{2-11}$$

The third term in (2-9) can be integrated by parts to obtain

$$\int \theta_r \frac{\vec{F}_r}{m_r} \cdot \nabla_w f_r \, d\vec{w}_r = - \int \frac{f_r}{m_r} \nabla_w \cdot (\theta_r \vec{F}_r) d\vec{w}_r$$
$$= - \frac{n_r}{m_r} \langle \nabla_w \cdot \theta_r \vec{F} \rangle_r \quad ,$$

where the first equality follows from the assumption that f_r vanishes on the infinite velocity surface. For velocity-independent forces

$$\langle \nabla_w \cdot \theta \vec{F} \rangle_r = \langle \vec{F} \cdot \nabla_w \theta \rangle_r \quad . \tag{2-12}$$

But this equation also holds for velocity dependent forces which are perpendicular to the velocity (e.g. $q\vec{w} \times \vec{B}/c$). Since all velocity-dependent external

forces to be treated in this work are of this nature, equation (2-12) may be used, with the result

$$\int \theta_r \frac{\vec{F}_r}{m_r} \cdot \nabla_w f_r \, d\vec{w}_r = - \frac{n_r}{m_r} \langle \vec{F} \cdot \nabla_w \theta \rangle_r \quad . \tag{2-13}$$

Substituting equations (2-10), (2-11), and (2-13) into (2-9) gives

$$\frac{\partial}{\partial t} (n_r \langle \theta \rangle_r) + \nabla \cdot (n_r \langle \theta \vec{w} \rangle_r) - \frac{n_r}{m_r} \langle \vec{F} \cdot \nabla_w \theta \rangle_r = \int \theta_r \left(\frac{\partial f_r}{\partial t} \right)_c d\vec{w}_r \quad . \tag{2-14}$$

This equation (or ones very similar) is variously referred to in the literature as Maxwell's transport equation (Sutton and Sherman, 1965), equation of change of molecular properties (Chapman and Cowling, 1970), or transfer equation (Burgers, 1969).

In its present form the transport equation is quite general (except for inelastic effects) and no improvement over the Boltzmann equation in terms of computational requirements, since the distribution function must first be known before the average quantities in equation (2-14) can be determined. The purpose of this formulation is to establish a bridge between the microscopic properties of the gas, which can be inferred from theory and specialized experiments, and the macroscopic properties, which are observed under more general conditions.

2.2 SPECIES CONSERVATION EQUATIONS FOR MULTICOMPONENT GASES

Conservation equations are obtained by selecting for use in the general transport equation, those particle properties which are conserved in collisions. In particular, mass, momentum, and energy are the conserved quantities of interest here. The object is to obtain equations governing the macroscopic observables of the gas, i.e., number density, flow velocity and temperature. In this section only terms on the left side of the transport equation (2-14) are treated in detail; treatment of the right side (collision terms) is deferred to the next section.

2.2.1 Conservation of Mass ($\theta_r = m_r$)

Since m_r is simply a constant quantity, equation (2-14) can be written down immediately for $\theta_r = m_r$:

$$m_r \frac{\partial n_r}{\partial t} + m_r \nabla \cdot n_r \vec{v}_r = m_r \int \left(\frac{\partial f_r}{\partial t}\right)_c d\vec{w}_r, \tag{2-15}$$

where equation (2-7) was used. The common factor m_r can be cancelled out unless it is desired to work in terms of mass density. If the right side of equation (2-15) is denoted by $\dot{\rho}_r$, this equation can be rewritten

$$\frac{\partial n_r}{\partial t} + \nabla \cdot n_r \vec{v}_r = \frac{\dot{\rho}_r}{m_r} \quad . \tag{2-16}$$

2.2.2 Conservation of Momentum ($\theta_r = m_r \vec{w}_r$)

With $\theta_r = m_r \vec{w}_r$, equation (2-14) becomes

$$m_r \frac{\partial n_r}{\partial t} \langle w \rangle_r + m_r \nabla \cdot n_r \langle \vec{w}\,\vec{w} \rangle_r - n_r \langle \vec{F} \cdot \nabla_w \vec{w} \rangle_r$$

$$= m_r \int \vec{w}_r \left(\frac{\partial f_r}{\partial t}\right)_c d\vec{w}_r \equiv \vec{P}_r \quad , \tag{2-17}$$

where $\vec{P}_r$ represents the total momentum transferred to the species r through collisions. In the second term, the tensor $\langle \vec{w}\,\vec{w} \rangle_r$ can be expanded, using equations (2-5), (2-7), and (2-8):

$$\langle \vec{w}\,\vec{w} \rangle_r = \langle \vec{c}\,\vec{c} \rangle_r + \langle \vec{w} \rangle_r \langle \vec{w} \rangle_r \quad . \tag{2-18}$$

In keeping with the method of defining all macroscopic parameters for each species in the species frame of reference, the species pressure tensor is defined by

$$\overline{\overline{p}}_r \equiv n_r m_r \langle \vec{c}\,\vec{c} \rangle_r \tag{2-19}$$

and the species temperature by

$$n_r k T_r \equiv \frac{1}{3} n_r m_r \langle c^2 \rangle_r = p_r \quad , \tag{2-20}$$

where p_r is the scalar pressure of species r. Equation (2-20) is seen to be the perfect gas law (for species r) and comparison with (2-19) shows that the

scalar pressure is the mean value of the diagonal elements of the pressure tensor. These definitions correspond to values which would be measured by appropriate gauges sensitive only to the species r and drifting with the species r at a velocity $\vec{v}_r$. Equation (2-18) can now be written

$$\langle \vec{w}\,\vec{w} \rangle_r = \frac{\overline{\overline{p}}_r}{n_r m_r} + \vec{v}_r \vec{v}_r \quad , \tag{2-21}$$

where equation (2-7) is used. The second term in (2-17) may then be written

$$m_r \nabla \cdot n_r \langle \vec{w}\,\vec{w} \rangle_r = \nabla \cdot \overline{\overline{p}}_r + m_r [n_r (\vec{v}_r \cdot \nabla)\vec{v}_r + \vec{v}_r \nabla \cdot (n_r \vec{v}_r)], \tag{2-22}$$

where the last two terms follow from Chapman and Cowling (1970, p. 19).

The third term of equation (2-17) follows directly from a standard vector identity to be

$$n_r \langle \vec{F} \cdot \nabla_w \vec{w} \rangle_r = n_r \langle \vec{F} \rangle_r \quad .$$

With these results equation (2-17) may be rewritten as

$$m_r \frac{\partial}{\partial t} (n_r \vec{v}_r) + \nabla \cdot \overline{\overline{p}}_r + n_r m_r (\vec{v}_r \cdot \nabla)\vec{v}_r + m_r \vec{v}_r \nabla \cdot (n_r \vec{v}_r) - n_r \langle \vec{F} \rangle_r = \vec{P}_r \quad . \tag{2-23}$$

2.2.3 Conservation of Energy ($\theta_r = \frac{1}{2} m_r w_r^2$)

In the literature the thermal energy moment ($1/2\ m_r\ c^2$) is more frequently used in obtaining an energy equation than is the total kinetic energy moment ($1/2\ m_r\ w_r^2$) used here. Since in those treatments, drift velocities are generally small compared with thermal velocities, the practical consequences of this distinction are negligible. In the ionosphere, however, flow velocities of ions and neutral particles can attain magnitudes of the same order as thermal velocities. It is therefore important to treat the energy contribution of both flow and thermal components.

For $\theta_r = 1/2\ m_r\ w_r^2$, equation (2-14) becomes

$$\frac{1}{2} m_r \frac{\partial}{\partial t} (n_r \langle w^2 \rangle_r) + \frac{1}{2} m_r \nabla \cdot (n_r \langle w^2 \vec{w} \rangle_r) - \frac{1}{2} n_r \langle \vec{F} \cdot \nabla_w w^2 \rangle_r$$

$$= \frac{1}{2} m_r \int w_r^2 \left(\frac{\partial f_r}{\partial t} \right)_c d\vec{w}_r \equiv E_r \quad , \tag{2-24}$$

where E_r represents the rate at which energy is transferred to the species r by collisions with other species. Again, a more usable form is obtained from a term by term examination.

In the first term the time derivative can be expanded:

$$\frac{1}{2} m_r \frac{\partial}{\partial t} (n_r \langle w^2 \rangle_r) = \frac{1}{2} m_r \langle w^2 \rangle_r \frac{\partial n_r}{\partial t} + \frac{1}{2} m_r n_r \frac{\partial \langle w^2 \rangle_r}{\partial t} \quad . \tag{2-25}$$

Although, as an independent coordinate, w_r (and hence w_r^2) is independent of t, this is not true for $\langle w^2 \rangle_r$, due to the time dependence of the distribution function over which w_r^2 is averaged. From equations (2-5), (2-7), and (2-8)

$$\langle w^2 \rangle_r = \langle c^2 \rangle + v_r^2 \quad , \tag{2-26}$$

since the cross term vanishes. With the definition of species temperature, equation (2-20), equation (2-26) can be written

$$\langle w^2 \rangle_r = \frac{3 k T_r}{m_r} + v_r^2 \quad . \tag{2-27}$$

This is equivalent to the statement that average total kinetic energy is the sum of the average thermal energy and the average flow energy. Equation (2-25) now becomes

$$\frac{1}{2} m_r \frac{\partial}{\partial t} (n_r \langle w^2 \rangle_r) = \left[\frac{3}{2} k T_r + \frac{1}{2} m_r v_r^2 \right] \frac{\partial n_r}{\partial t} + \frac{3}{2} n_r k \frac{\partial T_r}{\partial t}$$
$$+ n_r m_r \vec{v}_r \cdot \frac{\partial \vec{v}_r}{\partial t} \quad . \tag{2-28}$$

In treating the second term of equation (2-24), it is convenient to expand first the averaged velocity expression. Making use of equations (2-5), (2-7), and (2-8) yields

$$\langle w^2 \vec{w} \rangle = \langle (c^2 + 2\vec{c} \cdot \langle \vec{w} \rangle_r + \langle \vec{w} \rangle_r^2)\ (\vec{c} + \langle \vec{w} \rangle_r) \rangle_r$$

$$= \langle c^2 \vec{c} \rangle_r + 2\vec{v}_r \cdot \langle \vec{c}\,\vec{c} \rangle_r + \langle c^2 \rangle_r \vec{v}_r + v_r^2 \vec{v}_r \quad . \tag{2-29}$$

For species r the heat flux vector $\vec{q}_r$ is defined as

$$\vec{q}_r \equiv \frac{1}{2} n_r m_r \langle c^2 \vec{c} \rangle_r \quad , \tag{2-30}$$

representing the flow of thermal energy. With this and previously defined quantities, equation (2-29) can be substituted into the second term of equation (2-24), giving

$$\frac{1}{2} m_r \nabla \cdot (n_r \langle w^2 \vec{w} \rangle_r) = \nabla \cdot \vec{q}_r + \nabla \cdot (\vec{v}_r \cdot \overline{\overline{p}}_r) + \frac{3}{2} k \nabla \cdot (n_r T_r \vec{v}_r)$$

$$+ \frac{1}{2} m_r \nabla \cdot (n_r v_r^2 \vec{v}_r) \quad . \tag{2-31}$$

Most of these terms can be expanded readily in vector notation; however, the second term on the right is more easily manipulated in Cartesian tensor notation. Making use of the convention of summing over repeated indexes allows this term to be written

$$\nabla \cdot (\vec{v} \cdot \overline{\overline{p}}) = \frac{\partial}{\partial x_i} (v_j p_{ji})$$

$$= v_j \frac{\partial}{\partial x_i} p_{ji} + p_{ji} \frac{\partial}{\partial x_i} v_j \quad . \tag{2-32}$$

After Chapman and Cowling (1970, p. 16), the double product of two second rank tensors is defined as

$$\overline{\overline{A}} : \overline{\overline{B}} = A_{ij} B_{ji} \quad . \tag{2-33}$$

Then, since $\overline{\overline{p}}_r$ is a symmetric tensor (see equation (2-19)), equation (2-32) can be written in the form

$$\nabla \cdot (\vec{v}_r \cdot \overline{\overline{p}}_r) = \vec{v}_r \cdot (\nabla \cdot \overline{\overline{p}}_r) + \overline{\overline{p}}_r : \nabla \vec{v}_r \quad . \tag{2-34}$$

Using this result and expanding other terms in equation (2-31) gives

$$\frac{1}{2} m_r \nabla \cdot (n_r \langle w^2 \vec{w} \rangle_r) = \nabla \cdot \vec{q}_r + \vec{v}_r \cdot (\nabla \cdot \overline{\overline{p}}_r) + \overline{\overline{p}}_r : \nabla \vec{v}_r$$

$$+ \frac{3}{2} n_r k T_r \nabla \cdot \vec{v}_r + \frac{3}{2} n_r k \vec{v}_r \cdot \nabla T_r + \frac{3}{2} k T_r \vec{v}_r \cdot \nabla n_r$$

$$+ \frac{1}{2} m_r v_r^2 \vec{v}_r \cdot \nabla n_r + n_r m_r \vec{v}_r \cdot [(\vec{v}_r \cdot \nabla)\vec{v}_r]$$

$$+ \frac{1}{2} n_r m_r v_r^2 \nabla \cdot \vec{v}_r \quad . \tag{2-35}$$

The third term in equation (2-24) is straightforward:

$$\vec{F} \cdot \nabla_w w^2 = 2\vec{F} \cdot \vec{w} \quad . \tag{2-36}$$

It was previously noted that the only velocity dependence of F to be considered has the form of a cross product in velocity, for which the scalar product in equation (2-36) vanishes. Therefore, the third term in equation (2-24) may be written, using equation (2-7),

$$- \frac{1}{2} n_r \langle \vec{F} \cdot \nabla_w w^2 \rangle = - n_r \langle \vec{F} \rangle_r \cdot \vec{v}_r \quad . \tag{2-37}$$

Combining results from equations (2-28), (2-35), and (2-37) permits equation (2-24) to be placed in the following form:

$$\frac{3}{2} n_r k \frac{\partial T_r}{\partial t} + n_r m_r \vec{v}_r \cdot \frac{\partial \vec{v}_r}{\partial t} + \left[\frac{3}{2} k T_r + \frac{1}{2} m_r v_r^2\right] \frac{\partial n_r}{\partial t}$$

$$+ \nabla \cdot \vec{q}_r + \vec{v}_r \cdot (\nabla \cdot \overline{\overline{p}}_r) + \overline{\overline{p}}_r : \nabla \vec{v}_r + \frac{3}{2} n_r k T_r \nabla \cdot \vec{v}_r$$

$$+ \frac{3}{2} n_r k \vec{v}_r \cdot \nabla T_r + \frac{3}{2} k T_r \vec{v}_r \cdot \nabla n_r + \frac{1}{2} m_r v_r^2 \vec{v}_r \cdot \nabla n_r$$

$$+ m_r n_r \vec{v}_r \cdot [(\vec{v}_r \cdot \nabla)\vec{v}_r] + \frac{1}{2} n_r m_r v_r^2 \nabla \cdot \vec{v}_r$$

$$- n_r \langle \vec{F} \rangle_r \cdot \vec{v}_r = E_r \quad . \tag{2-38}$$

The energy equation in this form is rather cumbersome; and since further modifications will be made subsequently, a detailed description of the physical

significance is deferred. However, for future reference, attention is directed to the final term on the left side of equation (2-38). This represents work done on species r particles by external forces. In the ionosphere, if F represents an electrostatic field, this term is called the "Joule heating" contribution (Cole, 1962). A generalization of this concept will be discussed when the conservation equations are placed in final form.

2.2.4 Formal Modifications of the Conservation Equations

Equations (2-16), (2-23), and (2-38), as a coupled set of time-dependent partial differential equations are inconvenient to use in calculations because the quantities of interest are coupled in the time derivatives of the equations. A more workable form is to have the time derivative of only one of the macroscopic variables n_r, $\vec{v}_r$, T_r in each equation. Each equation then describes the time evolution of a single observable, although coupling remains present in other terms. Fortunately, obtaining this result is a straightforward operation, and the results are well worth the effort.

Equation (2-16), the continuity equation, already has the desired form. It is used to eliminate the time derivative of n_r from the momentum equation (2-23). That time derivative can then be written

$$m_r \frac{\partial}{\partial t}(n_r \vec{v}_r) = m_r n_r \frac{\partial \vec{v}_r}{\partial t} + m_r \vec{v}_r \left[\frac{\dot{\rho}_r}{m_r} - \nabla \cdot (n_r \vec{v}_r) \right] . \qquad (2\text{-}39)$$

Substitution of equation (2-39) into (2-23) gives

$$m_r n_r \frac{\partial \vec{v}_r}{\partial t} + m_r n_r (\vec{v}_r \cdot \nabla)\vec{v}_r + \nabla \cdot \overline{\overline{p}}_r - n_r \langle \vec{F} \rangle_r = \vec{P}_r - \dot{\rho}_r \vec{v}_r , \qquad (2\text{-}40)$$

where all collision terms are collected on the right side.

For the energy equation both equations (2-16) and (2-40) are used to eliminate time derivatives of n_r and $\vec{v}_r$. After considerable algebra, equation (2-38) becomes

$$\frac{3}{2} n_r k \frac{\partial T_r}{\partial t} + \frac{3}{2} n_r k \vec{v}_r \cdot \nabla T_r + \nabla \cdot \vec{q}_r + \overline{\overline{p}}_r : \nabla \vec{v}_r$$

$$= E_r - \vec{v}_r \cdot \vec{P}_r + \frac{\dot{\rho}_r}{m_r} \left[\frac{1}{2} m_r v_r^2 - \frac{3}{2} k T_r \right] . \qquad (2\text{-}41)$$

This represents a substantial simplification in the form of the energy equation. One consequence of this simplification is the absence of an external force term, which for an electrostatic force was termed the "Joule heating" term in the previous section. It will be seen in the following section that this contribution is contained implicitly in the collision terms, where it physically belongs.

Since the left sides of the conservation equations are now in final (and simplest) form, the physical meaning of the terms can be examined briefly. Examination of the collision terms is deferred until the next section. In the continuity equation (2-16), the first term represents the explicit time rate of change of n_r, while the second represents the net change in n_r due to more or less r-particles flowing into a small volume than out.

In the momentum equation (2-40), the first term gives the explicit time rate of change of momentum of species r particles. The second term is the nonlinear term which gives the change of momentum of particles in a small cell flowing with the species r particles at velocity $\vec{v}_r$ due to the variation of $\vec{v}_r$ in space. The third term gives change in momentum due to internal forces within species r, that is, pressure and viscous forces. Finally, the fourth term gives momentum changes due to external forces, excluding collision (frictional) forces which are treated explicitly.

The energy equation (2-41) is seen now to involve only thermal or random energy. All directed (mechanical) energy contributions may be recovered from the momentum equation which governs directed motion. The first term in equation (2-41) gives the explicit time rate of change of temperature while the second gives the temperature change of a cell moving at velocity $\vec{v}_r$ due to spatial differences in temperature. Net changes in thermal energy due to more or less thermal energy flowing into a small volume than out are given by the

third term. The fourth term gives the thermal energy of viscous dissipation, that is, the randomizing effect of collisions of r particles among themselves when the drift velocity $\vec{v}_r$ varies in space.

The net effect of the mathematical manipulations in this section has been the transformation from microscopic to macroscopic variables. The resulting equations separately describe the time evolution of number density, directed motion, and random motion, while remaining closely coupled. Although the physical situation has been improved in the sense that the equations can be interpreted in terms of physically measurable quantities, the mathematical problem is no less complicated. The terms treated to this point involve only the averaged interactions of species r particles with themselves and with external force fields. Interactions with other species is the object of the next section.

Section III

FORMAL TRANSFER INTEGRALS

3.1 GENERAL FORM OF THE TRANSFER INTEGRAL

The transfer integrals to be treated are those obtained from the right side of equation (2-14) when mass, momentum, and kinetic energy are successively substituted for θ_r. Initially, however, the form of the transfer integral for arbitrary θ_r is determined. For this an expression for $(\partial f_r/\partial t)_c$, the collision integral, is required. In the standard formulation of the collision integral, only elastic collisions are considered, and particle potentials are assumed to be spherically symmetric and of sufficiently short range that only binary collisions need be considered. This latter assumption is too restrictive to include Coulomb collisions. However, for electron-ion collisions use of the Boltzmann equation has been found to give the same results as the Fokker-Planck equation, which treats many simultaneous but independent collisions (cf Shkarofsky, et al., 1966 or Burgers, 1969). So for convenience, the Boltzmann collision integral will also be used for electron-ion collisions.

With these assumptions, the collision term in the Boltzmann equation (2-2) for species r is given by

$$\left(\frac{\partial f_r}{\partial t}\right)_c = \sum_s \int [f_r(\vec{w}_r') \, f_s(\vec{w}_s') - f_r(\vec{w}_r) \, f_s(w_s)] g \, b\,db \, d\phi \, d\vec{w}_s \,, \qquad (3\text{-}1)$$

where $f_{r,s}$ = distribution function for species r,s

$\vec{w}_{r,s}$ = total velocity of species r,s particle before collision

$\vec{w}_{r,s}'$ = total velocity of species r,s particle after collision

$g \equiv |\vec{w}_s - \vec{w}_r|$ = relative speed

b = impact parameter

ϕ = aximuthal angle.

The summation extends over all species and the range of integration over all $\vec{w}_s$-space. A schematic diagram of the collision process is given in Figure 3-1.

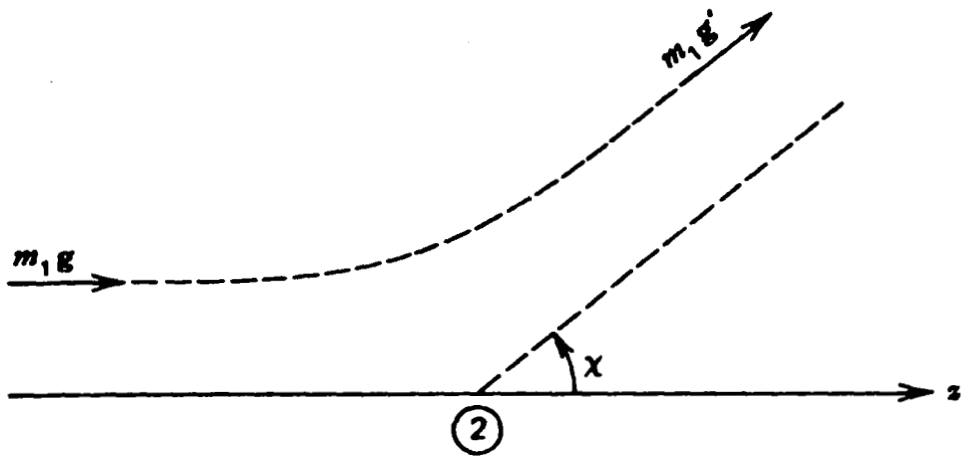

Figure 3-1. GEOMETRY FOR ELASTIC SCATTERING

The derivation of equation (3-1) is presented in many books (eg. Chapman and Cowling, 1970; Sutton and Sherman, 1965; Huang, 1963) and is not repeated here. For notational convenience, only collisions between species r and species s are considered for most of this section; appropriate summations are reinstated as needed.

When equation (3-1) is substituted in the right side of equation (2-14), the transfer integral has the form

$$\int_{\theta_r} \left(\frac{\partial f_r}{\partial t}\right)_c d\vec{w}_r = \int_{\theta_r} [f'_r f'_s - f_r f_s] g \, b db d\phi \, d\vec{w}_s \, d\vec{w}_r, \qquad (3\text{-}2)$$

where $f' \equiv f(w')$. By means of symmetry arguments, Chapman and Cowling (1970, Chapter 3) show that an equivalent form of equation (3-2) is

$$\int_{\theta_r} \left(\frac{\partial f_r}{\partial t}\right)_c d\vec{w}_r = \int (\theta'_r - \theta_r) \, f_r f_s g \, b db \, d\phi d\vec{w}_r \, d\vec{w}_s, \qquad (3\text{-}3)$$

where θ'_r corresponds to post-collision values of the property θ_r. This is the form of the transfer integral on which subsequent calculations are based.

3.2 SPECIFIC TRANSFER INTEGRALS

At this point, it is helpful to define carefully the plasma system to be encompassed by the model being developed. The ionospheric plasma of interest is the thermal plasma, i.e. the low energy plasma with generally random velocities. Plasma particles in this category have energies $\lesssim$2eV, with predominantly Maxwellian distributions characterized by temperatures of a few hundred to a few thousand degrees Kelvin. This distinction is important because occupying the same space may be charged particles with energies of order 10eV (photoelectrons), of order 1-10 KeV (auroral particles) and of order 100 KeV - 10 MeV (trapped radiation). In general, number densities of these higher energy particles are orders of magnitude smaller than that of the thermal particles in the ionosphere; and they do not have the approximately Maxwellian velocity distribution associated with the thermal particles. Because of these substantially different properties, it is convenient and plausible to treat the higher energy particles as separate entities and, in fact, to consider them as external to the system being treated. Although a

strictly consistent, complete treatment of the problem would require inclusion of all such elements in the system (e.g. S.T.Wu, 1970), considerable success in ionospheric investigations has been achieved by means of this distinction because it has a sound physical basis and it greatly simplifies a number of bookkeeping and computational problems.

In addition to practical considerations, there is some theoretical justification for taking this approach. From numerical solutions of Boltzmann-Fokker-Planck equations, Carleton (1968) and Ashihara and Takayanagi (1973, 1974) have found that for electron energies less than about 1 eV, the energy distribution is very nearly Maxwellian; above those energies significant deviations from a Maxwellian distribution occur. Solving a similar equation for the atomic oxygen ion distribution function, Banks and Lewak (1968) determined that for ionospheric conditions the ion distribution is only slightly distorted from Maxwellian in the steady-state nonequilibrium ($T_n \leq T_i \leq T_e$) case.

With these ideas in mind, discussion of the collision terms can proceed. For the case $\theta_r = m_r$, the right side of (3-3) clearly vanishes, since at the low energies considered here mass is unaffected by an elastic collision. From equation (2-16), this implies $\dot{\rho} = 0$. Here, however, recognition of the physical situation described above must be taken into account. This result is a direct consequence of ignoring inelastic collisions, chemical reactions and higher energy particles. Although these effects cannot be included in the present formal treatment of collisions, their place in the equations can be retained by simply retaining the $\dot{\rho}$ notation until details can be filled in appropriate to the specific conditions of a problem. Hereafter, $\dot{\rho}_r/m_r$ is viewed as a source/sink term resulting from processes external to the system, in the sense described above.

For $\theta_r = m_r\vec{w}_r$, equation (3-3) takes the form

$$m_r \int \vec{w}_r \left(\frac{\partial f_r}{\partial t}\right)_c d\vec{w}_r = m_r \int (\vec{w}_r' - \vec{w}_r)\, f_r f_s\, gbdb\, d\phi\, d\vec{w}_r\, d\vec{w}_s \equiv \vec{P}_{rs} \quad (3\text{-}4)$$

Because of the presence of the relative speed g in the integrand, it is necessary to transform the velocities to the center-of-mass system. New velocity coordinates are the center-of-mass velocities,

$$\vec{G} \equiv \frac{m_r \vec{w}_r + m_s \vec{w}_s}{m_r + m_s} = \vec{G}', \tag{3-5a}$$

(right equality follows from conservation of momentum) and the relative velocities

$$\vec{g} = \vec{w}_r - \vec{w}_s \tag{3-5b}$$

$$\vec{g}' = \vec{w}_r' - \vec{w}_s' \quad . \tag{3-5c}$$

Equations (3-5a, b, c) can be solved for $\vec{w}_r$ and $\vec{w}_s$ to obtain the inverse relations

$$\vec{w}_r = \vec{G} + \frac{\mu_{rs}}{m_r} \vec{g}, \qquad \vec{w}_s = \vec{G} - \frac{\mu_{rs}}{m_s} \vec{g}, \tag{3-6}$$

where $\mu_{rs} \equiv m_r m_s/(m_r + m_s)$ is the reduced mass, and similar relations hold for post-collision velocities. From conservation of momentum and energy it can be shown that

$$g = g' \ , \tag{3-7}$$

so that only the direction of relative motion is changed by the collision.

From these relations, the change in velocity of particle r due to the collision can be expressed as

$$(\vec{w}_r' - \vec{w}_r) = \frac{\mu_{rs}}{m_r} (\vec{g}' - \vec{g}). \tag{3-8}$$

The scattering angle χ (see Figure 3-1) is given by

$$\frac{\vec{g} \cdot \vec{g}'}{g^2} = \cos \chi, \tag{3-9}$$

where equation (3-7) has been used. It follows that in the direction of $\vec{g}$

$$\vec{g}' - \vec{g} = -\vec{g}\,(1 - \cos\chi). \tag{3-10}$$

Because of azimuthal symmetry in the scattering, other components of the vector $(\vec{g}' - \vec{g})$, when averaged over many collisions, will not contribute to the integral in equation (3-4). That integral may therefore be written

$$\vec{P}_{rs} = -\mu_{rs} \int \vec{g}g\,(1 - \cos\chi)\, f_r f_s\, b\, db\, d\phi\, d\vec{w}_r\, d\vec{w}_s\,. \tag{3-11}$$

The cross section for momentum transfer is defined to be

$$Q_{rs}(g) \equiv \int (1 - \cos\chi)\, b\, db\, d\phi, \tag{3-12}$$

where the g dependence follows from the fact that $\chi = \chi(g, b)$ in general. From the transformation equations it can be shown that

$$d\vec{w}_r\, d\vec{w}_s = d\vec{g}\, d\vec{G},$$

so that equation (3-11) can be written

$$\vec{P}_{rs} = -\mu_{rs} \int \vec{g}\, g\, Q(g)\, f_r f_s\, d\vec{g}\, d\vec{G}, \tag{3-13}$$

where now $f_{r,s} = f_{r,s}(\vec{g}, \vec{G})$ from equations (3-6). This is the form which is used for calculations with specified distribution functions.

For $\theta_r = 1/2\, m_r w_r^2$, equation (3-3) becomes

$$\frac{1}{2} m_r \int w_r^2 \left(\frac{\partial f_r}{\partial t}\right)_c d\vec{w}_r = \frac{1}{2} m_r \int (w_r'^2 - w_r^2) g\, f_r f_s\, b\, db\, d\phi\, d\vec{w}_r\, d\vec{w}_s$$

$$\equiv E_{rs} \tag{3-14}$$

From equations (3-6), it follows that

$$\frac{1}{2} m_r (w_r'^2 - w_r^2) = \mu_{rs}(\vec{g}' - \vec{g}) \cdot \vec{G} \qquad (3\text{-}15)$$

As previously, averaged over many collisions, the vector $(\vec{g}' - \vec{g})$ contributes to the integral only in the component parallel to $\vec{g}$. Making use of equations (3-10), (3-12), and (3-15) permits equation (3-14) to be written

$$E_{rs} = - \mu_{rs} \int g \, \vec{g} \cdot \vec{G} \, Q(g) \, f_r f_s \, d\vec{g} \, d\vec{G} \, . \qquad (3\text{-}16)$$

In this form the energy transfer integral is evaluated for specific distribution functions.

3.3 TRANSFER INTEGRALS FOR MAXWELLIAN DISTRIBUTION FUNCTIONS

3.3.1 Background

Before a lengthy calculation of this nature is begun, it is appropriate to question the need and the physical and mathematical justification for it and to review previous efforts in this direction. In order to evaluate the momentum and energy transfer integrals, $\vec{P}_{rs}$ and E_{rs}, some form for the distribution functions f_r and f_s must be used. The simplest, physically reasonable choices are two Maxwellian distributions with a common temperature and zero average velocity; reasons for choosing a Maxwellian distribution were discussed previously. In this case, however, application of energy conservation in equations (3-1) or (3-2) shows that the collision terms vanish. Moreover, such conditions do not in general hold in the E and F regions of the inosphere. It has been well established from both ground-based and *in situ* measurements that electron and neutral temperatures differ up to several thousand degrees Kelvin with ion temperatures intermediate to these. Flow velocity differences, while generally small ($\lesssim 10^2$ cm s^{-1}), may reach magnitudes of $\sim 10^5$ cm s^{-1} under certain conditions; this is of the order of ion and neutral thermal velocities.

Burgers (1969) has treated the transfer equations in considerable detail and considered these conditions specifically. He refers to the situation of small relative differences in temperatures and flow velocities as the fully

linear case. Large temperature differences but small differences in flow velocities constitute the semilinear case. By extension, unrestricted differences in both temperatures and flow velocities are termed here the nonlinear case. Although this terminology is not widely used, partially because the nonlinear case has received little attention, it aptly describes the range of approximations for this aspect of ionosphere modeling.

A completely rigorous treatment should also consider distortions of the Maxwellian distribution, for example, by use of a Chapman-Enskog method (cf Burgers, 1969). This is not attempted here because the calculational requirements are large and the degree of accuracy to which basic data, such as momentum transfer cross sections, are known does not presently warrant such an effort. Moreover, as noted previously, theoretical determinations of distribution functions for ionospheric conditions have found deviations from the Maxwellian distributions to be small for the thermal energies considered here. The most important contributions to the transfer integrals are expected to be due to temperature and flow velocity differences, rather than distortions of the distribution functions.

A variation of the semilinear approximation considers arbitrary temperature differences, but assumes static gases. This problem has been treated in detail for Maxwellian distribution functions by Banks (1966 a, c) among others. It can be considered a limiting case for the nonlinear problem and is so used later in examining results. Treatments of flow velocities (i.e. displaced Maxwellian distributions) have not been so complete in either the semilinear or nonlinear approximations.

Morse (1963) has made analytic calculations in the semilinear approximation, presenting both general expressions (arbitrary interaction potential) and specific results for Maxwell, Coulomb, and hard sphere interactions for both momentum and energy transfer. However, his energy transfer integral is based on the thermal (random) energy moment ($1/2\ mc^2$) rather than on the total energy moment ($1/2\ mw^2$ - see equation (3-14)) considered here. Noting this

distinction, Ingold (1968) has presented specific analytic results in the nonlinear approximation for Maxwell and Coulomb interactions. However, he has presented no general equations, except in the semilinear approximation.

Apparently without knowledge of these other studies, Stubbe (1968) has also investigated this problem. He has treated only the momentum transfer integral, obtaining a general result in series form, which can readily be shown to reduce Morse's (1963) closed form integral. His specific results are obtained numerically and apply to charge transfer interactions. Burgers (1969) has presented a comprehensive, systematic development of the fluid dynamic equations from the Boltzmann equation. However, although he has laid out the Chapman-Enskog procedure for treating the nonlinear problem, he has not attempted to solve it. Rather his treatment of this problem extends only to hard sphere interactions, using displaced Maxwellian distribution functions.

Recently Horwitz and Banks (1973), apparently independently of the others cited, have applied the consideration of large flow velocity differences to the ionosphere for both momentum and energy transfer in the nonlinear approximation. However, they provide no general expressions; and their results, although pertaining to charge transfer collisions, are in an approximation corresponding to a hard sphere interaction. As with Burgers' (1969) similar results, the energy transfer calculation is based on the thermal energy moment rather than the total energy moment.

A notable feature of this brief review is the number of times this type of problem has been investigated, generally independently, in a piecemeal manner. It indicates an interest in the problem for a variety of reasons. For ionospheric research in particular, there is good reason for interest. Much attention is currently being directed towards high latitudes where large electrostatic fields are observed driving the ionospheric plasma at high velocities. The previous partial treatments have been found to be inadequate for the present study, particularly with respect to the energy transfer integral. So one of the objectives of this investigation is to present a complete formal treatment of the nonlinear problem, in the approximation of two displaced

Maxwellian distribution functions, and to provide a set of specific results which should be adequate for most requirements. Below, general formal expressions are developed for arbitrary interactions. In the Appendix, the formal results are applied to several specific interactions to obtain analytic expressions suitable for numerical evaluation.

3.3.2 Momentum Transfer

Momentum transferred to species r by species s through elastic collisions is calculated from equation (3-13). Both distribution functions are assumed to be displaced Maxwellians, given by

$$f_r = n_r \left(\frac{m_r}{2\pi k T_r}\right)^{3/2} \exp\left[-\frac{m_r}{2kT_r}(\vec{w}_r - \vec{v}_r)^2\right]$$

$$f_s = n_s \left(\frac{m_s}{2\pi k T_s}\right)^{3/2} \exp\left[-\frac{m_s}{2kT_s}(\vec{w}_s - \vec{v}_s)^2\right] , \qquad (3\text{-}17)$$

where parameters $\vec{v}_r$, $\vec{v}_s$, T_r, T_s have arbitrary values. Placing these expressions in equation (3-13) gives

$$\vec{P}_{rs} = -\mu_{rs} n_r n_s \left(\frac{m_r m_s}{4\pi^2 k^2 T_r T_s}\right)^{3/2} \int g\, \vec{g}\, Q_{rs}(g)$$

$$\cdot \exp\left[-\frac{m_r}{2kT_r}(\vec{w}_r - \vec{v}_r)^2 - \frac{m_s}{2kT_s}(\vec{w}_s - \vec{v}_s)^2\right] d\vec{g}\, d\vec{G} \qquad (3\text{-}18)$$

The exponent of the exponential function must now be transformed to the center-of-mass system, using equations (3-6). When this is accomplished, the exponent, denoted by $X(\vec{g}, \vec{G})$, can be written in the form

$$X(\vec{g}, \vec{G}) = -(Ag^2 + BG^2 + C\vec{g} \cdot \vec{G} + D\,\vec{\alpha} \cdot \vec{g} + E\,\vec{\beta} \cdot \vec{G} + F), \qquad (3\text{-}19)$$

where $$A \equiv \frac{\mu_{rs}}{2k}\left[\frac{m_r T_r + m_s T_s}{m_r m_s T_r T_s}\right] \qquad (3\text{-}20a)$$

$$B \equiv \frac{m_r T_s + m_s T_r}{2k\, T_r T_s} \tag{3-20b}$$

$$C \equiv \frac{\mu_{rs}}{k}\left[\frac{T_s - T_r}{T_r T_s}\right] \tag{3-20c}$$

$$D \equiv -\frac{\mu_{rs}}{kT_r T_s} \quad , \quad \vec{\alpha} \equiv (\vec{v}_r T_s - \vec{v}_s T_r) \tag{3-20d}$$

$$E \equiv -\frac{1}{kT_r T_s} \quad , \quad \vec{\beta} \equiv (m_r \vec{v}_r T_s + m_s \vec{v}_s T_r) \tag{3-20e}$$

$$F \equiv \frac{m_r v_r^2}{2kT_r} + \frac{m_s v_s^2}{2kT_s} \quad . \tag{3-20f}$$

Since the only unknown in equation (3-18) is the momentum transfer cross section which is a function of g only, the integration over $\vec{G}$-space can be carried out immediately. For notational convenience, the integral in equation (3-18) is denoted by $\vec{I}_p$, which can be rewritten as

$$\vec{I}_p = \int d\vec{g}\; g\; \vec{g}\; Q_{rs}(g)\; \exp[-(Ag^2 + D\,\vec{\alpha}\cdot\vec{g} + F)]$$

$$\cdot \int \exp[-BG^2 - \vec{G}\cdot(C\vec{g} + E\vec{\beta})]\, d\vec{G} \; . \tag{3-21}$$

With the notation

$$\vec{S} \equiv C\vec{g} + E\vec{\beta} \; , \tag{3-22}$$

the integration over $\vec{G}$-space can be performed by completing the square, giving

$$\int \exp[-BG^2 - \vec{G}\cdot\vec{S}]d\vec{G} = \left(\frac{\pi}{B}\right)^{3/2} \exp(S^2/4B). \tag{3-23}$$

When this result is substituted back into equation (3-21), together with definition (3-22), $\vec{I}_p$ may be expressed as

$$\vec{I}_p = \left(\frac{\pi}{B}\right)^{3/2} \int g\, \vec{g}\, Q(g)\, \exp[-(A' g^2 + \vec{\gamma}' \cdot \vec{g} + C')]\, d\vec{g} \qquad (3\text{-}24)$$

where

$$A' \equiv \frac{A - C^2}{4B} = \frac{\mu_{rs}}{2kT} \qquad (3\text{-}25a)$$

$$\gamma' \equiv D\vec{\alpha} - \frac{CE\vec{\beta}}{2B} = -\frac{\mu_{rs}}{kT}\,(\vec{v}_r - \vec{v}_s) \qquad (3\text{-}25b)$$

$$C' \equiv F - \frac{E^2\beta^2}{4B} = \frac{\mu_{rs}}{kT}\,(\vec{v}_r - \vec{v}_s)^2 \quad . \qquad (3\text{-}25c)$$

The right sides of equations (3-25) follow from equations (3-20) and the definition of a center-of-mass temperature

$$T \equiv \mu_{rs}\left[\frac{T_r}{m_r} + \frac{T_s}{m_s}\right] . \qquad (3\text{-}26a)$$

For convenience the following notation is also introduced:

$$\vec{v}_o \equiv \vec{v}_r - \vec{v}_s \qquad (3\text{-}26b)$$

$$K \equiv \mu_{rs}/2kT \qquad (3\text{-}26c)$$

Equation (3-24) may then be expressed concisely as

$$\vec{I}_p = \left(\frac{\pi}{B}\right)^{3/2} \int g\, \vec{g}\, Q_{rs}(g)\, \exp[-K(\vec{g} - \vec{v}_o)^2]\, d\vec{g} \quad . \qquad (3\text{-}27)$$

If a spherical coordinate system is selected for $\vec{g}$-space, the angular integration can be performed immediately. This can be accomplished by means of symmetry arguments (e.g. Mathews and Walker, 1965, Chapter 3). Since $\vec{v}_o$ is the only direction specified in the integral, $\vec{I}_p$ must be parallel or anti-parallel to it; this is specified mathematically by

$$\vec{I}_p = A_o\, \vec{v}_o \ , \qquad (3\text{-}28)$$

where A_o is a proportionality constant to be determined. Let $\vec{v}_o$ designate the polar direction in a spherical coordinate system in $\vec{g}$-space. Then from equations (3-27) and (3-28)

$$A_o = \frac{\vec{v}_o \cdot \vec{I}_P}{v_o^2} = \frac{1}{v_o^2} \left(\frac{\pi}{B}\right)^{3/2} \int v_o g^2 \cos\theta \; Q_{rs}(g) \; \exp[-K(g^2 + v_o^2 - 2v_o g \cos\theta)] \cdot g^2 dg \sin\theta d\theta d\phi \quad . \tag{3-29}$$

Because of azimuthal symmetry, the variable ϕ may be integrated out directly and the θ integral evaluated. For that part of the integral involving only angles, the result is

$$2\pi \int_{-1}^{1} \cos\theta \exp(2Kgv_o \cos\theta) \, d\cos\theta$$

$$= \frac{4\pi}{2Kgv_o} \left\{ \cosh(2Kgv_o) - \frac{1}{2Kgv_o} \sinh(2Kgv_o) \right\} \quad .$$

Placing this result in equation (3-29) gives

$$A_o = \frac{4\pi kT}{\mu_{rs}} \left(\frac{\pi}{B}\right)^{3/2} \frac{\exp(-Kv_o^2)}{v_o^2} \int_o^\infty Q(g) \exp(-Kg^2) \left[\cosh(2Kgv_o) - \frac{\sinh(2Kgv_o)}{2Kgv_o} \right] g^3 dg \quad . \tag{3-30}$$

With the relation

$$\frac{d}{dg} \left[\frac{\sinh(2Kgv_o)}{2Kgv_o} \right] = \frac{1}{g} \left[\cosh(2Kgv_o) - \frac{\sinh(2Kgv_o)}{2Kgv_o} \right], \tag{3-31}$$

equation (3-30) can be modified and substituted into equations (3-28), with the result

$$\vec{I}_P = \frac{4\pi kT}{\mu_{rs}} \left(\frac{\pi}{B}\right)^{3/2} \frac{\exp(-Kv_o^2)}{v_o^2} \vec{v}_o \int_o^\infty Q_{rs}(g) \exp(-Kg^2) g^4 d \left[\frac{\sinh(2Kgv_o)}{2Kgv_o} \right]. \tag{3-32}$$

Since $\vec{I}_p$ represents the integral in equation (3-18), that equation may now be written

$$\vec{P}_{rs} = -n_r n_s \frac{\mu_{rs}}{\sqrt{\pi K}} \frac{\exp(-Kv_o^2)}{v_o^2} \vec{v}_o \int_o^\infty Q_{rs}(g) \exp(-Kg^2) g^4 d\left[\frac{\sinh(2Kgv_o)}{2Kgv_o}\right]. \tag{3-33}$$

An effective collision frequency for momentum transfer ν_{rs} is now defined by the relation (Stubbe, 1968)

$$\vec{P}_{rs} \equiv -n_r \nu_{rs} \mu_{rs} \vec{v}_o \quad . \tag{3-34}$$

Comparison with equation (3-33) identifies the collision frequency as

$$\nu_{rs}(v_o) = 2\sqrt{\frac{K}{\pi}} n_s \frac{\exp(-Kv_o^2)}{v_o^2} \int_o^\infty Q_{rs}(g) \exp(-Kg^2) g^4 d\left[\frac{\sinh(2Kgv_o)}{2Kgv_o}\right]. \tag{3-35}$$

Equation (3-35) formally generalizes the collision frequency obtained by Banks (1966a) for two gases at different temperatures to include the effects of average relative motion between the gases. This equation is equivalent to the expression obtained by Morse (1963). It is also equivalent to the series form obtained by Stubbe (1968), as may be verified by expanding the hyperbolic sine in equation (3-35) in a power series. In the Appendix it is shown that in the limit $\vec{v}_o \to 0$, equation (3-35) has the form

$$\nu_{rs}(0) = \frac{8}{3} n_s \sqrt{\frac{K}{\pi}} K^2 \int_o^\infty Q_{rs}(g) \exp(-Kg^2) g^5 dg, \tag{3-36}$$

which is the expression obtained by Banks (1966a). Equation (3-35) is evaluated analytically in the Appendix for a number of forms of the momentum transfer cross section, corresponding to collisional interactions of general interest. Specific collision frequencies of aeronomical interest are compiled in Section V.

3.3.3 Energy Transfer

Total energy transferred to species r by species s through elastic collisions is calculated from equation (3-16). When displaced Maxwellians, equations (3-17), are assumed for the distribution functions, equation (3-16) may be written

$$E_{rs} = -\mu_{rs}\, n_r n_s \left(\frac{m_r m_s}{4\pi^2 k^2 T_r T_s}\right)^{3/2} \int d\vec{g}\; g\; Q_{rs}(g) \exp[-(Ag^2 + D\vec{\alpha}\cdot\vec{g} + F]\vec{g}$$

$$\cdot \int \vec{G} \exp[-(BG^2 + \vec{G}\cdot(C\vec{g} + E\vec{\beta})]d\vec{G}, \qquad (3\text{-}37)$$

where the constants are as defined in equations (3-20). Denote the integral over $\vec{G}$-space by $\vec{I}_E$. Since the exponent in $\vec{I}_E$ is the same as previously, equation (3-22) can be used to write

$$\vec{I}_E = \exp(S^2/4B) \int \vec{G} \exp[-B(\vec{G} + \frac{\vec{S}}{2B})^2]d\vec{G} \quad . \qquad (3\text{-}38)$$

If variables are changed to $\vec{\xi} = \vec{G} + \vec{S}/2B$, equation (3-38) becomes

$$\vec{I}_E = \exp(S^2/4B) \int (\vec{\xi} - \frac{\vec{S}}{2B}) \exp(-B\xi^2)d\vec{\xi} \; . \qquad (3\text{-}39)$$

The integral of the first term vanishes since the integrand is an odd function of each cartesian component of $\vec{\xi}$ over the symmetric, infinite range. Integration of the second term then gives

$$\vec{I}_E = -\exp(S^2/4B)\, \frac{\vec{S}}{2B} \left(\frac{\pi}{B}\right)^{3/2} \quad , \qquad (3\text{-}40)$$

by equation (3-23).

With this result equation (3-37) becomes

$$E_{rs} = n_r n_s\, \mu_{rs} \left(\frac{K}{\pi}\right)^{5/2} \frac{2\pi k^2 T_r T_s}{m_r m_s} \int \vec{g}\cdot[C\vec{g} + E\vec{\beta}]gQ_{rs}(g)$$

$$\cdot \exp[-K(\vec{g} - \vec{v}_o)^2]d\vec{g} \quad . \qquad (3\text{-}41)$$

Designate the first and second terms on the right by I_1 and I_2 respectively and consider I_2 first. The integral in I_2 is basically the same as I_P; so from equations (3-32) through (3-35) I_2 can be evaluated immediately:

$$I_2 = n_r n_s \frac{\mu_{rs}}{m_r m_s} 2\pi k^2 T_r T_s \left(\frac{K}{\pi}\right)^{5/2} E \vec{\beta} \cdot \int \vec{g}\, g\, Q_{rs}(g) \exp[-K(\vec{g} - \vec{v}_o)^2] d\vec{g}$$

$$= -n_r \left(\frac{\mu_{rs}}{m_r + m_s}\right) \left(\frac{\vec{\beta} \cdot \vec{v}_o}{T}\right) \nu_{rs}(v_o) \quad , \tag{3-42}$$

where E has been evaluated from equation (3-20).

For I_1 the integration over angles can be carried out directly:

$$2\pi \int_{-1}^{1} \exp[2Kgv_o \cos\theta] d\cos\theta = 2\pi \frac{\sinh(2Kgv_o)}{Kg\, v_o} \quad . \tag{3-43}$$

I_1 is then given by

$$I_1 = -n_r n_s \left(\frac{\mu_{rs}}{m_r + m_s}\right) \left(\frac{K}{\pi}\right)^{3/2} 4\pi k(T_r - T_s) \frac{\exp(-Kv_o^2)}{v_o} \int_o^\infty g^4 Q_{rs}(g)$$

$$\cdot \exp(-Kg^2) \sinh(2Kgv_o) dg \quad . \tag{3-44}$$

By differentiating with respect to v_o, the following equation can be verified from equations (3-31) and (3-35):

$$\int_o^\infty g^4 Q(g) \exp(-Kg^2) \sinh(2Kgv_o) dg$$

$$= \frac{1}{2n_s} \sqrt{\frac{\pi}{K}} \left\{ \frac{1}{2K} \frac{\partial}{\partial v_o} [v_o^2 \exp(Kv_o^2) \nu_{rs}(v_o)] + \frac{v_o}{2K} \exp(Kv_o^2) \nu_{rs}(v_o) \right\} \quad . \tag{3-45}$$

When this equation is substituted into equation (3-44) and part of the differentiation carried out, the result can be written

$$I_1 = - n_r \left(\frac{\mu_{rs}}{m_r + m_s} \right) \left(\frac{T_r - T_s}{T} \right) \left[v_o kT \frac{\partial \nu_{rs}}{\partial v_o} + (3kT + \mu_{rs} v_o^2) \nu_{rs} \right] \quad . \quad (3\text{-}46)$$

With equations (3-42) and (3-46), equation (3-41) can be written

$$E_{rs} = - n_r \left(\frac{\mu_{rs}}{m_r + m_s} \right) \left(\frac{T_r - T_s}{T} \right) \left[v_o kT \frac{\partial \nu_{rs}}{\partial v_o} + \left(3kT + \mu_{rs} v_o^2 + \frac{\vec{\beta} \cdot \vec{v}_o}{T_r - T_s} \right) \nu_{rs} \right] \quad . \quad (3\text{-}47)$$

This is the desired result.

Equation (3-47) expresses the energy gained by species s due to elastic collisions in terms of the effective collision frequency for momentum transfer. This formulation in terms of momentum transfer collision frequency is original, and it is useful in simplifying both calculations and interpretation of collisional energy transfer. Expressed in this way, terms which depend on temperature differences or average velocity differences or both are clearly separated. The high velocity correction ($\partial \nu_{rs} / \partial v_o$) term is an isolated term as opposed to a set of factors (e.g., Horwitz and Banks, 1973). This permits a more direct assessment of the importance of the correction involved. Once the collision frequency is determined, the additional term is found by differentiation, which is simpler than performing the additional integral required by other formulations. This is illustrated in detail by the analytical evaluations in the Appendix.

Consideration of some special cases aids interpretation of equation (3-47). If the species flow velocities are the same ($\vec{v}_r = \vec{v}_s$), then $\vec{v}_o = 0$. In the Appendix it is demonstrated that in this limit $\partial \nu_{rs}(0) / \partial v_o \to 0$. Equation (3-47) then has the limiting form

$$E_{rs} = - n_r \left(\frac{\mu_{rs}}{m_r + m_s} \right) 3k (T_r - T_s) \nu_{rs}(0), \quad (3\text{-}48)$$

where $\nu_{rs}(0)$ is given by equation (3-36). This is the result derived by Banks (1966a) for these conditions. It can therefore be concluded that the term $3kT\nu_{rs}$ in brackets in equation (3-47) represents the transfer of random energy (heat) from one gas to the other due to temperature differences.

For $T_r = T_s$ the energy transfer given by equation (3-47) is

$$E_{rs} = n_r(m_r + m_s)\left[\frac{\mu_{rs}}{m_r} v_o^2 - \vec{v}_r \cdot \vec{v}_o\right] \nu_{rs}(v_o) \quad , \tag{3-49}$$

where the definitions of $\vec{\beta}$, T, and $\vec{v}_o$ (equations (3-20a), (3-26a), (3-26b) have been used. Comparison with corresponding results of Morse (1963) shows that the second term in equation (3-49) constitutes the difference between taking the total energy moment and the random (thermal) energy moment of the collision integral. This term is seen to represent the rate of work done on species r by the frictional force $-(m_r + m_s)\nu_{rs}\vec{v}_o$ due to the difference in flow velocities. Thus the term $(\vec{\beta} \cdot \vec{v}_o)/(T_r - T_s)$ in equation (3-47), which is the right side of equation (3-49), is seen to have two components, one representing a transfer of directed energy and the other a conversion of directed energy to random energy. The collision of two monoenergetic beams is a limiting example of this case.

The remaining terms in brackets in equation (3-47), $v_o kT\, \partial\nu_{rs}/\partial v_o$ and $\mu_{rs} v_o^2 \nu_{rs}$, correspond to cross terms in the sense that both conditions $T_r \neq T_s$ and $\vec{v}_r \neq \vec{v}_s$ must be satisfied for a nonvanishing contribution. The first of these depends on the interaction potential for its sign as well as its magnitude. Neither term has a straightforward physical interpretation, due to the dual requirement for a finite value.

In the energy conservation equation (2-41), the elastic collision terms are $(E_r - \vec{v}_r \cdot \vec{P}_r)$. The first term is the rate at which total kinetic energy is transferred to species r through collisions. From this is subtracted (second term) the rate at which work is done on species r by collisions, that is, the rate of transfer of directed energy. What remains is the random energy part, which is consistent with the left side of equation (2-41). The collision

terms can be evaluated in terms of the momentum transfer collision frequency from equations (3-34) and (3-47) (with a summation over all species). The result, after lengthy but straightforward algebra, is

$$E_{rs} - \vec{v}_r \cdot \vec{P}_{rs} = \frac{n_r \mu_{rs}}{m_r + m_s} \left[m_s v_o^2 \nu_{rs} - k(T_r - T_s)\left(3\nu_{rs} + v_o \frac{\partial \nu_{rs}}{\partial v_o}\right)\right] . \tag{3-50}$$

Since, from discussion above, the right side of equation (3-50) must represent thermal energy, the physical meaning of the terms can be obtained. In the case of thermal equilibrium ($T_r = T_s$), but $v_o \neq 0$, only the first term remains. This term thus represents the conversion of directed energy to thermal energy, which is a generalization of the Joule heating usually associated with electric fields. In this form, Joule heating (or frictional heating) is seen to result from any forces which cause the gases r and s to move with different average velocities; and this difference in velocities may be due to the nature of the force (for example, electric field) or due to conditions of the medium (for example, a third species which couples preferentially with species r or s). From the form of equation (3-50), it can be inferred that for a two-component system, the total rate of Joule heating is $n_r \mu_{rs} v_o^2 \nu_{rs}$ with a fraction $m_s/(m_r + m_s)$ going to species r (Banks and Kockarts, 1973, Chapter 22).

If $v_o = 0$ but $T_r \neq T_s$, only the second term in equation (3-50) remains. This gives the rate of transfer of thermal energy to species r due to the temperature difference. For the third term not to vanish three conditions must be met: (1) $T_r \neq T_s$, (2) $\vec{v}_r \neq \vec{v}_s$, (3) ν_{rs} must vary with velocity. This term represents a correction term for large relative average velocities, but only if the gases are in thermal nonequilibrium, and only if ν_{rs} is velocity dependent.

3.4 FINAL FORM FOR FORMAL CONSERVATION EQUATIONS FOR MULTICOMPONENT CASES

Results of Section II for the left sides and Section III for the right sides of the conservation equations can now be combined to obtain the final forms. For multicomponent gases the species conservation equations are:

(i) Continuity Equation (equation (2-16))

$$\frac{\partial n_r}{\partial t} + \nabla \cdot (n_r \vec{v}_r) = \frac{\dot{\rho}_r}{m_r} \tag{3-51}$$

(ii) Momentum equation (equations (2-40) and (3-34))

$$\frac{\partial \vec{v}_r}{\partial t} + (\vec{v}_r \cdot \nabla)\vec{v}_r + \frac{1}{n_r m_r} \nabla \cdot \overline{\overline{p}}_r - \frac{\langle \vec{F}_r \rangle}{m_r} =$$

$$- \sum_s \frac{\mu_{rs}}{m_r} \nu_{rs} (\vec{v}_r - \vec{v}_s) - \frac{\dot{\rho}_r}{n_r m_r} \vec{v}_r \tag{3-52}$$

(iii) Thermal energy equation (equations (2-41) and (3-50))

$$\frac{3}{2} n_r k \frac{\partial T_r}{\partial t} + \frac{3}{2} n_r k \vec{v}_r \cdot \nabla T_r + \nabla \cdot \vec{q}_r + \overline{\overline{p}}_r : \nabla \vec{v}_r$$

$$= n_r \sum_s \left(\frac{\mu_{rs}}{m_r + m_s} \right) \left[m_s \nu_{rs} v_{rs}^2 - k (T_r - T_s) \left(3\nu_{rs} + v_{rs} \frac{\partial \nu_{rs}}{\partial v_{rs}} \right) \right]$$

$$+ \frac{\dot{\rho}_r}{m_r} \left[\frac{1}{2} m_r v_r^2 - 3/2 \, k \, T_r \right] \tag{3-53}$$

where the notation $\vec{v}_{rs} \equiv \vec{v}_r - \vec{v}_s$ has replaced the $\vec{v}_o$ previously used.

These equations are formal in the sense that specific interactions must be known before ν_{rs} can be computed from equation (3-35) and $\dot{\rho}_r$ must be specified. In addition, there is a closure problem for the system of equations. Although these five equations are sufficient to solve for n_r, $\vec{v}_r$, and T_r, the additional unknowns associated with $\overline{\overline{p}}_r$ and $\vec{q}_r$ require considerably more information than is given in these equations. And finally, as with such partial differential equations, initial and boundary conditions must be specified.

Part of the additional information required can be determined from general ionospheric conditions, and some simplification of the equations can be obtained

by considering such. These matters are treated in the next section. Some insight can be obtained from investigations of transport properties under controlled conditions, obtaining results which can be applied more generally. This aspect is examined in Section V. Finally, certain information must await the particular problem to be solved for specification. This latter category is by its nature a catchall, since every variable which has not been tied down by previous efforts must be approximated or specified by assumption before the problem can be solved. Section VI illustrates this procedure in a numerical calculation.

THIS PAGE INTENTIONALLY LEFT BLANK

Section IV

THREE-FLUID IONOSPHERIC MODEL

4.1 CONSERVATION EQUATIONS IN THE THREE-FLUID APPROXIMATION

In the three-fluid approximation, macroscopic properties of the electrons, ions, and neutrals are treated separately, while differences of these properties among the various ion or neutral species are assumed negligible. Specifically, all ion species are assumed to have a common temperature T_i and flow velocity $\vec{v}_i$, and all neturals are similarly assumed to have common temperature T_n and flow velocity $\vec{v}_n$. With these assumptions, discussed in Section I, the relevant conservation equations for ions and neutrals can be obtained by summing over the species comprising these gases. Electron equations are given directly by the species equations since a single species constitutes the gas.

From equation (3-51), the electron continuity equation is

$$\frac{\partial N_e}{\partial t} + \nabla \cdot (N_e \vec{v}_e) = \frac{\dot{\rho}_e}{m_e} \quad . \tag{4-1}$$

For number densities, the notation N will hereafter denote the total number density of the (ion or neutral) gas, while n will denote a species number density. These are then related by

$$N = \sum_j n_j \quad . \tag{4-2}$$

To avoid cumbersome notation, subscript i will denote ion and n, neutral; summations will imply summation over all relevant ion or neutral species, as specified by an i and/or an n. Thus, these subscripts serve the double function of summation index and gas indicator. In practice, this should cause less confusion than a proliferation of subscripts. Summing equation (3-51) over all ion species gives

$$\sum_i \frac{\partial n_i}{\partial t} + \sum_i \nabla \cdot (n_i \vec{v}_i) = \sum_i \frac{\dot{\rho}_i}{m_i} \quad .$$

From charge neutrality, $N_i = N_e$, so that interchanging the order of summation and differentiation allows this equation to be rewritten as

$$\frac{\partial N_e}{\partial t} + \nabla \cdot (N_e \vec{v}_i) = \sum_i \frac{\dot{\rho}_i}{m_i} \tag{4-3}$$

where $\vec{v}_i$ was factored out of the summation. In a similar manner the neutral continuity equation is found to be

$$\frac{\partial N_n}{\partial t} + \nabla \cdot (N_n \vec{v}_n) = \sum_n \frac{\dot{\rho}_n}{m_n} \tag{4-4}$$

If a problem involves composition change as one of the significant physical processes, this formulation is inadequate; a separate continuity equation (3-51) must then be used for each ion and neutral species

Equations of motion are obtained from equation (3-52). For electrons the equation may be written down directly:

$$\frac{\partial \vec{v}_e}{\partial t} + (\vec{v}_e \cdot \nabla)\vec{v}_e + \frac{1}{N_e m_e} \nabla \cdot \overline{\overline{p}}_e - \frac{\langle \vec{F}_e \rangle}{m_e}$$

$$= - \sum_{s=i,n} \nu_{es} (\vec{v}_e - \vec{v}_s) - \frac{\vec{v}_e}{N_e} \left(\frac{\dot{\rho}_e}{m_e} \right) , \tag{4-5}$$

where the approximation $\mu_{es} \simeq m_e$ has been used for the reduced mass of the electron with any ion or neutral particle. To obtain the momentum equation for ions and neutrals, it is convenient to multiply equation (3-52) by the number density and mass before summing. The ion equation of motion may then be written

$$\sum_i n_i m_i \frac{\partial \vec{v}_i}{\partial t} + \sum_i n_i m_i (\vec{v}_i \cdot \nabla)\vec{v}_i + \sum_i \nabla \cdot \overline{\overline{p}}_i - \sum_i n_i \langle \vec{F}_i \rangle$$

$$= - \sum_{i,s=e,n} n_i \mu_{is} \nu_{is} (\vec{v}_i - \vec{v}_s) - \vec{v}_i \sum_i \dot{\rho}_i \quad . \tag{4-6}$$

Let the mean mass per particle $\bar{m}$ of a gas (ion or neutral) and the mass density ρ be defined by

$$\rho = N \bar{m} \equiv \sum_s n_s m_s \quad . \tag{4-7}$$

Similarly, let the mean effective collision frequency for momentum transfer between gas r and gas s (if r represents ions, then s represents neutrals and vice versa) be defined by

$$\bar{\nu}_{rs} \equiv \frac{1}{\rho_r} \sum_{r,s} n_r \mu_{rs} \nu_{rs} \quad . \tag{4-8}$$

With these definitions and the fact that the three-fluid approximation allows the flow velocities to be factored out of the summations, equation (4-6) can be rewritten as

$$\frac{\partial \vec{v}_i}{\partial t} + (\vec{v}_i \cdot \nabla)\vec{v}_i + \frac{1}{\rho_i} \nabla \cdot \sum_i \overline{\overline{p}}_i - \frac{1}{\rho_i} \sum n_i \langle \vec{F}_i \rangle$$

$$= - \bar{\nu}_{in}(\vec{v}_i - \vec{v}_n) - \bar{\nu}_{ie}(\vec{v}_i - \vec{v}_e) - \frac{\vec{v}_i}{\rho_i} \sum_i \dot{\rho}_i \quad . \tag{4-9}$$

Following the same procedure for neutrals gives the neutral equation of motion:

$$\frac{\partial \vec{v}_n}{\partial t} + (\vec{v}_n \cdot \nabla)\vec{v}_n + \frac{1}{\rho_n} \nabla \cdot \sum_n \overline{\overline{p}}_n - \frac{1}{\rho_n} \sum_n n_n \langle \vec{F}_n \rangle$$

$$= - \bar{\nu}_{ni}(\vec{v}_n - \vec{v}_i) - \bar{\nu}_{ne}(\vec{v}_n - \vec{v}_e) - \frac{\vec{v}_n}{\rho_n} \sum_n \dot{\rho}_n \quad . \tag{4-10}$$

It is helpful at this point to establish the relation between $\bar{\nu}_{rs}$ and $\bar{\nu}_{sr}$. The total momentum transferred to gas r due to collisions with gas s is given by (cf equations (3-34) and (4-6))

$$\sum_{r,s} n_r \mu_{rs} \nu_{rs}(\vec{v}_r - \vec{v}_s) = \rho_r \bar{\nu}_{rs}(\vec{v}_r - \vec{v}_s) \tag{4-11}$$

by equation (4-8). From equation (3-35) it can be seen that

$$n_r \nu_{rs} = n_s \nu_{sr} \quad . \tag{4-12}$$

When equation (4-12) is used on the left side of (4-11), the result obtained is

$$\sum n_s \mu_{rs} \nu_{sr} \equiv \rho_s \bar{\nu}_{sr} = \rho_r \bar{\nu}_{rs} \quad . \tag{4-13}$$

The distinction between equations (4-12) and (4-13) is sometimes confused. It can be seen that the proper relation depends on whether the momentum transfer term in the momentum equation is written as in equation (4-6) (use equation (4-12)) or as in equation (4-10) (use equation (4-13)). Consistent use of the notation introduced above should eliminate any confusion in the remainder of this study. Application of equations (4-13) and (4-8) gives the following specific relations:

$$\bar{\nu}_{ei} = \sum_i \nu_{ei} \quad , \qquad \bar{\nu}_{ie} = \frac{m_e}{\bar{m}_i} \bar{\nu}_{ei} \tag{4-14a}$$

$$\bar{\nu}_{en} = \sum_n \nu_{en} \quad , \qquad \bar{\nu}_{ne} = \frac{N_e \, m_e}{N_n \, \bar{m}_n} \bar{\nu}_{en} \tag{4-14b}$$

$$\bar{\nu}_{in} = \frac{1}{N_e \, \bar{m}_i} \sum_{i,n} n_i \, \mu_{in} \, \nu_{in} \, , \qquad \bar{\nu}_{ni} = \frac{N_e \, \bar{m}_i}{N_n \, \bar{m}_n} \bar{\nu}_{in} \quad . \tag{4-14c}$$

This allows all collision terms to be expressed in terms of the three collision frequencies ν_{ei}, ν_{en} and ν_{in} or, alternatively, their averaged counterparts $\bar{\nu}_{ei}$, $\bar{\nu}_{en}$, $\bar{\nu}_{in}$.

The energy equations are obtained from equation (3-53). For electrons this can be written

$$\begin{aligned} &\frac{3}{2} N_e \, k \frac{\partial T_e}{\partial t} + \frac{3}{2} N_e \, k \, \vec{v}_e \cdot \nabla T_e + \nabla \cdot \vec{q}_e + \bar{\bar{p}}_e : \nabla \vec{v}_e \\ &\quad = N_e \, m_e (\bar{\nu}_{ei} \, v_{ei}^2 + \bar{\nu}_{en} \, v_{en}^2) - N_e \, k (T_e - T_i) \left[3\bar{\nu}_{ei} + \nu_{ei} \sum_i \frac{\partial \nu_{ei}}{\partial v_{ei}} \right] \\ &\quad - N_e \, k (T_e - T_n) \left[3\bar{\nu}_{en} + \nu_{en} \sum_n \left(\frac{\partial \nu_{en}}{\partial v_{en}} \right) \right] \\ &\quad + \frac{\dot{\rho}_e}{m_e} \left[\frac{1}{2} m_e \, v_e^2 - \frac{3}{2} k \, T_e \right] \end{aligned} \tag{4-15}$$

where $v_{rs} \equiv \left| \vec{v}_r - \vec{v}_s \right|$. Equations for ions and neutrals follow from procedures used above. For ions the result is

$$\frac{3}{2} N_e k \frac{\partial T_i}{\partial t} + \frac{3}{2} N_e k \vec{v}_i \cdot \nabla T_i + \nabla \cdot \sum_i \vec{q}_i + \sum_i \bar{\bar{p}}_i : \nabla \vec{v}_i$$

$$= N_e m_e^2 \nu_{ei}^2 \sum_i \frac{\nu_{ei}}{m_i} - N_e m_e k(T_i - T_e) \sum_i \left[3 \frac{\nu_{ei}}{m_i} + \frac{\nu_{ei}}{m_i} \frac{\partial \nu_{ei}}{\partial \nu_{ei}} \right]$$

$$+ \nu_{in}^2 \sum_{i,n} n_i \frac{\mu_{in}^2}{m_i} \nu_{in} - k(T_i - T_n) \sum_{i,n} \frac{n_i \mu_{in}}{(m_i + m_n)} \left[3\nu_{in} + \nu_{in} \left(\frac{\partial \nu_{in}}{\partial \nu_{in}} \right) \right]$$

$$+ \frac{1}{2} v_i^2 \sum_i \dot{\rho}_i - \frac{3}{2} k T_i \sum_i \frac{\dot{\rho}_i}{m_i} \qquad (4\text{-}16)$$

where equation (4-12) and the fact that $v_{rs} = v_{sr}$ have been used freely. The corresponding equation for the neutral gas is

$$\frac{3}{2} N_n k \frac{\partial T_n}{\partial t} + \frac{3}{2} N_n k \vec{v}_n \cdot \nabla T_n + \nabla \cdot \sum_n \vec{q}_n + \sum_n \bar{\bar{p}}_n : \nabla \vec{v}_n$$

$$= N_e m_e^2 \nu_{en}^2 \sum_n \frac{\nu_{en}}{m_n} - N_e m_e k(T_n - T_e) \sum_n \left[3 \frac{\nu_{en}}{m_n} + \frac{\nu_{en}}{m_n} \left(\frac{\partial \nu_{en}}{\partial \nu_{en}} \right) \right]$$

$$+ \nu_{in}^2 \sum_{i,n} n_i \frac{\mu_{in}^2}{m_n} \nu_{in} - k(T_n - T_i) \sum_{i,n} \frac{n_i \mu_{in}}{m_i + m_n} \left[3\nu_{in} + \nu_{in} \frac{\partial \nu_{in}}{\partial \nu_{in}} \right]$$

$$+ \frac{1}{2} v_n^2 \sum_n \dot{\rho}_n - \frac{3}{2} k T_n \sum_n \frac{\dot{\rho}_n}{m_n} \quad . \qquad (4\text{-}17)$$

This completes the set of conservation equations in the three-fluid approximation.

4.2 IONOSPHERIC CONDITIONS AND CORRESPONDING APPROXIMATIONS

Representative ionospheric conditions were indicated in Section I, Figures 1-1 through 1-4. Here the interest is not so much in typical conditions as in the extremes likely to be encountered in a wide variety of potential applications. The objective is to strip the conservation equations of unnecessary terms without limiting the scope of applications. This is accomplished by considering the range of values of variables and parameters likely to be encountered under usual and unusual conditions, then, from order-of-magnitude estimates, discarding those terms of negligible contribution throughout the range. At this stage a conservative approach is taken -- borderline or questionable

terms are retained. There is ample opportunity for further reduction of the equations when a particular problem is defined and physical conditions are known more precisely.

Extremes of ionospheric variables generally correspond to different altitudes, different geographic locations, and different times. Values given are based on observations or inferences from observations and should be taken as indications of order of magnitude rather than as absolute limits. With that caution, extreme values are presented in Table 4-1. These values will be used as the basis for order-of-magnitude estimates in the remainder of this section.

Table 4-1. EXTREME VALUES FOR SELECTED IONOSPHERIC PARAMETERS

Masses:	$m_e/m_s \sim 10^{-4}$, s = i, n
Number Densities:	$N_e/N_n \lesssim 10^{-3}$
Flow Velocities†:	$10^2 \lesssim v \lesssim 10^5$ cm s^{-1}
Temperatures:	$10^2 \lesssim T \lesssim 10^4$ °K
Spatial Scales*(L)	$10^6 \lesssim L \lesssim 10^8$ cm
Time Scales*:	$T \gtrsim 1$ s
Electric Fields:	$0 \lesssim \lvert\vec{E}\rvert \lesssim 150$ mV m^{-1}

† *Lower limit is a practical limit of interest and observability.*

* *Restriction - not a natural extreme.*

4.2.1 Continuity Equation

As noted in Section III, the term $\dot{\rho}/m$ on the right side of the continuity equation is a phenomenological term in this study because only elastic collisions are treated systematically. It is appropriate at this point to discuss this term and its role in the ionosphere more specifically. Rather than a single term it actually represents the net sum of all processes which add or remove particles of the appropriate type to or from a given volume element. This can be represented mathematically by

$$\dot{\rho}_s/m_s = \sum_s (P_s - L_s) \quad , \qquad s = i, n, e \tag{4-18}$$

where P denotes particle production processes and L particle loss processes.

For ionization, the electron and ion processes are the same; and since only singly ionized ions are present, ions and electrons are produced and lost at the same rate. In the notation of equation (4-18), this is written

$$P_e = \sum_i P_i \quad , \qquad L_e = \sum_i L_i \quad . \tag{4-19}$$

The "P" terms originate primarily from photoionization of neutral atoms and molecules by extreme ultraviolet radiation ($\lambda \lesssim 1029$ Å for primary constituents). An extensive set of chemical kinetic processes modifies the ion composition from that due to photoionization. Photoelectrons produced in this way are not the thermal electrons of interest here, but since they quickly become thermalized, the photoionization rate is generally taken to be the thermal electron production rate. Collisional ionization is another source of thermal plasma, but its importance is restricted primarily to high latitude regions where large numbers of relatively high energy (>1 keV) charged particles frequently penetrate to the altitudes of interest here (90 km to 800 km).

The important loss process for charged particles is dissociative recombination, represented schematically by

$$X\,Y^+ + e \rightarrow X^* + Y^*$$

where the asterisk denotes a possible excited state. Of secondary significance is radiative recombination

$$X^+ + e \rightarrow X^* \rightarrow X + h\nu$$

which may play a significant role only in the upper F region where atomic neutral species predominate. Three-body recombination is important only below the E region where three-body collisions can occur frequently enough to be significant.

Despite the apparent coupling between the source-loss terms of the charged particle and neutral particle continuity equations, they are independent, except for possible coupling in the transport terms. This results from the low degree of ionization, particularly at altitudes where production and loss rates are highest (110 km to 250 km); that is, the number of particles involved in ionization and recombination is negligible compared with the total neutral number densities. More important is the photodissociation of molecular species, especially molecular oxygen. For many problems it is adequate to set this term to zero. Such considerations, however, are best left to particular applications. For a detailed discussion of these terms the work by Banks and Kockarts (1973) (hereafter denoted B&K) may be consulted.

Finally, one of the consequences of the assumptions of (1) charge neutrality, (2) single ionization and (3) no negative ions can be obtained from the continuity equations. Use of equations (4-18) and (4-19) in (4-1) and (4-3) gives

$$\frac{\partial N_e}{\partial t} + \nabla \cdot (N_e \vec{v}_e) = P_e - L_e \tag{4-20}$$

and

$$\frac{\partial N_e}{\partial t} + \nabla \cdot (N_e \vec{v}_i) = P_e - L_e \quad . \tag{4-21}$$

Current density is defined as

$$\vec{j} = \sum_{s=e,i} q_s n_s \vec{v}_s$$

$$= e N_e (\vec{v}_i - \vec{v}_e) \tag{4-22}$$

where -e is the electron charge and the latter result follows from the assumtions. If equation (4-20) is subtracted from (4-21), the result can therefore be written

$$\nabla \cdot \vec{j} = 0 \tag{4-23}$$

where the vanishing of the time derivative of the space charge density, normally found in this equation, is a direct result of the charge-neutrality assumption.

For completeness the neutral continuity equation, corresponding to equations (4-20) and (4-21), is written as

$$\frac{\partial N_n}{\partial t} + \nabla \cdot (N_n \vec{v}_n) = P_n - L_n \quad . \tag{4-24}$$

4.2.2 Equations of Motion

A distinctive difference between the equations of motion of charged and neutral particles is the external force term. Electromagnetic forces, as noted previously, play an extremely important role in differentiating the motions of the charged and the neutral particles. Other forces are also operative in the upper atmosphere, however, and their importance must be assessed. These forces are the gravitational force and the coriolis force, the latter a consequence of working in an Earth-fixed, rotating coordinate system. For the neutral gas, the external force term may be written

$$\frac{1}{\rho_n} \sum_n n_n \langle \vec{F}_n \rangle = \vec{g} + 2\vec{v}_n \times \vec{\Omega}_E \tag{4-25}$$

where $\vec{g}$ is the gravitational acceleration, $\vec{\Omega}_E$ is the angular acceleration of the Earth and the brackets around $\vec{F}_n$ indicate that the average velocity, rather than particle velocity, is to be used. The gravitational term has a unique quality among all the terms in the momentum equations: for a given location it is constant in magnitude and direction. This makes it difficult to neglect in general because a situation can be conceived in which every term is, at some time or other, smaller than the gravitational term. So gravity should always be included unless it can be shown to be insignificant in a particular problem. No such general statement can be made of the coriolis term; it must be examined in the context of the other terms.

External force terms for the charged particles are similar to equation (4-25), with the addition of the appropriate electromagnetic terms:

$$\frac{\langle \vec{F}_e \rangle}{m_e} = -\frac{e}{m_e}\left(\vec{E} + \frac{\vec{v}_e}{c} \times \vec{B}\right) + \vec{g} + 2\vec{v}_e \times \vec{\Omega}_E$$

$$\frac{1}{\rho_i} \sum_i n_i \langle \vec{F}_i \rangle = \frac{e}{m_i}\left(\vec{E} + \frac{\vec{v}_i}{c} \times \vec{B}\right) + \vec{g} + 2\vec{v}_i \times \vec{\Omega}_E \quad .$$

The angular velocity of a charged particle gyrating about a field line is given by

$$\vec{\omega}_s = \frac{q_s \vec{B}}{m_s c} \quad , \tag{4-26}$$

the magnitude of which is the gyrofrequency. Using this notation in the above equations gives

$$\frac{\langle \vec{F}_e \rangle}{m_e} = - \omega_e \frac{\vec{E}}{B} c - \vec{v}_e \times \vec{\omega}_e + \vec{g} + 2\vec{v}_e \times \vec{\Omega}_E \quad , \tag{4-27}$$

$$\frac{1}{\rho_i} \sum_i n_i \langle \vec{F}_i \rangle = \bar{\omega}_i \frac{\vec{E}}{B} c + \vec{v}_i \times \vec{\bar{\omega}}_i + \vec{g} + 2\vec{v}_i \times \vec{\Omega}_E \quad , \tag{4-28}$$

where the bar on the ion gyrofrequency denotes an average value obtained by using the mean ion mass $\bar{m}_i$. Note that in the ion equation, for example, the magnetic and coriolis terms can be combined to obtain

$$\vec{F}_{imag} + \vec{F}_{icor} = \vec{v}_i \times (\vec{\bar{\omega}}_i + 2\vec{\Omega}_E) . \tag{4-29}$$

Since $\bar{\omega}_i \sim 10^2 \ s^{-1}$ while $\Omega_E = 7.29 \times 10^{-5} \ s^{-1}$, the coriolis force is negligible compared to the Lorentz force. The same holds true for the electron equation since $\omega_e \sim 10^7 \ s^{-1}$. So the coriolis force is retained only in the neutral equation.

The momentum equations may now be written with external force terms written out explicitly and the notation of equations (4-14a through 4-14c) incorporated in the collision terms. From equation (4-5) the electron momentum equation

$$\frac{\partial \vec{v}_e}{\partial t} + (\vec{v}_e \cdot \nabla)\vec{v}_e + \frac{1}{N_e m_e} \nabla \cdot \bar{\bar{p}}_e + \omega_e \frac{\vec{E}}{B} c + \vec{v}_e \times \vec{\omega}_e - \vec{g}$$

$$= - \bar{\nu}_{ei}(\vec{v}_e - \vec{v}_i) - \bar{\nu}_{en}(\vec{v}_e - \vec{v}_n) - \frac{\vec{v}_e}{N_e}(P_e - L_e) \quad . \tag{4-30}$$

Normally, the last term on the right side is negligible because

$$(P_e - L_e)/N_e << 1\ s^{-1}\ ,$$

while

$$\bar{\nu}_{en} \text{ or } \bar{\nu}_{ei} \gtrsim 10^2\ s^{-1}.$$

At certain times the ratio may approach the order of one, but collision or other terms would still dominate. So this term will be discarded. The other terms require closer examination.

To this point little has been said of the pressure tensor, $\bar{\bar{p}}_s$ (also called the momentum flux tensor), since its definition in equation (2-19). It was noted, following its definition in equation (2-20), that the scalar pressure p_s is one third of the trace of the pressure tensor. For convenience, these definitions are rewritten in Cartesian tensor notation:

$$p_{\alpha\beta} \equiv n\ m\langle c_\alpha\ c_\beta\rangle \qquad \alpha,\beta = 1, 2, 3 \qquad (4\text{-}31a)$$

$$p \equiv \frac{1}{3}\ n\ m\langle c_\alpha\ c_\alpha\rangle \qquad \alpha = 1, 2, 3 \qquad (4\text{-}31b)$$

where the summation convention is used for repeated indices. From these, the viscous-stress tensor (also called the zero-trace pressure tensor and shear-stress tensor) is defined by

$$\tau_{\alpha\beta} \equiv p_{\alpha\beta} - p\ \delta_{\alpha\beta} \qquad (4\text{-}32)$$

where $\delta_{\alpha\beta}$ is the Kronecker delta. Chapman and Cowling (1970, Section 7.41), following rigorous procedures, obtain an expression which can be written in the form

$$\tau_{\alpha\beta} = -\ \eta\left[\frac{\partial v_\alpha}{\partial x_\beta} + \frac{\partial v_\beta}{\partial x_\alpha}\right] + \frac{2}{3}\ \eta\ \delta_{\alpha\beta}\ \nabla \cdot \vec{v} \qquad (4\text{-}33)$$

where η is the coefficient of absolute viscosity. That derivation also provides a rigorous means for computing η; however, for present purposes that is less useful than the simple mean-free-path expression derived from physical arguments.

These expressions can now be considered in the context of the electron momentum equation (4-30). The question of immediate interest is whether the anisotropic part of pressure tensor is negligible compared with the scalar (isotropic) pressure. To determine this, an order-of-magnitude estimate is made based on a mean-free-path expression for η. Expressions of Mitchner and Kruger (1973, Section II-12), obtained for partially ionized gases, are employed. With factors of order unity ignored, the desired ratio can be written, for purposes of estimating order-of-magnitude only, as

$$\left| \frac{(\tau_e)_{\alpha\beta}}{p_e} \right| \simeq \frac{\eta_e}{p_e} \left| \frac{\partial v_{e_\alpha}}{\partial x_\beta} \right| \tag{4-34a}$$

The coefficient of viscosity is given approximately by

$$\eta_e \simeq N_e \, m_e \, \bar{c}_e \, \ell_e^{\,m} \tag{4-34b}$$

where $\bar{c}_e$ is the mean electron thermal velocity and $\ell_e^{\,m}$ is the electron momentum-randomization mean free path, which can be written

$$\ell_e^{\,m} \simeq \frac{\bar{c}_e}{\bar{\nu}_{ei} + \bar{\nu}_{en}} \quad . \tag{4-34c}$$

When these expressions, together with

$$p_e = N_e \, k \, T_e \simeq N_e \, m_e \, \bar{c}_e^{\,2} \quad , \tag{4-34d}$$

are introduced into equation (4-34a), the result is

$$\left| \frac{(\tau_e)_{\alpha\beta}}{p_e} \right| \simeq \frac{1}{(\bar{\nu}_{ei} + \bar{\nu}_{en})} \left| \frac{\partial (v_e)_\alpha}{\partial x_\beta} \right| . \tag{4-34e}$$

A conservative estimate is obtained by taking maximum values in the numerator and minimum values in the denominator. Possible extremes would be $\bar{\nu}_{ei} + \bar{\nu}_{en} \simeq 10 \ s^{-1}$, $\Delta(v_e)_\alpha \simeq 1 \ km \ s^{-1}$ and $\Delta x_\beta \simeq 10$ km, very unlikely to occur in this combination. From this it appears that

$$\left| \frac{(\tau_e)_{\alpha\beta}}{p_e} \right| \lesssim 10^{-2} \quad , \tag{4-34f}$$

so that only the scalar pressure part of the pressure tensor need be retained in the electron momentum equation.

Rewriting equation (4-30) to include only the retained terms gives

$$\frac{\partial \vec{v}_e}{\partial t} + (\vec{v}_e \cdot \nabla)\vec{v}_e + \frac{1}{N_e m_e} \nabla p_e + \omega_e \frac{\vec{E}}{B} c + \vec{v}_e \times \vec{\omega}_e - \vec{g}$$

$$= - \bar{\nu}_{ei}(\vec{v}_e - \vec{v}_i) - \bar{\nu}_{en}(\vec{v}_e - \vec{v}_n) \quad . \tag{4-35}$$

It is now convenient to estimate the range of values each of these terms may be expected to have based on values listed in Table 4-1. These are given in Table 4-2. In the last two cases, values of 10^4 s^{-1} and 10^5 s^{-1} were used for maximum values of $\bar{\nu}_{ei}$ and $\bar{\nu}_{en}$ respectively.

Several considerations apply to the judicious use of these numbers. First, some terms can vanish or almost vanish, and in a number of problems this can be reasonably assumed. However, maximum values for these terms are much less likely. Second, values for some of these terms scale with the electron velocity, making a better comparison possible. Third, directions must be taken into account explicitly since the geomagnetic field makes the ionosphere quite anisotropic.

Individual terms can now be examined in light of these considerations. Because of the anisotropy due to the geomagnetic field, it is convenient to think in terms of components parallel and perpendicular to the geomagnetic field. This differentiation applies particularly to terms (4) and (5), which are potentially the largest. Since $\vec{\omega}_e$ is parallel to the magnetic field (equation (4-26)), term (5) affects only transverse components of electron velocity. Because the value of this term varies directly with electron velocity, it may be compared with terms (7) and (8) which may vary somewhat similarly. Since ω_e remains virtually constant while factors in terms (7) and (8) can become much smaller, these latter terms can be neglected in equations for the transverse components. Similarly, terms (1), (2), and (6) are negligible for transverse components (radio frequency driving forces would be

Table 4-2. ORDER-OF-MAGNITUDE ESTIMATES OF EXTREME VALUES FOR TERMS IN THE ELECTRON MOMENTUM EQUATION

TERM NUMBER	RANGE OF VALUES ($cm\ s^{-2}$)
(1)	$10^{-2} \leq \left\| \frac{\partial \vec{v}_e}{\partial t} \right\| \lesssim 10^{5}$
(2)	$10^{-5} \leq \|(\vec{v}_e \cdot \nabla)\vec{v}_e\| \lesssim 10^{4}$
(3)	$10^{4} \lesssim \left\| \frac{1}{N_e m_e} \nabla p_e \right\| \lesssim 10^{8}$
(4)	$0 \leq \left\| \omega_e \frac{\vec{E}}{B} c \right\| \lesssim 10^{12}$
(5)	$10^{9} \leq \|\vec{v}_e \times \vec{\omega}_e\| \lesssim 10^{12}$
(6)	$\|\vec{g}\| \simeq 10^{3}$
(7)	$0 \leq \|\bar{\nu}_{ei}(\vec{v}_e - \vec{v}_i)\| \lesssim 10^{9}$
(8)	$0 \leq \|\bar{\nu}_{en}(\vec{v}_e - \vec{v}_n)\| \lesssim 10^{10}$

required to make the first term significant). Term (3) can also be neglected, although it appears to be a borderline case, because there is little likelihood of the minimum value of term (5) occurring at the same location as the maximum of term (3). The former corresponds to a low or middle latitude location and the latter to high latitudes. This reduction leaves only terms (4) and (5), which can be solved explicitly for the transverse components of $\vec{v}_e$, giving

$$\vec{v}_{e\perp} = \frac{\vec{E} \times \vec{B}}{B^2} c \qquad (4\text{-}36)$$

This is frequently termed the E x B drift velocity or the Hall drift. Although equation (4-36) is expressed in Gaussian units, in the literature measured values of E are generally given in units of millivolts per meter. A convenient conversion for estimating drift velocities is that an electric field (transverse to $\vec{B}$) of 1 mV m^{-1} results in a drift velocity of about 20 m s^{-1} for B = .5 gauss.

For the equation of the component parallel to the geomagnetic field, the situation is entirely different because term (5) is not part of the equation. It may be recalled from discussions in Section I that the existence of an electric field component parallel to the geomagnetic field is controversial. For this reason term (4) is retained in the equation for possible use, but it is not used to eliminate other terms. Since terms (1), (2), (7), and (8) scale with electron velocity, comparisons among these terms allow (1) and (2) to be dropped. Gravity is parallel to the magnetic field only at the poles where the (vertical) pressure gradient will be closer to the maximum value, so term (6) can be dropped. The resulting equation can again be solved explicitly giving

$$v_{e\parallel} = \left(\frac{1}{\bar{\nu}_{ei} + \bar{\nu}_{en}}\right)\left[\bar{\nu}_{ei}\, v_{i\parallel} + \bar{\nu}_{en}\, v_{n\parallel} - \omega_e \frac{E_\parallel}{B} c - \frac{1}{N_e m_e} \nabla_\parallel p_e\right] . \qquad (4\text{-}37)$$

Equations (4-36) and (4-37) together comprise the electron momentum equations for the E and F regions of the ionosphere, within the few restrictions adopted.

Since rather similar considerations apply to the ion equation, it can be treated more briefly. From equations (4-9), (4-14), (4-18), (4-19), (4-28), and (4-32), the ion momentum equation can be written

$$\frac{\partial \vec{v}_i}{\partial t} + (\vec{v}_i \cdot \nabla)\vec{v}_i + \frac{1}{\rho_i}\nabla p + \frac{1}{\rho_i}\nabla \cdot \sum_i \overline{\overline{\tau}}_i - \vec{g} - \omega_i \frac{\vec{E}}{B}\, c$$
$$- \vec{v}_i \times \vec{\omega}_i = -\bar{\nu}_{in}(\vec{v}_i - \vec{v}_n) - \frac{m_e}{m_i}\nu_{ei}(\vec{v}_i - \vec{v}_e) - \vec{v}_i\left(\frac{P_e - L_e}{N_e}\right). \quad (4\text{-}38)$$

Corresponding to equation (4-34e), the ratio of the anisotropic part of the ion pressure tensor to the isotropic part is given by

$$\left|\frac{(\tau_i)_{\alpha\beta}}{p_i}\right| \simeq \frac{1}{\bar{\nu}_{ii} + \bar{\nu}_{in}}\left|\frac{\partial (v_i)_\alpha}{\partial x_\beta}\right| . \quad (4\text{-}39a)$$

As before, a maximum estimated value is obtained for $(\bar{\nu}_{ii} + \bar{\nu}_{in}) \sim .1\ s^{-1}$, $\Delta(v_i)_\alpha \sim 1\ km\ s^{-1}$ and $\Delta x_\beta \sim 10\ km$, with the result

$$\left|\frac{(\tau_i)_{\alpha\beta}}{p_i}\right| \lesssim 1 \quad . \quad (4\text{-}39b)$$

So in the following order-of-magnitude estimates, it is sufficient to consider only the scalar pressure gradient - the viscous-stress tensor divergence will be retained or discarded along with the pressure gradient.

Terms in equation (4-38) are evaluated from Table 4-1 as before, to obtain the estimates given in Table 4-3. Because the ion gyrofrequency is much smaller than the electron gyrofrequency, the electromagnetic terms do not dominate the ion momentum equation as completely as in the electron case. Comparison of terms (1), (2), (7), (8), and (9), all of which scale with $\vec{v}_i$ for the most part, allows all but term (7) to be dropped. The other terms do not scale together, and the ranges overlap sufficiently that none can be

Table 4-3. ORDER-OF-MAGNITUDE ESTIMATES OF EXTREME VALUES FOR TERMS IN THE ION MOMENTUM EQUATION

TERM NUMBERS	RANGE OF VALUES ($cm\ s^{-2}$)
(1)	$10^{-2} \lesssim \left\lvert \frac{\partial \vec{v}_i}{\partial t} \right\rvert \lesssim 10^{5}$
(2)	$10^{-5} \lesssim \lvert (\vec{v}_i \cdot \nabla)\vec{v}_i \rvert \lesssim 10^{4}$
(3)	$1 \lesssim \left\lvert \frac{1}{N_e \bar{m}_i} \nabla p_i \right\rvert \lesssim 10^{4}$
(4)	$\lvert \vec{g} \rvert \simeq 10^{3}$
(5)	$0 \lesssim \left\lvert \bar{\omega}_i \frac{\vec{E}}{B} c \right\rvert \lesssim 10^{7}$
(6)	$10^{4} \lesssim \lvert \vec{v}_i \times \vec{\bar{\omega}}_i \rvert \lesssim 10^{7}$
(7)	$0 \lesssim \lvert \bar{\nu}_{in}(\vec{v}_i - \vec{v}_n) \rvert \leq 10^{8}$
(8)	$0 \lesssim \left\lvert \frac{m_e}{\bar{m}_i} \bar{\nu}_{ei}(\vec{v}_i - \vec{v}_e) \right\rvert \lesssim 10^{4}$
(9)	$0 \lesssim \left\lvert \vec{v}_i \left(\frac{P_e - L_e}{N_e} \right) \right\rvert \lesssim 10^{5}$

totally ignored. Although the gravitational term is borderline, compared with term (6) (transverse components), it is convenient to retain it and write a single vector equation. The remaining terms can be placed in the form

$$\vec{v}_i = \vec{v}_n + \frac{1}{\bar{\nu}_{in}} \left[\bar{\omega}_i \frac{\vec{E}}{B} c + \vec{v}_i \times \vec{\omega}_i + \vec{g} - \frac{1}{\rho_i} \nabla p_i - \frac{1}{\rho_i} \nabla \cdot \sum_i \bar{\bar{\tau}}_i \right] \quad (4\text{-}40)$$

which is an implicit partial differential equation for $\vec{v}_i$. This is the final form for the ion equation of motion.

Similar procedures are followed in treating the neutral momentum equation. From equations (4-10), (4-14), (4-18), (4-25), and (4-32) this equation may be written

$$\frac{\partial \vec{v}_n}{\partial t} + (\vec{v}_n \cdot \nabla)\vec{v}_n + \frac{1}{\rho_n} \nabla p_n + \frac{1}{\rho_n} \nabla \cdot \sum_n \bar{\bar{\tau}}_n - \vec{g} - 2(\vec{v}_n \times \vec{\Omega}_E)$$

$$= - \frac{N_e \bar{m}_i}{N_n \bar{m}_n} \bar{\nu}_{in} (\vec{v}_n - \vec{v}_i) - \frac{N_e m_e}{N_n \bar{m}_n} \bar{\nu}_{en} (\vec{v}_n - \vec{v}_e) - \vec{v}_n \frac{(P_n - L_n)}{N_n} \quad .$$

The ratio of the magnitude of the viscous stress tensor to the scalar pressure, analogous to equation (4-39a) for ions, has an order of magnitude given by

$$\left| \frac{(\tau_n)_{\alpha\beta}}{p_n} \right| \simeq \frac{1}{\frac{N_e}{N_n} \bar{\nu}_{in} + \bar{\nu}_{nn}} \left| \frac{\partial (v_n)_\alpha}{\partial x_\beta} \right| \quad . \quad (4\text{-}41a)$$

A value of approximately 10^{-3} s^{-1} is used for $\bar{\nu}_{nn}$ at 800 km, based on a hard-sphere collision assumption. For neutrals, the scale size for significant variation is larger than for electrons and ions because the smaller scale sizes are associated with the geomagnetic field at high latitudes. These affect the neutrals only through collisions with charged particles; and because of the number density disparity, relatively long times are required to make significant changes in the neutral times. During this time, motions of the neutral gas cause the effects to diffuse to surrounding regions, that is, enlarging the spatial scale for significant variation. A conservative value

of 100 km is used for Δx_β. Together with an extreme value of 1 km s^{-1} for $\Delta(v_n)_\alpha$, equation (4-41a) yields

$$\left| \frac{(\tau_n)_{\alpha\beta}}{p_n} \right| \lesssim 10 \quad . \tag{4-41b}$$

As before, the scalar pressure term will be used to represent all pressure tensor terms in the following order-of-magnitude estimates, with due recognition of the above result in the event that the pressure gradient term appears negligible.

Order-of-magnitude estimates, based on values in Table 4-1 and the above considerations of spatial and time scales, are presented in Table 4-4. The estimate for term (8) is based on a photodissociation rate constant of 10^{-6} s^{-1} for molecular oxygen (B&K, 1973); this term is clearly negligible. Also, term (7) may be neglected compared with term (6).

For the neutral gas, gravity plays the prominent role in developing anisotropies in the motions, much as the magnetic field did for the charged particles, but in a qualitatively different way. Gravity clearly separates the vertical and horizontal directions for different treatment. Maximum observed vertical neutral velocities are on the order of tens of meters per second (Rees, 1969; Rieger, 1974), while horizontal velocities in excess of 1 km s^{-1} have been observed (Wu, et al., 1974). In addition, vertical scale lengths are of the order of tens of kilometers, while horizontal scales are at least an order of magnitude larger. When these considerations are taken into account, the vertical component equation reduces to terms (3), (4), and (6), with all terms except (4) contributing to the horizontal component equations. It may appear that term (5), the coriolis term, should be dropped. However, this is the only term which explicitly couples the different directions, resulting in a rotation of the wind direction. For sufficiently long-lived winds this effect is significant; hence it is retained in the neutral equation of motion. The final vector equation of motion for the neutral gas is then

Table 4-4. ORDER-OF-MAGNITUDE ESTIMATES OF EXTREME VALUES FOR TERMS IN THE NEUTRAL MOMENTUM EQUATION

TERM NUMBER	RANGE OF VALUES ($cm\ s^{-2}$)
(1)	$10^{-2} \lesssim \left\lvert \frac{\partial \vec{v}_n}{\partial t} \right\rvert \lesssim 10^{3}$
(2)	$10^{-6} \lesssim \lvert (\vec{v}_n \cdot \nabla)\vec{v}_n \rvert \lesssim 10^{3}$
(3)	$10^{-1} \lesssim \left\lvert \frac{1}{N_n \bar{m}_n} \nabla p_n \right\rvert \lesssim 10^{3}$
(4)	$\lvert \vec{g} \rvert \approx 10^{3}$
(5)	$10^{-2} \lesssim \lvert 2\vec{v}_n \times \vec{\Omega}_E \rvert \lesssim 10$
(6)	$0 \lesssim \left\lvert \frac{N_e}{N_n} \bar{\nu}_{in} (\vec{v}_n - \vec{v}_i) \right\rvert \lesssim 10^{4}$
(7)	$0 \lesssim \left\lvert \frac{N_e}{N_n} \frac{m_e}{\bar{m}_n} \bar{\nu}_{en} (\vec{v}_n - \vec{v}_e) \right\rvert \lesssim 1$
(8)	$0 \lesssim \left\lvert \vec{v} \left(\frac{P_n - L_n}{N_n} \right) \right\rvert \lesssim 10^{-1}$

$$\frac{\partial \vec{v}_n}{\partial t} + (\vec{v}_n \cdot \nabla)\vec{v}_n + \frac{1}{\rho_n}\nabla p_n + \frac{1}{\rho_n}\nabla \cdot \sum_n \bar{\bar{\tau}}_n - \vec{g} - 2(\vec{v}_n \times \vec{\Omega}_E)$$
$$= \frac{N_e \bar{m}_i}{N_n \bar{m}_n} \bar{\nu}_{in}(\vec{v}_n - \vec{v}_i) \quad . \tag{4-42}$$

This completes reduction of the momentum equations to forms appropriate to ionospheric conditions.

4.2.3 Energy Equations

The procedure for examining the energy equations is quite similar to that for the momentum equations, which is by now familiar. Only the heat flux vector has not been encountered in the previous equations. This was defined in equation (2-30) as

$$\vec{q} \equiv \frac{1}{2} n\, m\langle c^2 \vec{c}\rangle$$

where c is the random (thermal) velocity. Chapman and Cowling (1970, Section 7.4), in a rigorous derivation, show that the heat flux vector can be written in the form (second approximation)

$$\vec{q} = - K^T \nabla T \quad , \tag{4-43}$$

where K^T is the thermal conductivity coefficient (sometimes designated by λ).

With this result the electron energy equation may be written from equations (4-15), (4-18), (4-32), and (4-34f) as

$$\frac{3}{2} k \frac{\partial T_e}{\partial t} + \frac{3}{2} k \vec{v}_e \cdot \nabla T_e - \frac{1}{N_e}\nabla\cdot(K^T \nabla T) + \frac{1}{N_e}(\nabla p_e)\cdot \nabla \vec{v}_e$$
$$= m_e(\bar{\nu}_{ei} v_{ei}^2 + \bar{\nu}_{en} v_{en}^2) - k(T_e - T_i)\left[3\bar{\nu}_{ei} + v_{ei}\sum_i \frac{\partial \nu_{ei}}{\partial v_{ei}}\right]$$
$$- k(T_e - T_n)\left[3\bar{\nu}_{en} + v_{en}\sum_n\left(\frac{\partial \nu_{en}}{\partial v_{en}}\right)\right] + \frac{(P_e - L_e)}{N_e}\left[\frac{1}{2} m_e v_e^2 - \frac{3}{2} k T_e\right] \quad . \tag{4-44}$$

Some of these terms can be ignored forthwith by considering the relative magnitudes of flow and thermal energies. Maximum flow velocities are of the order of 10^5 cm s^{-1} while electron thermal velocities are of the order of 10^7 cm s^{-1}. Since energy varies as the square of the velocity, the ratio of flow to thermal energy is of order 10^{-4}; therefore, for electrons, flow energy can be neglected in comparison with thermal energy. Thus, all terms containing v_e^2 or v_{es}^2 can be dropped from the right side of equation (4-44). This is why Joule heating (conversion of bulk motion to random (thermal)) motion is negligible for electrons.

In the notation of Section III and the Appendix, the small ratio of flow to thermal energy corresponds to the condition $Kv_o^2 << 1$. From equations in subsection A.1 of the Appendix, in this limit the ratio of terms in brackets on the right side of equation (4-44) is given approximately by

$$\left(v_o \frac{\partial \nu}{\partial v_o}\right) 3\nu \simeq -\frac{2}{3} K v_o^2 \left[1 - \frac{K}{5} \frac{\int Q(g)\, g^7 \exp(-Kg^2)\, dg}{\int Q(g)\, g^5 \exp(-Kg^2)\, dg}\right]. \qquad (4\text{-}45)$$

If the momentum transfer cross section, Q(g), is assumed to vary as an integer power law n, within the range covered in the Appendix, then the ratio of integrals is given by

$$\frac{\int Q(g)\, g^7 \exp(-Kg^2)\, dg}{\int Q(g)\, g^5 \exp(-Kg^2)\, dg} = \begin{cases} \dfrac{r+1}{K} & n = \text{even}, \quad r = 0, 1, \ldots, 4 \\ \dfrac{2r+1}{2K} & n = \text{odd}, \quad r = 1, \ldots, 4 \end{cases} \qquad (4\text{-}46)$$

(Gradshteyn, I. S. and Ryzhik, I. M., 1965, Integrals 3.461-2,3). The bracketed factor in equation (4-45) is then of order unity or less so that

$$\left| v_o \left(\frac{\partial \nu}{\partial v_o}\right) \frac{1}{3\nu} \right| << 1 \quad . \qquad (4\text{-}47)$$

Terms containing the partial derivatives of collision frequencies may therefore be dropped from the right side of equation (4-44).

With these reductions, the remaining terms of the electron energy equation are

$$\frac{3}{2} k \frac{\partial T_e}{\partial t} + \frac{3}{2} k \vec{v}_e \cdot \nabla T_e - \frac{1}{N_e} \nabla \cdot (K_e^T \nabla T_e) + k T_e \nabla \cdot \vec{v}_e$$

$$= - 3k(T_e - T_i)\bar{\nu}_{ei} - 3k(T_e - T_n)\bar{\nu}_{en} - \frac{(P_e - L_e)}{N_e} \frac{3}{2} kT_e \ . \qquad (4\text{-}48)$$

Order-of-magnitude estimates of terms in this equation are presented in Table 4-5. The estimate for term (3) is based on a mean-free-path expression obtained by Mitchner and Kruger (1973, Section II-12):

$$K_e^T \simeq N_e \, k \, \bar{c}_e \, \ell_e^m \ . \qquad (4\text{-}49)$$

Term (7) is a consequence of the formalism, predicated on electrons being created with zero energy, thus requiring an average energy of 3/2 kT_e from the electron gas. For now, this term will be retained; the actual physical situation will be discussed later in this section. For the other terms, it appears that terms (2) and (4) are negligible compared with the others, leaving

$$\frac{3}{2} k \frac{\partial T_e}{\partial t} - \frac{1}{N_e} \nabla \cdot (K_e^T \nabla T_e) = - 3k(T_e - T_i)\bar{\nu}_{ei}$$

$$- 3k(T_e - T_n)\bar{\nu}_{en} - \frac{(P_e - L_e)}{N_e} \frac{3}{2} k T_e \ . \qquad (4\text{-}50)$$

The ion energy equation does not have the same simplifications because flow energies are comparable to thermal energies, when flow velocities approach 1 km s^{-1}. Consequently, neither the flow energy terms nor the derivatives of the collision frequencies can be neglected outright. From equations (4-16), (4-18), (4-19), (4-32), and (4-43) the ion energy equation can be written

$$\frac{3}{2} k \frac{\partial T_i}{\partial t} + \frac{3}{2} k \vec{v}_i \cdot \nabla T_i - \frac{1}{N_e} \nabla \cdot \sum_i K_i^T \nabla T_i + kT_i \nabla \cdot \vec{v}_i$$

$$+ \frac{1}{N_e} \sum_i \overline{\overline{\tau}}_i : \nabla \vec{v}_i = m_e^2 \, v_{ei}^2 \sum_i \frac{\nu_{ei}}{m_i} - m_e \, k(T_i - T_e) \sum_i \left[3 \frac{\nu_{ei}}{m_i} \right.$$

$$\left. + \frac{\nu_{ei}}{m_i} \frac{\partial \nu_{ei}}{\partial \nu_{ei}} \right] + \frac{\nu_{in}^2}{N_e} \sum_{i,n} n_i \frac{\mu_{in}^2}{m_i} \nu_{in}$$

$$- \frac{k(T_i - T_n)}{N_e} \sum_{i,n} \frac{n_i \, \mu_{in}}{(m_i + m_n)} \left[3\nu_{in} + \nu_{in} \frac{\partial \nu_{in}}{\partial \nu_{in}} \right]$$

Table 4-5. ORDER-OF-MAGNITUDE ESTIMATES OF EXTREME VALUES FOR TERMS IN THE ELECTRON ENERGY EQUATION

TERM NUMBER	RANGE OF VALUES ($eV\ s^{-1}$)
(1)	$10^{-5} \lesssim \left\lvert \frac{3}{2} k \frac{\partial T_e}{\partial t} \right\rvert \lesssim 10^{-1}$
(2)	$10^{-8} \lesssim \left\lvert \frac{3}{2} k \vec{v}_e \cdot \nabla T_e \right\rvert \lesssim 10^{-3}$
(3)	$10^{-10} \lesssim \left\lvert \frac{1}{N_e} \nabla \cdot (K_e^{\ T} \nabla T_e) \right\rvert \lesssim 1$
(4)	$10^{-8} \lesssim \lvert k T_e \nabla \cdot \vec{v}_e \rvert \lesssim 10^{-3}$
(5)	$0 \lesssim \lvert 3k(T_e - T_i)\bar{\nu}_{ei} \rvert \lesssim 10^{3}$
(6)	$0 \lesssim \lvert 3k(T_e - T_n)\bar{\nu}_{en} \rvert \lesssim 10$
(7)	$0 \lesssim \left\lvert \frac{3}{2} k T_e \left(\frac{P_e - L_e}{N_e} \right) \right\rvert \lesssim 10^{-1}$

$$+\left(\frac{1}{2}\bar{m}_i v_i^2 - \frac{3}{2} k T_i\right) \frac{(P_e - L_e)}{N_e} \quad . \tag{4-51}$$

As with the ion momentum equation the scalar pressure is taken to represent the entire pressure tensor in order-of-magnitude estimates. These estimates are presented in Table 4-6.

Only one term appears to be negligible under all likely conditions, term (5). Term (7), the generalized Joule heating term, has potentially the largest magnitude, depending on the magnitude of the ion-neutral relative flow velocity. Because the relative flow velocity is negligible in many problems, it cannot be used alone as a basis for discarding other terms. Term (9) will be discussed later with the corresponding electron term. There appears to be no simple means of estimating the magnitude of the collision frequency derivatives short of a detailed numerical calculation. These terms will therefore be retained until there is sufficient reason to drop them. The reduced ion energy equation is then

$$\frac{3}{2} k \frac{\partial T_i}{\partial t} + \frac{3}{2} k \vec{v}_i \cdot \nabla T_i - \frac{1}{N_e} \nabla \cdot \sum_i K_i^T + \nabla T_i + \frac{P_i}{N_e} \nabla \cdot \vec{v}_i + \frac{1}{N_e} \sum_i \bar{\bar{\tau}}_i : \nabla \vec{v}_i$$

$$= \frac{v_{in}^2}{N_e} \sum_{i,n} n_i \frac{\mu_{in}^2}{m_i} \nu_{in} - \frac{k(T_i - T_n)}{N_e} \sum_{i,n} \frac{n_i \mu_{in}}{(m_i + m_n)} \left[3\nu_{in} + v_{in} \frac{\partial \nu_{in}}{\partial v_{in}}\right]$$

$$- m_e k(T_i - T_e) \sum_i \left[3 \frac{\nu_{ei}}{m_i} + \frac{v_{ei}}{m_i} \frac{\partial \nu_{ei}}{\partial v_{ei}}\right]$$

$$+\left(\frac{1}{2}\bar{m}_i v_i^2 - \frac{3}{2} k T_i\right)\frac{(P_e - L_e)}{N_e} \quad . \tag{4-52}$$

The primary differences between the electron and ion energy equations were due to the disparity in masses. From that standpoint the neutral energy equation is similar to the ion equation. Here the main differences are due to the disparity in number densities. From equations (4-17), (4-18), (4-32), and (4-43), the neutral energy equation can be written as

Table 4-6. ORDER-OF-MAGNITUDE ESTIMATES OF EXTREME VALUES FOR TERMS IN THE ION ENERGY EQUATION

TERM NUMBER	RANGE OF VALUES ($eV\ s^{-1}$)
(1)	$10^{-5} \lesssim \left\lvert \frac{3}{2} k \frac{\partial T_i}{\partial t} \right\rvert \lesssim 10^{-1}$
(2)	$10^{-8} \lesssim \left\lvert \frac{3}{2} k \vec{v}_i \cdot \nabla T_i \right\rvert \lesssim 10^{-3}$
(3)	$10^{-13} \lesssim \left\lvert \frac{1}{N_e} \nabla \cdot (K_i^T \nabla T_i \right\rvert \lesssim 10^{-2}$
(4)	$10^{-8} \lesssim \left\lvert \frac{p_i}{N_e} \nabla \cdot \vec{v}_i \right\rvert \lesssim 10^{-3}$
(5)	$0 \lesssim \left\lvert \frac{m_e^2}{m_i} v_{ei}^2 \nu_{ei} \right\rvert \lesssim 10^{-6}$
(6)	$0 \lesssim \left\lvert \frac{m_e}{m_i} 3k(T_i - T_e)\nu_{ei} \right\rvert \lesssim 10^{-2}$
(7)	$0 \lesssim \left\lvert \frac{\mu_{in}^2}{m_i} v_{in}^2 \nu_{in} \right\rvert \lesssim 10^{3}$
(8)	$0 \lesssim \left\lvert \frac{\mu_{in}}{m_i + m_n} 3k(T_i - T_n)\nu_{in} \right\rvert \lesssim 10^{-1}$
(9)	$0 \lesssim \left\lvert \left(\frac{1}{2} m_i v_i^2 - \frac{3}{2} kT_i\right)\left(\frac{P_e - L_e}{N_e}\right) \right\rvert \lesssim 10^{-1}$

$$\frac{3}{2} k \frac{\partial T_n}{\partial t} + \frac{3}{2} k \vec{v}_n \cdot \nabla T_n - \frac{1}{N_n} \nabla \cdot \sum_n (K_n^T \nabla T_n) + k T_n \nabla \cdot \vec{v}_n$$
$$+ \frac{1}{N_n} \sum_n \overline{\overline{\tau}}_n : \nabla \vec{v}_n = \frac{N_e}{N_n} m_e^2 \nu_{en}^2 \sum_n \frac{\nu_{en}}{m_n} - \frac{N_e}{N_n} m_e k(T_e - T_n) \sum_n$$
$$+ \frac{\nu_{in}^2}{N_n} \sum_{i,n} n_i \frac{\mu_{in}^2}{m_n} \nu_{in} - \frac{k(T_n - T_i)}{N_n} \sum_{i,n} \frac{n_i \mu_{in}}{m_i + m_n} \left[3\nu_{in} + \nu_{in} \frac{\partial \nu_{in}}{\partial \nu_{in}} \right]$$
$$+ \left[\frac{1}{2} m_n v_n^2 - \frac{3}{2} k T_n \right] \left(\frac{P_n - L_n}{N_n} \right) \quad . \tag{4-53}$$

Order-of-magnitude estimates for terms in this equation are given in Table 4-7.

From these values it appears that collisions with charged particles play a very small role in neutral particle energetics, with the exception of the Joule heating term (7). Terms (5), (6), (8), and (9) are negligible, leaving the following equation:

$$\frac{3}{2} k \frac{\partial T_n}{\partial t} + \frac{3}{2} k \vec{v}_n \cdot \nabla T_n - \frac{1}{N_n} \nabla \cdot (K_n^T \nabla T_n) + k T_n \nabla \cdot \vec{v}_n$$
$$+ \frac{1}{N_n} \sum_n \overline{\overline{\tau}}_n : \nabla \vec{v}_n = \frac{\nu_{in}^2}{N_n} \sum_{i,n} n_i \frac{\mu_{in}^2}{m_n} \nu_{in} \quad . \tag{4-54}$$

Actually this equation is far from complete due to limitations of the formalism, specifically, omissions of inelastic collisions and interactions with the radiation field. These subjects are discussed in a limited way in the next subsection.

4.3 INELASTIC PROCESSES IN THE IONOSPHERE

At various points throughout preceding discussions allusions have been made to factors which, by assumption, have been excluded from the system under consideration. These include inelastic collisions, interactions with the (solar) radiation field and elastic collisions with high energy, nonthermal (non-Maxwellian velocity distribution) particles. Formal inclusion of these effects has been accomplished by S. T. Wu (1969, 1970) using the Chapman-Enskog method of successive approximation. The resulting increase in formal

Table 4-7. ORDER-OF-MAGNITUDE ESTIMATES OF EXTREME VALUES FOR TERMS IN THE NEUTRAL ENERGY EQUATION

TERM NUMBER	RANGE OF VALUES ($eV\ s^{-1}$)
(1)	$10^{-5} \lesssim \left\lvert \frac{3}{2} k \frac{\partial T_n}{\partial t} \right\rvert \lesssim 10^{-1}$
(2)	$10^{-8} \lesssim \left\lvert \frac{3}{2} k \vec{v}_n \cdot \nabla T_n \right\rvert \lesssim 10^{-3}$
(3)	$10^{-5} \lesssim \left\lvert \frac{1}{N_n} \nabla \cdot (K_n{}^T \nabla T_n \right\rvert \lesssim 10^{-1}$
(4)	$10^{-8} \lesssim \lvert k T_n \nabla \cdot \vec{v}_n \rvert \lesssim 10^{-3}$
(5)	$0 \lesssim \left\lvert \frac{N_e}{N_n} \frac{m_e^2}{m_i} v_{en}^2 \nu_{en} \right\rvert \lesssim 10^{-11}$
(6)	$0 \lesssim \left\lvert \frac{N_e}{N_n} \frac{m_e}{m_n} 3k(T_e - T_n)\nu_{en} \right\rvert \lesssim 10^{-7}$
(7)	$0 \lesssim \left\lvert \frac{N_e}{N_n} \frac{\mu_{in}^2}{m_n} v_{in}^2 \nu_{in} \right\rvert \lesssim 10^{-3}$
(8)	$0 \lesssim \left\lvert \frac{N_e}{N_n} k(T_n - T_i)\nu_{in} \right\rvert \lesssim 10^{-6}$
(9)	$0 \lesssim \left\lvert \left(\frac{1}{2} \bar{m}_n v_n^2 - \frac{3}{2} k T_n\right)\left(\frac{P_n - L_n}{N_n}\right) \right\rvert \lesssim 10^{-7}$

complexity makes use of this approach somewhat formidable for numerical calculations. For applications which exercise the full extent of the formal framework, this added complexity may be no more than is required for a complete treatment in a less rigorous and consistent manner. But for the ionosphere, a simpler approach appears more efficient. Furthermore, the method formulated by S. T. Wu (1969, 1970) is based on expansions of species temperatures and flow velocities in a center-of-mass system for the gas as a whole. It has been noted previously that such an approach is less useful for the ionosphere than explicit use of distinct equations for various gases, due to the relatively loose coupling observed among them. Because large differences in temperature and flow velocities can occur among ionospheric electrons, ions and neutrals, it is not clear that the expansions used by S. T. Wu (1969, 1970) (to first order) would converge, so that truncation with the linear terms could yield inaccurate results. For these reasons the approach adopted for this study has been to formulate a complete, consistent treatment based on elastic interactions, with nonelastic effects included phenomenologically when and where they are required.

A thorough examination of these topics exceeds the scope of this investigation; such a treatment is given in the recent two-volume work by Banks and Kockarts (1973). The purpose here is to discuss briefly those physical processes which may affect the conservation equations. In a few limited instances, explicit expressions are provided to allow these processes to be taken into account directly in the conservation equations. Generally, however, the treatment must be limited to qualitative discussion, because no convenient closed form expressions of direct applicability are available. In these cases recent reviews or model calculations are cited, where information required for numerical calculations can be obtained. As in previous discussions of the conservation equations, the continuity, momentum and energy equations are discussed in turn.

Because the source/loss terms of the continuity equation were introduced into the momentum and energy equations in the process of eliminating time derivatives of number densities in those equations, it was expedient to

examine those terms preceding the order-of-magnitude estimates of the previous section. For present purposes, nothing need be added to that discussion of the processes whereby particles are added or lost to the various gases. However, the concomitant effects on the momentum and energy equations require elaboration. First, momentum transferred from solar radiation to upper atmospheric gases is negligible. Since photoelectrons tend to be emitted in the direction of polarization of the photon (Heitler, 1954), and since solar radiation incident on the upper atmosphere is predominantly unpolarized, there is azimuthal symmetry in the emission of photoelectrons about the direction of the solar radiation. The result is that on the average essentially no net momentum is added to any of the gases as a result of photoionization. So newly formed ions on the average should have the average neutral velocity, resulting in an effective transfer of momentum from the neutral to the ion gas. Isotropy in the recombination process results in the reverse effect. In general, net production or loss involves only a small portion of the ion population, particularly at altitudes where ion and neutral flow velocity differences are largest. Even though the reasoning here differs from that used in the previous analysis of this term, order-of-magnitude estimates are the same in both cases. So the previous results, that the source/loss terms of the continuity equation have negligible effects in all the momentum equations, remain unchanged.

Different considerations apply to the energy equations. In photoionization, since momentum must be conserved, the mass disparity between the newly formed electron and ion causes the photoelectron to carry away all but about one part in 10^4 of the photon energy exceeding the ionization potential. The energy left to the ion ($\sim 10^{-3}$eV) is small relative to thermal energies and, from the discussion of momentum, randomly directed. Newly formed ions therefore have a temperature which may be expressed as $T_n + \Delta T$, where, $\Delta T << T_n$. In the ion energy equation (4-52), the last terms reflect the effects of deviations of the average properties of added and lost ions from the average ion gas properties. For the lost ions, data on the energy dependence of rate coefficients for loss processes presented by Ferguson (1974) in a recent

review indicate that such deviations are small. The last term in equation (4-52) should therefore be replaced with

$$Q_p = \frac{P_e}{N_e} \frac{3}{2} k(T_n + \Delta T - T_i) \quad . \tag{4-55}$$

For altitudes below about 300 km, $T_n \simeq T_i$, so that the temperature factor is small where the source factor P_e is maximal; above 300 km where temperature differences become large, P_e/N_e is quite small. In terms of previous order-of-magnitude estimates, however, this term cannot be dropped as negligible under all conditions. It should be noted that equation (4-55) applies only to photoionization. For collisional ionization, as in auroral activity, a thorough reformulation would be required.

For the electron energy equation a different physical situation prevails. Photoelectrons are generally created with several tens of electron volts of energy, which places them outside the energy range of particles considered part of the system, as discussed previously. The energy they provide to the thermal gases is treated as if it were due to an external heat source. Thus, photoelectrons are placed in the incongruous roles of being counted as new particles in the system in the continuity equation, but being considered as an external heat source in the energy equation. These roles are somewhat reconciled by the fact that at sufficiently low altitudes thermalization of the photoelectron takes place rapidly; that is, through inelastic collisions with neutral particles and finally through elastic collisions with thermal electrons the photoelectrons energy is quickly reduced to less than a few electron volts. When the delay between creation and thermalization is short, few problems of consistency arise in the time evolutions of the conservation equations over the time scales of interest.

More serious is the distance the photoelectron travels before it is thermalized. Photoelectrons created above ~300 km and moving upward approximately parallel to the geomagnetic field may suffer no collisions to inhibit their motion until they traverse the entire field line to the conjugate ionosphere. Charge neutrality assures that the local rate of photoionization

remains the local rate of electron production, because newly created ions will not travel far. However, photoelectron energy may be deposited nonlocally. In a recent review, Cicrone (1974) has concluded that photoelectron transport and energy loss within the ionosphere (local effects) are well understood; however, understanding of nonlocal effects due to photoelectron transport between conjugate ionospheres along geomagnetic field lines remains rudimentary. For detailed discussions of photoelectron properties with effects on ionospheric gases, and for problems requiring source functions due to photoionization, the review by Cicerone (1974) and references therein can be consulted. Such source functions should replace the final term in equation (4-50) which does not adequately represent the physical situation.

In previous discussion of the neutral continuity equation it was noted that photodissociation is the primary source term. When order-of-magnitude estimates were made for this process, effects in the energy equation were found to be negligible. However, once again this estimate failed to consider nonelastic effects, in particular excess energy of the photon beyond that required for dissociation. This contribution will be compared with those of other nonelastic processes below; here it is sufficient to note that although the final term in equation (4-53) is dropped, the physical process behind it, photodissociation, does make a contribution in another form.

The conclusion to be drawn from these discussions is that in the ionosphere, the source/loss terms of the continuity equation do not contribute significantly to the momentum equation. They do have significant effects in the energy equation, although not in the form suggested by the formalism. This is due to the neglect of inelastic processes in the formalism, and these processes are the basis for effects in the energy equation.

To this point, discussion has been centered on particle sources and losses and the associated effects on momentum and energy equations. Sources and sinks of momentum and energy themselves must now be considered. Source/loss terms for the momentum equations are already included in the form of the external force terms; these require no further discussion. However, in the

energy equations, as in the continuity equations, major source/loss mechanisms are not included within the elastic-collision formalism developed above. These involve energy transfer through inelastic collisions and radiative sources and sinks of energy. The former is important primarily for electrons and neutrals, the latter for neutrals alone. This separation of effects can be understood from the properties of the gases in the upper atmosphere.

The importance of inelastic collisions for electron energy transfer is another consequence of the disparity between electron and heavy-particle masses. Equation (3-48) shows that energy transferred per elastic collision between ions and neutral particles is equivalent to the difference in mean particle energies, while for electrons and neutrals it is this energy difference reduced by a factor of (m_e/m_n). Consequently the elastic collision is an efficient means for the transfer of energy from ions to neutrals, but rather inefficient for electrons to neutrals. In this context the relative magnitudes of elastic and inelastic cross sections must be considered. Elastic cross sections are of the order 10^{-15}-10^{-16} cm^2 while inelastic cross sections are generally of the order 10^{-17}-10^{-18} cm^2 or smaller at energies of an electron volt or less. Since the most efficient inelastic collisions for energy transfer will be those with transition energies near the kinetic energies of the colliding particles, the relative magnitudes of these cross-sections indicate that energy transfer for ions through inelastic collisions is negligible compared with elastic collisions. However, for electrons the smaller inelastic cross section is more than compensated by increased energy transfer per inelastic collision, making this the predominant means of electron energy transfer, up to heights where electron-neutral collisions become less important than electron-ion collisions.

The importance of a given inelastic process for electrons depends on the transition energy for the process and the electron energy distribution. Conservation of energy requires that the kinetic energy of the collision partners equal or exceed the transition energy in order for the cross section to be nonzero. Thus, the significant transitions are those with energies of the order of or less than the mean thermal electron energies -- a few tenths of an

electron volt. For the primary neutral species of the upper atmosphere, rotational and vibrational excitation of N_2 and O_2 and excitation of the fine structure levels of the ground state of atomic oxygen meet this criterion. For unusually high electron temperatures ($T_e \gtrsim 4500°K$), excitation of electronic states of atomic and molecular oxygen becomes significant. These and other inelastic collisions have been reviewed by Dalgarno (1969). The application of these processes to electron energetics has been examined by a number of investigators, notably Dalgarno, et al. (1968). To facilitate computer calculations, these investigators have developed analytic expressions for electron energy transfer rates due to inelastic collisions; these will be extracted from the literature and presented here without detailed discussion of their derivation.

For energy transfer due to electron collisional excitation of the rotational levels of N_2, the expression given by Dalgarno (1969) is

$$N_2(\text{ROT}): \quad Q_L = - N_e \, n_{N_2} \times (2.9 \times 10^{-14})(T_e - T_n)/T_e^{1/2} \text{ eV cm}^{-3} \text{ s}^{-1} \tag{4-56}$$

where n_{N_2} is the number density of N_2. The corresponding energy transfer rate for O_2, also given by Dalgarno (1969), is

$$O_2(\text{ROT}): \quad Q_L = - N_e \, n_{O_2} (6.9 \times 10^{-14})(T_e - T_n)/T_e^{1/2} \text{ eV cm}^{-3} \text{ s}^{-1} . \tag{4-57}$$

The energy transfer rate due to electron excitation of the vibrational states of N_2, as presented by Stubbe and Varnum (1972), is

$$N_2(\text{VIB}): \quad Q_L = - N_e \, n_{N_2} \times (2.99 \times 10^{-12}) \exp\left[f\left(\frac{T_e - 2000}{2000 \, T_e} \right) \right] \times \left\{ 1 - \exp\left[- g \left(\frac{T_e - T_n}{T_e \, T_n} \right) \right] \right\} \text{eV cm}^{-3} \text{ s}^{-1} , \tag{4-58}$$

where

$$f = 1.06 \times 10^4 + 7.51 \times 10^3 \tanh[1.10 \times 10^{-3}(T_e - 1800)]$$

and

$$g = 3300 + 1.233(T_e - 1000) - 2.056 \times 10^{-4}(T_e - 1000)(T_e - 4000) \quad .$$

The corresponding expression for O_2, given by Prasad and Furman (1973), is

$$O_2(\text{VIB}): \quad Q_L = - N_e \, n_{O_2} \times (5.196 \times 10^{-13}) \exp\left[f\left(\frac{T_e - 700}{700 \, T_e}\right)\right] \times \left\{1 - \exp\left[- 2770 \left(\frac{T_e - T_n}{T_e \, T_n}\right)\right]\right\} \text{eV cm}^{-3} \text{ s}^{-1} \qquad (4\text{-}59)$$

where

$$f = 3300 - 839 \sin[1.91 \times 10^{-4}(T_e - 2700)] \quad .$$

Electronic excitation of atomic oxygen ($O(^3P) \rightarrow O(^1D)$: transition energy = 1.97 eV) becomes significant for high electron temperatures such as are found in aurora and stable mid-latitude red arcs (SAR-arc). An expression for energy transferred by electrons to O by this method, also provided by Stubbe and Varnum (1972), is

$$O(^1D): \quad Q_L = - N_e \, n_O \times (1.57 \times 10^{-12}) \exp\left[f\left(\frac{T_e - 3000}{3000 \, T_e}\right)\right] \times \left\{1 - \exp\left[- 22713 \left(\frac{T_e - T_n}{T_e \, T_n}\right)\right]\right\} \text{eV cm}^{-3} \text{ s}^{-1} \qquad (4\text{-}60$$

where

$$f = 2.4 \times 10^4 + .3(T_e - 1500) - 1.947 \times 10^{-5}(T_e - 1500)(T_e - 4000) \quad .$$

Excitation of electronic states of molecular oxygen is less likely to be significant because at altitudes where molecular oxygen is more important, electron temperatures are not likely to be high. However, conditions for

these processes to be significant might be found in aurora. Therefore, the following expressions obtained by Prasad and Furman (1973) are presented:

$$(O_2(^3\Sigma_g^-) \rightarrow O_2(^1\Delta_g): \quad \text{transitional energy} = .98 \text{ eV})$$

$$O_2(^1\Delta_g): \quad Q_L = -N_e\, n_{O_2} \times (1.143 \times 10^{-14}) \exp\left[f\left(\frac{T_e - 1500}{1500\, T_e}\right)\right] \times \left\{1 - \exp\left[-11400\left(\frac{T_e - T_n}{T_e\, T_n}\right)\right]\right\} \tag{4-61}$$

where

$$f = \left\{13200 + 1410 \sin[2.41 \times 10^{-4}(T_e - 500)]\right\} \times \left\{1 + \exp[(T_e - 14011)/1048]\right\};$$

$$(O_2(^3\Sigma_g^-) \rightarrow O_2(^1\Sigma_g^+): \quad \text{transitional energy} = 1.64 \text{ eV})$$

$$O_2(^1\Sigma_g): \quad Q_L = -N_e\, n_{O_2} \times (1.616 \times 10^{-16}) \exp\left[g\left(\frac{T_e - 1500}{1500\, T_e}\right)\right] \times \left\{1 - \exp\left[11400\left(\frac{T_e - T_n}{T_e\, T_n}\right)\right]\right\} \tag{4-62}$$

where

$$g = \left\{19225 + 560 \sin[3.83 \times 10^{-4}(T_e - 1000]\right\} \times \left\{1 + \exp[(T_e - 16382)/1760]\right\} .$$

Fine structure excitation of ground state atomic oxygen requires a more extended discussion (1) because its cross section is of the order of the elastic cross section, (2) because it is thought to be the dominant mechanism whereby electrons lose energy to neutrals, and (3) because the cross sections have recently been recalculated, casting some doubt on the previous assertion. Atomic oxygen has a ^1P_J ground state with nondegenerate total angular momentum states, the J = 0 and J = 1 states lying .028 eV and .02 eV above the J = 2

ground state respectively. Dalgarno and Degges (1968) first suggested that this mechanism might be an efficient means of cooling ionospheric electrons. They presented electron cooling rates based on collision strengths computed by Breig and Lin (1966). The importance of this mechanism for electron energetics was confirmed by Dalgarno, et al. (1968). New calculations of cross sections for this process were reported at a recent American Physical Society meeting by Tambe and Henry (1973). Cooling rates calculated from these new cross sections are about a factor of three smaller than for the previous ones (G. A. Victor, 1974). Since these recent developments have not yet appeared in the open literature, their implications for electron energetics are not yet clear. However, it appears that some caution is in order in making and interpreting calculations involving the electron energy equation.

In the absence of an available electron cooling rate expression based on the new atomic oxygen fine structure excitation cross sections, that based on the previous cross sections is provided, recognizing that it is likely to be superseded in the near future. A detailed derivation of the cooling rate due to fine structure (FS) excitation of atomic oxygen, demonstrating the book-keeping required for a multi-state system, is presented by Comfort (1970). That expression, determined from the collision strengths of Breig and Lin (1966), is

$$
\begin{aligned}
\text{O(FS):}\quad Q_L = - & \frac{N_e\, n_o\, (6.217 \times 10^{-13}) T_e 1/2}{5 + 3\exp(-.02/k\,T_n) + \exp(-.028/k\,T_n)} \\
& \times \Big\{ 6[\exp(-.02/k\,T_e) - \exp(-.02/k\,T_n)] \\
& \times [1.323 - 1.028/f^2] + 2.8[\exp(-.028/k\,T_e) \\
& - \exp(-.028/k\,T_n)]\,[.9911 - .9555/f^2] + .8\exp(-.02/k\,T_n) \\
& \times [\exp(-.008/k\,T_e) - \exp(-.008/k\,T_n)] \\
& \times [1.505 - 1.510/f^2]\ \text{eV cm}^{-3}\ \text{s}^{-1} \Big\}\,, \qquad (4\text{-}63)
\end{aligned}
$$

where $f = 8k\,T_e + 1$.

As noted above, the cross section for excitation of the fine structure levels of ground state atomic oxygen is of the order of the elastic momentum transfer cross section ($\sim 10^{-16}$ cm^2). The basis for ignoring momentum transfer in inelastic collision was previously stated to be that inelastic cross sections were much smaller than momentum transfer cross sections; the frequency of inelastic collisions would therefore be so much smaller than that of elastic collisions that the total momentum transferred through inelastic collisions would be negligible by comparison. Since for this inelastic process, such reasoning is invalid, Schunk and Walker (1970) have suggested that an effective increase in the momentum transfer collision frequency, due to fine structure excitation of atomic oxygen, could have a significant effect on ionospheric electron transport properties. It would therefore be desirable to take this into account quantitatively. However, Itikawa (1972) has discussed the effect of inelastic processes on the momentum transfer cross section and concluded that the presently available formalism is inadequate to treat this problem. Moreover, given the uncertainties in the fine structure excitation cross sections noted above, it appears unprofitable to attempt a quantitative estimate of such effects at this time. This effect must therefore remain an uncertainty in any calculated results, to be taken into account in their interpretation.

For ions, neither inelastic collisions nor radiative interactions play a significant role in the energy balance. Excitation energies for ions are too high for thermal particles of the upper atmosphere to interact with them inelastically to any significant degree. Similarly, too few ions absorb or emit radiation to affect the energy balance appreciably. Interest in ion excited states is restricted primarily to auroral emissions, as indicators of interactions with nonthermal particles.

Neutral energetics, on the other hand, depend to a high degree on radiative and inelastic processes. Chandra and Sinha (1973) have recently presented model calculations of the neutral thermal energy budget. Results of their calculations for local noon show that below 300 km primary heat sources for neutrals are inelastic collisions with photoelectrons and photo-dissociation by solar ultraviolet radiation. Above 300 km inelastic interactions with the thermal plasma deliver energy comparable to the photoelectron contribution,

while photo-dissociation is a negligible heat source. Energy losses are due primarily to thermal conduction and, to a lesser extent, infrared emissions. Smaller heat sources in the calculation include chemical energy (energy released in dissociative recombination processes) and neutral wind energy (Joule or frictional heating in collisions with ions due to flow velocity differences). At night, of course, heat sources based on solar radiation vanish, resulting in a very different heat budget. Also, since the calculations of Chandra and Sinha (1973) are based on middle latitude conditions, a rather different set of relationships can be expected at auroral latitudes. This simply emphasizes that the importance of a given energy source depends on the conditions associated with each problem. Each problem, therefore, requires a detailed review of energy sources and sinks in order to include all that are of possible importance without including unnecessary computational burdens. The paper by Chandra and Sinha (1973) and B&K (1973), as well as references therein, may be consulted for quantitative expressions and detailed discussions.

This discussion of inelastic and radiative processes has been necessarily incomplete and, for the most part, qualitative. Its primary purpose has been to note physical considerations of importance which are not contained in the formalism previously developed. In many cases, these involve complicated problems requiring extensive computations in their own right. Since they are generally treated in this manner, it is more practical to incorporate results of such treatment into a calculation phenomenologically than to include everything into the formalism and solve it in one computational effort. This approach is illustrated in the problem treated in Section VI. References cited in the discussion above should provide reasonable resources for obtaining the detailed information required for specific calculations.

4.4 CONSERVATION EQUATIONS APPROPRIATE TO THE IONOSPHERE

The results of this section are summarized in the final conservation equations which have evolved from consideration of the physical conditions in the ionosphere. These equations represent the starting points for the investigation of particular ionospheric problems. For convenient reference they are collected here.

4.4.1 Continuity Equations

$$\text{Plasma:}\quad \frac{\partial N_e}{\partial t} + \nabla \cdot (N_e \vec{v}_e) = P_e - L_e \tag{4-64a}$$

$$\text{Neutral:}\quad \frac{\partial N_n}{\partial t} + \nabla \cdot (N_n \vec{v}_n) = P_n - L_n \tag{4-64b}$$

4.4.2 Momentum Equations

$$\text{Electrons:}\quad \vec{v}_{e\perp} = \frac{\vec{E} \times \vec{B}}{B^2} c \tag{4-65a}$$

$$v_{e\parallel} = \left[\frac{1}{\bar{\nu}_{ei} + \bar{\nu}_{en}}\right]\left[\bar{\nu}_{ei}\, v_{i\parallel} + \bar{\nu}_{en}\, v_{n\parallel} - \omega_e \frac{E_\parallel}{B} c - \frac{1}{N_e m_e} \nabla_\parallel p_e\right] \tag{4-65b}$$

$$\text{Ions:}\quad \vec{v}_i = \vec{v}_n + \frac{1}{\bar{\nu}_{in}}\left[\bar{\omega}_i \frac{\vec{E}}{B} c + \vec{v}_i \times \vec{\omega}_i + \vec{g} - \frac{1}{\rho_i} \nabla p_i - \frac{1}{\rho_i} \nabla \cdot \sum_i \bar{\bar{\tau}}_i\right] \tag{4-65c}$$

$$\text{Neutrals:}\quad \frac{\partial \vec{v}_n}{\partial t} + (\vec{v}_n \cdot \nabla)\vec{v}_n + \frac{1}{\rho_n} \nabla p_n + \frac{1}{\rho_n} \nabla \cdot \sum_n \bar{\bar{\tau}}_n - \vec{g} - 2\vec{v}_n \times \vec{\Omega}_E = -\frac{\rho_i}{\rho_n} \bar{\nu}_{in} (\vec{v}_n - \vec{v}_i) \tag{4-65d}$$

4.4.3 Energy Equations

$$\text{Electrons:}\quad \frac{3}{2} k \frac{\partial T_e}{\partial t} - \frac{1}{N_e} \nabla \cdot (K_e^T \nabla T_e) = -3k(T_e - T_i)\bar{\nu}_{ei} - 3k(T_e - T_n)\bar{\nu}_{en} + \frac{1}{N_e} \sum_{P,L} Q_e \tag{4-66a}$$

$$\text{Ions:}\quad \frac{3}{2}k\frac{\partial T_i}{\partial t} + \frac{3}{2}k\vec{v}_i\cdot\nabla T_i - \frac{1}{N_e}\nabla\cdot\sum_i K_i^T\nabla T_i$$

$$+ kT_i\nabla\cdot\vec{v}_i + \frac{1}{N_e}\sum_i \overline{\overline{\tau}}_i:\nabla\vec{v}_i = \frac{v_{in}^2}{N_e}\sum_{i,n} n_i\frac{\mu_{in}}{m_i}\nu_{in}$$

$$- \frac{k(T_i - T_n)}{N_e}\sum_{i,n}\frac{n_i\mu_{in}}{m_i + m_n}\left[3\nu_{in} + v_{in}\frac{\partial\nu_{in}}{\partial v_{in}}\right]$$

$$- m_e\,k(T_i - T_e)\sum_i\left[3\frac{\nu_{ei}}{m_i} + \frac{v_{ei}}{m_i}\frac{\partial\nu_{ei}}{\partial v_{ei}}\right] \qquad (4\text{-}66b)$$

$$\text{Neutrals:}\quad \frac{3}{2}k\frac{\partial T_n}{\partial t} + \frac{3}{2}k\vec{v}_n\cdot\nabla T_n - \frac{1}{N_n}\nabla\cdot(K_n^T\nabla T_n)$$

$$+ k\,T_n\nabla\cdot\vec{v}_n + \frac{1}{N_n}\sum_n\overline{\overline{\tau}}_n:\nabla\vec{v}_n$$

$$= \frac{v_{in}^2}{N_n}\sum_{i,n} n_i\frac{\mu_{in}^2}{m_n}\nu_{in} + \frac{1}{N_n}\sum_{P,L} Q_n \qquad (4\text{-}66c)$$

In the electron and neutral energy equations, the final terms represent sums over inelastic and/or external energy production (P) and loss (L) processes, as discussed in subsection 4.3 of this section (for example equations (4-55) through (4-63)).

THIS PAGE INTENTIONALLY LEFT BLANK

Section V

TRANSPORT PROPERTIES

5.1 MACROSCOPIC APPROACH TO TRANSPORT PROPERTIES

In the derivation of the conservation equations (Section II), a set of velocity moment equations is generated by multiplying the Boltzmann equation by successively higher powers of velocity (terminated at v^2 here) and integrating over velocity space. An infinite number of moment equations could be generated in this way. However, the second term on the left side of the Boltzmann equation (2-2) contains velocity as a factor, resulting in a velocity moment one order higher than the moment of interest. Effectively, this introduces an additional variable into the system of equations. As a consequence, any finite sequence of velocity moment equations generated from the Boltzmann equation is an indeterminate system of equations. However, if the highest order moment can be related to lower order moments, essentially independently of the system of moment equations, the system can be closed and solved, in principle. This is one of the mathematical motivations for studying transport properties.

Physical motivation stems from the possibility of better understanding the relative importance of different mechanisms which convey particle properties from one location to another. At the elemental level, a particle can be thought of as having certain average properties, characteristic of its location. In the context of a Boltzmann binary collision, a particle moves undisturbed (except for external force fields) from one collision to another; these collisions determine the length of a free path. Thus, the particle carries the average properties characteristic of the beginning of the free path to the other end of the free path. For this reason, Chapman and Cowling (1970) use the term "free path" phenomena as an alternate to "transport" phenomena. Clearly, if average particle properties at both ends of a free path are the same, nothing is changed. So the effects of transport depend on a spatial gradient in the property of interest. With a spatial gradient, the total effect of transport then depends on the length of the free path, which in turn depends on velocities, number densities, and collisional interaction potentials.

Using mean free path arguments of this nature, Chapman and Cowling (1970) derive expressions for diffusion, viscosity, and thermal conductivity coefficients, which relate to gradients in number density, flow velocity, and temperature, respectively. These expressions are useful for physical understanding and order-of-magnitude estimates. However, for rigorous derivations with accurate results, Chapman and Cowling (1970) (and others) use the Boltzmann equation.

For charged particles, the effects of electric and magnetic fields must be considered in addition to spatial gradients. An immediate consequence of an external magnetic field is that it renders the medium anisotropic. This is easily seen in terms of the simple free path arguments. For a strong magnetic field ($\omega_b >> \bar{\nu}$), the effective free path in the transverse direction is no longer determined by collisions, but by the gyroradius. In the parallel direction, of course, collisions are still the limiting factor. Furthermore, the Lorentz force causes the transverse component of external forces to drive particles in a direction transverse to both the driving force and the magnetic field, for example, equation (4-36). The situation is more complicated when the collision frequency and the gyrofrequency are comparable, for example, ions in the E region; both collisions and the magnetic field then affect the transverse free path. The mathematical consequence of these physical effects is that each transport coefficient must be replaced by a three dimensional tensor of rank two.

Shkarofsky (1961) has developed a method for calculating electron transport tensor components, explicitly including the effects of a magnetic field of arbitrary strength and an arbitary degree of ionization. Use of this method in calculating transport tensor components is rather difficult for the general case. However, if electron-neutral collision frequencies vary with velocity according to a power law r, Shkarofsky (1961) presents results with all the integrals evaluated. Although these results still require lengthy calculations, they represent a considerable reduction of effort over the general case.

With this motivation, methods have been developed for determining an effective power law for electron-neutral collision frequencies of arbitary

velocity dependence. This makes complete results of the Shkarofsky formulation immediately accessible. Derivation of this technique is presented first. This is followed by a discussion of specific elastic collision frequencies for upper atmospheric gases. The power law approximation method is applied to the electron-neutral collision frequencies as an example of its use. With these parameters available, expressions for electron transport tensor calculations are extracted from the derivation by Shkarofsky (1961). These are examined briefly for consistency with order-of-magnitude estimates in the previous section. Expressions of more limited applicability are presented for ions with a discussion of the consequences. Finally, available expressions for neutral transport coefficients are presented.

5.2 POWER LAW REPRESENTATION FOR COLLISION FREQUENCIES

As noted previously, calculations of transport coefficients by the method of Shkarofsky (1961) are considerably simplified if the collision frequency varies as a power law in velocity. Recognizing this, Schunk and Walker (1970) presented a technique for determining an approximate power law representation for electron-neutral collision frequencies when the velocity dependencies of the momentum transfer cross sections are expressed as polynomials. An alternate technique has been developed which offers the following advantages over the Schunk and Walker (1970) method. It gives a power law representation for arbitrary velocity dependence; it has a simple extension to multi-species gases; and it is derived straightforwardly without approximation from the defining equation. Most importantly, comparisons of this method and the Schunk and Walker (1970) method with results of exact calculations in a model study for the ionosphere demonstrate this method to be the more accurate (Comfort, 1975).

In the following derivation, it is convenient to adopt the notation of Shkarofsky (1961). This permits an orderly introduction of that notation with relationships to notation used here; in the later presentation of transport tensor components, use of this notation will facilitate reference to the source work.

From equation (A-3) in the Appendix, it is seen that beyond the first term in the expansion of the momentum transfer collision frequency, all terms are of order (Kv_o^2) or higher. For electron-heavy particle collisions $K \simeq m_e/2kT_e$, which is approximately the reciprocal of the electron mean square thermal speed. Since v_o is the magnitude of the relative flow velocity $\left|\vec{v}_e - \vec{v}_j\right|$ $(j = i, n)$, $\sqrt{K}\, v_o$ is the ratio of relative flow velocity to mean thermal velocity, which is of order 10^{-2} or less in the ionosphere. Thus, electron collision frequencies may always be computed in the limit $v_o \to 0$, given by equation (3-36). This is consistent with the expressions of Banks (1966a), Shkarofsky (1961), and Itikawa (1971, 1973).

When the isotropic part of the electron velocity distribution is assumed to be Maxwellian, the total effective electron-neutral collision frequency for momentum transfer is given by Shkarofsky (1961) as

$$\langle \nu_m \rangle = \frac{8}{3\sqrt{\pi}} K^{5/2} \int_0^\infty v^4\, \nu_m(v)\, \exp(-Kv^2)dv, \tag{5-1}$$

where K is as above, v is the total electron velocity (approximately the total relative velocity g of Section III), and $\nu_m(v)$ is the velocity-dependent collision frequency. For a single neutral species, $\nu_m(v)$ is related to the momentum transfer cross section by

$$\nu_m(v) = N_n\, v\, Q_m(v) \quad . \tag{5-2}$$

With this definition, equation (5-1) is seen to be equivalent to equation (3-36); hence $\langle \nu_m \rangle = \nu_{en}$. If $\nu_m(v)$ varies with v as a power law of the form

$$\nu_m(v) = c\, v^r \ , \tag{5-3}$$

where c is proportionality constant and r need not be an integer, the integration in equation (5-1) can be carried out immediately, yielding

$$\langle \nu_m \rangle = c\, K^{-r/2}\, \Gamma\left(\frac{r+5}{2}\right)/\Gamma\left(\frac{5}{2}\right) \quad . \tag{5-4}$$

For ν_m given by equation (5-3), Shkarofsky (1961) gives the following relation (his equation (99)):

$$(W^2\nu_m)_a/(W\nu_m)_a = 1/2\ (r + 5)\ , \tag{5-5}$$

where $W \equiv Kv^2$ and, for arbitrary function ϕ, the average $(\ )_a$ is defined by

$$(\phi)_a \equiv 4\pi \left(\frac{K}{\pi}\right)^{3/2} \int_0^\infty \phi\ \exp(-Kv^2)v^2 dv\ . \tag{5-6}$$

Equation (5-5) can be verified by straightforward integration; however, an alternate method indicates a convenient method for determining the effective power index r. From equations (5-1) and (5-6), the denominator and numerator of the left side of (5-5) are given by

$$(W\nu_m)_a = 3/2\ \ <\nu_m> \tag{5-7}$$

and

$$(W^2\nu_m)_a = \frac{4K}{\sqrt{\pi}}^{7/2} \int_0^\infty \nu_m v^6\ \exp(-Kv^2)dv\ . \tag{5-8}$$

Let I(K) denote the integral in equation (5-1); thus from that equation,

$$I(K) = \frac{3\sqrt{\pi}}{8}\ K^{-5/2}\ <\nu_m>\ . \tag{5-9}$$

Then the integral in equation (5-8) may be written as

$$\int_0^\infty \nu_m\ v^6\ \exp(-Kv^2)dv = -\frac{\partial}{\partial K} I(K) = -\frac{3\sqrt{\pi}}{8}\ \frac{\partial}{\partial K}\ (K^{-5/2}\ \ <\nu_m>), \tag{5-10}$$

in which the order of integration and differentiation has been reversed. Equation (5-8) may therefore be rewritten

$$(W^2\nu_m)_a = -\frac{3}{2}\ K^{7/2}\ \frac{\partial}{\partial K}\ (K^{-5/2}\ <\nu_m>)\ . \tag{5-11}$$

If ν_m varies as a power law in v, as in equation (5-3), equation (5-4) can be used in (5-11) and the differentiation carried out. The result, together with equation (5-7), verifies equation (5-5). It should be emphasized that the steps leading from equation (5-8) to equation (5-11) depend on a Maxwellian velocity distribution for electrons, but place no particular restriction on the velocity dependence of ν_m.

In the following, it is assumed that $\langle\nu_m\rangle$ is a known function of K (that is, T_e), based on a knowledge of ν_m and equation (5-1). Equation (5-5) is now taken to define an effective value of r for those cases in which ν_m does not have the simple form of equation (5-3). Solving equation (5-5) for r yields

$$r = -2\left[\frac{5}{2} - \frac{(W^2\nu_m)_a}{(W\nu_m)_a}\right] . \tag{5-12}$$

Substitution of equations (5-7) and (5-11) into (5-12) and performing part of the differentiation results in

$$r = -\frac{2K}{\langle\nu_m\rangle}\frac{\partial}{\partial K}\langle\nu_m\rangle , \tag{5-13}$$

which provides a convenient means for evaluating r, once $\langle\nu_m\rangle$ is known as a function of T_e. It is noted that result (5-13) follows from the defining equation (5-5) without approximation; and the functional form of $\langle\nu_m\rangle$ is unrestricted.

Although equation (5-13) is sufficiently flexible to treat multi-component gases, a more convenient form for such gas mixtures is easily obtained. Let j designate the j^{th} neutral species. For each neutral species an effective power law index r_j is computed from equation (5-13). The total electron-neutral collision frequency is just the sum of the individual species collision frequencies

$$\langle\nu_m\rangle = \sum_j \langle\nu_j\rangle = \sum_j c_j K^{-r_j/2}\,\Gamma\left(\frac{r_j+5}{2}\right)\Big/\Gamma(5/2) , \tag{5-14}$$

where each $\langle \nu_j \rangle$ is represented by equation (5-4), using the computed value of r_j. When equation (5-14) is used to evaluate the derivative in equation (5-13), the result may be written as

$$r = \frac{1}{\langle \nu_m \rangle} \sum_j r_j \langle \nu_j \rangle \quad . \tag{5-15}$$

This specifies r simply as the mean of the power law indexes weighted by the corresponding species effective collision frequencies.

A brief application of these results to ionospheric collision frequencies is given in the following subsection. Accuracy of this representation is discussed in terms of ionospheric transport tensor component calculations by Comfort (1975). It is found that for the collision frequencies presented in the next section, use of the above approximation results in deviations from exact calculations of less than 2 percent, in a model calculation.

5.3 EFFECTIVE MOMENTUM TRANSFER COLLISION FREQUENCIES FOR THE IONOSPHERE

Formal expressions for collision frequencies have been derived in Section III and the integrals for particular velocity dependencies evaluated in the Appendix. Here explicit expressions for the different species of the ionosphere are presented in a form suitable for computer evaluation. Some of these are obtained directly from the literature; others are introduced here based on momentum transfer cross sections or other information in the literature.

5.3.1 Electron–Neutral Collisions

The most recent reviews of momentum transfer cross-section information (experimental data and theoretical calculations) are those of Itikawa (1971, 1973), based on results available at the end of 1971. Itikawa (1971, 1973) defines two effective collision frequencies, one for computing a. c. conductivities, the other for d. c. conductivities. That for d. c. conductivities is designated $\langle \nu_{eff} \rangle$ and is defined as in equation (5-1). Itikawa (1971) shows that $\langle \nu_{eff} \rangle$ is appropriate for use in the transport calculations of interest here; accordingly those collision frequencies are presented here.

Collision frequencies are given by Itikawa (1973) as functions of T_e in tabular form. If, for each neutral species, ν_j is written in the form

$$\nu_j = n_j \sum_{k=0}^{m} a_{jk} v^k \quad , \tag{5-16}$$

then equation (5-4) can be used to obtain

$$\langle \nu_j \rangle = \frac{n_j}{\Gamma(5/2)} \sum_{k=0}^{m} a_{jk} \left(\frac{2k_B T_e}{m_e} \right)^{k/2} \Gamma \left(\frac{k+5}{2} \right) , \tag{5-17}$$

where $K = m_e / 2k_B T_e$ has been used. A fourth degree polynomial in $T_e^{1/2}$ has been fit to the collision frequency data of Itikawa (1973), Table II). Equation (5-17) has then been used to determine the a_{jk} coefficients from the curve fit coefficients; these a_{jk} coefficients are listed in Table 5-1. The resulting polynomial approximations represent Itikawa's (1973) tabulated collision frequencies within 2 percent over the range $200°K \leq T_e \leq 5000°K$.

Table 5-1. COEFFICIENTS FOR ITIKAWA'S (1973) ELECTRON-NEUTRAL COLLISION FREQUENCIES (CGS UNITS)

j	a_{j1}	a_{j2}	a_{j3}	a_{j4}
N_2	-2.32×10^{-16}	6.60×10^{-23}	-1.28×10^{-30}	9.12×10^{-39}
O_2	1.50×10^{-16}	3.87×10^{-25}	3.24×10^{-31}	-2.86×10^{-39}
O	5.38×10^{-17}	4.32×10^{-24}	5.10×10^{-32}	-4.85×10^{-40}
H_e	4.90×10^{-16}	5.84×10^{-24}	-4.69×10^{-32}	8.02×10^{-41}
H	4.23×10^{-15}	7.07×10^{-24}	-9.76×10^{-31}	6.50×10^{-39}

As an application of the power law representation for collision frequencies, derived in the previous section, equation (5-17) can be substituted into equation (5-13) and the differentiation carried out to obtain

$$r_j = \frac{n_j}{\langle \nu_j \rangle \Gamma(5/2)} \sum_{k=1}^{4} k \, a_{jk} K^{-k/2} \Gamma \left(\frac{k+5}{2} \right) , \tag{5-18}$$

which is readily evaluated with the a_{jk} coefficients in Table 5-1. Numerical results are given by Comfort (1975). Equations (5-17), (5-18), and (5-15) are particularly convenient forms for computer evaluation.

5.3.2 Electron–Ion Collisions

Collisions among charged particles in plasmas have received extensive attention in the literature and in many texts, so that a detailed discussion need not be presented here. It is nevertheless worth noting that a variety of methods have been used, each focusing on a particular physical aspect of the process. To first order, all rely on either truncating the Coulomb potential at the Debye length (R_D) or using the screened Coulomb (or Debye) potential ($\propto \exp(-r/R_D)/r$) with or without truncation at R_D. The physical idea behind these approximations is that charges of a given sign are effectively screened by charges of the opposite sign, so that beyond a certain distance (R_D) there is negligible interaction. Among the approaches used to compute the effects of charged particle collisions are the binary collision concept, the Fokker-Planck equation, and two-particle distribution functions. These are examined in detail by Shkarofsky, et al. (1966, Chapter 7) and Burgers (1969, Chapter 4).

To first order, the various approaches arrive at results which can be placed in the same form, with differences incorporated into the Coulomb logarithm ($\ell n\ \Lambda$). Numerically, ionospheric collision frequencies resulting from these methods agree within 10-15 percent. Since there appears to be little consensus favoring one result over others, and given the reasonable agreement among them relative to other uncertainties in ionospheric calculations, the basis for selection here is simplicity and consistency with other factors in the study.

With that rationale, the derivation of the electron-ion collision frequency is outlined in the context of the binary collision formalism developed in Section III. It is well-known that both classical and quantum mechanical treatments yield the Rutherford differential cross section for scattering in a Coulomb potential:

$$\sigma(g,\chi) = \left(\frac{Z_r Z_s e^2}{2\mu_{rs} g^2}\right)^2 \frac{1}{\sin^4(\chi/2)} \quad , \tag{5-19a}$$

in the notation of Section III, with Z_r and Z_s the number of charge units for species r and s. The momentum transfer cross section for this process is then given by equation (3-12) as

$$Q_{rs}(g) = 2\pi \left(\frac{Z_r Z_s e^2}{2\mu_{rs} g^2}\right)^2 \int_0^{\pi/2} (1-\cos\chi) \frac{\sin\chi}{\sin^4(\chi/2)} d\chi. \tag{5-19b}$$

Here the relation between the impact parameter and the differential cross section,

$$bdb = -\sigma(g,\chi) \sin\chi d\chi, \tag{5-19c}$$

has been used.

Since the integral in equation (5-19b) diverges at the lower limit, which corresponds to forward scattering and infinite impact parameter, the standard technique for avoiding this problem is to set a new lower limit χ_m. This is determined by assuming that because of screening by charges of the opposite sign, the potential of a given particle does not effectively extend beyond the Debye length

$$R_D = \left[\frac{kT_e}{4\pi N_e e^2}\right]^{1/2} . \tag{5-19d}$$

With this assumption and the condition that densities be sufficiently high that the Debye sphere contain many charged particles, the integration in equation (5-19b) can be carried out and the result placed in the form

$$Q_{rs}(g) \simeq 16\pi \left(\frac{Z_r Z_s e^2}{2\mu_{rs} g^2}\right)^4 \ell n\left[\frac{\mu_{rs} g^2}{Z_r Z_s e^2} R_D\right] . \tag{5-19e}$$

At this point, the usual approximation is to argue that the logarithmic factor varies sufficiently slowly with velocity that the mean velocity can be used in its argument and the logarithm can be factored out of the integral in the collision frequency. For the electron-ion collision frequency, $Z_r=Z_s=1$, $\mu_{rs}=m_e$ and equation (3-36) is used for the integration over relative velocities, giving the result

$$\bar{\nu}_{ei} \equiv \langle \nu_{ei} \rangle = \frac{4}{3} \sqrt{\frac{2\pi}{M_e}} \frac{N_e e^4}{(kT_e)^{3/2}} \ell n\Lambda, \qquad (5\text{-}20a)$$

where the argument of the Coulomb logarithm ($\ell n\ \Lambda$) is given by

$$\Lambda = \frac{3kT_e}{e^2} \left(\frac{kT_e}{4\pi N_e e^2} \right)^{1/2} . \qquad (5\text{-}20b)$$

This form for the collision frequency is consistent with those of Banks (1966a), Shkarofsky, et al. (1966) and Itikawa (1971) among others. The form for the Coulomb logarithm is one of the most common in the literature. However, it neglects the effects of ion motion both in charge shielding and in contributing to the relative collision speed. Since the ion thermal speed is about one percent of the electron thermal speed, these effects are relatively small; but they contribute to the numerical differences discussed above. For present purposes, equations (5-20a) and (5-20b) are considered adequate.

5.3.3 Ion–Neutral Collisions

Ion-neutral collisions have special significance for several reasons. First, elastic collisions are an efficient means for transferring momentum and energy between ions and neutrals, so that the formalism developed in Section III applies directly. Second, it was shown above that all collisions involving electrons could be computed in the limit of vanishing relative flow velocity. However, this is not true for ions in general. Hence, the full mathematical framework developed in Section III, taking into account the effects of the relative flow velocity on momentum and energy transfer, must be used for ion-neutral collisions and only for those collisions. Third, because the masses

of ions and neutrals are comparable, electrostatic fields of external (magnetospheric) origin give momentum to the charged particles; and this is transferred to neutrals primarily through collisions with ions. In other words, the ions are the agent through which magnetospheric electric fields interact with the neutral atmosphere. Some effects of this interaction are examined in the following section.

Since there are five major neutral species and five major ion species, a total of 25 different collision frequencies are possible. However, all of these species are not important in the same altitude region. Thus, some possible combinations are not required. Those that are required may be conveniently grouped into two categories: collisions between ions and unlike neutrals, and resonance charge exchange collisions between ions and parent neutrals. Interactions in each category are the same, differing only in strength, so that only two different expressions are required to express all the collision frequencies. These are discussed separately below.

5.3.3.1 Collisions Between Ions and Unlike Neutrals. The longest range interaction between ions and neutrals results from an induced dipole potential of the form

$$\phi = -\alpha e^2/2r^4, \tag{5-21}$$

where α is the dipole polarizability of the neutral atom. This interaction predominates at low temperatures, below about 300°K. Due to lack of experimental data for higher temperatures, little is known reliably of the actual shorter range interactions (Mason, 1970). Depending on the nature of these shorter range interactions, the momentum transfer cross section can either increase or decrease with increasing temperature. So in the absence of reliable information, the simple approach is taken: the polarization interaction is assumed to predominate for all ionospheric temperatures. Corresponding to the induced dipole interaction, equation (5-21), is the momentum transfer cross section (see Dalgarno, et al. (1958))

$$Q_{rs}(g) = \frac{2.21\pi}{g}\left(\frac{\alpha e^2}{\mu_{rs}}\right)^{1/2} \text{ cm}^2, \tag{5-22}$$

where r designates an ion species and s a neutral species. This is recognized as the momentum transfer cross section for Maxwellian molecules, for which the collision frequency is independent of temperature. From equation (A-43d) the collision frequency for this cross section is

$$\nu_{rs} = 2.21\pi\left(\frac{\alpha e^2}{\mu_{rs}}\right)^{1/2} n_s \text{ s}^{-1}. \tag{5-23}$$

When values for the dipole polarizability given by Banks and Kockarts (1973, Chapter 9) are used in equation (5-23), collision frequencies may be written in the form

$$\nu_{rs} = A_{rs} n_s , \tag{5-24}$$

where the A_{rs} coefficients are given in Table 5-2.

Table 5-2. COEFFICIENTS FOR ION COLLISIONS WITH UNLIKE NEUTRALS FROM DIPOLE POLARIZABILITIES OF BANKS AND KOCKARTS (1973)

ION-NEUTRAL	A_{rs} (10^{-9}cm^{3}s^{-1})	ION-NEUTRAL	A_{rs} (10^{-9}cm^{3}s^{-1})
$O^+ - N_2$	.89	$O^+ - H$	2.18
$O_2^+ - O$	.70	$H_e^+ - N_2$	1.84
$NO^+ - N_2$	.90	$H_e^+ - O$	1.29
$NO^+ - O_2$	.83	$H_e^+ - H$	2.36
$NO^+ - O$	.71	$H^+ - N_2$	3.50
$O^+ - N_2$	1.08	$H^+ - O_2$	3.32
$O^+ - O_2$	1.00	$H^+ - O$	2.37
$O^+ - H_e$	.66	$H^+ - H_e$	1.33

The order corresponds to the altitude region of primary importance, with those listed first (left side) most important in the E region. Since H_e^+ and H^+ ions are negligible at altitudes of interest here, those collision frequencies are included only for completeness.

A significant feature of these collision frequencies is that they are constant. This is associated with the type of interaction assumed (that of Maxwellian molecules) rather than any approximation involving dropping small terms. Since the derivative with respect to relative flow velocity vanishes for this type of collision frequency, that term will be absent from the ion energy transfer equation (4-66b) for these collisions.

5.3.3.2 Collisions Between Ions and Parent Neutrals. For collisions between ions and parent neutrals, resonant charge exchange interactions become more important than induced dipole polarization interactions as temperature increases (Mason, 1970). Such collisions are quite important for the exchange of momentum and energy between ions and neutrals. In a single collision, a fast ion becomes a fast neutral and a slow neutral becomes a slow ion. Because both momentum and kinetic energy of the particles are conserved in the collision, the collision may be treated as if it were elastic, by the formalism developed in Section III. Indeed, the small-angle charge exchange collision is indistinguishable from a large angle elastic collision. Therefore, these collisions are discussed here in the context of elastic collisions and in that mathematical framework.

Banks (1966c) has examined the transition from induced dipole polarization interactions at low temperatures to charge exchange interactions at higher temperatures. He finds that the transition takes place over a temperature range of a few hundred degrees. Outside this range, he determines that the individual interactions dominate almost totally in their respective temperature regions. Banks (1966c) therefore takes the approach of extrapolating experimental or theoretical curves of cross section versus temperature for each interaction into the temperature region of the other. Where they cross defines the transition temperature and expressions for each interaction are used alone in their respective regions of dominance.

Stubbe (1968) takes an alternate approach. In a semi-classical calculation, he corrects the contribution of charge exchange to the momentum transfer cross section by including contributions of induced Dipole polarization for impact parameters beyond a critical value. Solving the resulting equations numerically, he presents graphic results for the momentum transfer cross section of (O^+, O) and (H^+, H) for $g \leq 2.5 \times 10^5$ cm s^{-1}, as well as collision frequencies as functions of relative flow velocity, with T as a parameter, for $|\vec{v}_i - \vec{v}_n| \leq 3 \times 10^5$ cm s^{-1}. He also approximates the collision frequencies at zero relative velocities as power laws in temperature for other charge exchange collisions of aeronomical interest.

In comparing his results for (O^+, O) with those of Banks (1966c), Stubbe (1968) finds his results greater than Banks' (1966c) ranging from about 35 percent at 500°K (transition region) to 22 percent at 2000°K. Stubbe (1968) appears to interpret these differences at high temperatures as due to dipole polarization effects, ignored by Banks (1966c) at high temperatures. However, since they used slightly different charge exchange cross sections, exact agreement should not be expected. Stubbe's (1968) own data indicate that at 2000°K the polarization effect is less than 9 percent. In view of uncertainties in the source data, such differences are not necessarily the limiting factors in the accuracy of the results.

For present purposes, it is not so much the assessment of accuracy as the form of the results that leads to the use of Stubbe's (1968) results for the present study. The desirable feature is a single representation of the velocity dependence of the momentum transfer cross section over the entire velocity range of ionospheric interest. Numerical results of this type are presented graphically by Stubbe (1968) in his Figures 6 and 7. Since these momentum transfer cross sections clearly vary inversely with relative velocity (g), second order polynomials in (1/g) have been fit to these curves over the velocity ranges presented by means of least squares curve fits. Momentum transfer cross sections are then represented analytically in the form

$$Q_j(g) = A_{jo} + \frac{A_{j1}}{g} + \frac{A_{j2}}{g^2} , \qquad (5\text{-}25)$$

where the A_{jr} are curve-fit coefficients of appropriate units. Values of these coefficients are given in Table 5-3. These coefficients used in equation (5-25) reproduce the graphic values within 2 percent over the entire velocity range of the graphs. It is assumed that this expression can be used in collision frequency integrations for all velocities.

Table 5-3. COEFFICIENTS FOR STUBBE'S (1968) MOMENTUM TRANSFER CROSS SECTIONS (CGS UNITS)

COEFFICIENT	$O^+ - O$	$H^+ - H$
A_{jo}	$.67067 \times 10^{-14}$	1.4056×10^{-14}
A_{j1}	$.33298 \times 10^{-9}$	1.1572×10^{-9}
A_{j2}	$.11465 \times 10^{-4}$	$.64445 \times 10^{-4}$

With the momentum transfer cross section represented by equation (5-25), collision frequencies can be obtained directly from equations (A-43 c-e). Thus, the collision frequencies have the form

$$\nu_{in}(v_o) = n_j \left\{ A_{j1} + \frac{\exp(-Kv_o^2)}{\sqrt{\pi K}} \left[\left(\frac{1}{2Kv_o^2} + 1 \right) A_{jo} + \frac{A_2}{v_o^2} \right] \right.$$

$$\left. + \operatorname{erf}(\sqrt{K}\, v_o) \left[\left(Kv_o^2 + 1 - \frac{1}{4Kv_o^2} \right) \frac{A_{jo}}{Kv_o} + (2Kv_o^2 - 1) \frac{A_{j2}}{2Kv_o^3} \right] \right\}, \quad (5\text{-}26)$$

where $v_o = |\vec{v}_i - \vec{v}_n|$, $K = 4kT/m_j$, $T = 1/2\ (T_i + T_n)$ and the A_{jr}'s are given in Table 5-2.

When equation (5-26) is evaluated for (O^+, O) collisions, using various values for v_o and T, comparison with corresponding graphic data presented by Stubbe (1968, Figure 9) shows exact agreement, within the precision of the graph. However, similar comparison for (H^+, H) collisions (Stubbe, 1968, Figure 10) shows a temperature-dependent discrepancy. Since both calculations are made by the same computer program, changing only the A_{jr} coefficients, the agreement for (O^+, O) validates the equation and the program. Similarly,

the same computer program computed and checked both sets of curve fit coefficients; so the (O^+, O) results validate that procedure. Review of the input data reveals no error there. It appears that for (H^+, H) collisions, the momentum transfer cross sections presented by Stubbe (1968, Figure 7) are inconsistent with his collision frequencies (his Figure 10). Collision frequencies computed from the cross sections by equation (5-26) are consistently larger than Stubbe's (1968) graphic values by amounts ranging from about 6 percent at 500°K to 18 percent at 3000°K ($v_o = 0$). For present purposes, this is no problem since H^+ is generally a minor ion below 800 km. In addition, the size of the discrepancy is within the uncertainties associated with ion neutral collision frequencies.

In addition to the collision frequencies above, Stubbe (1968) provides the following approximate expressions, for 500°K $\leq$ T $\leq$ 3000°K and $v_o = 0$:

$$\nu(O_2^+, O_2) = 1.17 \times 10^{-9} \, (T/1000)^{.28} \, n_{O_2} \, s^{-1} \qquad (5\text{-}27a)$$

$$\nu(N_2^+, N_2) = 2.11 \times 10^{-9} \, (T/1000)^{.38} \, n_{N_2} \, s^{-1} \qquad (5\text{-}27b)$$

$$\nu(N^+, N) = 1.75 \times 10^{-9} \, (T/1000)^{.34} \, n_N \, s^{-1} \qquad (5\text{-}27c)$$

$$\nu(He^+, He) = 2.92 \times 10^{-9} \, (T/1000)^{.37} \, n_{He} \, s^{-1} \, . \qquad (5\text{-}27d)$$

Of these only $\nu(O_2^+, O_2)$ is likely to be significant below 800 km. For most of this region, $\nu(O^+, O)$ is the single most important ion-neutral collision frequency because O^+ is the major ion species throughout the F region (above about 180 km, see Figure 1-1c) and resonant charge exchange is the most important collision process.

5.4 METHODS FOR COMPUTING TRANSPORT TENSOR COMPONENTS

Rigorous calculations of transport properties are inherently difficult, requiring numerical solution of coupled sets of integro-differential equations. As the number of independent parameters with which the transport properties vary increases, it even becomes difficult to place the numerical results in a form usable in practical calculations. Thus, when arbitrary degree of ionization and magnetic field strength must be considered in addition to number density and temperature as independent parameters, the problem becomes formidable indeed. This is why the method of Shkarofsky (1961) is so useful: it includes all these effects in a basically simple form. For the power law representation derived in Section 5.2., the more complicated mathematics has been worked out by Shkarofsky (1961), who presents expressions requiring only the evaluation of determinants. Recent experimental data supports Shkarofsky's (1961) treatment of partial ionization (Albares, 1973). The primary disadvantage is that only electron motions are treated.

Shkarofsky, et al., (1966) treat the ion pressure tensor in a manner similar to that for electrons. However, only a fully ionized plasma is considered (ion-neutral collisions are neglected) and only transport associated with gradients in flow velocity (i.e. viscosity/pressure tensor) are treated. For the ionosphere, this set of limitations makes the results of little practical value. At high altitudes where the fully ionized gas approximation is most nearly approached, the strong magnetic field limit ($<\nu_{in}> << \omega_i$) applies to the ions, so that ion transport is restricted to the parallel direction. In this case, less complicated results for no magnetic field can be employed. Also, gradients in flow velocity are likely to be much smaller at high altitudes than in the E region (e.g. see Section VI) where the magnetic field competes with neutral collisions for dominance of ion motions. The fact of this competition, however, means that the fully ionized approximation is inapplicable. The net result of these considerations is that for ions Shkarofsky's method offers too little for the effort required to be useful for ionospheric applications.

Alternate expressions for ion transport coefficients are therefore adopted. Although these lack the thoroughness of the electron treatment, the effects on practical calculations are probably small, as discussed below. For neutrals different complications arise, due to the multiplicity of neutral species. However, adequate expressions are available from the literature, and these are presented.

5.4.1 Computation of Electron Transport Tensor Components

The Shkarofsky method for computing electron transport coefficients is described in detail in several works (Shkarofsky, 1961; Shkarofsky, et al., 1966; Hochstim and Massel, 1969; Mitchner and Kruger, 1973); a lengthy description is inappropriate here. Since calculation of the transport tensor components is the primary objective here, the assumptions and approach used are summarized briefly. Then those equations necessary for making the calculations are extracted from the sources above.

Assumptions made in the derivation of the Shkarofsky method are listed by Shkarofsky (1961, Section 2) and, in a slightly different form, by Shkarofsky et al., (1966, Chapter 4). These have been placed in the context of the ionosphere by Schunk and Walker (1970), who also demonstrate that ionospheric conditions are consistent with the assumptions (where appropriate). In the form given by Schunk and Walker (1970) the assumptions and conditions are as follows

1. Only electron current and heat flow are considered; contributions due to ion motions are ignored.

2. Only elastic collisions are considered (see discussion of fine structure excitation of atomic oxygen in subsection 4.3 on the validity of this assumption).

3. A steady state is assumed - for the ionosphere this is valid because time scales for changes in macroscopic properties are long relative to electron relaxation times.

4. The angular dependence of the electron distribution function is expanded in Legendre polynomials, truncated after the second term. Schunk and Walker (1970) note that this requires the electron flow velocity be much less than the mean thermal speed and that the electron mean free path be much less than the electron scale height; they demonstrate that both hold in the ionosphere.

5. The collision frequency is a function of velocity only, not of position; i.e. scatterers are uniformly distributed. This is valid if electron mean free paths are much smaller than both electron and neutral scale heights.

6. Driving forces (electric fields and gradients) are sufficiently small that the equilibrium Maxwellian distribution is not disturbed; i.e. the isotropic part of the distrution function is assumed to be Maxwellian. This holds if the flow velocity is much smaller than the mean thermal speed.

7. Applied electric and magnetic fields are uniform in space.

8. The perturbation to the equilibrium Maxwellian distribution is expanded in a series of generalized Laguerre polynomials, truncated after four terms. (Hochstim and Massel (1969) carry out the expansion to 20 terms in order to investigate convergence properties. Examination of their results indicates that for the ionosphere four terms gives sufficient accuracy.)

These items fairly well indicate the approach as well as the assumptions and conditions for the calculation. The electron distribution function is expanded first in Legendre polynomials in the form

$$f = f_o + \vec{f}_1 \cdot \frac{\vec{v}}{v} + \ldots \qquad (5\text{-}28)$$

in the notation of subsection 5.2. This form is then used in the Boltzmann equation, together with the previous assumptions. The resulting equations relate $\vec{f}_1$ to f_o. From these relations general expressions for the transport tensors are obtained. To solve the equations, $\vec{f}_1$ is expanded in terms of generalized Laguerre polynomials (four terms). Once $\vec{f}_1$ is known the expressions for the transport tensors can be evaluated. The end products of this rather lengthy procedure are presented below.

Since the required equations are taken from Shkarofsky (1961), this work is denoted by SI for ease of reference in the remainder of this section. Insofar as feasible, the notation of SI is followed to facilitate reference to the complete derivation in that work. The treatment in SI includes a.c. electric fields; these effects are suppressed in the results below since they are not included in this study.

Consistent with the assumption above, the electron current is related to the electric field and gradients in T_e and N_e by (SI, equation (70))

$$\vec{J}_e = \overline{\overline{\sigma}} \cdot \vec{E} - e\overline{\overline{D}} \cdot \nabla N_e - \overline{\overline{T}} \cdot \nabla T_e \,. \tag{5-29}$$

(An equation of this form can be obtained from the electron momentum equation (4-35) for the steady-state case.) Here $\overline{\overline{\sigma}}$ is the d.c. electrical conductivity tensor, $\overline{\overline{D}}$ is the diffusion current tensor, and $\overline{\overline{T}}$ is the current flow tensor due to thermal gradients at constant density (SI uses $\overline{\overline{\tau}}$ instead of $\overline{\overline{T}}$, but here $\overline{\overline{\tau}}$ is used to denote the viscous stress tensor). Correspondingly, the total energy flow $\vec{H}$ due to electrons is related to the electric field and gradients in T_e and N_e by (SI, equation (72a))

$$\vec{H} = \overline{\overline{\mu}} \cdot \vec{E} - e\overline{\overline{Q}} \cdot \nabla N_e - \overline{\overline{K}} \cdot \nabla T_e \,. \tag{5-30}$$

Here $\overline{\overline{\mu}}$ is the energy flow tensor due to electric fields, $\overline{\overline{Q}}$ is the energy diffusion tensor and $\overline{\overline{K}}$ is the thermal conductivity tensor at constant density. These transport tensors are not independent, being related by (SI, equation (76))

$$\overline{\overline{D}} = \frac{kT\,\overline{\overline{\sigma}}}{e^2 N_e} \,, \quad \overline{\overline{Q}} = \frac{kT}{N_e e^2}\,\overline{\overline{\mu}}, \tag{5-31}$$

known as Einstein relationships. Calculations are therefore limited to $\overline{\overline{\sigma}}$, $\overline{\overline{T}}$, $\overline{\overline{\mu}}$, and $\overline{\overline{K}}$.

In Shkarofsky's formulation, the transport tensor components are expressed in a compact notation with a deceptively simple form. Only in the limiting cases does simplicity remain as the parameters are expanded for evaluation. In order to present this expansion in a coherent manner, the approach taken here is to begin with the final result required - the transport tensor. These are related to other parameters, which are in turn related to still other parameters, until all parameters can be related to the fundamental properties of the system: electron temperature, electron number density, collision frequencies, magnetic field strength and physical constants.

All of the transport tensors have the form

$$\overline{\overline{X}} = \begin{pmatrix} X_{11} & -X_{21} & 0 \\ X_{21} & X_{11} & 0 \\ 0 & 0 & X_{33} \end{pmatrix} , \tag{5-32}$$

where the 3-component lies in the direction of the magnetic field. The relatively simple form is due to the fact that the only anisotropy of the medium is due to the magnetic field; off-diagonal terms are due to the Lorentz force. Because of the symmetries in the matrix elements, they can be compactly expressed for the general case in the following manner (SI, equations (82)):

$$\sigma_{11} \mp i\sigma_{21} = \frac{N_e e^2}{M_e(\langle\nu_g\rangle g_{\sigma\mp} + i\omega_b h_\sigma)} \tag{5-33a}$$

$$T_{11} \mp iT_{21} = \frac{N_e ek}{M_e(\langle\nu_g\rangle g_{T\mp} + i\omega_b h_T)} \tag{5-33b}$$

$$\mu_{11} \mp i\mu_{21} = \frac{5N_e ek\, T_e}{2M_e(\langle\nu_g\rangle g_{\mu\mp} + i\omega_b h_\mu)} \tag{5-33c}$$

$$K_{11} \mp iK_{21} = \frac{5N_e k^2 T_e}{M_e(\langle\nu_g\rangle g_{K\mp} + i\omega_b h_K)} \tag{5-33d}$$

In these equations $\langle\nu_g\rangle$ is the total effective electron collision frequency, given by (see notation in subsection 5.2.)

$$\langle\nu_g\rangle = \langle\nu_m\rangle + \langle\nu_{ei}\rangle . \tag{5-34}$$

The g and h coefficients are correction factors which incorporate the effects of the degree of ionization and magnetic field strength into the tensor components. The complex notation is a device for compact expression; it has no physical significance. To obtain the X_{33} components, simply set $\omega_b \equiv \omega_e = 0$ in equations (5-33); these correspond to the zero magnetic field case.

In equations (5-33) the only unknown quantities, in the context of the fundamental properties noted above, are the g and h correction factors; so it remains only to determine them. They are computed from (SI, equations (92 a-h)):

$$g_\sigma = \frac{\langle \nu_{ei} \rangle}{\langle \nu_g \rangle} \; R_e \left(\frac{|\Delta|}{|\Delta_{00}|} \right) \tag{5-35a}$$

$$h_\sigma = \frac{\langle \nu_{ei} \rangle}{\mp \omega_b} \; I_m \left(\frac{|\Delta|}{|\Delta_{00}|} \right) \tag{5-35b}$$

$$g_T = \frac{\langle \nu_{ei} \rangle}{\langle \nu_g \rangle} \; R_e \left(\frac{|\Delta|}{|\Delta_{00}| + \frac{5}{2}|\Delta_{01}|} \right) \tag{5-35c}$$

$$h_T = \frac{\langle \nu_{ei} \rangle}{\mp \omega_b} \; I_m \left(\frac{|\Delta|}{|\Delta_{00}| + \frac{5}{2}|\Delta_{01}|} \right) \tag{5-35d}$$

$$g_\mu = \frac{\langle \nu_{ei} \rangle}{\langle \nu_g \rangle} \; R_e \left(\frac{|\Delta|}{|\Delta_{00}| + |\Delta_{01}|} \right) \tag{5-35e}$$

$$h_\mu = \frac{\langle \nu_{ei} \rangle}{\mp \omega_b} \; I_m \left(\frac{|\Delta|}{|\Delta_{00}| + |\Delta_{01}|} \right) \tag{5-35f}$$

$$g_K = \frac{2\langle \nu_{ei} \rangle}{\langle \nu_g \rangle} \; R_e \left(\frac{|\Delta|}{|\Delta_{00}| + \frac{7}{2}|\Delta_{01}| + \frac{5}{2}|\Delta_{11}|} \right) \tag{5-35g}$$

$$h_K = \frac{2\langle \nu_{ei} \rangle}{\mp \omega_b} \; I_m \left(\frac{|\Delta|}{|\Delta_{00}| + \frac{7}{2}|\Delta_{01}| + \frac{5}{2}|\Delta_{11}|} \right) \tag{5-35h}$$

(The factor 2 in these last two equations was erroneously omitted from equations (92g) and (92h) in SI, as determined from SI equations (82) and (91) and verified by comparisons of numerical results.) Signs $\mp$ in the h factors correspond to $\overline{+}$ in equations (5-33).

In equations (5-35) the notation $|\Delta_{00}|$ denotes the 00 minor of the determinant $|\Delta|$, with similar meanings for the other determinants. Matrix Δ is given by (SI, equations (55c), (63a))

$$\Delta = \frac{1}{\langle \nu_{ei} \rangle} \begin{pmatrix} H_{00} \pm i\omega_b & H_{01} & H_{02} & 0 \\ H_{01} & H_{11} \pm i\frac{5}{2}\omega_b & H_{12} & 0 \\ H_{02} & H_{12} & H_{22} \pm i\frac{35}{8}\omega_b & 0 \\ 0 & 0 & 0 & H_{33} \pm i\frac{105}{16}\omega_b \end{pmatrix} \tag{5-36}$$

The matrix (H_{ij}) is an interaction matrix, with contributions due to collisions of electrons with ions, electrons, and neutrals:

$$H_{ij} = \langle \nu_{ei} \rangle H_{ij}^{ei} + \langle \nu_{ei} \rangle \sqrt{2}\, H_{ij}^{ee} + \langle \nu_m \rangle H_{ij}^{en} . \tag{5-37}$$

(In SI the collision frequencies in this equation are included in the definitions of H_{ij}^{ei}, H_{ij}^{ee}, and H_{ij}^{en}.)

For the first two matrices in equation (5-37), the interaction is known and fixed; the matrix elements are therefore constants. These are given by (SI, equations (49), (53), (63b, c))

$$(H_{ij})^{ei} = \begin{pmatrix} 1 & 3/2 & 15/8 & 35/16 \\ 3/2 & 13/4 & 69/16 & 165/32 \\ 15/8 & 69/16 & 433/64 & 1077/128 \\ 35/16 & 165/32 & 1077/128 & 2957/256 \end{pmatrix} \tag{5-38}$$

and

$$(H_{ij})^{ee} = \begin{pmatrix} 0 & 0 & 0 & 0 \\ 0 & 1 & 3/4 & 15/32 \\ 0 & 3/4 & 45/16 & 309/128 \\ 0 & 15/32 & 309/128 & 5657/1024 \end{pmatrix} . \tag{5-39}$$

The matrix $(H_{ij})^{en}$ contains effects of electron-neutral interactions; its elements vary with the velocity dependence of the momentum transfer cross sections for electron-neutral collisions. In general, these matrix elements are given by integrals over velocity-weighted products of the momentum transfer cross section and electron distribution function (isotropic part). For the case of a simple power law dependence (see equations (5-2) and (5-3)), these matrix elements have been evaluated in SI. The purpose of the method derived in section 5.2. was to permit use of these results for arbitrary velocity dependence. From SI, equations (48) and (63d), the electron-neutral interaction matrix is given by

$$(H_{ij})^{en} = \begin{pmatrix} 1 & -\frac{r}{2} & \frac{r(r-2)}{8} & -\frac{r(r-2)(r-4)}{48} \\ -\frac{r}{2} & \frac{r^2+2r+10}{4} & -\frac{r(r^2+2r+20)}{16} & \frac{r(r-2)(r^2+2r+30)}{96} \\ \frac{r(r-2)}{8} & -\frac{r(r^2+2r+20)}{16} & H_{22}^{en} & -\frac{r(r^4+4r^3+68r^2+8r+420)}{384} \\ -\frac{r(r-2)(r-4)}{48} & \frac{r(r-2)(r^2+2r+30)}{96} & -\frac{r(r^4+4r^3+68r^2+8r+420)}{384} & H_{33}^{en} \end{pmatrix} \quad (5\text{-}40a)$$

where

$$H_{22}^{en} = (r^4 + 4r^3 + 52r^2 + 96r + 280)/64 \quad (5\text{-}40b)$$

$$H_{33}^{en} = (r^6 + 6r^5 + 142r^4 + 528r^3 + 3952r^2 + 6864r + 15120)/2304. \quad (5\text{-}40c)$$

In SI this matrix is expressed in terms of "m", which is related to r by

$$m = (r+3)/2. \quad (5\text{-}41)$$

The notation used above seems more convenient and compact.

Once the power law index r has been determined by the procedure in subsection 5.2., all information necessary for the calculation of the transport tensor components is available in terms of the fundamental properties desired. These equations hold for the general case of arbitrary degree of ionization and magnetic field strength. For the ionosphere, there is a simplification associated with the fact that for electrons the magnetic field is always in the strong field limit ($\omega_b >> \langle\nu_m\rangle$). This applies, of course, only to the transverse components.

In the strong magentic field limit, transverse components of the transport tensors are expressed in the following manner (cf. equations (5-33) above):

$$\sigma_{11} \pm i\sigma_{21} = \frac{N_e e^2}{kT_e}\left(\frac{\pm i}{h_\sigma \omega_b} + \frac{g_\sigma \langle\nu_g\rangle}{h_\sigma^2 \omega_b^2}\right) \tag{5-42a}$$

$$T_{11} \pm iT_{21} = \frac{N_e ek}{kT_e}\left(\frac{\pm i}{h_T \omega_b} + \frac{g_T \langle\nu_g\rangle}{h_T^2 \omega_b^2}\right) \tag{5-42b}$$

$$\mu_{11} \pm i\mu_{21} = \frac{5N_e ek T_e}{2M_e}\left(\frac{\pm i}{h_\mu \omega_b} + \frac{g_\mu \langle\nu_g\rangle}{h_\mu^2 \omega_b^2}\right) \tag{5-42c}$$

$$K_{11} \pm iK_{21} = \frac{5N_e k^2 T_e}{M_e}\left(\frac{\pm i}{h_K \omega_b} + \frac{g_K \langle\nu_g\rangle}{h_K^2 \omega_b^2}\right), \tag{5-42d}$$

from SI, equation (98). The limiting expressions for the correction factors are then (SI, equations (99a) - (99d)):

$$h_\alpha = 1 \text{ for } \alpha = \sigma, T, \mu, K \tag{5-43}$$

$$g_\sigma = 1 \tag{5-44a}$$

$$g_T = \frac{1}{2}\left[\frac{-1 + (r+2)\langle\nu_m\rangle/\langle\nu_{ei}\rangle}{1 + \langle\nu_m\rangle/\langle\nu_{ei}\rangle}\right] \tag{5-44b}$$

$$g_\mu = \frac{2}{5}\left[\frac{1 + \frac{1}{2}(r+5)\langle\nu_m\rangle/\langle\nu_{ei}\rangle}{1 + \langle\nu_m\rangle/\langle\nu_{ei}\rangle}\right] \tag{5-44c}$$

$$g_K = \frac{1/10 + \sqrt{2}/5 + [(r+5)(r+4)\langle\nu_m\rangle/20\langle\nu_{ei}\rangle]}{1 + \langle\nu_m\rangle/\langle\nu_{ei}\rangle} \tag{5-44d}$$

Since the transverse components can be evaluated from equations (5-42) - (5-44), the lengthy procedure involving the interaction matrices can be avoided. This is not so for the parallel (3, 3) components; however, for this component there is a small simplification. Because this component is obtained by setting ω_b to zero, it is seen from equation (5-36) that

$$\Delta_{ij} = H_{ij}/\langle\nu_{ei}\rangle, \text{ all } i,j \ , \tag{5-45}$$

in computing the parallel component only. With g correction factors given by equations (5-35a, c, e, g), the parallel components are then computed from (cf. equations (5-33)):

$$\sigma_o \equiv \sigma_{33} = \frac{N_e e^2}{M_e \langle\nu_g\rangle g^\circ_\sigma} \tag{5-46a}$$

$$T_o \equiv T_{33} = \frac{N_e ek}{M_e \langle\nu_g\rangle g^\circ_T} \tag{5-46b}$$

$$\mu_o \equiv \mu_{33} = \frac{5N_e ek\, T_e}{2M_e \langle\nu_g\rangle g^\circ_\mu} \tag{5-46c}$$

$$K_o \equiv K_{33} = \frac{5N_e k^2 T_e}{M_e \langle\nu_g\rangle g^\circ_K} \ , \tag{5-46d}$$

where the subscript and superscript o denotes no magnetic field.

To make use of these transport tensors in the context of the conservation equations, it is necessary to relate them to the unknown quantities, in particular to the heat flux vector $\vec{q}_e$. In SI this quantity is denoted by $\vec{H}_h$ and is shown to be related to the total energy flux $\vec{H}$ by (SI, p. 1656).

$$\vec{q}_e \simeq \vec{H} - 5kT_e\vec{J}/2e \ . \tag{5-47}$$

In the ionosphere it is frequently assumed that the current parallel to magnetic field lines vanishes. Physically this is interpreted as a steady state condition in which an electric field has built up in such a way that it cancels current contributions due to gradients in temperature and density; this is termed the thermoelectric effect (Spitzer and Harm, 1953). The effect in equation (5-47) is to make $\vec{q}_e$ equal to $\vec{H}$. It is shown by Hochstim and Massel (1969, p. 160) that for this case the heat flux parallel to the magnetic field can be computed from

$$\vec{q}_e \simeq -K_{eff} \nabla T_e \ , \tag{5-48}$$

where

$$K_{eff} = \frac{5N_e k^2 T_e}{M_e <\nu_g> (g_K^\circ)_{eff}} \tag{5-49}$$

and

$$\frac{1}{(g_K^\circ)_{eff}} \equiv \frac{1}{g_K^\circ} - \frac{g_\sigma^\circ}{2g_\mu^\circ g_T^\circ} \tag{5-50}$$

in notation introduced above.

In view of the approximations made in Section IV regarding transverse components in the electron equations, it is worthwhile to examine briefly the transport tensor expressions for consistency with those approximations. Let X denote any one of the transport tensors, and consider the ratios of transverse to parallel components. The component parallel to a transverse driving force is X_{11}. From equations (5-42) for the strong field transverse case and (5-46) for the parallel (zero field) case, the ratio is

$$\frac{X_{11}}{X_{33}} = \left(\frac{\langle \nu_g \rangle}{\omega_b}\right)^2 \left| g_\perp \; g^\circ \right| . \tag{5-51}$$

In SI a rather comprehensive set of tables is provided, giving g and h correction factors for $-3 \leq r \leq 3$ with magnetic field strength ranging from zero to infinitely strong and degrees of ionization from essentially zero to completely ionized. The g correction factors are of order unity, always satisfying $|g| \leq 3$. Disregarding them and using maximum values of $\langle \nu_g \rangle$ consistent with those used for order-of-magnitude estimates in Section IV gives

$$\left| \frac{X_{11}}{X_{33}} \right| \lesssim 10^{-4} . \tag{5-52}$$

Similarly for the off diagonal component, corresponding to transport which is transverse to both the magnetic field and a transverse driving force, the ratio is

$$\left| \frac{X_{21}}{X_{33}} \right| = \left| \frac{\langle \nu_g \rangle}{\omega_b} \; g^\circ \right| \lesssim 10^{-2} \tag{5-53}$$

In both cases the direction of the magnetic field clearly dominates the transport for isotropic driving forces. However, there may be no driving force in the parallel direction, as is frequently assumed to be the case for steady-state ionospheric electrostatic fields. The pertinent ratio is then the ratio of the transverse component parallel to the driving force (X_{11}) to the component transverse to both the magnetic field and the driving force (X_{21}):

$$\left| \frac{X_{11}}{X_{21}} \right| = \left| \frac{\langle \nu_g \rangle}{\omega_b} \; g_\perp \right| \lesssim 10^{-2} . \tag{5-54}$$

In words, transport parallel to the driving force is negligible compared to that perpendicular to the driving force in the transverse plane. When the driving force is an electric field, the current (conductivity) parallel to the electric field (in the transverse plane) is called the Pedersen current (conductivity), while that perpendicular to the electric field is the Hall

current (conductivity). It is readily recognized that only the Pedersen component represents work done by the electric field on the electrons. Since, according to equation (5-54), most electron transport transverse to the magnetic field occurs through Hall motion, Joule heating ($\propto \vec{E} \cdot \vec{J}$) of electrons will be small.

These considerations are consistent with the results of Section IV and this is evident from examination of equations (4-65a) and (4-66a). In the momentum equations, the transverse and parallel component are uncoupled with only the Hall drift remaining in the transverse equation. Joule heating was dropped from the electron energy equation by comparison with thermal energy exchange terms. The additional conclusion that can now be drawn is that the spatial gradients in the electron energy equation (4-66a) need be taken only parallel to the magnetic field, since the transverse components of $\overline{\overline{K}}$ are small compared with K_{33}. Mathematically, this is written (consistent with equation (5-48))

$$\frac{-1}{N_e} \nabla \cdot (\overline{\overline{K}} \cdot \nabla T_e) \simeq \frac{-1}{N_e} \frac{\partial}{\partial s} \left(K_{eff} \frac{\partial T_e}{\partial s} \right), \tag{5-55}$$

where s is arc length along a magnetic field line (see Banks, 1966b).

Equations presented in this part should be adequate for any ionospheric investigation of electron transport.

5.4.2 ION Transport

The formalism for a complete treatment of the ion transport problem, including arbitrary degree of ionization and arbitrary magnetic field strength, has been developed by S. T. Wu (1968); however, its form is impractical for numerical calculations. In the absence of a complete, usable method, only what is needed for the conservation equations and is readily available in the literature is presented. The term "readily" is used advisedly, since Mitchner and Kruger (1973) note that with proper precautions, the Chapman-Enskog approach, as applied by Hirschfelder, Curtiss, and Bird (1954), can be used in computing

both ion and neutral transport coefficients (for the zero-magnetic field case). Some indication of the steps required for such a procedure are provided by Chapman (1954) in his evaluation of the viscosity and thermal conductivity coefficients for a fully ionized gas without a magnetic field. Rather than engage in such an effort, the results of Chapman (1954) are presented; limitations on their applicability and consequent effects on calculations are then examined briefly.

References to equations (4-65c), (4-66b) and (4-33) shows that only coefficients of viscosity and thermal conductivity are required for the ion conservation equations. In the previous section, it was seen that in a magnetic field the thermal conductivity becomes a tensor of rank two. Shkarofsky, et al. (1966, Chapter 8-8) show that viscosity is affected in a similar manner, although the results are included in the stress tensor rather than in an explicit tensor viscosity. They note that a scalar viscosity is applicable only if $\omega_i << \langle \nu_{ii} \rangle$; this condition seldom holds in the ionosphere. Thus coefficients derived for a fully ionized gas in the absence of a magnetic field apply only for directions parallel to the field lines. For these conditions Chapman (1954) obtains the following expressions for viscosity and thermal conductivity coefficients of a single ion species:

$$\eta_i = \frac{5}{2}\sqrt{\frac{M_i}{\pi}}\ \frac{(kT)^{5/2}}{e^4\, A_2(2)} \tag{5-56}$$

$$K_i^T = \frac{15k}{4M_i}\,\eta_i \quad . \tag{5-57}$$

In the work cited, $A_2(2)$ is an integral based on a cutoff at the mean separation of particles. This has subsequently been modified in Chapman and Cowling (1970, p. 178) to use a Debye length cutoff, although the form of the result is unchanged. Thus $A_2(2)$ can be expressed in terms of the argument of the Coulomb logarithm, Λ, equation (5-20b), as

$$A_2(2) = 2\,[\ell n(1+\Lambda^2) - \Lambda^2/(1+\Lambda^2)]. \tag{5-58a}$$

Since $\Lambda >> 1$ (Spitzer, 1956; Banks, 1966a), this can be written to a good approximation as

$$A_2(2) \simeq 2[2\ell n\Lambda - 1].$$

For consistency with the results for electron-ion collisions, this should further be approximated by

$$A_2(2) \simeq 4\ \ell n\ \Lambda\ . \tag{5-58b}$$

In the ionosphere $\ln\Lambda \gtrsim 10$ (see Spitzer, 1956). It may now be noted that Chapman and Cowling (1970) use an expression corresponding to Λ which differs from equations (5-20) by a factor 4/3. Such a difference is inconsequential in terms of the approximation leading to equation (5-58b).

Equation (5-56) can thus be rewritten as

$$\eta_i = \frac{5}{8}\sqrt{\frac{M_i}{\pi}}\frac{(kT)^{5/2}}{e^4\ \ln\ \Lambda}\ , \tag{5-59}$$

while equation (5-57) remains unchanged. This result may be compared with a similar result obtained by Shkarofsky et al. (1966, equation (8-140)). That form can be shown to be the same with a factor $3/[4\sqrt{2}(.7326)]$ in place of 5/8 in equation (5-59). These numbers have decimal values of .7239 and .6250 respectively. However, the expression obtained by Chapman and Cowling (1970) is in the first approximation (Chapman - Enskog method of successive approximations). They note that in the second approximation, the expression for the first approximation is simply multiplied by 1.15. When this is done, the numerical constant is .7188, in very close agreement with the result of Shkarofsky et al. (1966). The corresponding correction factor for K_i^T in the second approximation is 1.25. So the recipe for accurate ion transport coefficients is to compute η_i from equation (5-59). With this value, evaluate K_i^T; then multiply the former by 1.15 and the latter by 1.25.

As indicated at the outset, these expressions are of limited applicability. The question is, how important are the limitations? Consider first the effect of the geomagnetic field. Chapman and Cowling (1970, Chapter 19) find that transport perpendicular to the magnetic field is reduced from the zero field case by a factor $1/[1 + (\omega_i\tau)^2]$ for direct transport and by a factor $(\omega_i\tau)/[1 + (\omega_i\tau)^2]$ for transverse transport. The terms direct and transverse, as used in this sense, refer to directions parallel to and perpendicular to the driving force (external force or gradient) in the plane perpendicular to the magnetic field. τ is a relaxation time which is given approximately by the inverse of the total ion collision frequency. Thus at low altitudes ($\lesssim$130km) where $\omega_i \lesssim \bar{\nu}_i$, direct transport is little affected by the magnetic field, while transverse transport varies approximately as $\omega_i/\bar{\nu}_i$. At high altitudes, on the other hand, where $\omega_i >> \bar{\nu}_i$, direct transport varies as $(\omega_i/\bar{\nu}_i)^{-2}$ and transverse transport as $(\omega_i/\bar{\nu}_i)^{-1}$. Hence, at high altitudes transport is confined to directions parallel to the magnetic field (except for strong transverse electric field driving forces).

For thermal conduction, observation and theory agree that ions have approximately the neutral temperature up to altitudes of 250km to 300km. So below that transition, thermal conduction is unimportant for the ions. Above this transition $\omega_i >> \bar{\nu}_i$ so that ion thermal conduction transverse to the geomagnetic field is unimportant. Thus, the thermal conduction coefficient for the zero-magnetic-field case is sufficient for practical purposes. Furthermore, above the thermal transition region, ion-neutral collision frequencies are small compared with collision frequencies of ions with charged particles. Hence, the ion thermal conductivity for a fully ionized gas is appropriate. In sum, the limitations on the application of the ion thermal conductivity coefficient, given by equation (5-52), should have little practical effect on ionospheric calculations.

For viscosity, the physical situation is rather different and not so well-defined, since less is known about ionospheric velocity fields than about its thermal structure. According to present understanding, significant ion flow velocities have two origins: electric fields and neutral

flow (via collisions). As discussed in Sections I and IV, electrostatic fields in the ionosphere are predominately transverse to the geomagnetic field. At high altitudes, where $\omega_i >> \bar{\nu}_{in}$, the Hall drift ($\vec{E}\vec{X}\vec{B}$) results (e.g. electron momentum equation (4-36)). At low altitudes, where $\bar{\nu}_{in} >> \omega_i$, ions essentially move with the neutral flow. A transition between these motions occurs at intermediate altitudes where $\bar{\nu}_{in} \approx \omega_i$ (~120km - 140km), resulting in vertical velocity gradients. Since large electric fields are observed primarily at high latitudes where geomagnetic field lines are almost vertical, large ion drifts due to electric fields are primarily horizontal. Thus, in this case, the flow is mainly horizontal with primarily vertical gradients which are largest in the region where $\bar{\nu}_{in} \approx \omega_i$. This qualitative picture is given quantitative substance in the next section.

When neutral flow causes the ion motion, a similar situation results. Collisional coupling at low altitudes ($\bar{\nu}_{in} >> \omega_i$) causes ions to move with the (horizontal) neutral wind. With increasing altitude the ion coupling undergoes a transition from collision dominated to geomagnetic field dominated, until at high altitudes the ions move primarily along magnetic field lines in the absence of transverse electric fields. Although this picture is somewhat complicated by geomagnetic field geometry variation with latitude, the physical results are basically the same as above. Velocity gradients are predominately vertical and strongest in the dynamic transition region ($\bar{\nu}_{in} \sim \omega_i$).

Physically, viscosity represents momentum transport due to spatial gradients in velocity. From the discussion above, this corresponds essentially to the transport of horizontal momentum in vertical directions. Since the physical conditions for maximum velocity gradients are now more precisely defined ($\bar{\nu}_{in} \sim \omega_i$) than those used for order-of-magnitude estimates in Section IV, a new estimate may be useful. In equation (4-39a) the same values are used to obtain a maximum velocity gradient (~.1 s^{-1}), but the collision frequency is now restricted to the order of the gyrofrequency (~10^2 s^{-1}). Under these conditions the ratio of the viscous stress tensor to scalar pressure is

$$\left| \frac{\tau_{i\,\alpha\beta}}{p_i} \right| \lesssim 10^{-3} \quad . \tag{5-60}$$

Hence viscous effects on ion motion are negligible in the dynamic transition region and below.

At high altitudes, where the total ion collision frequency is much reduced, it might appear that viscosity could be important. However, since the primary driving force for ion flow at high altitudes is electric fields, this is unlikely for the following reasons. The largest measured electric fields occur at high latitudes; that is, they are of magnetospheric origin and mapped into the ionosphere along geomagnetic field lines (see Figure 1-4). Because magnetic field lines are approximately equipotentials and the magnetic field is almost uniform over the altitude range of interest here, the electric field varies little along a field line over this range. Correspondingly, there is little variation in the $\vec{E}x\vec{B}$ drift velocity, resulting in very small velocity gradients. Consequently, along with the reduction in collision frequency at high altitudes, there is a reduction in the vertical velocity gradient, due to a uniformity in altitude of the driving force. So viscosity is unlikely to be important for ions at either high or low altitudes. If it is significant, it will probably be at high altitudes and for gradients along field lines, conditions for which the viscosity coefficient above is appropriate.

5.4.3 Neutral Transport

Neutral gas transport is not complicated by considerations of magnetic fields or degrees of ionization. Moreover, the kinetic theory for transport in single species monatomic gases is well-established (see Chapman and Cowling, 1970). However, difficulties arise in gas mixtures, particularly mixtures involving polyatomic molecules. These difficulties are discussed in some detail by Chapman and Cowling (1970, chapters 12-14) and will not be elaborated here. Using approximate formulas and some inspired curve-fitting, Banks and Kockarts (1973, chapter 14) have devised simple, yet reasonably accurate expressions for the viscosity and thermal conductivity coefficients for the mixture of neutral gases in the upper atmosphere. These are presented below.

The temperature dependence of the viscosity coefficients of all primary neutral species has been approximated in a common power law form, based on

experimental data for all except atomic hydrogen. Thus all the viscosity coefficients vary as $T^{.69}$ for $200°K \leq T \leq 2000°K$, a range adequate for most upper atmospheric conditions. Because of this common temperature dependence, Banks and Kockarts (1973) have been able to reduce the viscosity for the mixture to the following simple form:

$$\eta_n = A\, T^{.69} , \tag{5-61a}$$

where

$$A = \sum_n A_n n_n / \sum_n n_n . \tag{5-61b}$$

The summation runs over all neutral species, and the A_n coefficients are given in Table 5-4.

Table 5-4. COEFFICIENTS FOR COMPUTING THE NEUTRAL VISCOSITY COEFFICIENT (BANKS AND KOCKARTS, 1973)

NEUTRAL SPECIES	A_n (10^{-6}gm cm^{-1} s^{-1})
N_2	4.03
O_2	3.43
O	3.90
H_e	3.84
H	1.22

Thermal conductivity is treated in a similar manner. If all upper atmospheric gases were monatomic, a relation similar to equation (5-57) for ions could be used to obtain the thermal conductivity coefficient from the viscosity coefficient. However, the internal degrees of freedom associated with the diatomic molecules N_2 and O_2 also affect the thermal conductivity. Analysis of experimental data allows correct inclusion of these effects. Banks and Kockarts (1973) are again able to express all temperature variations in a common power law form, permitting the thermal conductivity for the mixture to be written

$$K_n^T = BT^{.69} \tag{5-62a}$$

where

$$B = \sum_n B_n n_n / \sum_n n_n \ . \tag{5-62b}$$

The B_n coefficients are given in Table 5-5.

Table 5-5. COEFFICIENTS FOR COMPUTING THE NEUTRAL THERMAL CONDUCTIVITY COEFFICIENT (BANKS AND KOCKARTS, 1973)

NEUTRAL SPECIES	B_n (erg cm^{-1} s^{-1} $°K^{-1}$)
N_2	56.0
O_2	56.0
O	75.9
H_e	299.0
H	379.0

These relations may be used over the temperature range $200°K \leq T_n \leq 2000°K$. Although the error in O_2 due to curve fitting approximations approaches 20 percent at 2000°K, at altitudes where O_2 is important, temperatures and errors are much lower. Errors for the other gases are smaller than for O_2.

Since viscosity and thermal conductivity are the only transport coefficients appearing in the conservation equations, none others are required for closure of the neutral equations.

THIS PAGE INTENTIONALLY LEFT BLANK

Section VI

NEUTRAL WINDS IN THE AURORAL E REGION DURING GEOMAGNETIC DISTURBANCES

The conservation equations developed in previous sections are somewhat general in the sense that only those approximations appropriate to all E and F region conditions have been applied. For the particular physical circumstances of any specific study, further approximations may be justified. Moreover, observational data may be used to specify some variables so that certain of the equations need not be solved at all, or may be greatly simplified. Also, numerical constraints may require simplifying assumptions which limit the applicability of the results to special circumstances. For these reasons, results of the previous sections must be regarded as appropriate starting points for a wide variety of upper atmospheric investigations, rather than as finished products. The present section is an example of one such investigation, and it illustrates various methods for bridging the gap between the initial set of conservation equations and the final working equations which can be solved numerically within computational constraints.

6.1 INTRODUCTION

Since the incoherent scatter radar facility at Chatanika, Alaska, became operational in 1971, thermal, dynamic, and electrical properties of the ionosphere above that location have been observed under a variety of conditions (e.g. Watkins and Banks, 1974; Brekke, et al., 1973, 1974a, b). Of particular interest are winds generated during geomagnetic disturbances. It is well established that global disturbances of both the charged and neutral components of upper atmospheric gases are associated with geomagnetic storms (Jacchia, et al., 1966; DeVries, 1972; Matuura, 1972; Wu, et al., 1974). The mechanisms by which these disturbances occur at low and middle latitudes remain under study; but neutral winds originating in the auroral region are proposed in some theoretical explanations (e.g., Obayashi and Matuura, 1972). Such winds have apparently been observed in the E region at low latitudes following a magnetic storm (Smith, 1968), and simple estimates, based on observations at high latitudes, support the plausibility of such occurrences (Rees, 1971a).

Hence, extended observations of these neutral winds in the vicinity of their origin, may provide decisive information in establishing the validity of these and other theories.

In this study, attention is directed toward certain aspects of the neutral winds as determined by incoherent scatter radar observations. Because ion velocities, rather than neutral velocities, are observed directly by the radar, the neutral wind velocities must be derived from the ion velocities. One of the approximations required to determine the neutral velocity is that this velocity is uniform over an altitude range of 25 km to 50 km in the E region. Although Brekke, et al. (1973, 1974a) recognize that this condition does not hold, no quantitative estimates of its effects on the derived neutral winds are provided. One of the objectives here is to examine the effect of the neutral velocity altitude structure on neutral velocities derived from the incoherent scatter radar data.

A second objective concerns the origin of neutral winds during geomagnetically disturbed conditions. Brekke, et al. (1974a) note that incoherent scatter radar data alone provides insufficient information to separate the effects of ion drag (collisional coupling) and Joule heating on neutral winds. From observations of high latitude rocket-borne chemical releases at E region altitudes and ground-based magnetometer data, Rees (1971a) concludes that the neutral winds are generated by collisional coupling with electric-field-driven ions. This view is shared by Meriwether, et al. (1973), based on similar data for altitudes above 200 km. On the other hand, from chemical release data below 180 km, Rothwell, et al. (1974) concur in the conclusion of Stoffregen (1972), based on similar data for higher altitudes, that during geomagnetic disturbances, the deviations of observed neutral winds from theoretical models are due to high latitude heating and resultant pressure gradients.

To examine this problem, an approach which is partially direct and partially indirect is employed. In the direct approach, the effects of collisional coupling are computed by numerically solving the ion and neutral momentum equations simultaneously, based on observed electric fields as the driving

force and omitting pressure gradients. If there is good agreement between the calculated and observed velocities, this indicates that collisional coupling is adequate to explain the observations and that effects of pressure gradients are inconsequential. On the other hand, large discrepancies would indicate the opposite. Then, the indirect approach is employed: the discrepancy between the observed and calculated velocities is used to estimate the omitted driving force (pressure gradient).

Data used to carry out the calculations and to provide the observational reference velocities are described in subsection 6.2. In subsection 6.3 details of the theoretical and numerical methods are presented. Model calculations are presented in subsection 6.4 to demonstrate in a simple context the effects to be encountered under realistic conditions with observed electric fields. In subsection 6.5 a series of calculations, designed to meet the objectives outlined above, are discussed in detail. Finally, results of this study are discussed and summarized in subsection 6.6.

6.2 OBSERVATIONAL DATA

6.2.1 Characteristics of the Data

Data used in the calculations and comparisons below were obtained by the incoherent scatter radar facility at Chatanika, Alaska on 15 May 1974. This facility became operational in July, 1971; and early observations have been reported recently in the literature (Doupnik, et al. 1972; Brekke, et al., 1973, 1974 a, b; Banks, et al., 1973; Banks, et al., 1974; among others).

Leadabrand, et al. (1972) have described the equipment and its operating characteristics; and Banks and Doupnik (1974) have recently reviewed the experimental methods and operational modes used with the radar. Therefore, only those aspects pertinent to the analysis of the present data need be summarized here.

Location and geomagnetic field characteristics of Chatanika, Alaska, are given in Table 6-1. Operating at a frequency of 1290 MHz, the Chatanika incoherent scatter radar has a completely steerable dish antenna with a beam width

of .6 degrees. For the experiment on 15 May 1974 the recently developed azimuth scan procedure (Banks and Doupnik, 1974) was employed. Elevation of the antenna was held constant at 76.5 degrees above horizontal and the antenna azimuth was changed at the rate of 1 degree per second. Data were integrated over 15 second intervals (15 degrees in azimuth) to obtain estimates of ion drift velocity vectors and electron density profiles. The 24 estimates, for each 360 degree scan, were then analyzed, using a Fourier analysis technique, to obtain the ion velocity vector in 8 separate range gates and a time-averaged electron density profile for the 6 minute time period. At azimuth 299 degrees (geomagnetic west) on each scan, the direction of antenna rotation was reversed.

Table 6-1. CHATANIKA, ALASKA: LOCATION AND GEOMAGNETIC FIELD PROPERTIES

LOCATION:	Geographic - 65.1°N, 147.45°W Geomagnetic Dipole - 64.75°N, 105°W
TIME:	Alaskan Standard Time (AST) = UT-10 hours
GEOMAGNETIC FIELD:	Dip Angle (I) = 76.5° Magnetic Declination (δ) = 29° East of Geographic North Magnetic Field Intensity (B) = .54 Gauss

A diagram of the azimuth scan method of sampling the ionosphere is presented in Figure 6-1. It is seen that in addition to time-averaging over 6 minutes, this technique averages spatially. For example, the centers of the first two range gates correspond to altitudes of 109 km and 167 km; given the elevation angle, the radar beam samples over horizontal distances of 55 km and 85 km at these altitudes. In addition, due to the time length (τ) of the radar pulse, the radar signal averages ionospheric properties over the spatial extent of the pulse ($c\tau$). Brekke, et al. (1973) note that although the total extent of each range gate is 96 km, the effective length is reduced to 25 km to 50 km due to weighting of the radar signal. This weighting has three components: (1) a triangular factor which is unity at the center of the range gate, decreasing linearly to zero at the ends; (2) a factor which decreases as the inverse square of the range; and (3) the electron number density. The

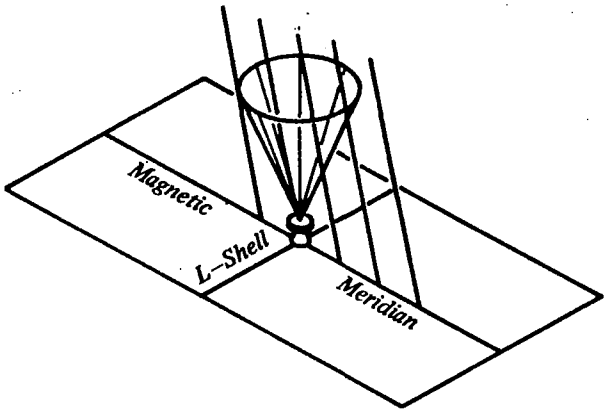

Figure 6-1. DIAGRAM OF THE AZIMUTH SCAN MODE OF OBSERVATION FOR THE INCOHERENT SCATTER RADAR AT CHATANIKA, ALASKA (BANKS AND DOUPNIK, 1974)

first two of these multiplied together are designated by W(z) and are presented graphically by Brekke, et al. (1973); those results are used here with appropriate translation to the proper altitude.

Interspersed with the long radar pulses, used for velocity measurements, were short pulses (with greater range resolution) for electron density determination. Beginning at a range of 73.6 km (71.6 km in altitude, due to the elevation angle), successive values are spaced at range increases of 4.5 km (4.38 km altitude). However, since the signal samples a range of 10 km, adjacent electron density values are not totally independent (Doupnik, 1975). Doupnik (1975) also notes that for electron densities below 10^4 cm^{-3}, true densities are underestimated by the radar because the Debye length becomes comparable to the radar wavelength. In addition, measured densities must be multiplied by a factor of $(1 + T_e/T_i)/2$ to obtain true values. For E region altitudes, $T_e/T_i = 1$ may be a reasonable approximation, however, not for higher altitudes. Since present interest is in the E region (and in the absence of temperature measurements), the electron density measurements are used without modification.

Geomagnetic activity during the experiment was relatively high globally; 15 May 1974 was designated one of the 5 disturbed days for that month (Lincoln, 1974). Values of the global three-hour geomagnetic range index K_p varied from 3- to 5+, averaging about 4. These, together with local index K for College, Alaska, are shown in Table 6-2.

Table 6-2. GLOBAL (K_p) AND LOCAL (K) (COLLEGE, ALASKA) THREE-HOUR GEOMAGNETIC RANGE INDICES FOR 15 MAY 1974

PERIOD:	1	2	3	4	5	6	7	8
K_p	4+	3-	4-	5-	5+	4+	3	4+
K	4	2	3	6	7	6	3	3

6.2.2 Data Analysis

From the ion flow velocities measured in different range gates, values of the electric field and the altitude-averaged E region neutral wind can be determined. The procedure for accomplishing this is described in some detail by Brekke, et al. (1973); it will be summarized here. This procedure is followed exactly since it provides the currently-accepted observed values from the incoherent scatter radar method. Part of the objective of this study is to compare theoretical calculations with standard observed values; so in treating the data, the established procedures are used without deviation.

At high altitudes where $\omega_i >> \nu_{in}$, ions move with the Hall drift velocity ($\vec{E} \times \vec{B}\, c/B^2$) (cf. electron momentum equation (4-36)). The vector equation relating the ion velocity to the electric field can then be solved for the electric field in terms of the ion velocity at high altitudes. At low altitudes where $\omega_i \lesssim \nu_{in}$, collisions with neutrals as well as the electric field affect the ion motion. With the electric field known from the high altitude ion velocity measurements, the ion velocities observed at low altitudes can be used to determine the neutral wind velocity.

These qualitative considerations can now be put on a quantitative basis. If gravitational and pressure gradient terms are assumed to be small compared with electric and magnetic field terms, the ion momentum equation (4-40) can

be written in the form

$$\frac{\bar{\nu}_{in}}{\bar{\omega}_i} (\vec{v}_n - \vec{v}_i) + \frac{\vec{E}}{B} c + \vec{v}_i \times \frac{\vec{B}}{B} = 0 \quad . \tag{6-1}$$

From this equation it is apparent that if $\bar{\omega}_i >> \bar{\nu}_{in}$, the electric field components transverse to the magnetic field can be obtained from ion flow velocities from the equation

$$\vec{E} + \frac{\vec{v}_i}{c} \times \vec{B} = 0 \quad . \tag{6-2}$$

Brekke, et al. (1973) find that the ion velocity measured in the second range gate (centered at 167 km) shows little rotation from those at higher range gates. They conclude that the electric field can be adequately determined from equation (6-2), using observed ion velocities from the second range gate. In the model to be discussed later (similar to that used by Brekke, et al. (1973)), it is found that at this altitude $\bar{\nu}_{in}/\bar{\omega}_i \sim .05$, thus the collision term in equation (6-1) is expected to be unimportant, consistent with the observations.

By taking scalar and cross products of $\vec{B}$ with equation (6-1), that equation can be solved explicitly for $\vec{v}_i$, with the result

$$\vec{v}_i = \left[\frac{1}{1 + (\bar{\omega}_i/\bar{\nu}_{in})^2}\right]\left[\vec{v}_n + \frac{\bar{\omega}_i}{\bar{\nu}_{in}} \frac{\vec{E}}{B} c + \frac{\bar{\omega}_i}{\bar{\nu}_{in}} \vec{v}_n \times \frac{\vec{B}}{B} + \left(\frac{\bar{\omega}_i}{\bar{\nu}_{in}}\right)^2 \frac{\vec{E} \times \vec{B}}{B^2} c + \left(\frac{\bar{\omega}_i}{\bar{\nu}_{in}}\right)^2 \frac{\vec{v}_n \cdot \vec{B}}{B}\right] , \tag{6-3}$$

where the component of $\vec{E}$ parallel to $\vec{B}$ has been assumed to be negligible compared to the components transverse to $\vec{B}$. Equation (6-3) holds at each altitude; however, observed ion velocities are weighted averages over altitude. Therefore, similar averaging must be applied to this equation.

Based on the weighting of the incoherent scatter radar signal, discussed in the previous section, Brekke, et al. (1973) determine that the weighted averages can be represented as

$$\bar{\vec{v}}_i = \int_{z_1}^{z_2} N_e(z)\, W(z)\, \vec{v}_i(z)\, dz \Big/ \int_{z_1}^{z_2} N_e(z)\, W(z)\, dz \quad . \tag{6-4}$$

Limits of integration correspond to the boundaries of the range gate; this is accomplished in effect by the vanishing of the weighting function W(z) at these boundaries. This weighting function represents the linear decrease from the center of the range gate divided by the square of the range; it is shown for the first range gate in Figure 6-2. It is a consequence of this weighting by W(z) and $N_e(z)$ that the effective width of the first range gate is reduced from 96 km to 25 km to 50 km.

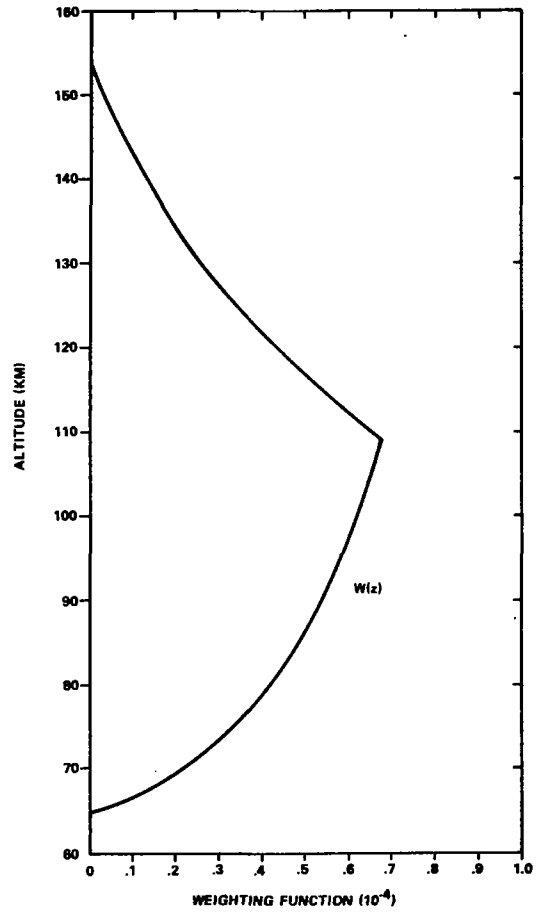

Figure 6-2. INCOHERENT SCATTER RADAR WEIGHTING FUNCTION W(Z) (BREKKE, ET AL. 1973)

In order to apply this averaging technique to the right side of equation (6-3) and obtain useful results, Brekke, et al. (1973) make the following assumptions: (1) the neutral wind velocity has a uniform value $\vec{V}_n$ throughout the first range gate; (2) the electric field determined from the second range gate is mapped down magnetic field lines to the bottom of the first range gate with no change in either magnitude or direction. Under these conditions,

equation (6-3) can be multiplied by $N_e(z)\ W(z)$, integrated over altitude and normalized by the denominator on the right side of equation (6-4) to obtain

$$\vec{V}_i = \kappa_3 \vec{V}_n + \kappa_1 \vec{V}_n \times \vec{B}/B + \kappa_1 \frac{\vec{E}}{B} c + \kappa_2 \frac{\vec{E} \times \vec{B}}{B^2} c$$

$$+ \kappa_2 (\vec{V}_n \cdot \vec{B})\vec{B}/B^2 \quad . \tag{6-5}$$

The κ-coefficients are given by

$$\kappa_1 = \frac{1}{I_W} \int_{z_1}^{z_2} \frac{\bar{\omega}_i\ \bar{\nu}_{in}(z)\ N_e(z)\ W(z)}{\bar{\nu}_{in}^2(z) + \bar{\omega}_i^2}\ dz \quad , \tag{6-6a}$$

$$\kappa_2 = \frac{1}{I_W} \int_{z_1}^{z_2} \frac{\bar{\omega}_i^2\ N_e(z)\ W(z)}{\bar{\nu}_{in}^2(z) + \bar{\omega}_i^2}\ dz \quad , \tag{6-6b}$$

$$\kappa_3 = 1 - \kappa_2 \quad , \tag{6-6c}$$

where

$$I_W = \int_{z_1}^{z_2} N_e(z)\ W(z)\ dz \quad . \tag{6-6d}$$

The ion velocity on the left side of equation (6-5) now represents the velocity as observed by the incoherent scatter radar.

To determine the neutral velocity, equation (6-5) is solved explicitly for $\vec{V}_n$, in the same manner as equation (6-3) was obtained, with the result

$$\vec{V}_n = \left[\frac{1}{\kappa_1^2 + \kappa_3^2}\right]\left[\kappa_3 \vec{V}_i - \kappa_1 \left(\vec{V}_i \times \frac{\vec{B}}{B} + \frac{\vec{E}}{B} c\right)\right.$$

$$\left. + \frac{(\kappa_1^2 - \kappa_2\kappa_3)}{B^2} [\vec{E} \times \vec{B}\ c + (\vec{V}_i \cdot \vec{B})\vec{B}]\right] . \tag{6-7}$$

(Equation (6-7) corrects a typographical error in equation (11) of Brekke, et al. (1973).) From this equation the height-averaged neutral wind is determined from incoherent scatter radar data. Ion velocity $\vec{V}_i$ is obtained from

the first range gate; $\vec{E}$ is obtained from ion velocities in the second range gate (through equation (6-2)); and the χ-coefficients are evaluated from electron number density measurements and a collision frequency model (to be discussed later).

By means of these techniques, Chatanika incoherent scatter radar observations made on 15 May 1974 have been analyzed. Resulting electric field values are shown in Figure 6-3a; and horizontal neutral velocities, determined from equation (6-7), are shown in Figure 6-3b. It should be noted that the x-component is defined positive to the south, while the meridional component in the figures of Brekke et al. (1973, 1974a) is defined positive to the north. Values shown in Figures 6-3a, b are used in the calculations and comparisons below.

The electric field components in Figure 6-3a show two distinct periods of enhancement, the first extending from about 06 to 11 hours UT and the second from about 12 to 18 hours UT. During the calm periods, electric fields have values generally less than about 10 mV m^{-1}, while during disturbances they have values of several tens of millivolts per meter. Rapid variations in magnitude are the rule; but reversals of direction which persist with the large magnitude electric fields, occur only once, shortly before local midnight (1000 UT). This reversal is a general feature of this local time period. It is associated with the Harang discontinuity (Heppner, 1973), originally observed as a reversal of ion flow direction.

Neutral velocities shown in Figure 6-3b are notable for their rapid and sometimes quite large fluctuations in both magnitude and direction. Since this indicates large variations during the peirod over which the data are averaged, large errors are likely (Brekke et al. 1973, 1974a). Nevertheless, the trend of the data is clear: except for occasional large fluctuations, magnitudes of the neutral velocity components are generally near or less than about 125 m s^{-1}. Periods of greatest velocity fluctuations correspond to periods of enhanced electric field. These results will be examined more closely in the comparisons with calculated velocities.

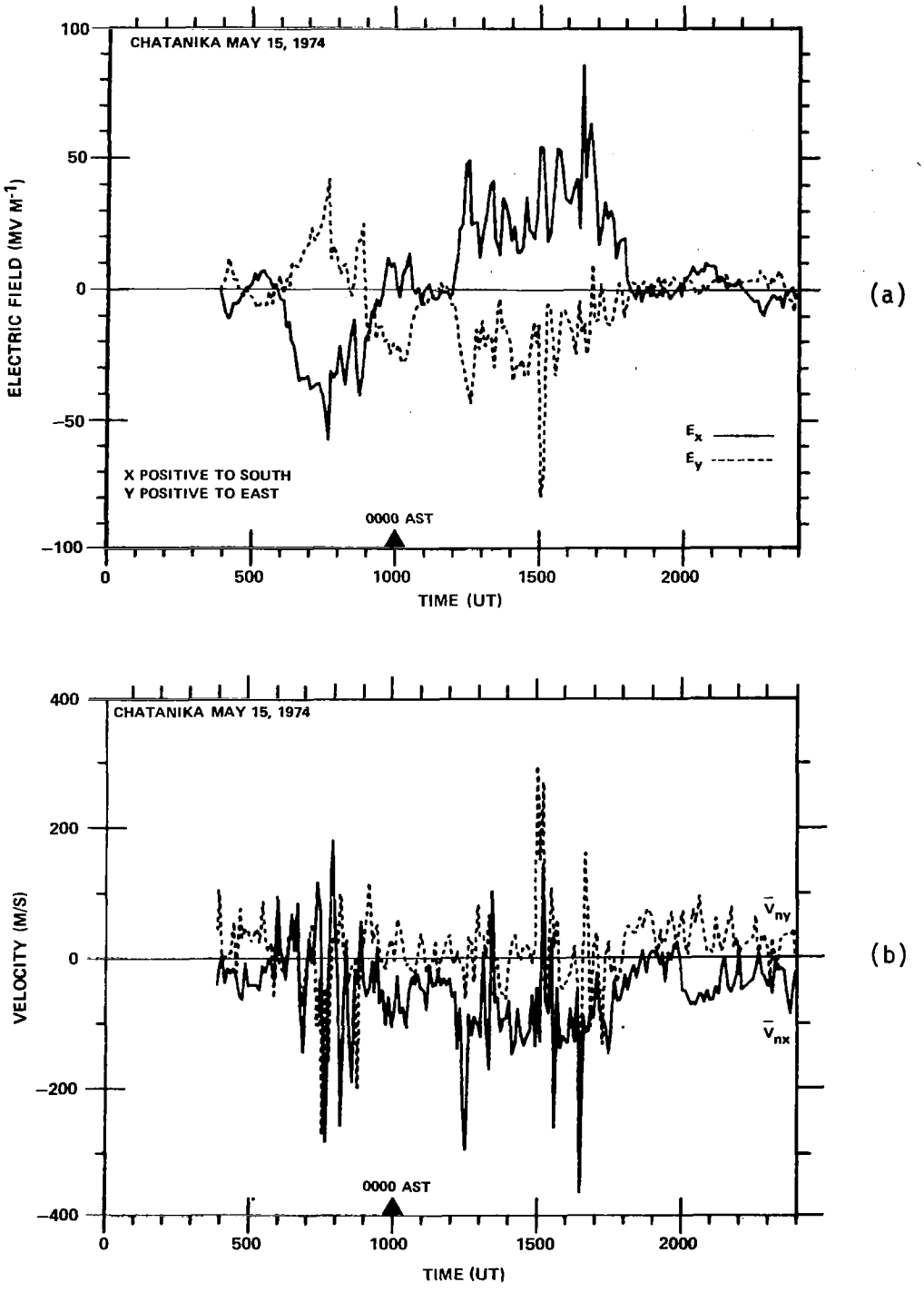

Figure 6-3. ELECTRIC FIELDS (a) AND NEUTRAL WINDS (b) IN GEOGRAPHIC COORDINATES, AS DETERMINED FROM INCOHERENT SCATTER RADAR OBSERVATIONS AT CHATANIKA, ALASKA ON 15 MAY 1974

6.3 THEORETICAL APPROACH

6.3.1 Physical and Mathematical Description

As noted previously, the effects of collisional coupling in neutral wind generation are to be determined. In simplest terms, an external electric field causes the ions to move. Collisions of ions with neutrals both modify the ion motion and cause the neutrals to move. It is the resultant motions of the neutrals, as functions of altitude and time, that are of particular interest. Model calculations of this nature have been presented by Fedder and Banks (1972). However, they differ from the present calculations in two important respects: theirs neglected coriolis effects and they were only model calculations with no explicit comparison with experiment possible. The first of these differences is examined in similar model calculations in subsection 6.4 to determine the importance of the coriolis term. The second difference, use of observed electric fields and comparison of corresponding calculated velocities with observed velocities, allows the importance of this collisional coupling in neutral wind generation to be assessed.

The theoretical framework has been developed in previous sections. Here, in the application of this framework, it remains to apply those additional approximations which the more restrictive conditions of a particular problem permit. And then a method for determining each remaining unknown quantity must be specified, either by including an appropriate equation in the system to be solved, or by adopting appropriate model values. This translation of the physical problem to a mathematical and numerical problem is accomplished below.

The coupled ion and neutral equations of motion (4-65c) and (4-65d) are the appropriate starting points. In consonance with discussions in Section V, the ion pressure tensor term is neglected in comparison with the scalar pressure term. Thus, the initial equations are

$$\vec{v}_i = \vec{v}_n + \frac{1}{\bar{\nu}_{in}}\left[\bar{\omega}_i \frac{\vec{E}}{B} c + \vec{v}_i \times \bar{\omega}_i + \vec{g} - \frac{1}{\rho_i} \nabla p_i\right], \qquad (6\text{-}8a)$$

$$\frac{\partial \vec{v}_n}{\partial t} = -(\vec{v}_n \cdot \nabla)\vec{v}_n - \frac{1}{\rho_n} \nabla p_n - \frac{1}{\rho_n} \nabla \cdot \overline{\overline{\tau}}_n$$

$$+ \vec{g} + 2\vec{v}_n \times \vec{\Omega}_E - \bar{\nu}_{ni}(\vec{v}_n - \vec{v}_i) \quad , \tag{6-8b}$$

where

$$(\overline{\overline{\tau}}_n)_{\alpha\beta} = -\eta_n \left[\frac{\partial v_{n\alpha}}{\partial x_\beta} + \frac{\partial v_{n\beta}}{\partial x_\alpha} \right] + \frac{2}{3} \eta_n \delta_{\alpha\beta} \nabla \cdot \vec{v}_n \tag{6-8c}$$

in Cartesian tensor notation (equation (4-33)).

In addition to being coupled to each other, these equations are coupled to the continuity and energy equations through mass densities (ρ_n, ρ_i), pressures (p_n, p_i) and collision frequencies ($\bar{\nu}_{in}$, $\bar{\nu}_{ni}$). Thus, additional information or equations are required in order to solve equations (6-8). From the incoherent scatter radar observations, electron number density profiles are available. Ion composition cannot be obtained from these observations, so an ion composition model, based on the rocket-borne mass spectrometer measurement of Kopp, et al. (1973) at high latitudes (68°N), is used. With this information, the ion continuity equation is no longer required. Since electric fields and velocities are generally large throughout the experiment, the order-of-magnitude estimates in Section IV indicate that the pressure gradient and gravitational terms can be dropped from the ion equation (6-8a). In addition, at the altitudes of interest (90 km to 200 km) the ion temperature can be assumed equal to the neutral temperature (required only for collision frequency calculations). These approximations and assumptions obviate the use of the ion energy equation.

To supplement the neutral equation of motion a model atmosphere is adopted to provide neutral number densities and temperatures. This approach is taken partly to keep the computational effort reasonable and partly due to lack of information. Since temperature measurements were not made in the experiment of 15 May 1974, there is no means for monitoring any theoretical calculations of temperature. Also, by using a static model for neutral temperature and

densities, the source of calculated velocity variations can be more easily identified. For a series of calculations of increasing complexity, this approach is a reasonable first step.

The neutral atmospheric model adopted is the Jacchia 1971 model (Jacchia, 1971; also cf. CIRA 1972) for an exospheric temperature of 1000°K (see Figure 1-3). Although this choice of exospheric temperature is arbitrary, it does correspond to the exospheric temperature used by Brekke, et al (1973, 1974a) in their data analysis (however, they employed a neutral model by Banks and Kockarts (1973)). Effects of model differences will be discussed later. It may be noted that recent temperature measurements reported by Watkins and Banks (1974) indicate that 1000°K is a reasonable choice for the exospheric temperature for a problem such as this. Their observations show no pronounced diurnal variations; however, temperature excursions of 100°K to 300°K over time periods of an hour, associated with large electric fields, are common.

As a result of using a model atmosphere, the continuity and energy equations are no longer required. However, there is an additional consequence for the neutral momentum equation. The Jacchia 1971 model is a static diffusion model in which it is assumed that each neutral constituent is in diffusive equilibrium. For present purposes the important feature of this condition is that the vertical pressure gradient exactly balances the gravitational acceleration in the momentum equation - there is no vertical motion. In reality, small vertical velocities are observed (Rieger, 1974). However, because the gravitational and pressure gradient terms are larger than the velocity terms, by factors of 10^2 to 10^3 under these conditions, a relatively small adjustment of the pressure gradient can counteract vertical motions, causing them to vanish or remain quite small. Consequently, vertical motions are suppressed in equations (6-8b) and (6-8c): diffusive equilibrium is assumed.

Finally, all horizontal gradients are neglected. This is required by the fact that all observations are made at a single location: no information on the horizontal variation of properties is available. Implicit in this assumption is horizontal uniformity, which is a bad assumption at high latitudes.

However, horizontal gradients affect only certain terms and if these terms are small relative to others, the consequences may be negligible. One of the objectives of this calculation is to test this assumption.

With the approximations and assumptions made, the ion equation of motion in equation (6-8a) reduces to

$$\vec{v}_i = \vec{v}_n + \frac{\bar{\omega}_i}{\bar{\nu}_{in}} \left[\frac{\vec{E}}{B} c + \vec{v}_i \times \frac{\vec{B}}{B} \right] , \qquad (6\text{-}9)$$

which is equivalent to equation (6-1). The neutral equation (6-8b) is correspondingly reduced to

$$\frac{\partial \vec{v}_n}{\partial t} = - \frac{1}{\rho_n} \nabla \cdot \bar{\bar{\tau}}_n - \bar{\nu}_{ni} (\vec{v}_n - \vec{v}_i) + 2\vec{v}_n \times \vec{\Omega}_E \quad , \qquad (6\text{-}10)$$

where the form of $\bar{\bar{\tau}}_n$ remains as given in (6-8a), but many of the terms vanish.

To solve equations (6-9) and (6-10) numerically, they must first be decomposed into scalar component equations. Based on physical considerations, it is convenient to treat these equations in two different Cartesian coordinate systems; the computer can easily transform the coordinates numerically as required for calculations. The ion equation is treated in a system designated here as "plasma" coordinates (1, 2, 3), in which the 3-component is parallel to $\vec{B}$, the 2- component is toward geomagnetic east in the plane transverse to $\vec{B}$, and the 1-component lies in the geomagnetic meridian plane; this is shown in Figure 6-4a. The neutral equation is decomposed in a local Cartesian coordinate system (x, y, z) oriented along geographic coordinates with x positive to the south, y positive to the east, and z positive vertically upward, as shown in Figure 6-4b. Angular relations between the coordinate systems are shown in Figure 6-4c. Transformation equations between these coordinates for an arbitrary vector $\vec{q}$ are:

(i) From plasma coordinates (1, 2, 3) to local geographic coordinates (x, y, z)

$$q_x = q_2 \sin \delta - \cos \delta (q_1 \sin I + q_3 \cos I) \qquad (6\text{-}11a)$$

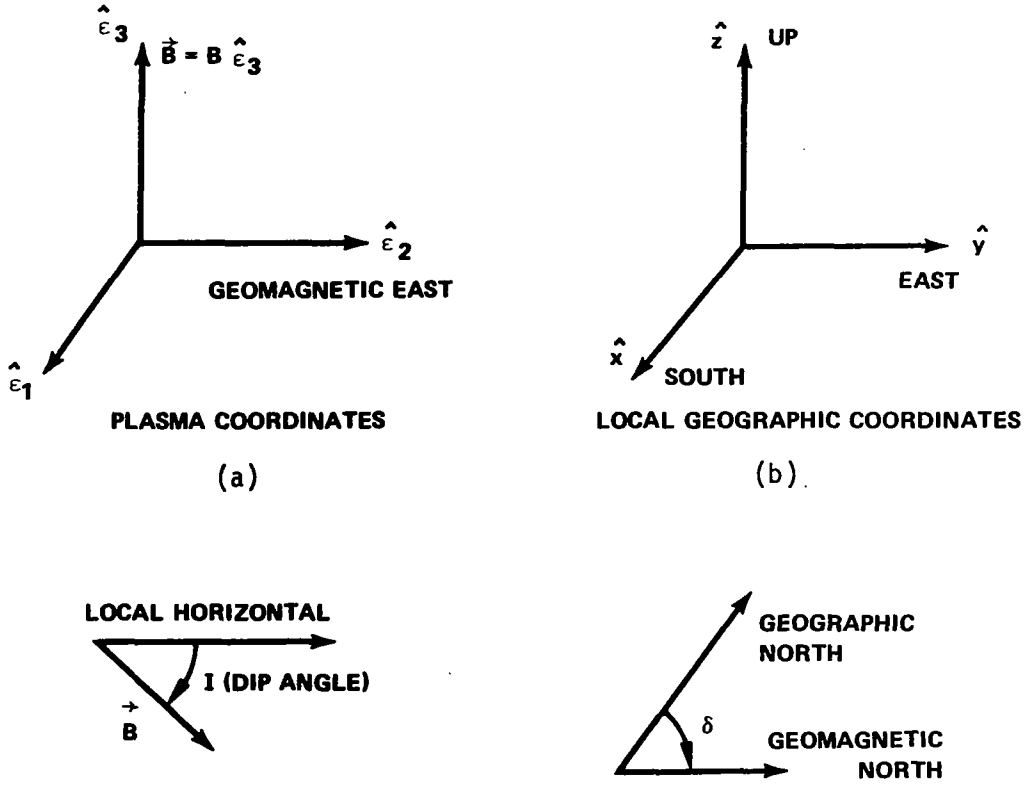

Figure 6-4. DEFINITIONS OF COORDINATE SYSTEMS AND ANGLES RELATING THEM

$$q_y = q_2 \cos\delta + \sin\delta(q_1 \sin I + q_3 \cos I) \tag{6-11b}$$

$$q_z = q_1 \cos I - q_3 \sin I \tag{6-11c}$$

(ii) From local geographic coordinates (x, y, z) to plasma coordinates (1, 2, 3)

$$q_1 = q_z \cos I - \sin I(q_x \cos\delta - q_y \sin\delta) \tag{6-12a}$$

$$q_2 = q_x \sin\delta + q_y \cos\delta \tag{6-12b}$$

$$q_3 = -q_z \sin I - \cos I(q_x \cos\delta - q_y \sin\delta) \quad . \tag{6-12c}$$

Consistent with the assumptions of Brekke, et al. (1973, 1974a) and discussions in Sections I and IV, the electric field is assumed to be uniform, and the component parallel to the geomagnetic field is assumed to be negligible. In the plasma coordinate system this is given by

$$E_3 = 0 \quad . \tag{6-13a}$$

If this is used in equation (6-12c), E_z can be expressed in the terms of E_x and E_y as

$$E_z = -\cot I(E_x \cos\delta - E_y \sin\delta) \quad . \tag{6-13b}$$

When the ion momentum equation (6-9) is written out in plasma coordinates, the directional coupling due to the Lorentz force can be removed algebraically giving the explicit results

$$v_{i1} = \left[\frac{1}{1 + (\bar{\omega}_i/\bar{\nu}_{in})^2}\right]\left[v_{n1} + \frac{\bar{\omega}_i}{\bar{\nu}_{in}}\left(\frac{E_1}{B}c + v_{n2}\right) + \left(\frac{\bar{\omega}_i}{\bar{\nu}_{in}}\right)^2 \frac{E_2}{B}c\right] \tag{6-14a}$$

$$v_{i2} = \left[\frac{1}{1 + (\bar{\omega}_i/\nu_{in})^2}\right]\left[v_{n2} + \frac{\bar{\omega}_i}{\bar{\nu}_{in}}\left(\frac{E_2}{B}c - v_{n1}\right) - \left(\frac{\bar{\omega}_i}{\bar{\nu}_{in}}\right)^2 \frac{E_1}{B}c\right] \tag{6-14b}$$

$$v_{i3} = v_{n3} \tag{6-14c}$$

The neutral velocity component equations in local geographic coordinates are

$$\frac{\partial v_{nx}}{\partial t} = \frac{\eta_n}{\rho_n}\frac{\partial^2 v_{nx}}{\partial z^2} - \bar{\nu}_{ni}(v_{nx} - v_{ix}) + 2v_{ny}\,\Omega_E \sin\lambda \qquad (6\text{-}15a)$$

$$\frac{\partial v_{ny}}{\partial t} = \frac{\eta_n}{\rho_n}\frac{\partial^2 v_{ny}}{\partial z^2} - \bar{\nu}_{ni}(v_{ny} - v_{iy}) - 2v_{nx}\,\Omega_E \sin\lambda \qquad (6\text{-}15b)$$

$$v_{nz} = 0\ , \qquad (6\text{-}15c)$$

where λ is geographic latitude. To obtain the viscous terms in this form, it is assumed that the viscosity coefficient varies slowly in altitude compared with neutral velocity variations, an assumption which has been found to be valid.

The set of neutral velocity component equations is seen to be a set of coupled (in the coriolis terms) partial differential equations, first order in time and second order in space. In addition to being coupled among themselves, these equations are coupled to the ion equations through the collision terms. Although the ion equations are of a time-independent form, the ion velocities are implicit functions of time through the time dependence of the electric field and the neutral velocities. Since $\vec{E}$ and $\bar{\nu}_{ni}$ (which varies directly with N_e) are specified outside the system of equations (from scatter radar observations), numerical solution is the only feasible approach.

Collision frequencies are computed according to equation (4-14c) and the species collision frequencies presented in subsection 5.3.3. Because static models of the neutral atmosphere and ion composition are employed, the ion-neutral collision frequencies $\bar{\nu}_{in}$ remain fixed throughout the calculation. However, as noted above, $\bar{\nu}_{ni}$ varies with N_e and must be updated from observation. The viscosity coefficient is evaluated from equations (5-61a, b). Since it depends only on the neutral model, the viscosity altitude profile is constant throughout the calculation.

6.3.2 Numerical Methods and Boundary Conditions

To solve equations (6-61a, b) an explicit finite difference technique is employed. For this discussion, let subscript m designate the spatial grid index and superscript n the time grid index, as shown in Figure 6-5. The partial derivative of a variable V with respect to time is approximated by the finite difference expression

$$\frac{\partial V}{\partial t} \simeq \frac{V_m^{n+1} - V_m^n}{\Delta t} \quad , \tag{6-16}$$

where Δt is the uniform grid spacing in the t direction. Similarly, the second partial derivative of V with respect to z is approximated by

$$\frac{\partial}{\partial z}\left(\frac{\partial V}{\partial z}\right) \simeq \frac{V_{m+1}^n - 2V_m^n + V_{m-1}^n}{(\Delta z)^2} \quad , \tag{6-17}$$

where Δz is the grid spacing in the x-direction.

To use these expressions, equations (6-15a, b) are first placed in the form

$$\frac{\partial v_{nx}}{\partial t} = Q(z) \frac{\partial^2 v_{nx}}{\partial z^2} + R(v_{nx}, v_{ny}, v_{ix}, z) \tag{6-18a}$$

$$\frac{\partial v_{ny}}{\partial t} = Q(z) \frac{\partial^2 v_{ny}}{\partial x^2} + S(v_{nx}, v_{ny}, v_{iy}, z) \quad , \tag{6-18b}$$

where the functions Q, R, S can be identified by comparison with equations (6-15a, b). When the derivatives in equations (6-18a, b) are replaced according to equations (6-16) and (6-17), the resulting equations can be placed in the form

$$(v_{nx})_m^{n+1} = (v_{nx})_m^n + \frac{\Delta t}{(\Delta z)^2} Q(z_m)[(v_{nx})_{m+1}^n - 2(v_{nx})_m^n + (v_{nx})_{m-1}^n]$$

$$+ \Delta t \, R((v_{nx})_m^n, (v_{ny})_m^n, (v_{ix})_m^{n+1}, z_m) \tag{6-19a}$$

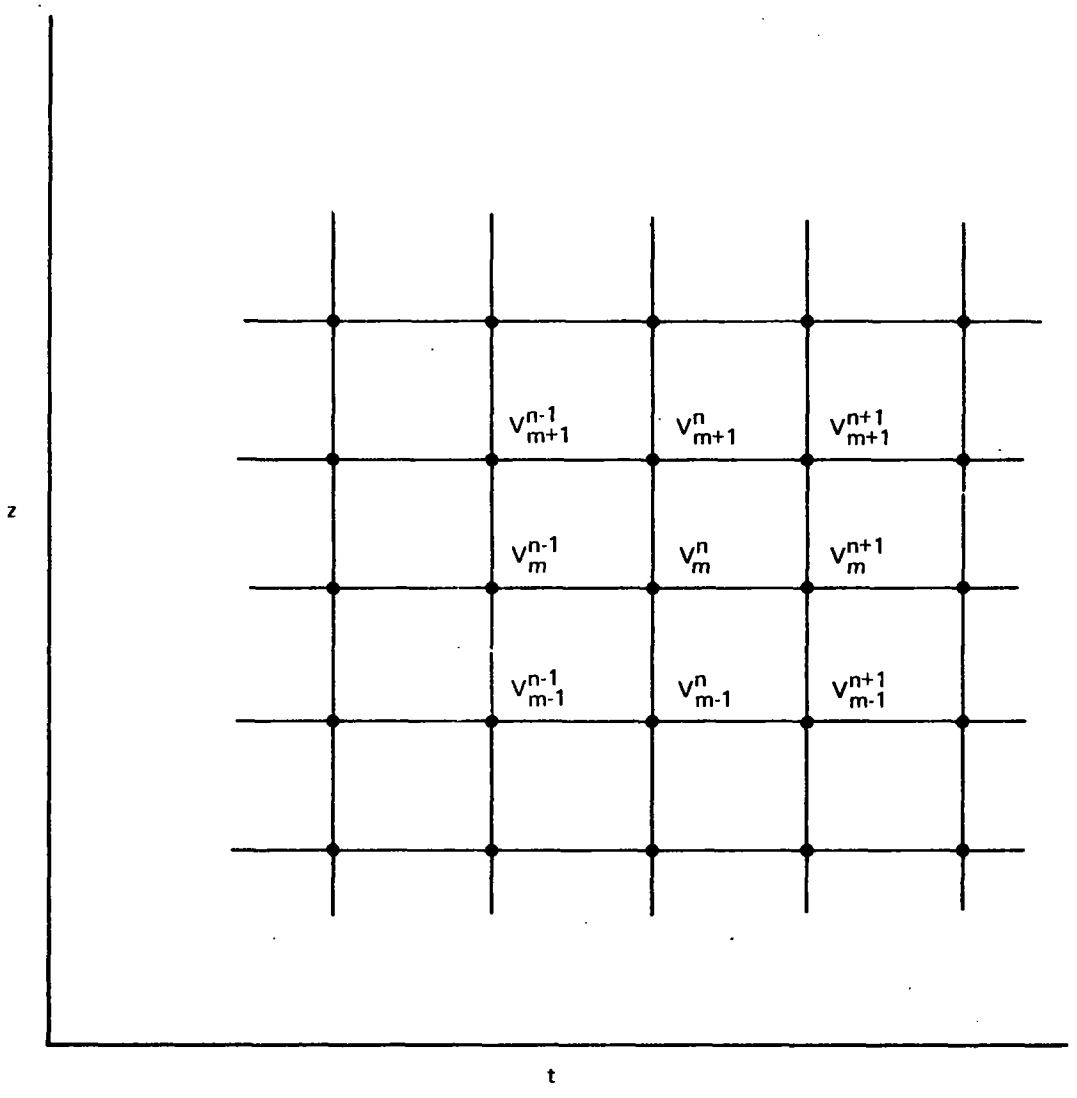

Figure 6-5. GRID POINT DESIGNATION IN DISCRETE z-t SPACE FOR A VARIABLE V

$$(v_{ny})_m^{n+1} = (v_{ny})_m^n + \frac{\Delta t}{(\Delta z)^2} Q(z_m)[(v_{ny})_{m+1}^n - 2(v_{ny})_m^n + (v_{ny})_{m-1}^n]$$

$$+ \Delta t\, S\left((v_{nx})_m^n,\ (v_{ny})_m^n,\ (v_{iy})_m^{n+1},\ z_m\right) \qquad (6\text{-}19b)$$

Evaluation of equations (6-19a, b) requires the specification of initial and boundary conditions. For initial conditions, the neutral velocities are taken to be zero. Consequences of this assumption will be discussed later. Because a second spatial derivative is involved; two boundary conditions must be specified. For finite difference equations of the form in (6-19), it is appropriate to specify one condition at each boundary in z. Thus, the lower boundary is taken to be 90 km and the neutral velocity is assumed to vanish there. At the upper boundary, z = 250 km, the vertical derivative of the neutral velocity is assumed to vanish. Tests involving changes of these boundary conditions have shown that the lower boundary condition has negligible effects at 100 km and above, while the upper boundary condition has negligible effects on results at and below 200 km. These results are consistent with similar results reported by Fedder and Banks (1972), who find that significant boundary condition effects are limited to within about one scale height of the boundary (scale heights are approximately 5 km at 90 km and 40 km at 250 km).

It has been found that the grid steps Δt and Δz cannot be selected independently, due to numerical instabilities. Although the form of equations (6-18a, b) is somewhat more complicated, the stability criterion for the usual diffusion equation (equations (6-18a,b) with R and S set to sero) has proved to be a reliable indicator. This criterion, as given by Potter (1973), requires that the inequality

$$\Delta t \leq \frac{1}{2} \frac{(\Delta z)^2}{Q(z)} \qquad (6\text{-}20)$$

be satisfied throughout the domain of the calculation. Accordingly, the grid steps employed are Δz = 5 km and Δt = 20 seconds. Inequality (6-20) is satisfied at all altitude from 90 km to 250 km, although the limit is approached at the upper boundary. Considerations of requirements of the physical problem, computer storage and processing times, and numerical stability were all taken

into account to arrive at the grid step sizes and location of the upper boundary for the calculation.

One of the early numerical tests performed with this set of equations was the use of the time-dependent ion equations of motion, to determine conditions for which the time-independent form is valid. The time-dependent ion equations of motion have the finite difference form (taking the 1-component as an example)

$$(v_{i1})_m^{n+1} = (v_{i1})_m^n + \Delta t \left[\bar{\omega}_i \frac{E_1}{B} c + \bar{\omega}_i (v_{i2})_m^n - \bar{\nu}_{in} [(v_{i1})_m^n - (v_{n1})_m^n] \right] \quad . \tag{6-21}$$

With an initial condition of $\vec{v}_i = 0$, it was found that for $\Delta t > \tau_{in}$, where $\tau_{in} = 1/\bar{\nu}_{in}$ is the mean time between ion-neutral collisions, numerical instabilities rapidly developed. This is easily understood from the equations. Initially, the electric field term is the only nonzero term in both ion and neutral equations. If it accelerates the ions for a time $\Delta t > \tau_{in}$, the ions attain an unrealistically large velocity. Neutrals respond slowly to ion collisions because of much larger number densities, so the neutral velocity remains close to zero. In the next time step and thereafter, the collision term in (6-21) dominates, with the result that the sign of the velocity alternates with each succeeding time step, and grows rapidly in magnitude. For $\Delta t < \tau_{in}$, this does not occur, and reasonable results can be obtained.

For a constant electric field, it was found that the ion velocity reaches essentially equilibrium values in 6 to 8 collision times (τ_{in}). Since τ_{in} varies from 3×10^{-5} seconds at 90 km to 1 second at 250 km (for models used here), a wide range of equilibrium times corresponds to the altitude range under study. The difficulties in using equation (6-21) under such circumstances are apparent. However, the important point of these results is not the range, but the fact that all times are short compared to the time scales of interest here. Since the Chatanika incoherent scatter radar observations are averaged over about 6 minutes, that is the time scale for change of the electric field. Hence, use of the time-independent ion momentum equations introduces

essentially no error into the calculation; and the ion velocity field can be considered to be always in equilibrium with the electric field and neutral velocity field. This results in a considerable reduction of the computational effort.

6.4 MODEL CALCULATIONS

Before performing an extended calculation and attempting to interpret the results, it is helpful to assess the importance of the various factors involved. While order-of-magnitude estimates are useful in judging the immediate effect of a variable on the system, total effects over extended periods of time are difficult to determine by this means. This is one purpose of the model calculations to be presented here. By adopting a simple electric field model and a static ion density model, the temporal response, or rise time, of the ion-neutral wind system can be determined. Effects of coriolis and viscous forces can be ascertained by selectively removing these terms from the equations and re-solving the problem. Once these effects are known, a better interpretation of the results for the physically realistic problem can be formulated.

A model calculation of this nature has been performed by Fedder and Banks (1972). They consider a polar cap case in which magnetic field lines are vertical; and they retain the time-dependent form for the ion equations. Otherwise, their assumptions, approximations and resulting equations correspond to those above, with one important exception: they neglect the coriolis term. Effects of the coriolis force have been found to be significant by Heaps (1972) in calculations of high-latitude thermospheric winds over extended times; and it is expected that they should be significant here also. Since the analysis of Fedder and Banks (1972) treated the effects of collisional coupling and viscosity in some detail, the model calculations here are primarily to supplement those results by including coriolis effects. To accomplish this most clearly, the quasi-step function electric field used by Fedder and Banks (1972) is employed here:

$$\vec{E} = -E(t)\hat{y} \qquad (6\text{-}22a)$$

where

where

$$E(t) = 0, \quad t < 0$$

$$E(t) \quad 20[1 - \cos(\pi t/1800)] \text{ mV m}^{-1}, \quad 0 \leq t \leq 1800 \text{ seconds}$$

$$E(t) = 40 \text{ mV m}^{-1}, \quad t > 1800 \text{ seconds}$$

(6-22b)

For these calculations, geomagnetic field geometry corresponding to Chatanika, Alaska is used. Differences in results between this geometry and the polar cap geometry of Fedder and Banks (1972) are small except for the vertical component of ion velocity, which is not considered in detail here. A representative ionization profile is used in conjunction with the ion composition and neutral atmospheric models previously discussed to compute required collision frequencies. The ionization-density profile and resulting collision-frequency and gyrofrequency profiles are shown in Figure 6-6.

Calculations for the electric field model in equations (6-22a, b) have been carried out for a period of 24 hours, both with and without the coriolis force. The ion and neutral horizontal velocity components (geographic coordinates) thus obtained are shown in Figure 6-7 as functions of time for altitudes of 115 km, 125 km, and 150 km. Velocities computed without the coriolis force in Figures 6-7 a, c are consistent with the results of Fedder and Banks (1972); the more rapid response of their neutral velocities to the ion velocity driving force is due to their use of larger collision frequencies.

In this approximation, it is seen that neutral velocity x-components (Hall drift direction) approach the ion-flow velocity over time periods of ten hours and more, the longer times corresponding to lower altitudes. This altitude variation of response times is understood in terms of neutral densities increasing exponentially with decreasing altitude, in effect reducing the degree of ionization, even for little change in ionization number density. At low altitudes, the neutral atmosphere thus requires a larger total transfer of momentum to achieve a given velocity than at higher altitudes. Since the rate of momentum transfer varies less with altitude than the neutral number density,

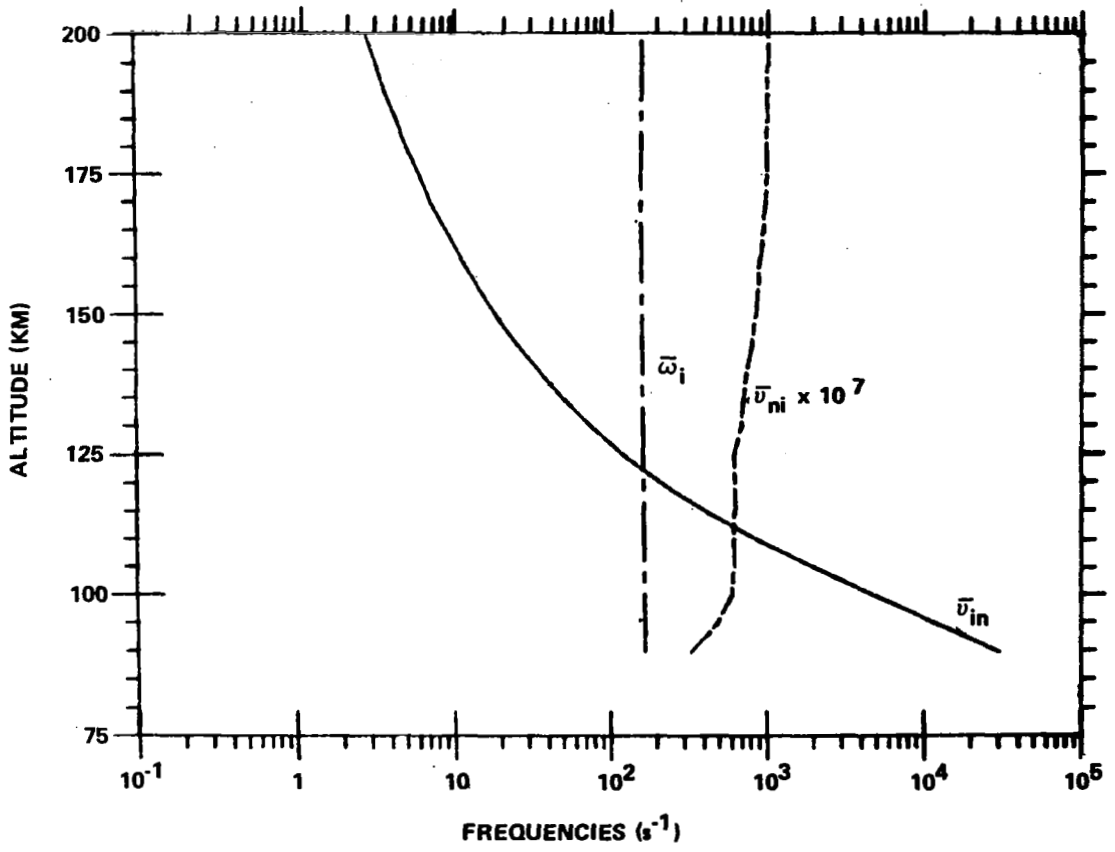

Figure 6-6. COLLISION FREQUENCIES AND GYROFREQUENCY USED IN MODEL CALCULATIONS

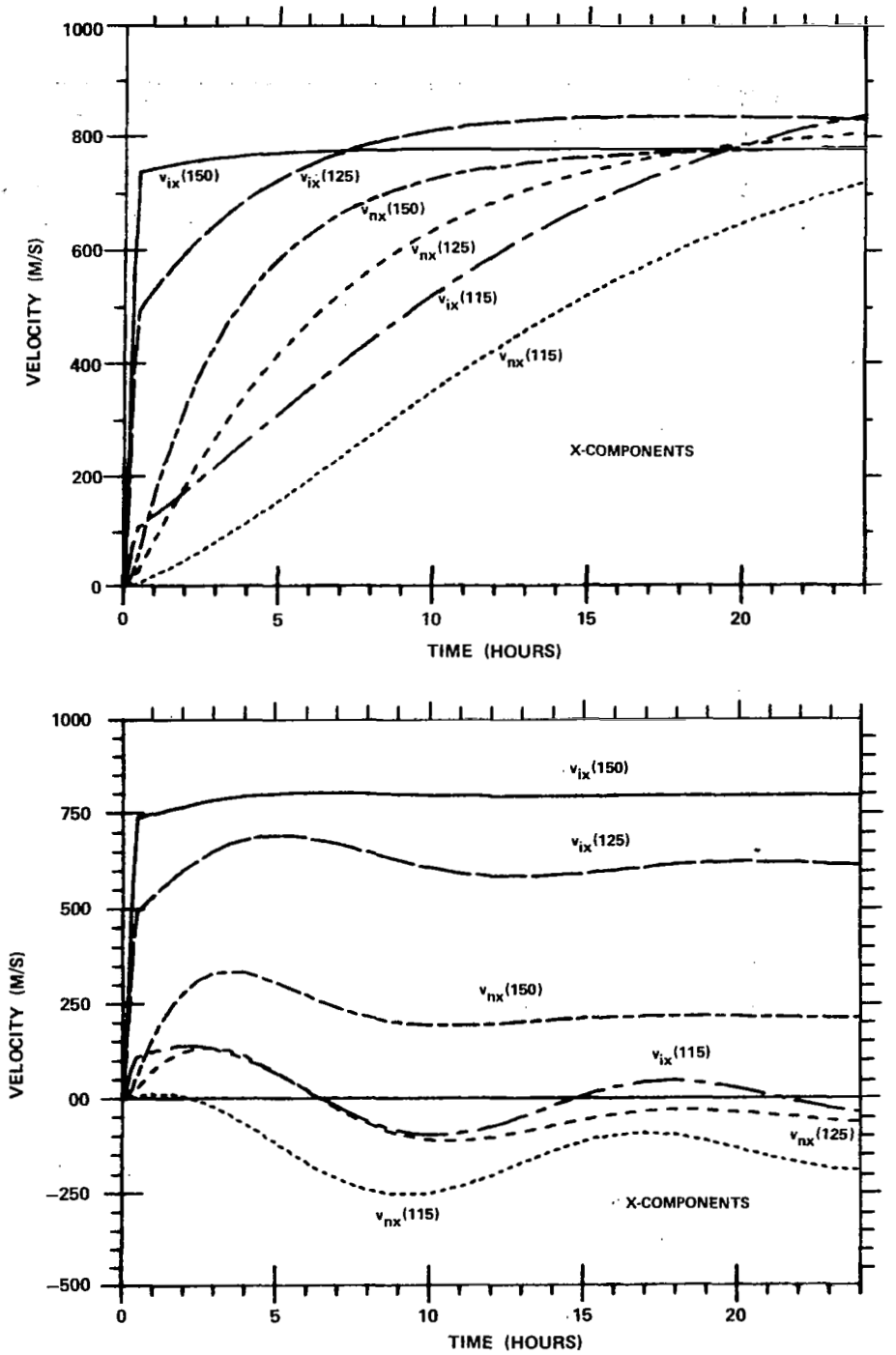

Figure 6-7. VELOCITY COMPONENTS AS FUNCTIONS OF TIME AT ALTITUDES 115 KM, 125 KM, AND 150 KM FROM MODEL CALCULATIONS: (a) x-COMPONENTS FOR CORIOLIS FORCE OMITTED; (b) x-COMPONENTS FOR CORIOLIS FORCE INCLUDED

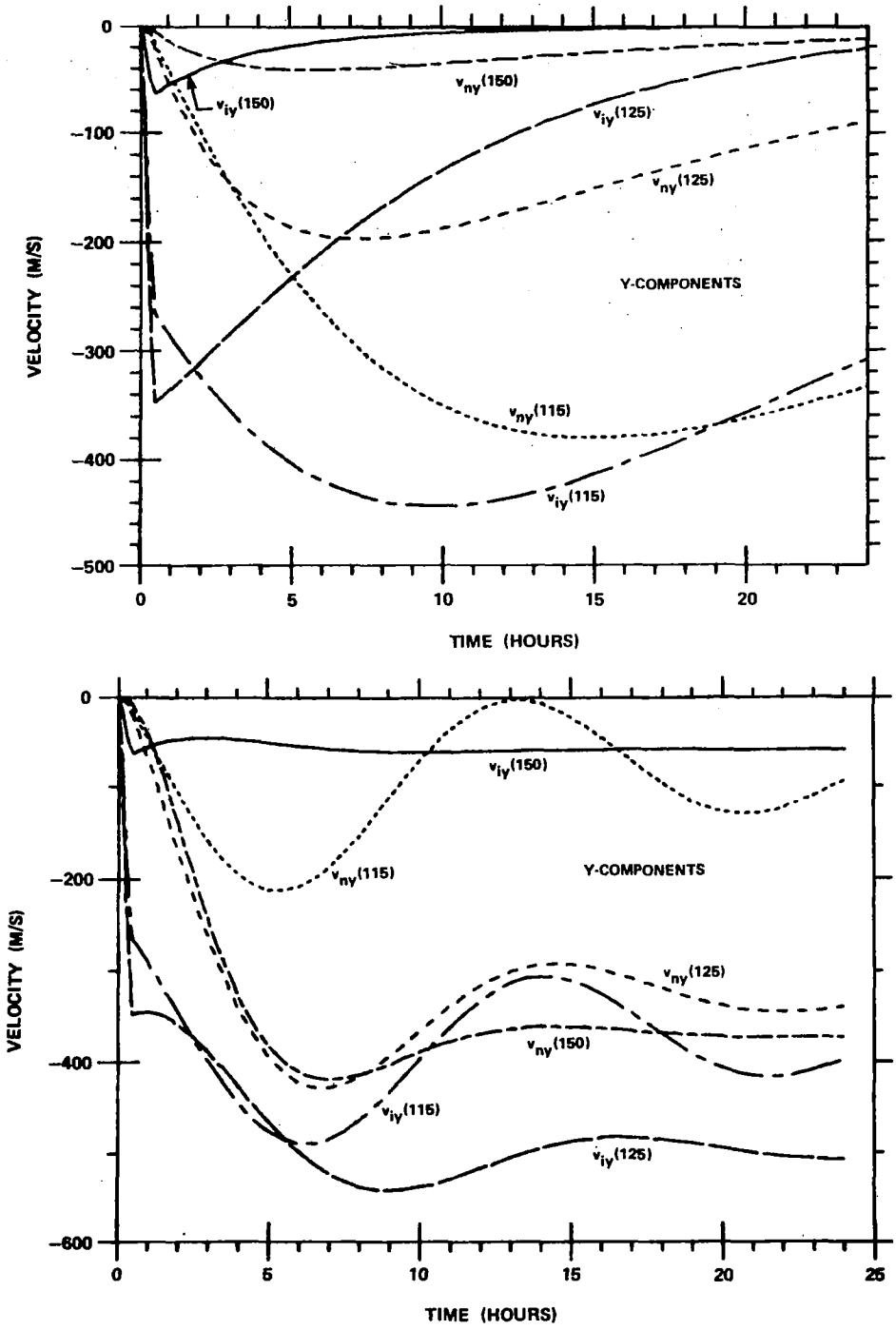

Figure 6-7. VELOCITY COMPONENTS AS FUNCTIONS OF TIME AT ALTITUDES 115 KM, 125 KM, AND 150 KM FROM MODEL CALCULATIONS: (c) y-COMPONENTS FOR CORIOLIS FORCE OMITTED; (d) y-COMPONENTS FOR CORIOLIS FORCE INCLUDED

more time is required for the neutral velocity at lower altitudes to come into equilibrium with the ion (collisional) driving force. From the opposite point of view, the effect of the neutrals on ions is clearly evident in the response of the ions to the electric field. At 115 km, this response time is very large and is closely coupled with the neutral response time because of the close collisional coupling of the ions to the neutrals.

The y-components are more difficult to understand immediately because they involve a balance between the geomagnetic field and collisional coupling with neutrals in controlling ion motions. However, upon reference to equations (6-14a, b), it is seen that because of ion-neutral collisions at lower altitudes, both components of both the electrical field and neutral velocity affect each component of ion velocity. This directional coupling is the origin of the relatively large ion velocities parallel to the electric field (Pedersen drift) in the early stages at 115 km and 125 km. The neutral velocities again respond to the collisional coupling and approach the ion velocity. However, because of the changing neutral velocity components the ion velocity y-component begins decreasing and becomes smaller than the neutral velocity. At this time the inertia of neutral gas results in a "coasting" motion, now becoming a driving force for the ions in maintaining their motion. At the same time neutral momentum is being diffused in altitude through viscous effects, as discussed in detail by Fedder and Banks (1972).

These results may now be compared with those of Figure 6-7b, d, for which the coriolis term is included. The effects on the neutral velocities are profound, and extend to the ion velocities at 125 km and 115 km where the collisional coupling of ions to neutrals is important. The magnitudes of the neutral velocity x-components are reduced to about one third of the equilibrium values being approached when coroilis forces are neglected, with the sign changing at lower altitudes. In the y-components of neutral velocity, the differences at different altitudes are particularly pronounced. Since the coriolis force basically couples the directions, the oscillatory behavior is a manifestation of a rotating velocity vector. The different effects at different altitudes are due to the variation of response times of the neutral velocity field with altitude.

For example, at 150 km, where the response time is somewhat smaller than the 13 hour period of the coriolis term, the x-component of neutral velocity begins to grow rapidly, as in Figure 6-6a. Through coriolis coupling, however, part of this motion is diverted into the y-component. When a final steady-state is achieved the y-component is much larger than for the previous case and the x-component is much smaller. This is not a simple case of just rotating the velocity vector however, because the magnitude of the velocity vector is smaller when the coriolis force is included. The neutral response to collisions with ions is not rapid enough for the neutral velocity to approach the ion velocity before coriolis effects significantly alter the direction of the former.

At 115 km, it appears from Figures 6-7b, d that the neutral velocity field will oscillate due to the coriolis force for a considerable period (of the order of days). This appears to be due to the fact that the response time of the neutrals to ion drag exceeds the coriolis period (see Figures 6-7 a,b).

An immediate consequence of these results is that large ion-neutral velocity differences are maintained at all altitudes, even when an equilibrium condition is reached. This is in contrast to the case when coriolis forces are ignored, in which the equilibrium condition is identical ion and neutral velocities. As a result, Joule heating, which varies as the square of the ion-neutral velocity difference (see equations (4-52) (4-54)) should remain relatively large under equilibrium conditions when the coriolis force is taken into account. This is consistent with the conclusions of Heaps (1974), who examined the effects of the coriolis force on Joule heating in a single-fluid-approximation calculation.

Effects of coriolis forces are now examined explicitly in terms of altitude structure. Calculated altitude profiles of the velocity fields are shown for t = 5 hours and t = 24 hours for no coriolis force in Figures 6-8a, c and with the coriolis force included in Figures 6-8b,d. Figure 6-8a shows the extent to which the equilibrium is approached in 5 hours and Figure 6-8c shows virtually the final state, when no coriolis coupling of directions is considered. At high altitudes the intuitive picture is fulfilled; below 125 km the

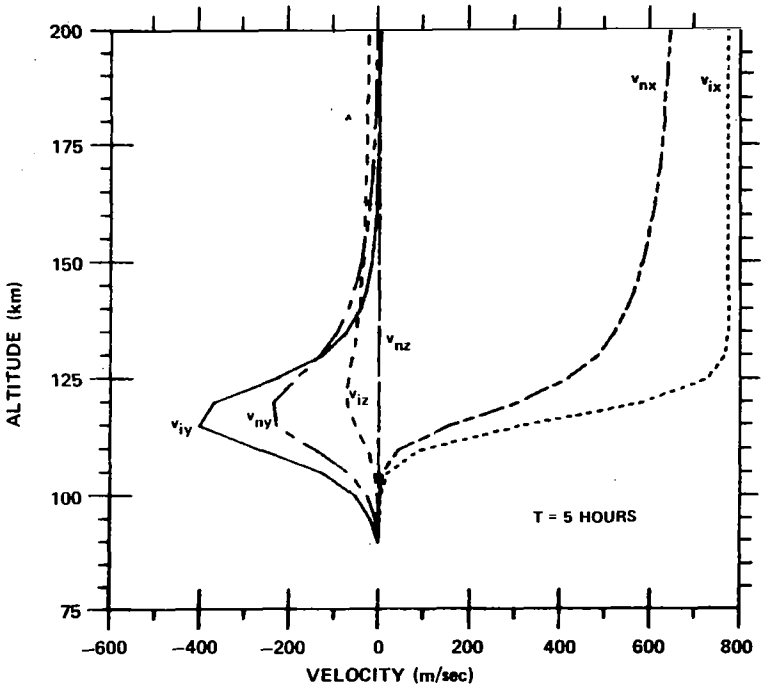

(a)

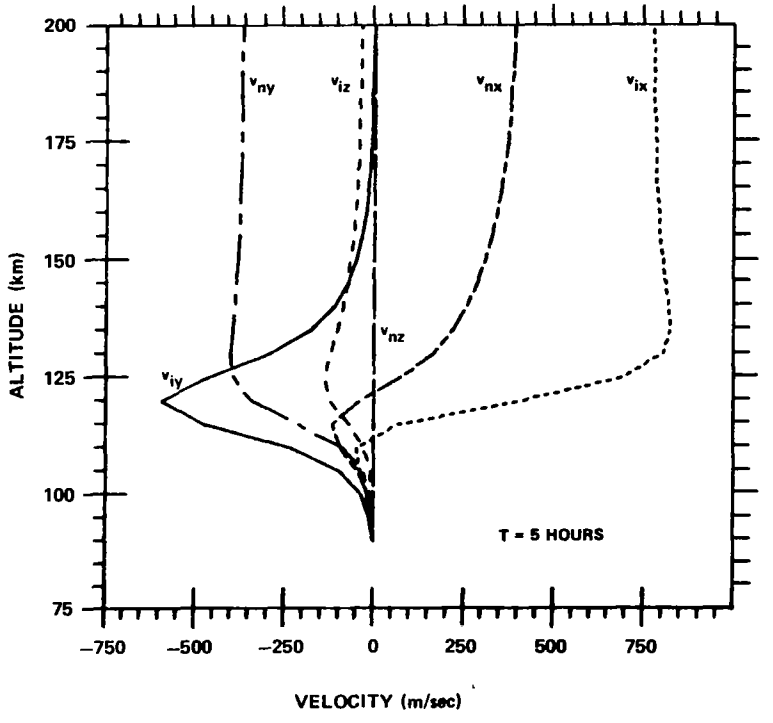

(b)

Figure 6-8. ALTITUDE STRUCTURE OF VELOCITY COMPONENTS FROM MODEL CALCULATIONS: (a) FOR T = 5 HOURS WITH CORIOLIS FORCE OMITTED; (b) FOR T = 5 HOURS WITH CORIOLIS FORCE INCLUDED

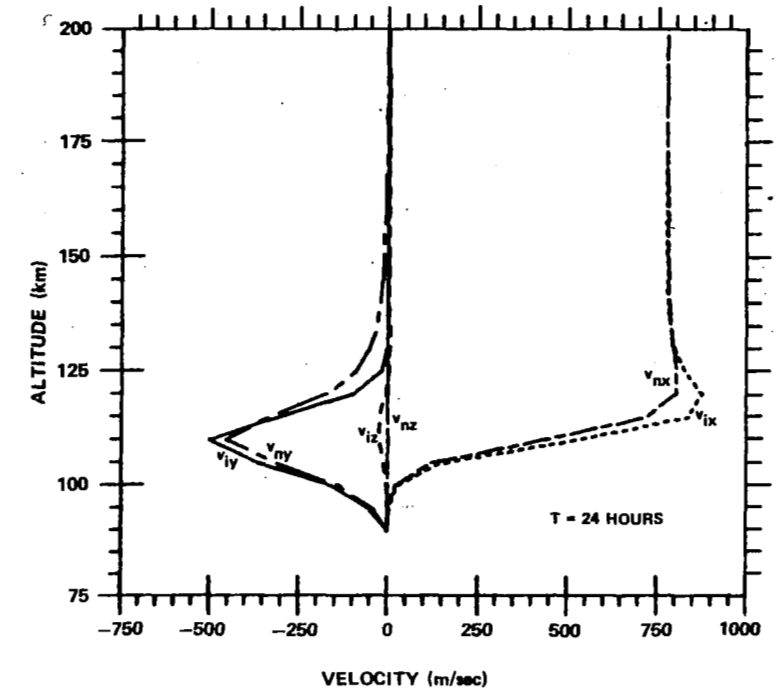

(c)

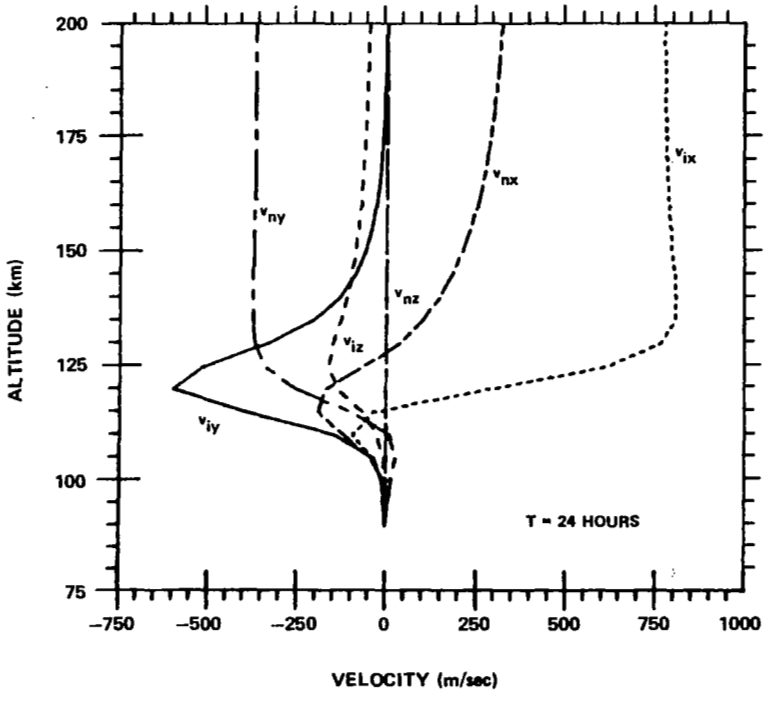

(d)

Figure 6-8. ALTITUDE STRUCTURE OF VELOCITY COMPONENTS FROM MODEL CALCULATIONS: (c) FOR T = 24 HOURS WITH CORIOLIS FORCE OMITTED; (d) FOR T = 24 HOURS WITH CORIOLIS FORCE INCLUDED

complexities introduced by the transition from ion-neutral collisional coupling to ion magnetic field coupling is evident, but with a similar end result: ion and neutral velocities are almost the same at all altitudes.

In contrast, altitude plots in Figure 6-8b, d, for which the coriolis force is included, show a very different altitude structure for ions and neutrals at all altitudes. Effects on the ion velocity are seen to be small except at low altitudes, as expected. At high altitudes, the profile in Figure 6-8d represents virtually an equilibrium configuration, while at low altitudes the structure can be expected to change somewhat, as discussed previously.

Similar calculations have been carried out with the viscous terms omitted. Results are not substantially different from those in which viscosity is included, however, so those results are not shown. The primary effect of viscosity is to diminish maximum values of the velocities and smooth out the altitude variations to a small extent. No significant differences in altitude structure of the velocity fields are seen. This is not really unexpected, due to the nature of viscous forces. It may be noted that Fedder and Banks (1972) found viscosity to be effective in transporting horizontal momentum through about one scale height. Their calculation was particularly designed to test this aspect by beginning with a strong vertical gradient at 155 km and no other driving force in the neutral wind equation. Because the collisional driving forces maintain the gradients in the present calculations, viscous forces are not seen so prominently. Under more realistic conditions, effects could well be more pronounced. Nevertheless, viscosity is not expected to alter the basic altitude configuration of the velocity fields to any great extent.

The inverse situation is now examined; that is, the decay of the velocity fields from an initial configuration is calculated for the case in which the electric field is set to zero. It is noted that this should correspond to a very unlikely condition, because even in the absence of an external electric field, a dynamo electric field would be generated by the E region wind system.

However, it was seen in Figure 6-3a that electric fields are observed to "turn off" rather abruptly; so this example may not be so unreasonable. In any event the purpose here is simply to gain some idea of the inertial properties of the wind system, primarily to see how important the initial conditions are to the calculated winds some hours later.

The initial wind configuration is that shown in Figure 6-7d, which is the calculated velocity field after 24 hours under the influence of the electric field in equation (6-22). The full set of equations (6-14) and (6-15) is employed, as it was to obtain the initial configuration. Temporal variations for the velocity components at 115 km, 125 km, and 150 km are shown for 10 hours in Figures 6-9a, b. Altitude structure of the velocity fields at 3 hours and 10 hours after decay begins are shown in Figures 6-9c, d. From the detailed numerical results it is found that the coriolis term dominates the motion, particularly at lower altitudes. This is evident in Figures 6-9a, b. Viscosity is found to be more important in the decay mode than when the velocity field is building up.

Perhaps the most important feature of these results, however, is the inertia in the 110 km to 120 km region. After 10 hours with no momentum input, velocities there are reduced by about one half, while at 200 km the velocities have all but vanished. This indicates that initial conditions for the calculations with observed electric fields may be significant for an extended period after the calculation begins. It also shows that small electric fields for the initial 2 or 3 hours of a calculation do not guarantee that initial neutral velocities will be small or will become small before the velocity fields are significantly affected by the larger electric fields of interest. This must be considered in the comparison of calculated and observed neutral velocities.

Results of interest from these model calculations may be summarized as follows. In the development of the velocity fields through collisional coupling alone, 8 to 10 hours are required at high altitudes ($\geq$150 km) for the neutral velocity to approach the ion velocity, while at low altitudes ($\leq$120 km)

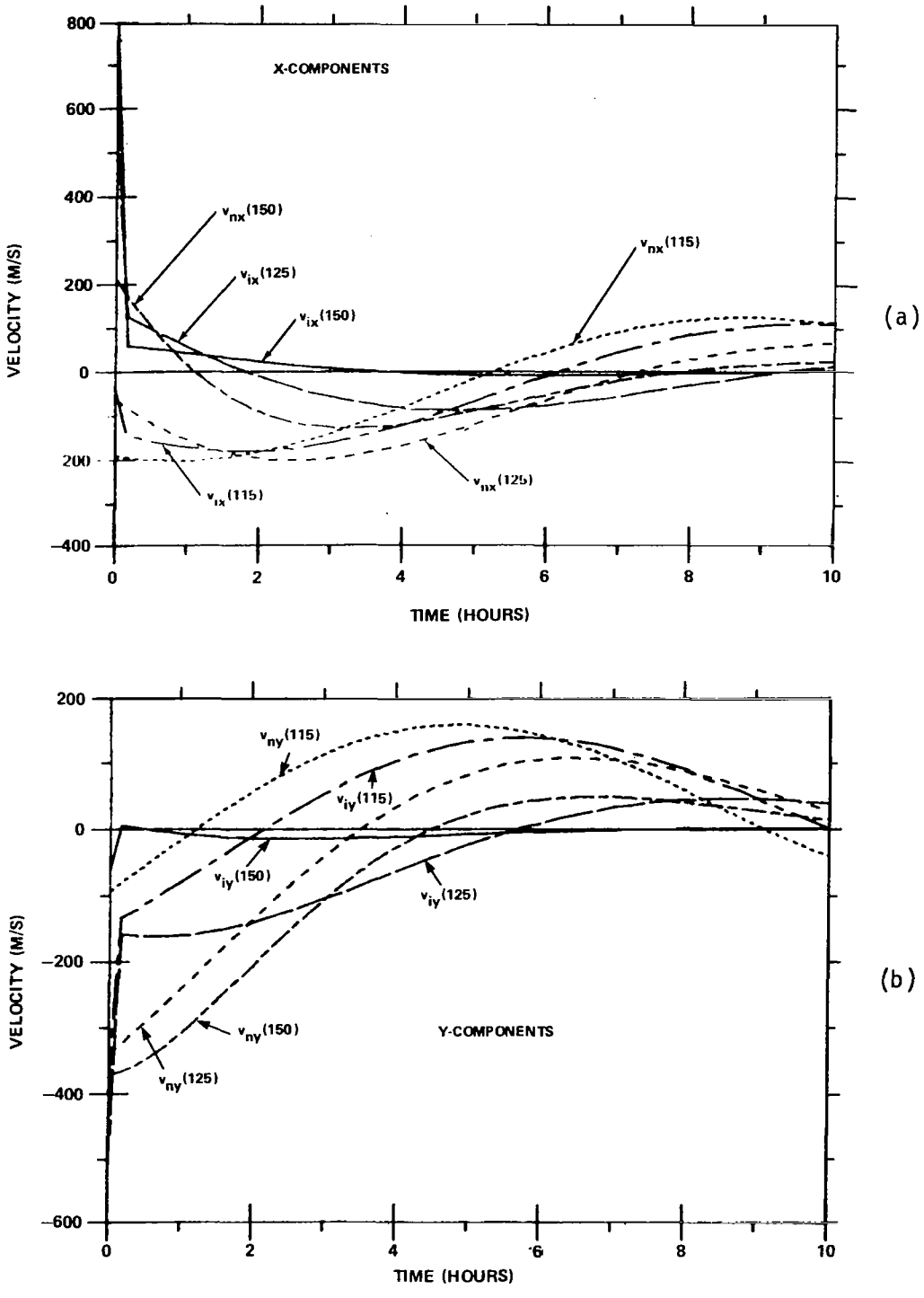

Figure 6-9. VELOCITY FIELD DECAY (NO ELECTRIC FIELD) FROM INITIAL CONFIGURATION GIVEN IN FIGURE 6-8d: (a) x-COMPONENTS AS FUNCTIONS OF TIME FOR ALTITUDES 115 KM, 125 KM, AND 150 KM; (b) SAME AS (a) FOR y-COMPONENTS;

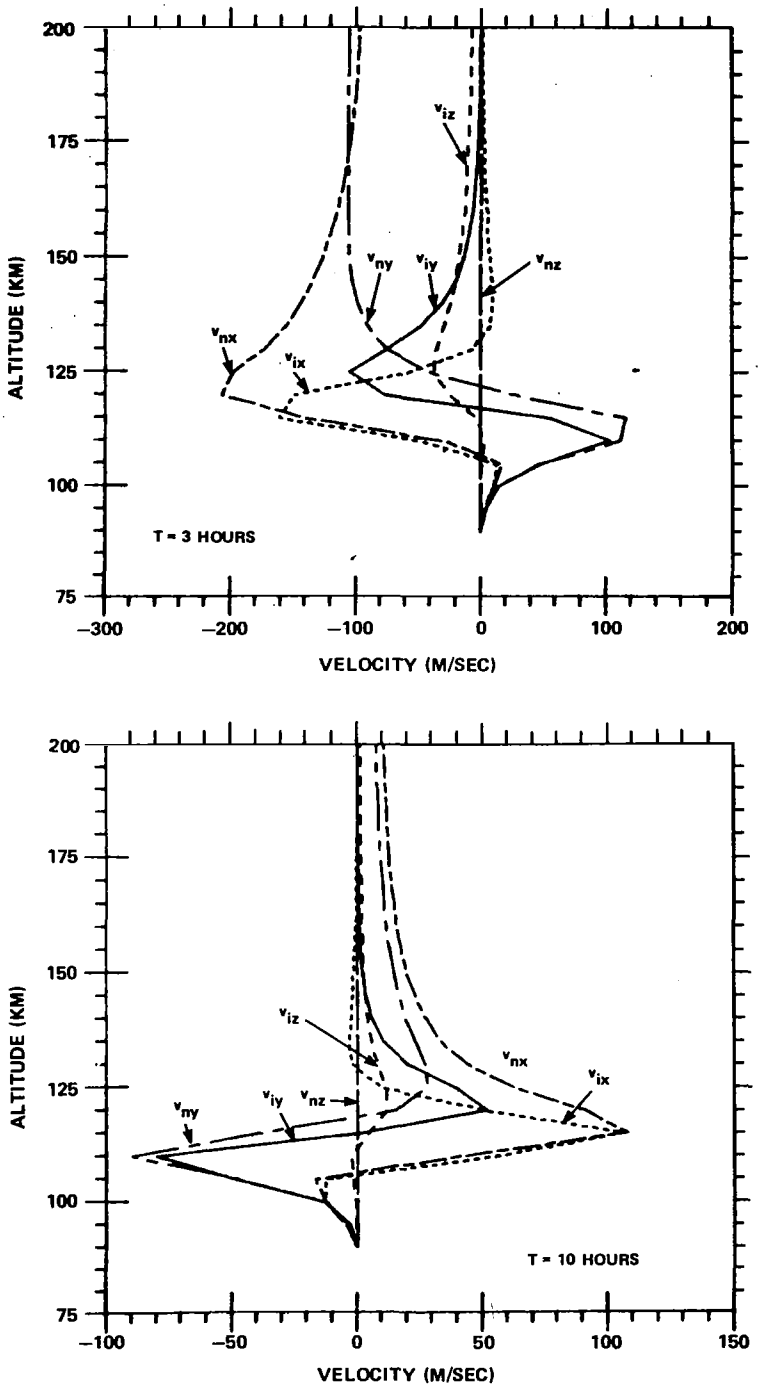

Figure 6-9. VELOCITY FIELD DECAY (NO ELECTRIC FIELD) FROM INITIAL CONFIGURATION GIVEN IN FIGURE 6-8d: (c) ALTITUDE PROFILES AT T = 3 HOURS: (d) ALTITUDE PROFILES AT T = 10 HOURS

more than 24 hours are required. The coriolis force plays a significant role in both development and decay of the velocity fields. It reduces the magnitude of the maximum neutral velocity attained, and maintains a larger ion-neutral velocity difference in a steady state. The coriolis term causes an increase in the time required for an equilibrium velocity field to be achieved, particularly at low altitudes. In the decay mode from large initital velocities in the absence of driving forces, the coriolis term is dominant. Finally, large initial velocities can persist without driving forces in excess of 10 hours at low altitudes; hence effects of initial conditions can be expected for several hours into a calculation at these altitudes.

6.5 VELOCITY CALCULATIONS FOR 15 MAY 1974

A series of calculations, based on observations made by the incoherent scatter radar facility at Chatanika, Alaska on 15 May 1974, are now presented. Since successive calculations are motivated by preceding ones, each set is examined and discussed in turn before presenting results of the next. This facilitates clarity and allows interpretation to be developed in an orderly manner.

6.5.1 Calculated Ion and Neutral Velocities as Functions of Altitude and Time

The first set of calculations is the simultaneous numerical solution of the ion and neutral momentum equations (6-14) and (6-15). The ion mean gyrofrequency $\bar{\omega}_i$ and ion-neutral mean effective collision frequency $\bar{\nu}_{in}$ vary with altitude but are constant in time under approximations above. From the incoherent scatter observations, electric field components are prescribed as functions of time (shown in Figure 6-3a) and assumed uniform throughout the region of interest. Remaining parameters in equations (6-14), speed of light c and geomagnetic field strength B, are constants. Neutral wind components are computed from equation (6-15), according to the numerical scheme discussed in subsection 6.3.2. Neutral mass density ρ_n and viscosity coefficient η_n are functions of altitude but constant in time. Geographic latitude λ and angular velocity Ω_E are constants. The neutral-ion mean effective collision frequency varies linearly with ionization density and, hence, varies in both altitude and time. To determine these collision frequencies a collision frequency profile

normalized to 1 ion cm^{-3} (which varies only with altitude) is multiplied by the ionization density profile appropriate to each time. A new electric field vector and ionization density profile are provided by the incoherent scatter radar at approximately 6 minute intervals; linear interpolation is used to determine values at intermediate time points.

Calculated values of the ion and neutral velocity components in geographic coordinates are shown as functions of time in Figure 6-10 for altitudes 110 km, 125 km, and 150 km. Altitude 110 km is shown in particular because it corresponds to the center of the first range gate, data for which is used to determine the neutral winds in Figure 6-3b. Several interesting features may be noted in these figures. First, the changing relations of the velocity components at different altitudes indicates changing altitude structure in the velocity fields. This is displayed more clearly in Figures 6-11a, b, c, which show the altitude structure of the velocity fields at UT = 1506, 1714, and 2234 hours. Although these times were selected to display some of the extreme velocities, the form of the altitude structure is not atypical, as reference to Figures 6-8 and 6-9 will indicate. Vertical gradients in the horizontal velocity components can be quite large, particularly at altitudes below 130 km. It is also of interest to observe in Figures 6-10 and 6-11 that the largest velocities for both ions and neutrals do not necessarily occur at the higher altitudes, but may also occur in the dynamic transition region, approximately 115 km to 130 km for this calculations.

A second significant feature of Figure 6-10 is the slow and almost sinusoidal variation of the neutral velocity components, in contrast with the highly structured temporal variation of the ion-velocity components. This latter structure clearly follows directly from similar structure in the electric field components, although the correspondence is not exact. Because of large numerical superiority, and therefore greater total inertia, the neutral gas averages over the short period fluctuations in the ion motions. This response is not unexpected, since it is consistent with the relatively long response times seen previously in the model calculations.

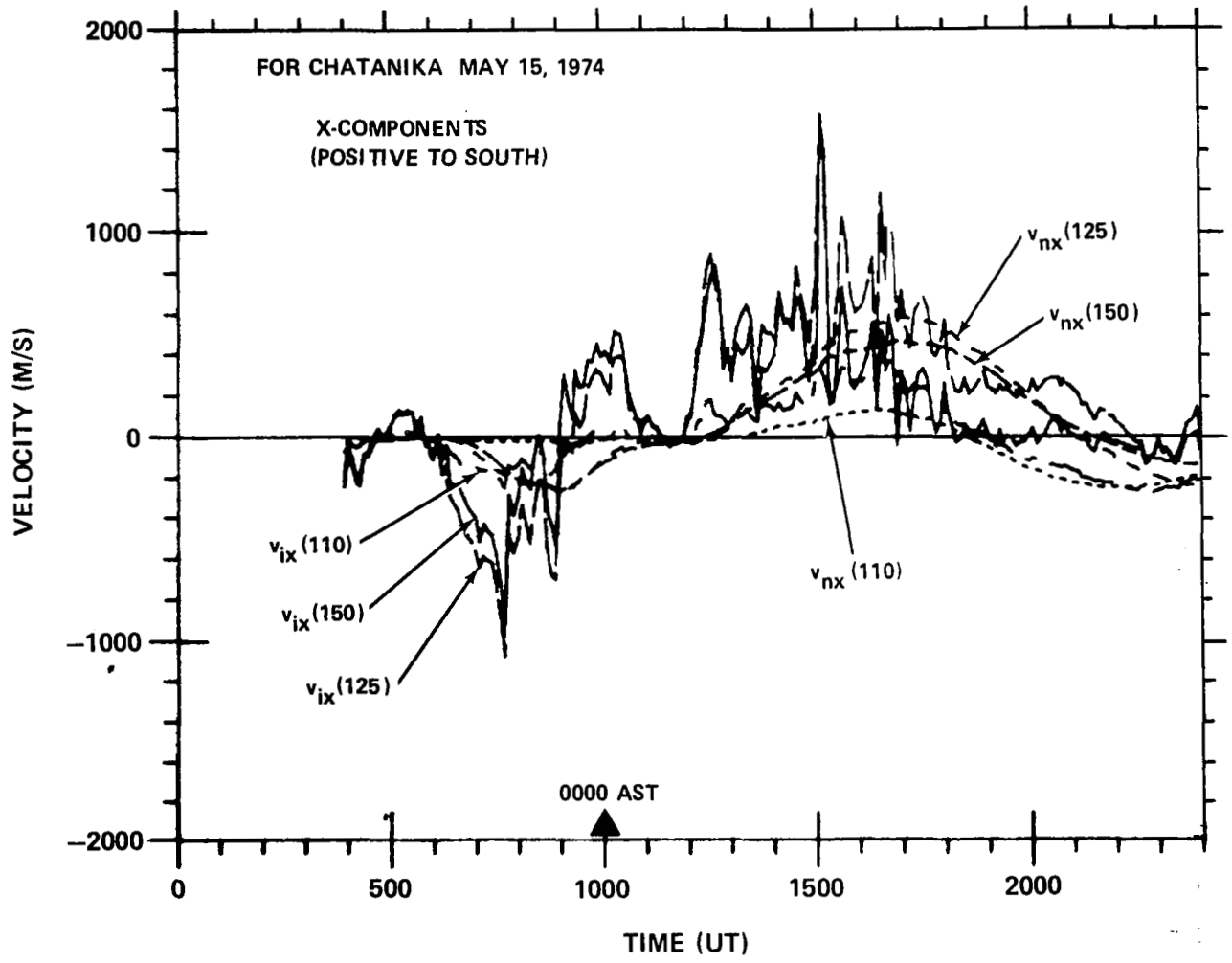

Figure 6-10. CALCULATED VELOCITIES AS FUNCTIONS OF TIME FOR ALTITUDES 110 KM, 125 KM, AND 150 KM, BASED ON OBSERVED ELECTRIC FIELDS AND ELECTRON DENSITIES: (a) x-COMPONENTS

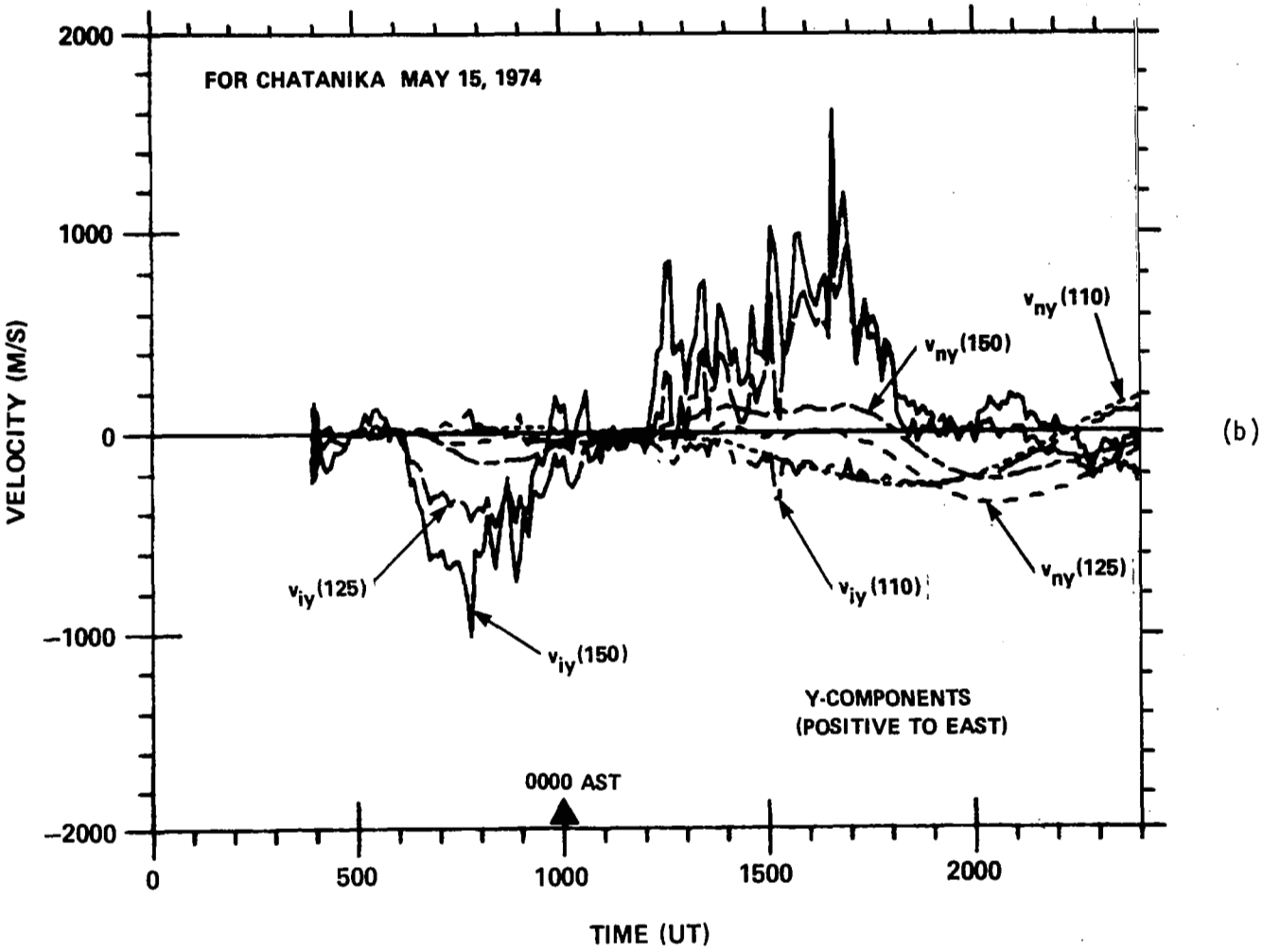

Figure 6-10. CALCULATED VELOCITIES AS FUNCTIONS OF TIME FOR ALTITUDES 110 KM, 125 KM, AND 150 KM, BASED ON OBSERVED ELECTRIC FIELDS AND ELECTRON DENSITIES: (b) y-COMPONENTS

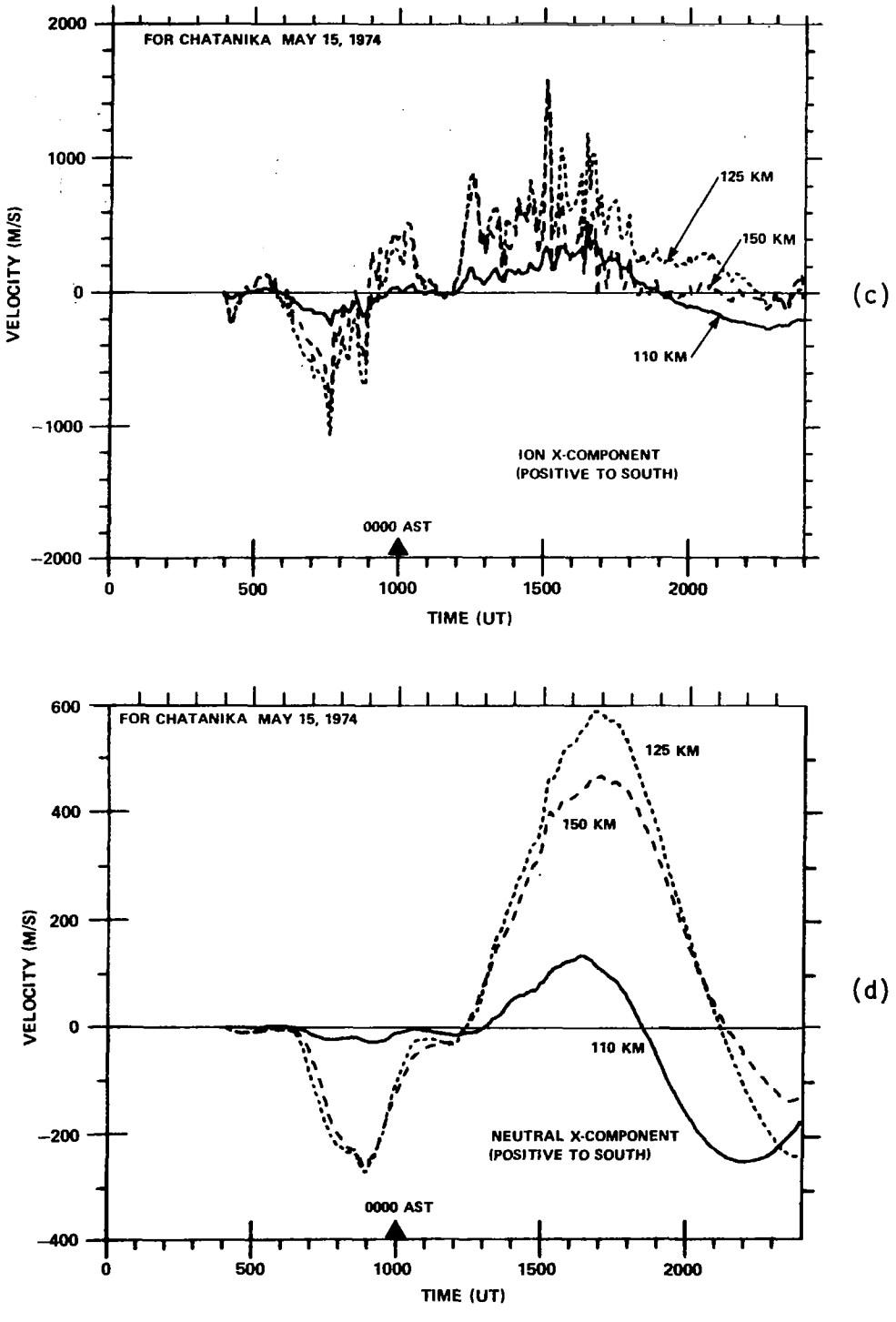

Figure 6-10. CALCULATED VELOCITIES AS FUNCTIONS OF TIME FOR ALTITUDES 110 KM, 125 KM, AND 150 KM, BASED ON OBSERVED ELECTRIC FIELDS AND ELECTRON DENSITIES: (c) x-COMPONENT, ION ONLY; (d) x-COMPONENT, NEUTRAL ONLY

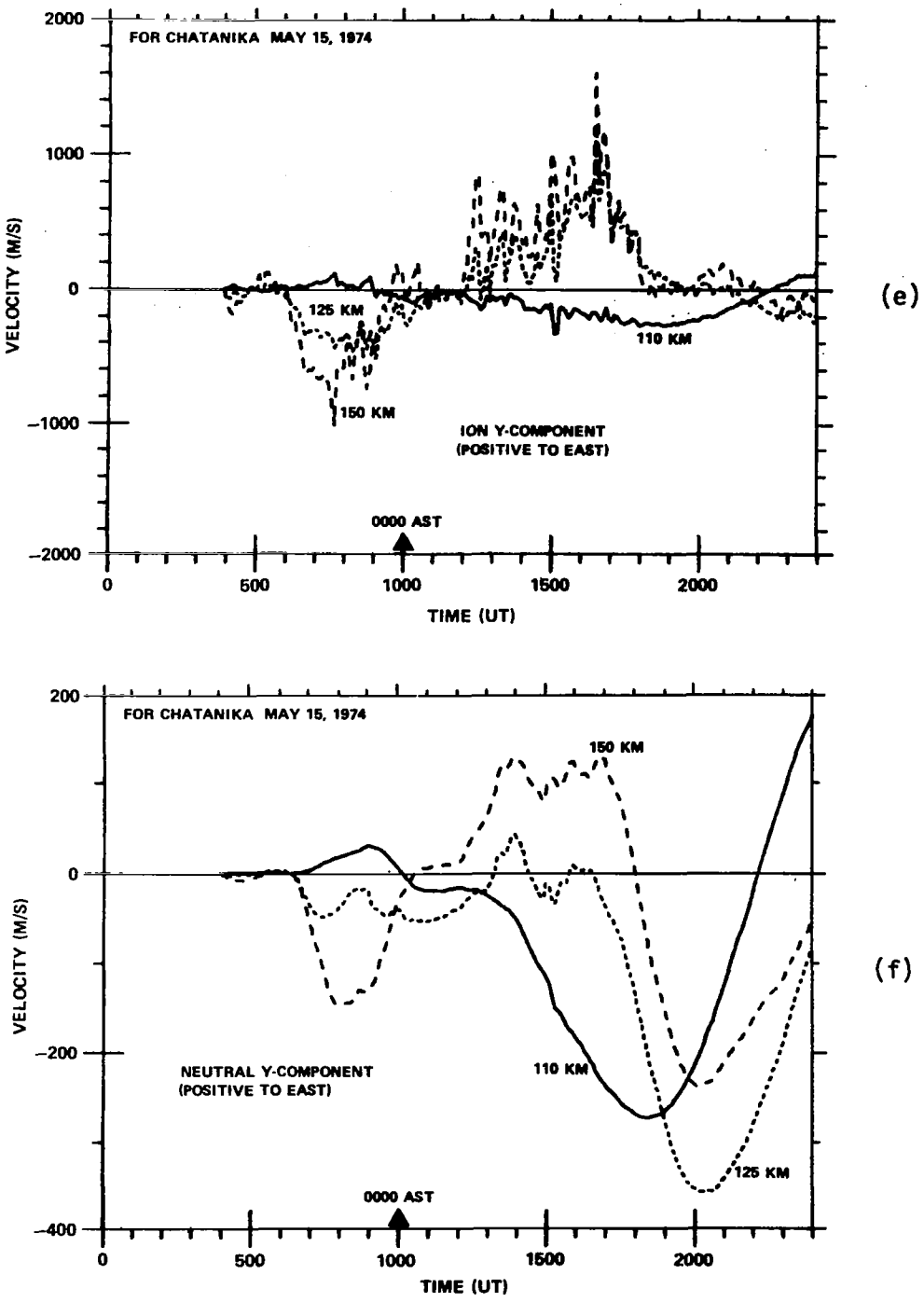

Figure 6-10. CALCULATED VELOCITIES AS FUNCTIONS OF TIME FOR ALTITUDES 110 KM, 125 KM, AND 150 KM, BASED ON OBSERVED ELECTRIC FIELDS AND ELECTRON DENSITIES: (e) y-COMPONENT, ION ONLY; (f) y-COMPONENT, NEUTRAL ONLY

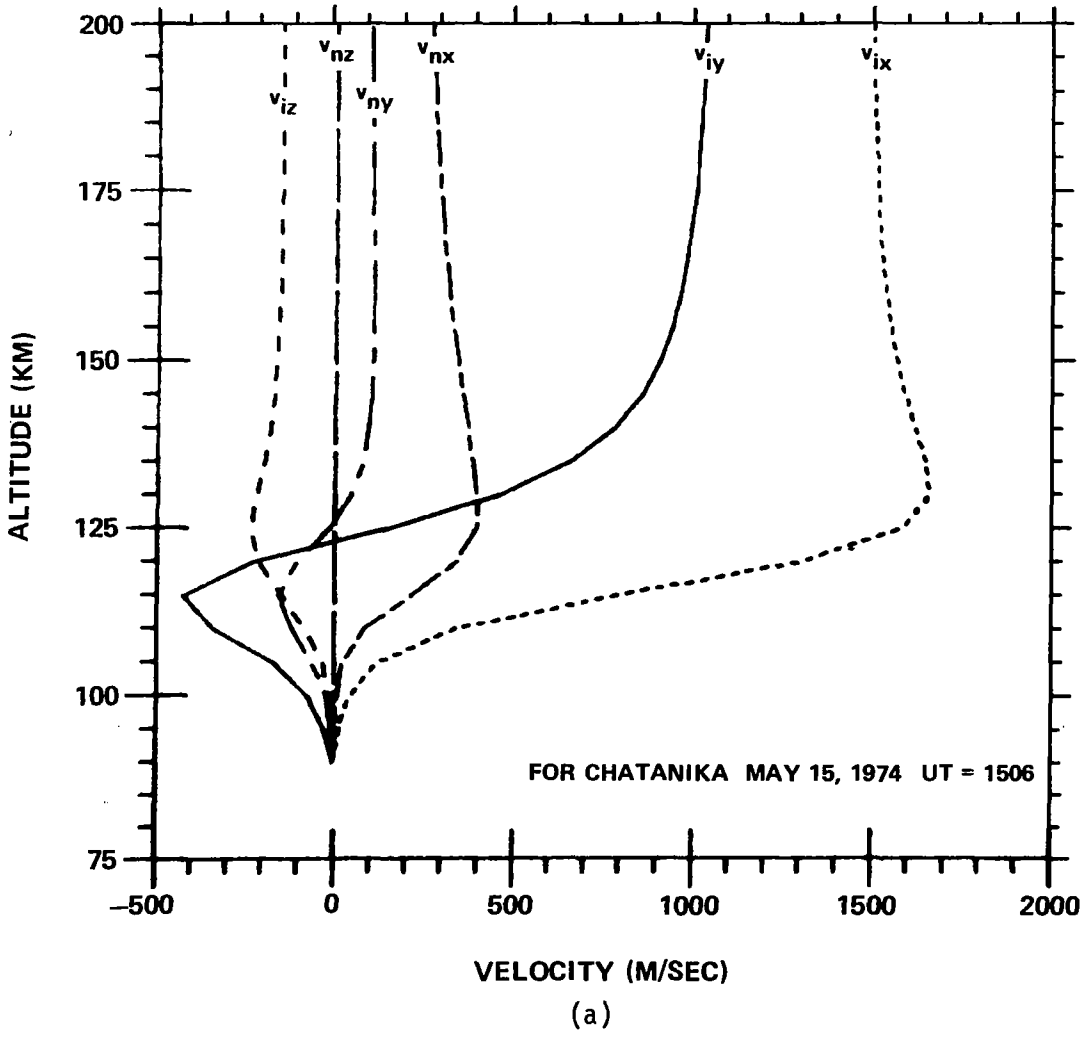

Figure 6-11. EXAMPLES OF ALTITUDE STRUCTURE FOR VELOCITIES OF FIGURE 6-10: (a) AT UT = 1506 HOURS

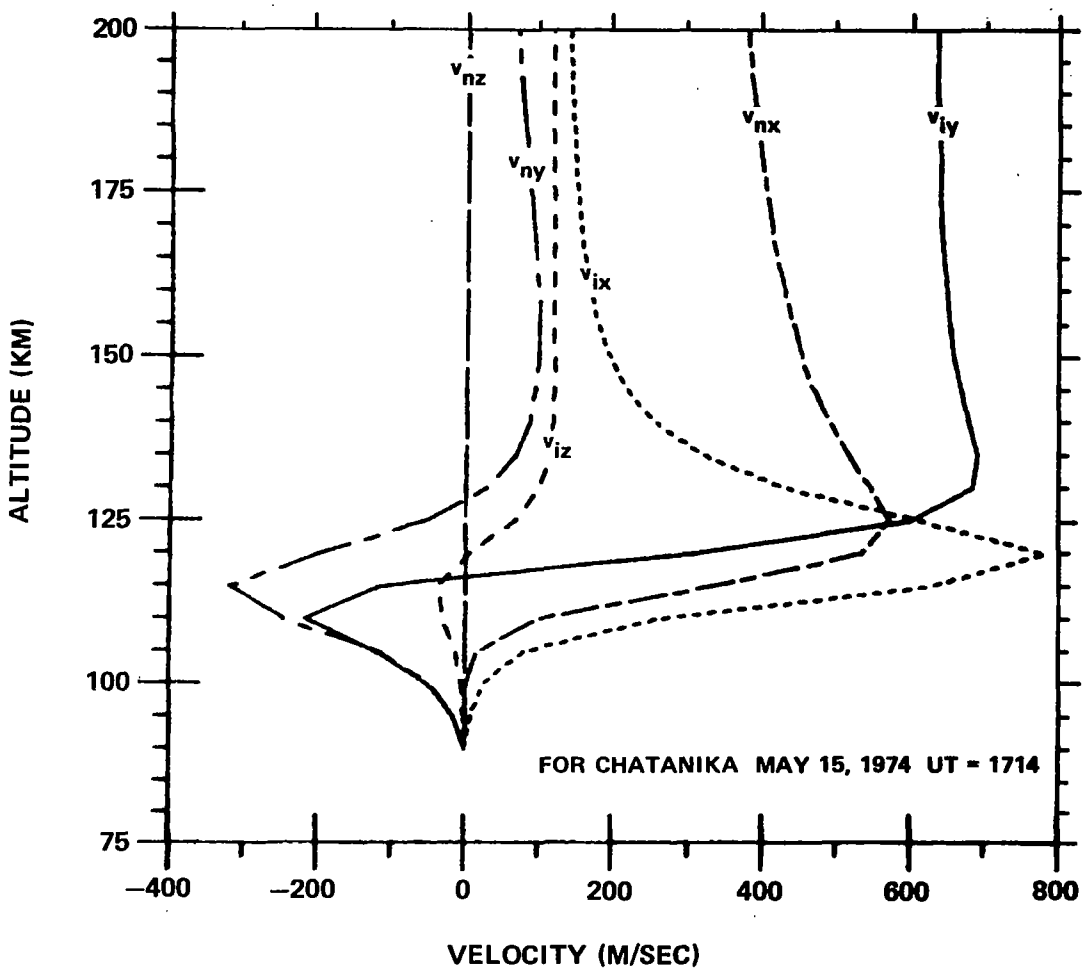

(b)

Figure 6-11. EXAMPLES OF ALTITUDE STRUCTURE FOR VELOCITIES OF FIGURE 6-10: (b) AT UT = 1714 HOURS

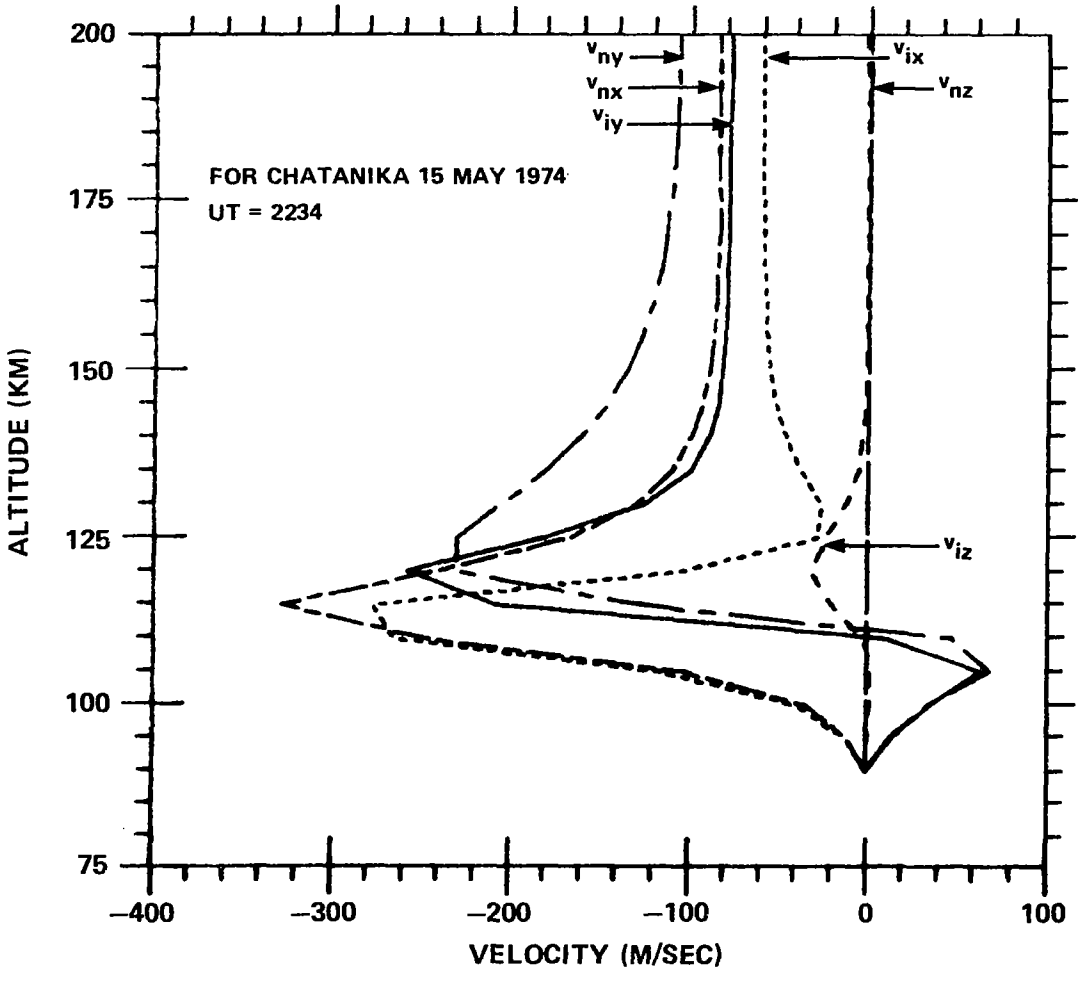

(c)

Figure 6-11. EXAMPLES OF ALTITUDE STRUCTURE FOR VELOCITIES OF FIGURE 6-10: (c) AT UT = 2234 HOURS

A major difference between this calculation and the model calculations, however, in addition to the large electric field fluctuations in this case, is large fluctuations in ionization density. This is illustrated in Figure 6-12 where the temporal variations of ionization density at 100 km, 110 km, 120 km, and 130 km are plotted. Large fluctuations at a given altitude in short times are frequent during the times of greatest electric field fluctuation. It might be suspected that resulting fluctuations in the neutral-ion collision frequency $\bar{\nu}_{ni}$ could induce similar variations in the neutral velocities. Upon examination of equations (6-15) however, it is recognized that an order of magnitude increase in the collision frequency $\bar{\nu}_{ni}$ has about the same effect as a similar increase in the ion velocity (electric field): an order of magnitude increase in the collision term. Over short times, neither produces a large variation in the neutral velocity, again because $N_i/N_n << 1$ at all altitudes.

Considerable attention is directed to the temporal variation in the neutral velocity components because the neutral velocity components inferred from the incoherent scatter radar observations, shown in Figure 6-3b, have large fluctuations in short times. Thus, the temporal structure of the observed neutral winds more closely resembles that of the calculated ion velocities than that of the calculated neutral velocities. Even without considering in detail the magnitudes of these velocities, the nature of this discrepancy indicates a problem. If the winds inferred from the radar observations are consistent with the assumptions made in the data anlaysis and are approximately correct (indicative of the actual neutral winds at that location), then from the discussion above, ion-neutral collision coupling alone cannot account for them: some important mechanism has been omitted. On the other hand, to the extent that collisional coupling is important, Figure 6-11 shows that one of the important assumptions in the radar data analysis for neutral wind determination is called into question. The data analysis procedure assumes a neutral wind which is uniform throughout the first range gate, and it is such a wind that is determined. Figure 6-10 shows that considerable altitude structure does exist in this region, unless collisional coupling is unimportant, in which case the data analysis procedure is invalid anyway (Brekke, et al. 1973).

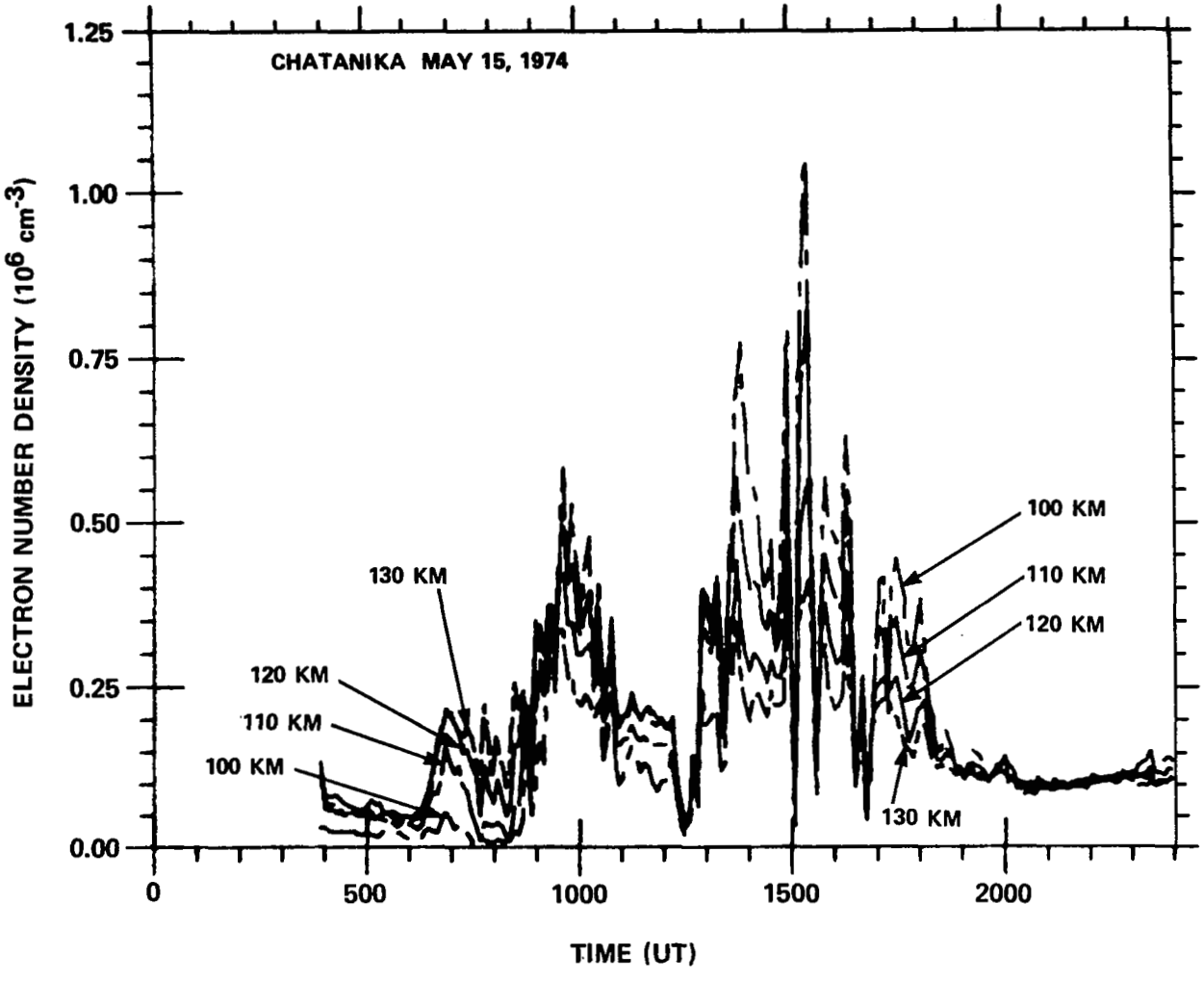

Figure 6-12. ELECTRON NUMBER DENSITIES AS FUNCTIONS OF TIME FOR ALTITUDES 100 KM, 110 KM, 120 KM, 130 KM

With respect to the effect of altitude structure on the analysis of radar data, two possibilities can be seen. The radar is assumed to average the observed ion velocity over altitude as in equation (6-4). Weighting the average are the electron (ion) density $N_e(z)$ and the radar weighting function $W(z)$. In Figure 6-12 it was seen that electron densities can change rapidly in time. Examples of how rapidly the altitude structure of $N_e(z)$ can change are shown by the altitude profiles in Figure 6-13. It is evident that even if the velocity structure remains constant, variation of the electron density profile can cause a shift in the altitudes most strongly weighted. From Figure 6-11, it is apparent that small shifts in altitude can correspond to large changes in velocity. Thus, the scatter radar observations of apparent temporal variations in ion velocity can result solely from variations in the electron density profiles, due to large vertical gradients in the velocity fields. Brekke, et al. (1974a) note this problem; although the mode of operation for the present experiment improves the situation somewhat, due to better time resolution, it nevertheless remains a difficulty.

A second possible effect is due to variation in the ion velocity altitude structure itself. Since the ion velocities are immediately affected by electric field variations, over a period of a few minutes the ion velocity altitude structure can change considerably, while that of the neutral velocity is virtually unaltered. If an effective altitude of observation is assumed to be defined as that altitude at which the weighted average velocity and the actual velocity agree, it can be seen that this effective altitude can shift by a change of ion velocity altitude structure, even for fixed electron density profiles.

It appears possible that some of these changes may be adequately compensated by the data analysis procedure, equations (6-6) and (6-7). For example, effects of variations in electron density profiles are taken into account to some extent by different values of κ-coefficients which essentially weight different altitudes (see Figure 3 of Brekke, et al. (1973); note, however, that their κ_1' and κ_2' labels are reversed). Also, since both the electric field and ion velocity appear in equation (6-7), changes in the one may

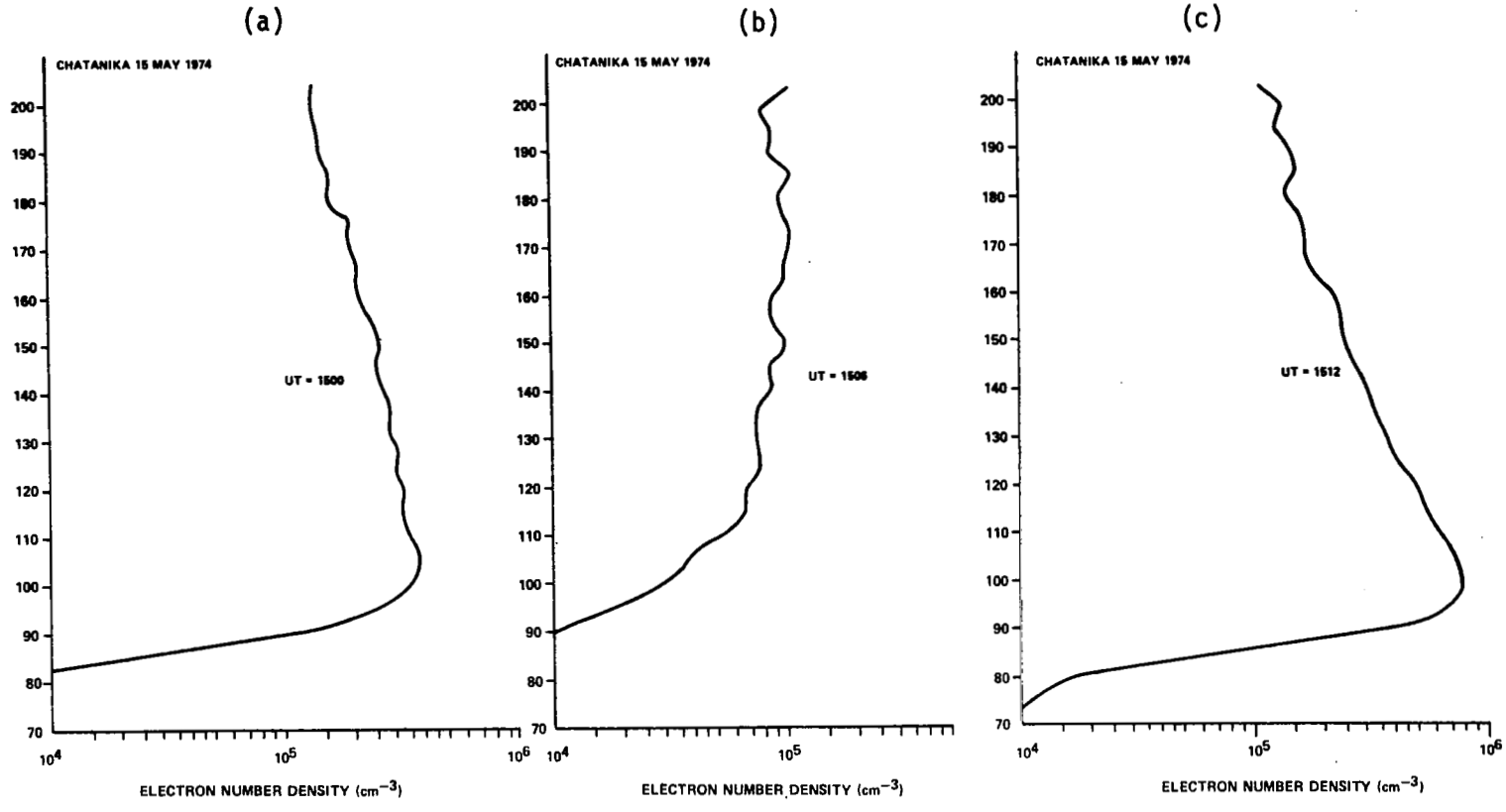

Figure 6-13. EXAMPLE ELECTRON DENSITY ALTITUDE PROFILES FOR CONSECUTIVE OBSERVATIONS: (a) UT = 1500 HOURS; (b) UT = 1506 HOURS; (c) UT = 1512 HOURS

compensate changes in the other, with little effect on the neutral velocity determined by that equation.

Nevertheless, the question remains, how are the calculated velocities of Figure 6-9 to be compared with the results of observation in Figure 6-3? Evidently, the answer is not to choose a fixed altitude and compare the calculated velocities as functions of time at that altitude with observed velocities. A promising approach, however, appears to lie in averaging the calculated velocities in altitude after the manner of the radar; that is, numerically simulate the radar averaging. This has the advantage of providing a common form for the observed and calculated velocities, making a valid comparison possible. It also offers prospects for resolving some of the difficulties noted above.

6.5.2 Weighted Altitude Averages of Calculated Velocities

Computation of weighted altitude averages of the calculated velocities presents no difficulties. Equation (6-4) defines the manner in which the average is weighted, and equations of this type are used to compute weighted altitude averages for both ion and neutral velocities. Numerically, the procedure is the same as that used in computing the κ-coefficients by equations (6-6a through c). For ion velocities this result should simulate the incoherent radar observation, to the extent that the calculated altitude structure corresponds to the actual altitude structure. For neutral velocities, the result represents what the radar would obtain if it were sensitive to the neutral gas in the way it is to ions.

This calculation also provides an opportunity for assessing the accuracy of the data analysis procedure for determining the neutral wind. On the one hand, the presumably accurate weighted altitude average of the neutral wind is obtained by direct numerical integration. On the other hand, the same is done for the ions, which should accurately represent the radar result. By treating this result as an observation, that is, by using it as an input to the data analysis procedure (equations (6-6) and (6-7)), neutral winds are obtained reflecting all systematic errors and inconsistencies inherent in the procedure.

Direct comparison with the accurate results then provides a test of the accuracy of the procedure under realistic conditions. It is emphasized that this is not a comparison of theory with observation; rather it is a test of the data analysis procedure (different theory) to see how well it represents what it is supposed to represent.

Before presenting results of these calculations, it is helpful to introduce some notational guides. Used consistently, these will help reduce confusion as different velocities are examined and discussed through the remainder of this section. Calculated velocities will be denoted by lower case $\vec{v}$, with subscript i or n indicating ion or neutral as before. A bar over the velocity, $\bar{\vec{v}}$, will indicate a weighted altitude average. Observed velocities, or those obtained from observations, will be denoted by capital $\bar{\vec{V}}$, where the bar indicates that it is a weighted altitude average. Within this framework, velocities will be distinguished by whatever means is appropriate, consistent with previous notation.

In terms of this notation, the weighted averages of the ion and neutral velocities obtained directly from equation (6-4) (or its analog) are denoted by $\bar{\vec{v}}_i$ and $\bar{\vec{v}}_n$. The neutral velocity obtained from $\bar{\vec{v}}_i$ by means of equation (6-7), as discussed previously, is denoted by $\bar{\vec{v}}_n'$. Horizontal components (geographic coordinates) of $\bar{\vec{v}}_n$ and $\bar{\vec{v}}_n'$ are presented in Figure 6-14.

Examination of $\bar{\vec{v}}_n$, with reference to $\vec{v}_n$ at constant altitudes in Figure 6-10, shows that the process of taking weighted altitude averages introduces considerable structure into the time variation of the velocity. It can be inferred that fluctuation of the electron density profile is the cause, since W(z) does not vary in time and the neutral wind is seen in Figure 6-10 to vary relatively slowly at all altitudes. If the general trend of $\bar{v}_{nx}$ is taken as a reference in Figure 6-14, it appears that perturbations of up to 50 percent can result from such shifts in the altitude weighting. The absence of similar large perturbations in the y-component appears to be due to the different altitude structure and smaller magnitude of this component during periods of large electron density fluctuations (see Figures 6-11 and 6-12). Finally, even though the weighting function W(z) is centered at 109 km, reference to

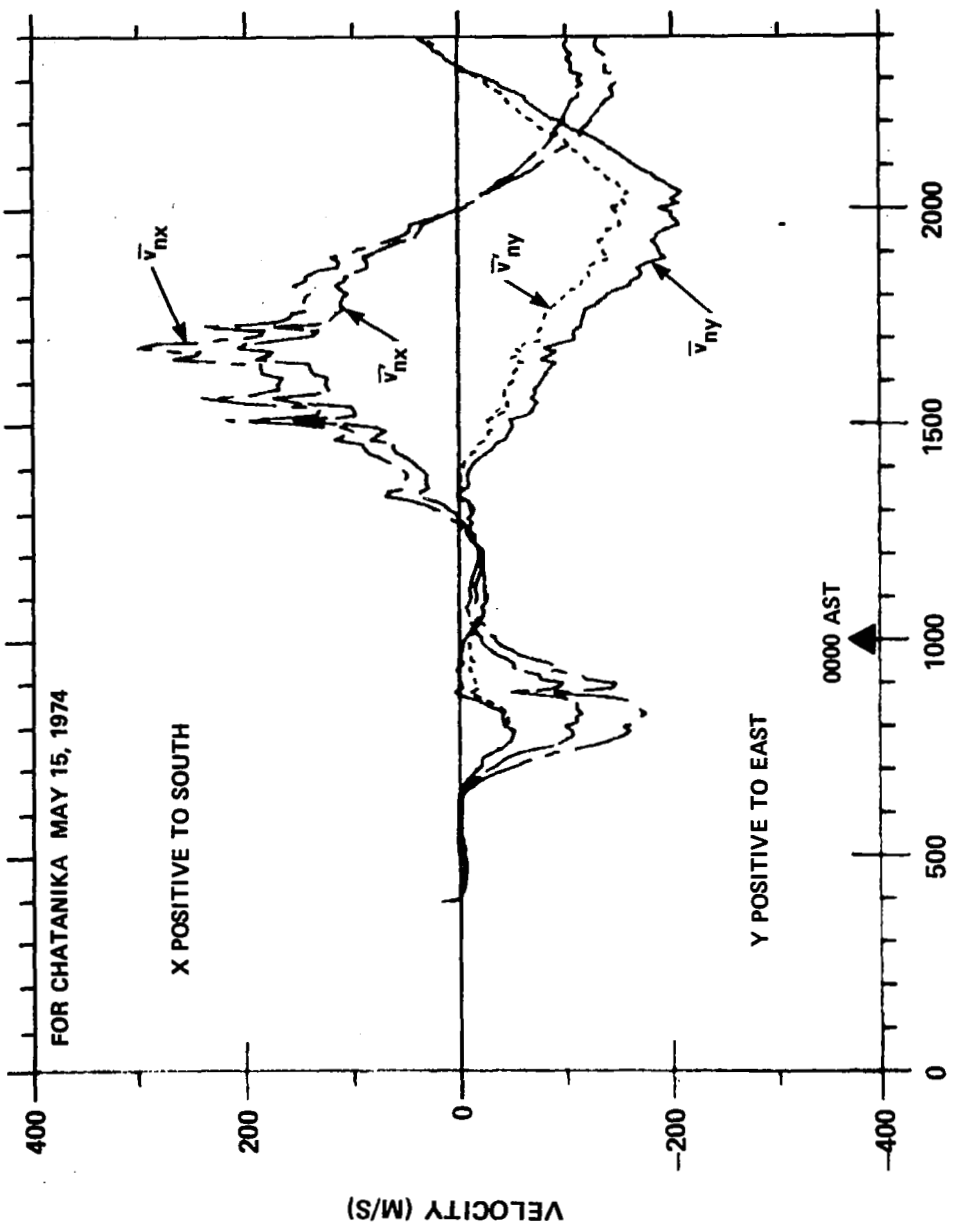

Figure 6-14. COMPARISON OF WEIGHTED ALTITUDE AVERAGES OF CALCULATED NEUTRAL VELOCITY COMPONENTS OBTAINED DIRECTLY BY NUMERICAL INTEGRATION ($\bar{v}_n$) AND OBTAINED INDIRECTLY THROUGH THE DATA ANALYSIS PROCEDURES ($\bar{v}_n'$)

Figure 6-10 shows that the magnitudes of $\bar{v}_{nx}$ and $\bar{v}_{ny}$ correspond to altitudes several kilometers higher, the exact altitudes varying with the electron density profiles.

The comparison of $\vec{\bar{v}}_n$ with $\vec{\bar{v}}_n'$ in Figure 6-14 demonstrates that the data analysis procedure consistently underestimates the actual magnitude of $\vec{\bar{v}}_n$ (and therefore $\vec{\bar{V}}_n$) by amounts ranging up to 40 percent. This appears to be a systematic effect associated with the altitude structure of the neutral wind, since the more transient effects of electron density fluctuations are evident in both $\vec{\bar{v}}_n$ and $\vec{\bar{v}}_n'$. The notable feature of this comparison, however, is how well the temporal variations of $\vec{\bar{v}}_n$ are reproduced by $\vec{\bar{v}}_n'$. With allowance for the systematic bias in magnitude, it is clear that the data analysis procedure does provide a reasonable representation of the weighted altitude average of the neutral velocity. However, it is equally clear that the time variation of this velocity is not the same as a straight altitude average of the neutral wind, because the weighting due to $N_e(z)$ has been seen to introduce some of this variation.

With regard to the magnitude of the velocities determined by equation (6-7), a brief digression is instructive. To assure that the data analysis procedure was being executed exactly as prescribed by Brekke, et al. (1973), a portion of the data for 15 May 1974 was processed through the computer program used for that study by J. R. Doupnik and P. M. Banks, and used to verify comparable calculations in this investigation. Proper use of the procedure has been comfirmed. However, in the course of this verification it has been seen how sensitive the magnitude of the velocity is to model values entering into the collision frequency $\bar{\nu}_{in}$. To compute ion-neutral collision frequencies, Brekke, et al. (1973, 1974a) have used the expression

$$\bar{\nu}_{in} = 7.5 \times 10^{-10} N_n \quad , \tag{6-23}$$

with the total neutral number density N_n obtained from a neutral atmospheric model given by Banks and Kockarts (1973), corresponding to an exospheric temperature of 1000°K. Collision frequencies used here are computed according to equation (4-14c) from the individual species collision frequencies given in

subsection 5.3.3. They also depend on the ion composition model and neutral atmosphere model discussed in subsection 6.3 When these different approaches are taken and the final values are computed and compared, the collision frequencies, used by Brekke, et al (1973, 1974) are larger than those used here by a factor of about 1.5 at 90 km, increasing with altitude to a factor of 2 at 160 km.

Neutral winds calculated according to equations (6-6) and (6-7) by Doupnik and Banks are denoted by $\vec{V}'$, while those calculated in this study are denoted by $\vec{V}$. This notation indicates that both are computed from the observational data. Horizontal components (geographic coordinates) of $\vec{V}'$ and $\vec{V}$ for 0600 hours UT to 1800 hours UT on 15 May 1974 are shown in Figure 6-15. It is emphasized that both of these represent "observed" neutral wind velocities, in the sense that they are obtained from observational data. The procedure for their calculation is the same; only the collision frequencies $\bar{\nu}_{in}$ differ significantly. This comparison shows basically the same temporal variation, but magnitudes are frequently substantially different. These differences are not systematic in an obvious manner.

The purpose of this comparison is to emphasize the sensitivity of the neutral winds derived from observation to the collision frequency model employed to deduce them. Because of uncertainties involved in the calculation of ion-neutral collision frequencies, from the pertinent interactions to the numbers of each species of ion and neutral particle actually present, it is difficult to support one set of collision frequencies against another. However, to the extent that a degree of arbitrariness is involved, its effects on the final results - neutral wind velocities - should be recognized and acknowledged.

In a study of this nature, such considerations do not undermine the comparison between observation and theory, so long as the same collision frequencies are used consistently in both the data analysis and the theoretical calculations. There is at least a rough scaling with collision frequency of neutral velocities obtained from both theory and data analysis, as indicated by Figure 6-14. One calculation which could be adversely affected, however,

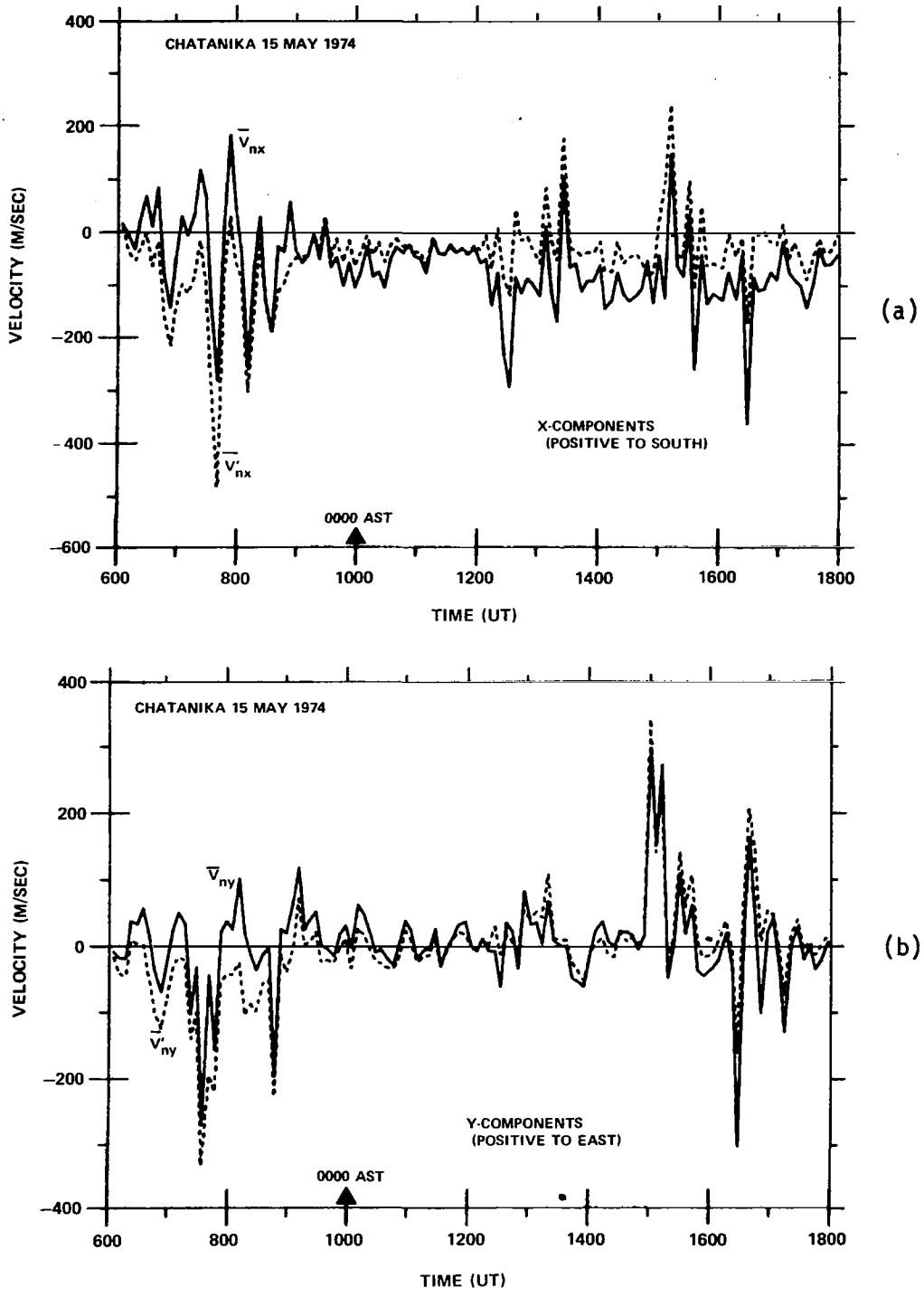

Figure 6-15. NEUTRAL VELOCITIES DETERMINED FROM INCOHERENT SCATTER RADAR OBSERVATIONS USING THE COLLISION FREQUENCIES OF THIS STUDY ($\bar{V}_n$ - SAME VELOCITIES AS FIGURE 6-3b)) AND USING THE COLLISION FREQUENCIES OF BREKKE ET AL. (1973) ($\bar{V}_n'$): (a) x-COMPONENTS; (b) y-COMPONENTS

is that of Joule heating, which depends on $(\vec{\overline{V}}_i - \vec{\overline{V}}_n)^2$. Since $\vec{\overline{V}}_i$ is determined directly by observation, its accuracy is affected only by the experimental error. However, because $\overline{V}_n$ is also subject to this additional bias in the data analysis, a Joule heating calculation is susceptible to similar error. This is merely noted for future studies because no such calculation is carried out here.

With that digression concluded, the primary comparison can be made between the theoretical weighted altitude average of the neutral velocity, $\vec{\overline{v}}_n$, and that determined from observation, $\vec{\overline{V}}_n$. These are presented in Figure 6-16. The initial impression is one of substantial disagreement. First, despite the temporal structure introduced into $\vec{\overline{v}}_n$ by taking the weighted altitude average, the temporal variation in $\vec{\overline{V}}_n$ is larger in both frequency and magnitude of fluctuations. From the comparison in Figure 6-14, it is clear that $\vec{\overline{V}}_n$ is a reasonably accurate reflection of the weighted altitude average of neutral velocity in terms of the observational data. However, Brekke, et al. (1974a) note that the data represent time averages - for this experiment over a period of 6 minutes. If velocities or electron densities are changing substantially during this time, the results will be inaccurate. It is evident that this happening when large differences are seen between consecutive measurements; and Figures 6-3a and 6-12a show this to occur frequently in this experiment. So these large rapid fluctuations must be taken as a qualitative indication of variability, rather than a quantitative measure of reality. The more stable quantities are a more accurate measure of the physical variables.

Even from this point of view, the discrepancy between $\vec{\overline{v}}_n$ and $\vec{\overline{V}}_n$ remains substantial. Two characteristics are apparent. First, the general magnitudes of $\overline{V}_{nx}$ and $\overline{V}_{ny}$ are considerably smaller than the broad maximums attained by $\overline{v}_{nx}$ and $\overline{v}_{ny}$. Secondly, the general directions of $\vec{\overline{V}}_n$ and $\vec{\overline{v}}_n$ bear little coherent relation to one another. Consequently it can be concluded that the theoretical basis for the calculated results is inadequate for describing the ionospheric conditions actually present when the observations were made. However, since the velocities calculated theoretically are somewhat larger in magnitude than those observed, the collisional coupling is evidently important. It

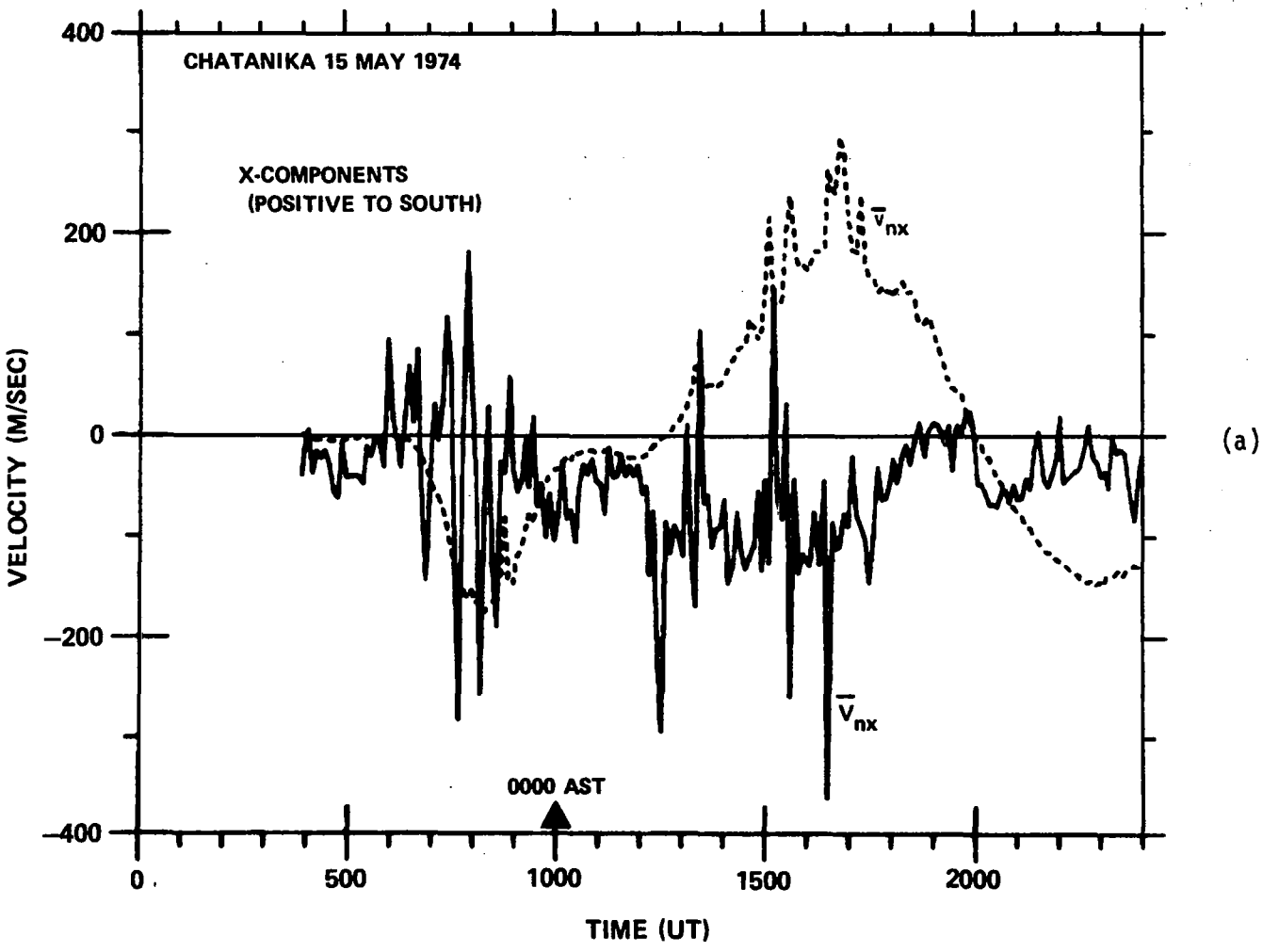

Figure 6-16. COMPARISON OF OBSERVED NEUTRAL VELOCITIES ($\bar{V}_n$) AND WEIGHTED ALTITUDE AVERAGES OF THE CALCULATED NEUTRAL VELOCITIES ($\bar{v}_n$) (a) x-COMPONENTS;

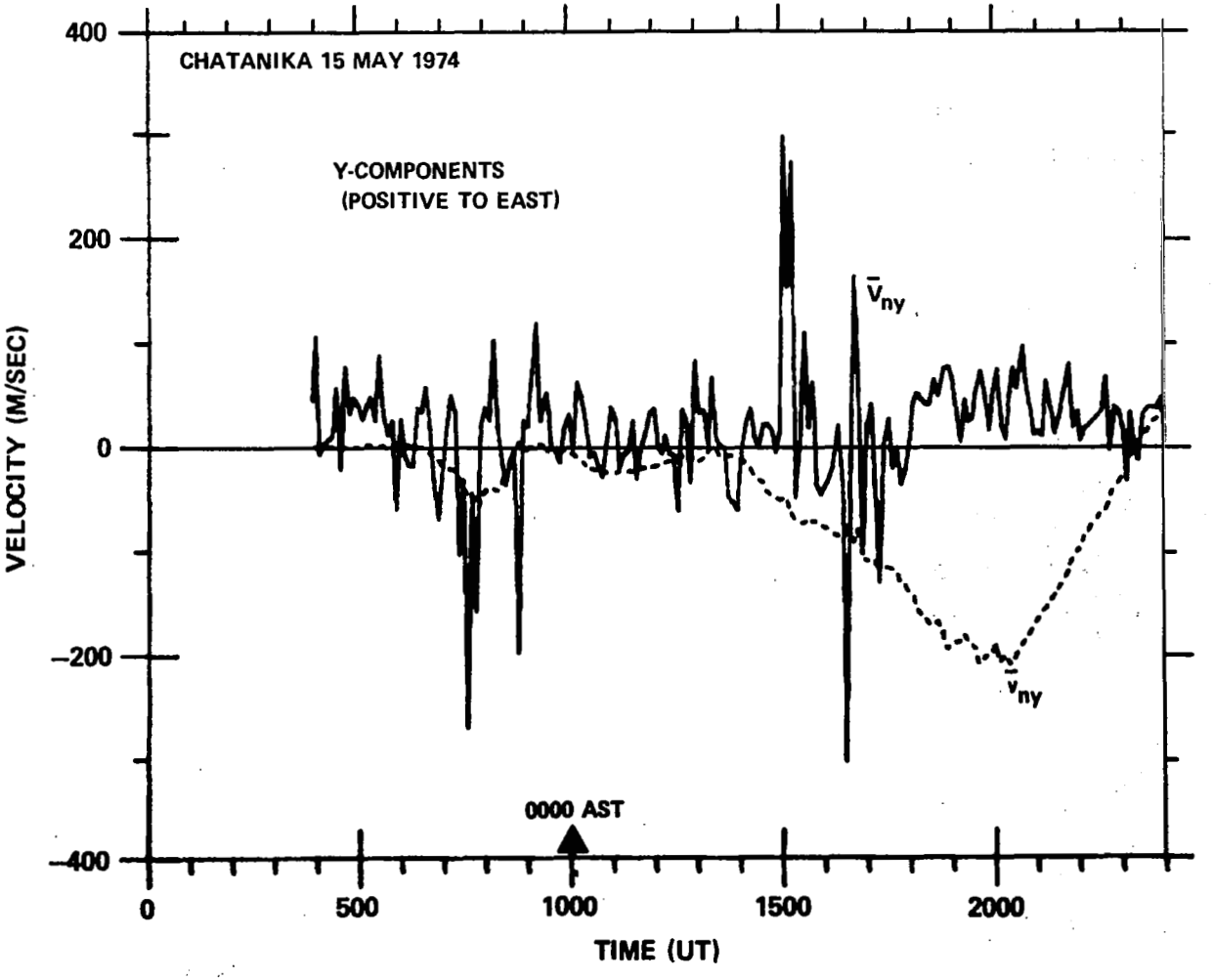

(b)

Figure 6-16. COMPARISON OF OBSERVED NEUTRAL VELOCITIES ($\bar{V}_n$) AND WEIGHTED ALTITUDE AVERAGES OF THE CALCULATED NEUTRAL VELOCITIES ($\bar{v}_n$) (b) y-COMPONENTS

appears that other mechanisms of comparable importance are operating in at least partial opposition to the collisional force so that the build-up of neutral velocities is inhibited.

It is helpful to recall briefly the basis of the theoretical calculation in order to see the implications of these results. The physical model is one of large electric fields of magnetospheric origin causing ions to move with large flow velocities. Some of this momentum is transferred to the neutral gas through collisions, causing it to move. The neutral gas motion is then modified somewhat by viscous and coriolis forces, these modifications being coupled back to the ions by collisions. From the comparisons in Figure 6-16, these processes are important, but insufficient to describe the actual physical behavior of the sytem. However, more information is now available than initially. Not only are velocities due to collisional coupling known, but the size of the discrepancy between these velocities and the observation velocities is known. This information can now be used to estimate the terms omitted form the theoretical analysis, that is, those terms required to resolve the discrepancy.

6.5.3 Estimates of Pressure Gradients

In order to carry out a calculation of this nature the original assumptions in subsection 6.3.1 must be reviewed. Those involving the ion momentum equation are on a sound physical basis and appear to require no modification. However, in the neutral momentum equation, the neglect of horizontal gradients was recognized as a mathematical expendient at the outset; this must now be reconsidered. The uncoupling of the neutral vertical component and use of static equilibrium model in its place remains an approximation, but probably not a major contributor to the discrepancies in the horizontal component. So, the primary requirement for more realistic horizontal neutral equations of motion appears to be the inclusion of horizontal gradients.

Thus, it is now assumed that the neutral velocities determined from incoherent scatter radar observations obey the following equations of motion:

$$\frac{\partial V_{nx}}{\partial t} = -\frac{1}{\rho_n}\frac{\partial p}{\partial x} + \frac{\eta_n}{\rho_n}\nabla^2 V_{nx} + \frac{\eta_n}{3\rho_n}\frac{\partial}{\partial x}(\nabla \cdot \vec{V}_n) - (\vec{V}_n \cdot \nabla)V_{nx}$$

$$- \bar{\nu}_{ni}(V_{nx} - V_{ix}) + 2V_{ny}\,\Omega_E \sin\lambda \qquad (6\text{-}24a)$$

$$\frac{\partial V_{ny}}{\partial t} = -\frac{1}{\rho_n}\frac{\partial p}{\partial y} + \frac{\eta_n}{\rho_n}\nabla^2 V_{ny} + \frac{\eta_n}{3\rho_n}\frac{\partial}{\partial y}(\nabla \cdot \vec{V}_n) - (\vec{V}_n \cdot \nabla)V_{ny}$$

$$- \bar{\nu}_{ni}(V_{ny} - V_{iy}) - 2V_{nx}\,\Omega_E \sin\lambda \quad . \qquad (6\text{-}24b)$$

In order to make use of the observational data, weighted altitude averages are required. This is accomplished formally by multiplying equations (6-24a, b) by $N_e(z)\,W(z)$, integrating over the first range gate, and normalizing to I_W (equation (6-6d)). When this is done the results may be written

$$\frac{\partial \bar{V}_{nx}}{\partial t} = -\frac{1}{I_W}\int \frac{N_e W}{\rho_n}\frac{\partial p}{\partial x}\,dz + \frac{1}{I_W}\int N_e W \frac{\eta}{\rho_n}\nabla^2 V_{nx}\,dz$$

$$+ \frac{1}{3I_W}\int N_e W \frac{\eta_n}{\rho_n}\frac{\partial}{\partial x}(\nabla \cdot \vec{V}_n)dz - \frac{1}{I_W}\int N_e W(\vec{V}_n \cdot \nabla)V_{nx}\,dz$$

$$-\bar{\nu}^*_{ni}(\bar{V}_{nx} - \bar{V}_{ix}) + 2\,\Omega_E\,\bar{V}_{ny}\sin\lambda \quad , \qquad (6\text{-}25)$$

where $\bar{\nu}^*_{ni}$ is the weighted altitude average of $\bar{\nu}_{ni}$, after the manner of equation (6-4). An analogous equation may be written for $\bar{V}_{ny}$.

Except for the last term in this equation, all terms in which the integral symbol is not written explicitly must be considered approximations, since they do not follow directly from equation (6-4). The left side in particular requires that electron densities vary slowly during the interval in which the time derivatives are evaluated. Since successive radar observations are used, this is consistent with the similar requirement for accurate observational data. It must be noted that only $\bar{V}_{nx}$ and $\bar{V}_{ny}$ are known from observational data. So those terms remaining as integrals are to be regarded as unknown quantities.

To make a comparison with the calculated results, a similar operation must be performed on the original equations (6-15a, b). This gives

$$\frac{\partial \bar{v}_{nx}}{\partial t} = \frac{1}{I_W}\int \frac{\eta_n N_e W}{\rho_n}\frac{\partial^2 v_{nx}}{\partial z^3}\,dz - \frac{1}{I_W}\int \bar{\nu}_{ni}(v_{nx} - v_{ix})N_e W\,dz$$

$$+ 2\,\Omega_E\,\bar{v}_{ny}\sin\lambda \qquad (6\text{-}26a)$$

$$\frac{\partial \bar{v}_{ny}}{\partial t} = \frac{1}{I_W}\int \frac{\eta_n}{\rho_n}\frac{\partial^2 v_{ny}}{\partial z^2} N_e W\,dz - \frac{1}{I_W}\int \bar{\nu}_{ni}(v_{ny} - v_{iy})N_e W\,dz$$

$$- 2\,\Omega_E\,\bar{v}_{nx}\sin\lambda\ . \qquad (6\text{-}26b)$$

Since v_{nx} and v_{ny} are known as functions of altitude, the integrals in these equations can be evaluated numerically without difficulty; that is, each term is a known quantity.

The difference between equations (6-25) and (6-26a) is now taken; this results in

$$\frac{\partial}{\partial t}\bar{V}_{nx} - \frac{\partial \bar{v}_{nx}}{\partial t} = \frac{1}{I_W}\int N_e W \frac{\eta_n}{\rho_n}\left[\frac{\partial^2 V_{nx}}{\partial z^2} - \frac{\partial^2 v_{nx}}{\partial z^2}\right]dz$$

$$+ \frac{1}{I_W}\int N_e W \frac{\eta_n}{\rho_n}\left[\frac{\partial^2 V_{nx}}{\partial x^2} + \frac{\partial^2 V_{nx}}{\partial y^2}\right]dz$$

$$+ \frac{1}{3I_W}\int N_e W \frac{\eta_n}{\rho_n}\frac{\partial}{\partial x}(\nabla\cdot\bar{V}_n)dz - \frac{1}{I_W}\int \frac{N_e W}{\rho_n}\frac{\partial p}{\partial x}\,dz$$

$$- \frac{1}{I_W}\int N_e W(\vec{V}_n\cdot\nabla)V_{nx}\,dz + 2\,\Omega_E\sin\lambda(\bar{V}_{ny} - \bar{v}_{ny})$$

$$- \bar{\nu}^*_{ni}(\bar{V}_{nx} - \bar{V}_{ix}) + \frac{1}{I_W}\int N_e W\,\bar{\nu}_{ni}(v_{nx} - v_{ix})\,dz \qquad (6\text{-}27)$$

with a similar equation for the y-component.

Several of these terms are probably small and can be omitted. The first term on the right side is negligibly small if the altitude structures of V_{nx} and v_{nx} are similar, or if both terms are small. This term for v_{nx} has been found in numerical calculations to be always at least one to two orders of magnitude smaller than the collision terms at these altitudes. Moreover, it seems unlikely that V_{nx} has larger vertical velocity gradients, since the magnitude of $\bar{V}_{nx}$ is generally smaller and vertical gradients in v_{nx} are themselves large. Hence, it appears reasonable to omit this term. As another approximation, the other viscous terms (second and third terms on the right side) are assumed negligible in comparison with the nonlinear term (fifth term on the right side). This seems reasonable from order of magnitude considerations, which can be specified more precisely than in Section IV because conditions are more restricted. The ratio of viscous to nonlinear terms is given by (order-of-magnitude only)

$$\left|\frac{(\eta_n V/\rho_n L^2)}{V^2/L}\right| \sim \left|\frac{\eta_n}{\rho_n V L}\right| \lesssim 10^{-2} \quad , \tag{6-28}$$

where $\eta_n \sim 10^{-4}$ poise, $V \sim 10^4$ cm s^{-1}, $\rho_n \gtrsim 2 \times 10^{-12}$ gm cm^{-3} and L is a typical horizontal scale length exceeding 10^6 to 10^7 cm.

With these approximations, equation (6-27) is simplified and rearranged so that unknown quantities appear on the left side while terms which can be evaluated are on the right. The result is

$$\frac{1}{I_W}\int N_e W\left[\frac{1}{\rho_n}\frac{\partial p}{\partial x} + (\vec{\bar{V}}_n \cdot \nabla)V_{nx}\right]dz = 2\,\Omega_E \sin\lambda(\bar{V}_{ny} - \bar{v}_{ny})$$
$$- \bar{\nu}^*_{ni}(\bar{V}_{nx} - \bar{V}_{ix}) + \frac{1}{I_W}\int N_e W \bar{\nu}_{ni}(v_{nx} - v_{ix})dz$$
$$- \left[\frac{\partial \bar{V}_{nx}}{\partial t} - \frac{\partial \bar{v}_{nx}}{\partial t}\right] \quad . \tag{6-29a}$$

The corresponding equation for the y-component is

$$\frac{1}{I_W}\int N_e\, W\left[\frac{1}{\rho_n}\frac{\partial p}{\partial y} + (\vec{V}_n \cdot \nabla)V_{ny}\right] dz = -\,2\,\Omega_E \sin\lambda(\bar{V}_{nx} - \bar{v}_{nx})$$
$$-\,\bar{\nu}^{*}_{ni}(\bar{V}_{ny} - \bar{V}_{iy}) + \frac{1}{I_W}\int N_e\, W\,\bar{\nu}_{ni}\,(v_{ny} - v_{iy})\,dz$$
$$-\left[\frac{\partial \bar{V}_{ny}}{\partial t} - \frac{\partial \bar{v}_{ny}}{\partial t}\right] \quad . \tag{6-29b}$$

The left side is seen to include both the pressure gradient and nonlinear terms. Their relative contributions can be estimated, based on observed velocities, if it is assumed that the horizontal scale length L is approximately the same for both pressure and velocity variations. With that provision, the ratio of nonlinear to pressure gradient terms is (order-of-magnitude)

$$\left|\frac{(\vec{V}_n \cdot \nabla)V_{nx}}{\frac{1}{\rho_n}\frac{\partial p}{\partial x}}\right| \sim \left|\frac{M_n V_n^2}{k T_n}\right| \quad . \tag{6-30a}$$

From Figure 6-16, observation values of V_n are of the order of 100 m s^{-1}. With assumed values of $m_n \sim 25$ AMU and $T_n \sim 400°K$, consistent with the neutral model employed, the ratio is

$$\left|\frac{(\vec{V}_n \cdot \nabla)V_{nx}}{\frac{1}{\rho_n}\frac{\partial p}{\partial x}}\right| \lesssim 10^{-1} \quad . \tag{6-30b}$$

Actually, velocities in Figure 6-16 sometimes exceed 100 m s^{-1} by factors of 2 to 4; and, on the other hand, T_n very likely exceeds 400°K by substantial amounts, on occasion, due to local heating. For this reason, the nonlinear term is retained in equations (6-29a, b). However, from (6-30b), it is clear that it is the pressure gradient which is generally being evaluated by these equations.

Numerical evaluation of terms on the right side of equations (6-29a, b) gives the accelerations shown in Figure 6-17a, c. These are based on the calculation and observation values shown in previous figures, and at time

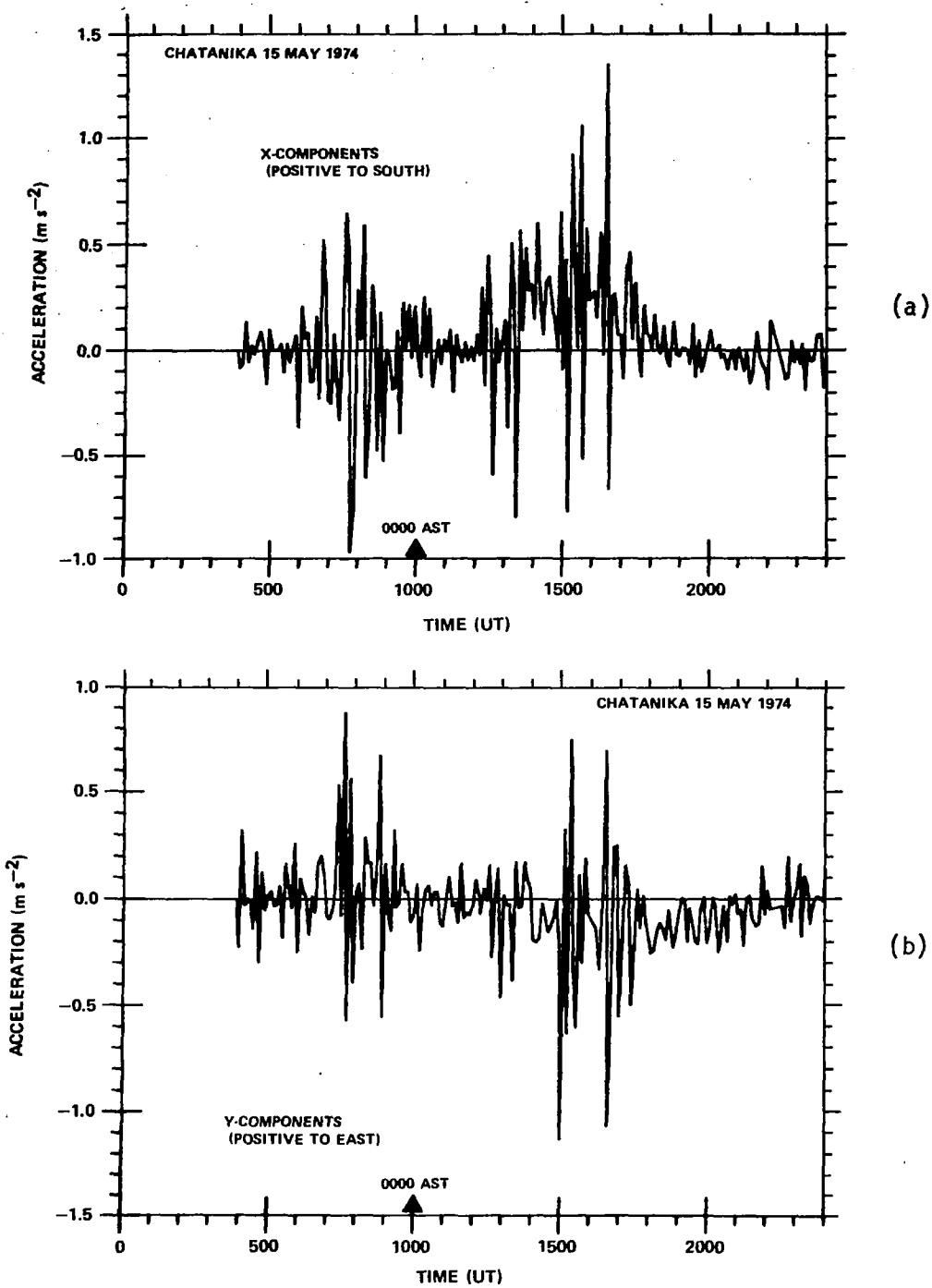

Figure 6-17. PRESSURE GRADIENT ACCELERATIONS AS DETERMINED FROM EQUATIONS (6-29a, b): (a) x-COMPONENT; (b) y-COMPONENT

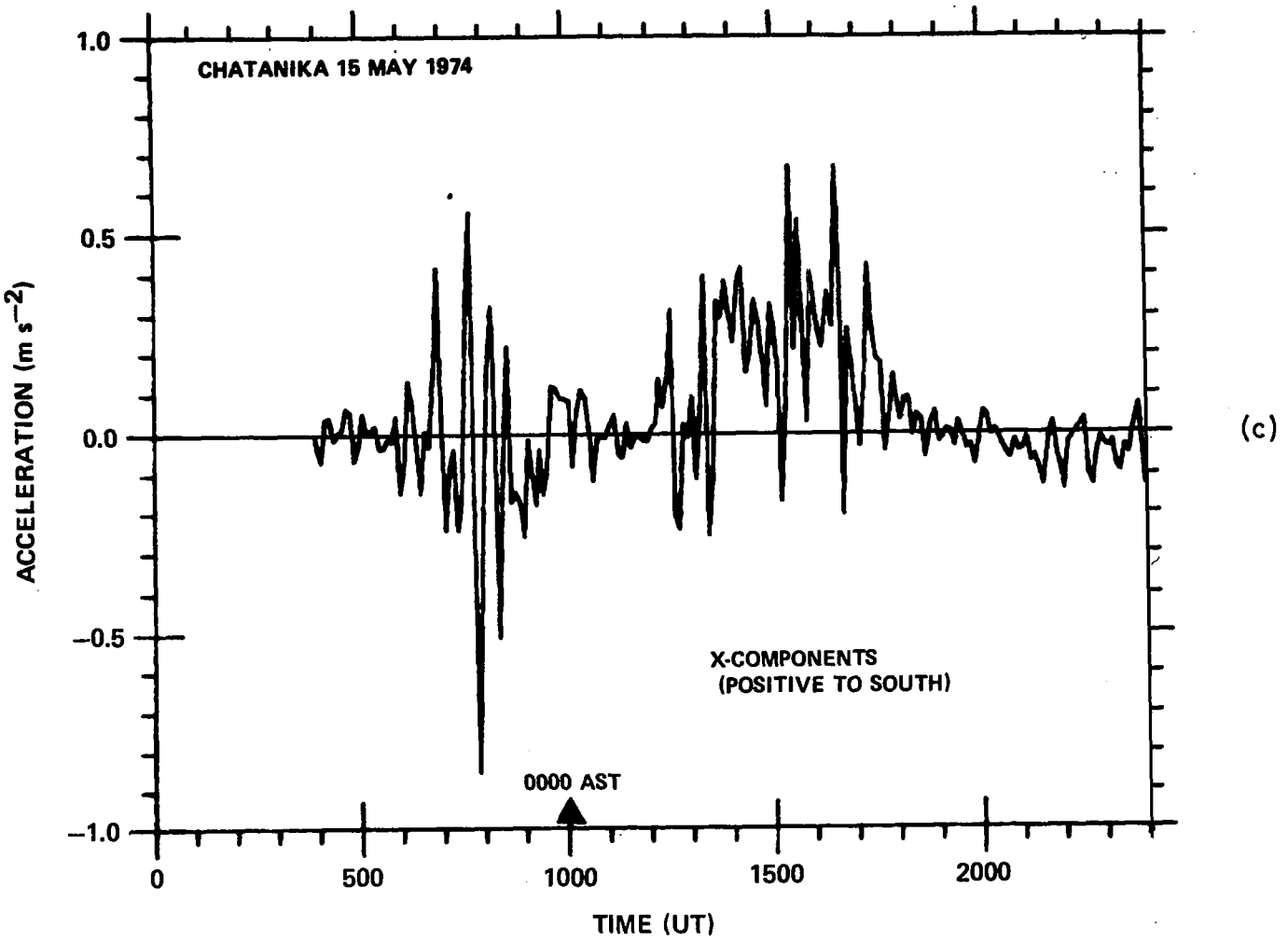

Figure 6-17. PRESSURE GRADIENT ACCELERATIONS AS DETERMINED FROM EQUATIONS (6-29a, b): (c) x-COMPONENT AVERAGED BETWEEN CONSECUTIVE OBSERVATION TIMES

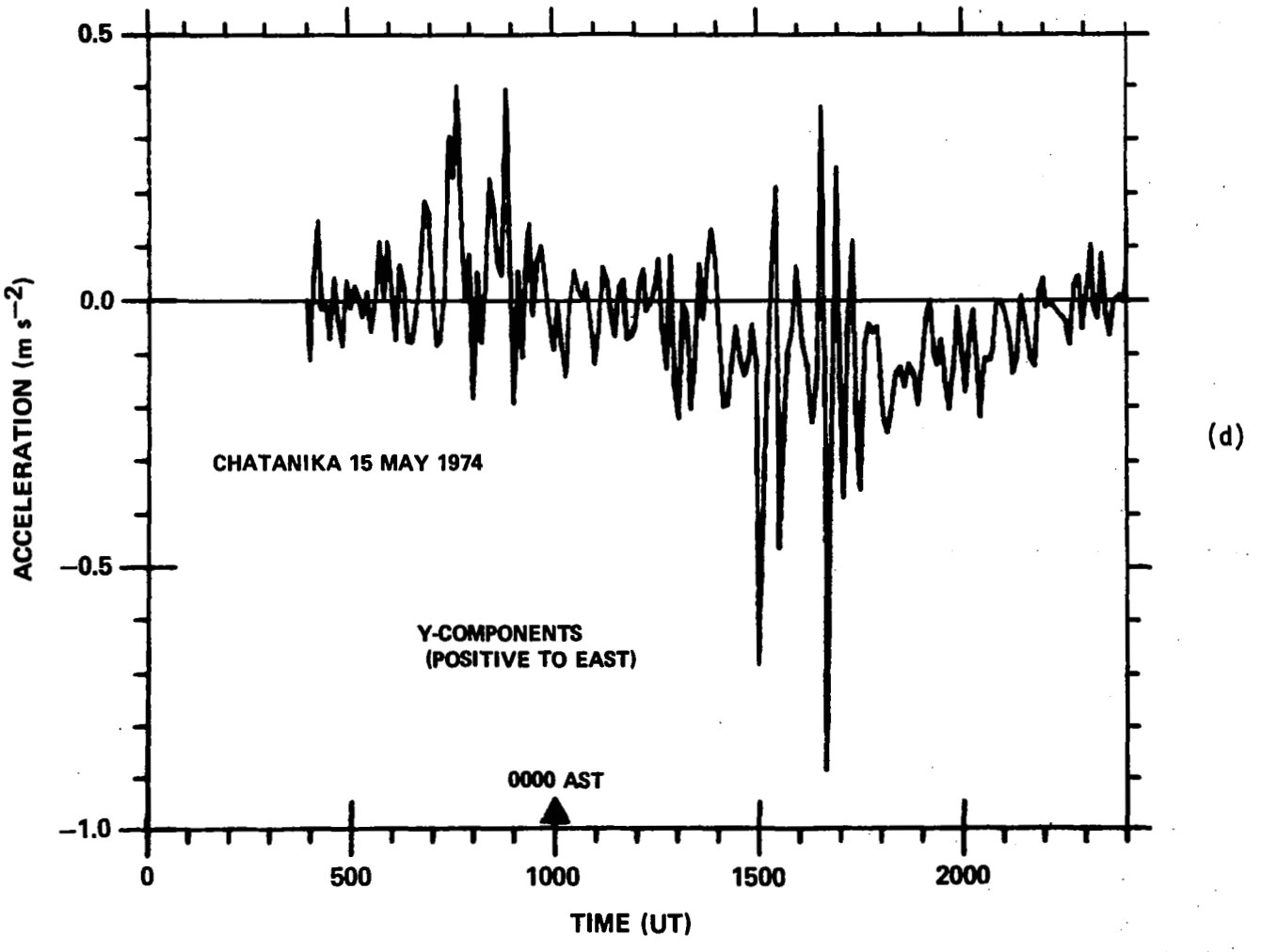

Figure 6-17. PRESSURE GRADIENT ACCELERATIONS AS DETERMINED FROM EQUATIONS (6-29a, b): (d) y-COMPONENTS AVERAGED BETWEEN CONSECUTIVE OBSERVATION TIMES

points corresponding to the observations. The rather large fluctuations which frequently occur between consecutive points tend to obscure the general trend. Since they may result from inaccuracies in the data, due to rapidly changing conditions, and from contributions from the nonlinear term for the larger velocities, these fluctuations do not necessarily represent good values of the pressure gradient. To see the general magnitude of this term more clearly, these fluctuations are smoothed somewhat by taking simple averages between consecutive points. These results are shown in Figure 6-17b, d.

Despite this averaging of results, considerable temporal structure remains. Nevertheless, trends in the magnitude and direction of the pressure gradient are now more apparent, particularly during the second electric field enhancement. In the x-component, the first two hours indicate no definite direction. During the first enhancement (0600 to 1100 hours UT; see Figure 6-3a) this component fluctuates considerably, but appears to be somewhat more negative than positive, indicating generally higher pressures (heat sources) to the north. Between enhancements, the pressure gradient is relatively small, and perhaps slightly more negative (northward) than positive. For the duration of the second electric field enhancement (1200 to 1800 hours UT), the meridional pressure gradient is predominately positive, indicating heat sources primarily to the south. Thereafter, this component becomes small, fluctuating about zero for about two hours, and then remains small but primarily negative (heat sources to the north) for the remainder of the experiment.

A similar examination of the y-component of the pressure gradient reveals both similarities and differences. The initial two hour period is again characterized by small magnitudes with indefinite direction. During the first electric field enhancement, the sign is more definite than for the x-component and the fluctuations smaller in amplitude. The predominately positive pressure gradient (heat source to the east) appears to become primarily negative shortly before 1000 hours UT and remains moderately small until about 1230 hours. For the duration of the second enhancement this component is primarily negative (heat sources to the west), although large rapid fluctuations occur between 1500 hours and 1800 hours UT. In contrast with the x-component,

however, the y-component does not become appreciably smaller in magnitude after termination of the second electric field enhancement. Rather it becomes more definite in its sign, still indicating heat sources to the west. This situation remains until about 2200 hours UT, when the sign becomes indefinite.

Magnitudes of these accelerations are seen to be a few tens of centimeters per second per second during electric field enhancements and a few centimeters per second per second otherwise. This distinction is less clear for the y-component, however, than for the x-component. These magnitudes may be compared with pressure gradient accelerations used in global theoretical models of the neutral wind system. Pressure gradients in the models of Kohl and King (1967) and Blum and Harris (1975) are both based on one of the neutral model atmospheres of Jacchia. Amplitudes of these pressure gradients for E region altitudes are $\lesssim 1$ cm s^{-2}. Thus, pressure gradients during disturbed conditions at high latitudes are typically at least an order of magnitude larger than those driving the global neutral wind models, which are due primarily to solar heating at low latitudes. It is therefore not surprising that observations of neutral winds at high latitudes under geomagnetically disturbed conditions frequently disagree with these models (e.g. Stoffregen, 1972; Meriwether, et al. 1973; Brekke, et al. 1974a; Rothwell, et al. 1974). For these conditions no other calculated or experimentally derived estimates of horizontal pressure gradients are known to be available for comparison. Accelerations due to ion drag are of the same order as these due to pressure gradients.

To interpret these results, it is important to note a significant difference between ion drag and pressure gradients as driving forces for neutral winds. For ion drag the direction of the electric field as well as its distribution and magnitude must be considered. Pressure gradients, however, depend only on the distribution (geometry) and magnitude of pressure enhancements (primarily heat sources). Since these results involve only pressure gradients, interpretation requires an explanation of the implied distribution of heat sources. Local heating, for example Joule heating associated with ion-neutral velocity differences at the point of observation, need not be considered, since it would represent a local maximum for which the local gradient would

vanish. Rather it is heat sources in surrounding regions, which are not observed by the radar, that must be considered.

Comparison of the electric fields in Figure 6-3a and the electron number densities at constant altitude in Figure 6-12 shows that periods of enhanced electric field occur during the same periods as auroral E layers. This is not meant on a (time) point by point basis, because large electric field magnitudes are often anticorrelated with E region electron densities; but rather periods of large rapid fluctuations in electric field magnitude coincide with similar fluctuations in E region electron densities. Since a developed auroral E layer is a reliable indicator of auroral activity, it can be concluded from Figure 6-12 that the ionosphere over Chatanika was in the auroral oval, that is, in the midst of auroral activity, from shortly after 0600 hours to about 1800 hours UT, with a possible exception during a brief period between 1200 hours and 1300 hours UT. Further, auroral heating in the form of both energetic particle precipitation and Joule heating was occurring concurrently in the same locations. Based on statistical models of the auroral oval (Feldstein and Starkov, 1967), it can be assumed that before and after this period, all auroral activity in the vicinity of Chatanika was to the north.

In this context the pressure gradients in Figures 6-17c, d can be examined. During the initial two hour period, no particular directionality is evident in the pressure gradient. After Chatanika enters the auroral oval near 0600 hours UT (2000 hours AST), the pressure gradient indicates that heating lies primarily to the north and east, which is consistent with the general picture of auroral activity being concentrated toward the local midnight and early morning sector (Akasofu, 1968). From 0900 hours to 1100 hours UT (1000 hours UT is AST midnight), no consistent directions are indicated; this can be viewed as a consequence of a somewhat symmetric distribution of heat sources about Chatanika. The period 1100 hours to 1300 hours is somewhat ambiguous; a more detailed discussion is deferred. During the second active period, from 1300 hours to 1800 hours UT (0300 hours to 0800 hours AST) the pressure gradients indicate predominant heating to the south and west. Again the heating toward the west is consistent with primary activity in the local midnight and

early morning sector of the auroral oval. The definite southward direction of the heat sources shows that Chatanika is well within the auroral oval. Soon after 1800 hours UT the electric field decreases abruptly to very small values, concurrent with the disappearance of the auroral E layer. Thus, Chatanika has left the auroral oval, or vice versa.

After 1800 hours UT, local activity is at a low level. The y-component of the pressure gradient, however, remains relatively large in magnitude with a definite westward direction, decaying slowly over the next 4 hours. It appears that heating on the night side has built up and maintained pressure differentials which are affecting the dayside region. In contrast, the x-component drops rapidly to very small magnitudes by 1830 hours UT, and remains small and essentially undirected for about an hour. Then it becomes definitely negative, indicating heat sources to the north where the dayside auroral-oval-cusp region is located.

Separation of spatial and temporal effects in observations at a single location is difficult, particularly when it involves a dynamic region like the auroral oval, which has a relatively fixed orientation with respect to the sun but can expand or contract due to magnetospheric electrodynamics. Nevertheless, some plausible inferences can be drawn. The period 1100 hours to 1300 hours is a good example. Between 1100 hours and 1200 hours UT the electric field (Figure 6-3a) has become quite small, while a small auroral E layer (Figure 6-12) persists. Between about 1215 hours and 1245 hours UT the auroral E layer vanishes and a large electric field develops. Several possible explanations for these observations exist: (1) the auroral oval could have contracted so that Chatanika was to the south of its equatorward border; (2) Chatanika could have encountered an extended region of low activity (first a region of low electric field, then low auroral precipitation), while activity continued in surrounding regions; this could occur by Chatanika rotating through a more or less fixed region of low activity, or the region could drift by Chatanika due to electrodynamic forces; or (3) activity could simply cease in time over a large spatial region due to source region temporal variations.

The first possibility does not seem to be supported by the available information. It could not have occurred except during the brief period when the auroral E layer vanished. Calculations of Jones and Rees (1973) show that an auroral E layer will decay to background levels in a minute or less after removal of the ionization source. This appears to happen near 1215 hours UT, but not prior to that time. However, during the period of no auroral E layer, a large electric field develops. For all other times in these observations, large electric fields occur in the immediate vicinity of auroral activity. Furthermore, during this same time a substantial pressure gradient develops directed first toward the south. This could not happen if Chatanika were to the south of the auroral oval at this time. For this same reason, the second explanation appears more likely than the third. It seems probable that Chatanika rotated into a slot between bands of activity oriented along the auroral oval. However, data from other locations would be required to substantiate this.

Similar considerations can be applied to the time period after 1800 hours UT. Here the evidence supports the view that the position of Chatanika relative to the auroral oval has shifted to the south. Electric fields and E layer number densities are consistent with this interpretation. Also the x-component of the pressure gradient favors this view. Heating to the south of Chatanika is indicated for several hours before. Shortly before 1730 hours UT, the pressure gradient begins to decline rapidly. This would be expected if the auroral oval were contracting northward so that pressures previously built up in the south were becoming balanced by pressures developing in the north. Such a balancing is more likely than a decay of the pressure in the south because these decay times are of the order of hours (Thomas and Ching, 1969; Rees, 1971b). From Figure 6-17c, it appears that approximate balance is achieved about 1830 hours UT, lasting for approximately an hour. Continued heating to the north then prevails, shifting the dominant pressure to the north of Chatanika.

While interpretations such as these cannot be proved without information covering an extended spatial region, they are consistent with the observations

at Chatanika and the general morphology of auroral activity. The results, as interpreted above, support the schematic model suggested by Stoffregen (1972) for explaining discrepancies between observed high latitude neutral winds and winds determined from the global theoretical wind models mentioned previously. Figure 6-18 shows his proposed schematic modification of global temperature distribution. This proposal is based on an analysis of 25 chemical release observations of neutral winds, restricted in local time to twilight hours, and for altitudes generally above 200 km in altitude. Nevertheless, the required heating would take place primarily in the E region and the general features of the diagram are consistent with the discussion of pressure gradients above. In particular the westward pressure gradient after 1800 hours UT (0800 hours AST) is satisfactorily explained, whereas the pressure gradient produced by solar heating alone should be eastward and of much smaller magnitude.

A possible period of inconsistency is in the first two hours of the experiment, when auroral heating would perhaps be expected to produce an eastward directed pressure gradient. However, effects of this heating may be small, so that some form of balance is achieved with the small westward pressure gradient associated with solar heating and heating in the afternoon sector of the auroral oval. Also because of uncertainties involving initial conditions, the earliest calculated results are not necessarily reliable; this could skew the pressure gradient calculation during that time period.

The broad features of the pressure gradient results have been discussed at some length because it is felt that they are more reliable than the small time scale features, due both to noise in the observational data, and to approximations required in deriving equations (6-29a, b). However, the temporal structure evident in Figure 6-17 requires comment. This structure is almost certainly not all real. Some is due simply to experimental uncertainties in the observed ion velocities. Likewise, some is due to altitude structure of the velocity fields and the weighted altitude averaging, as was seen to occur in $\vec{v}_n$. It should be reemphasized that the pressure gradients calculated are weighted altitude averages. The altitude structure of these horizontal pressure gradients is not known. Conceivably, close to rapidly varying

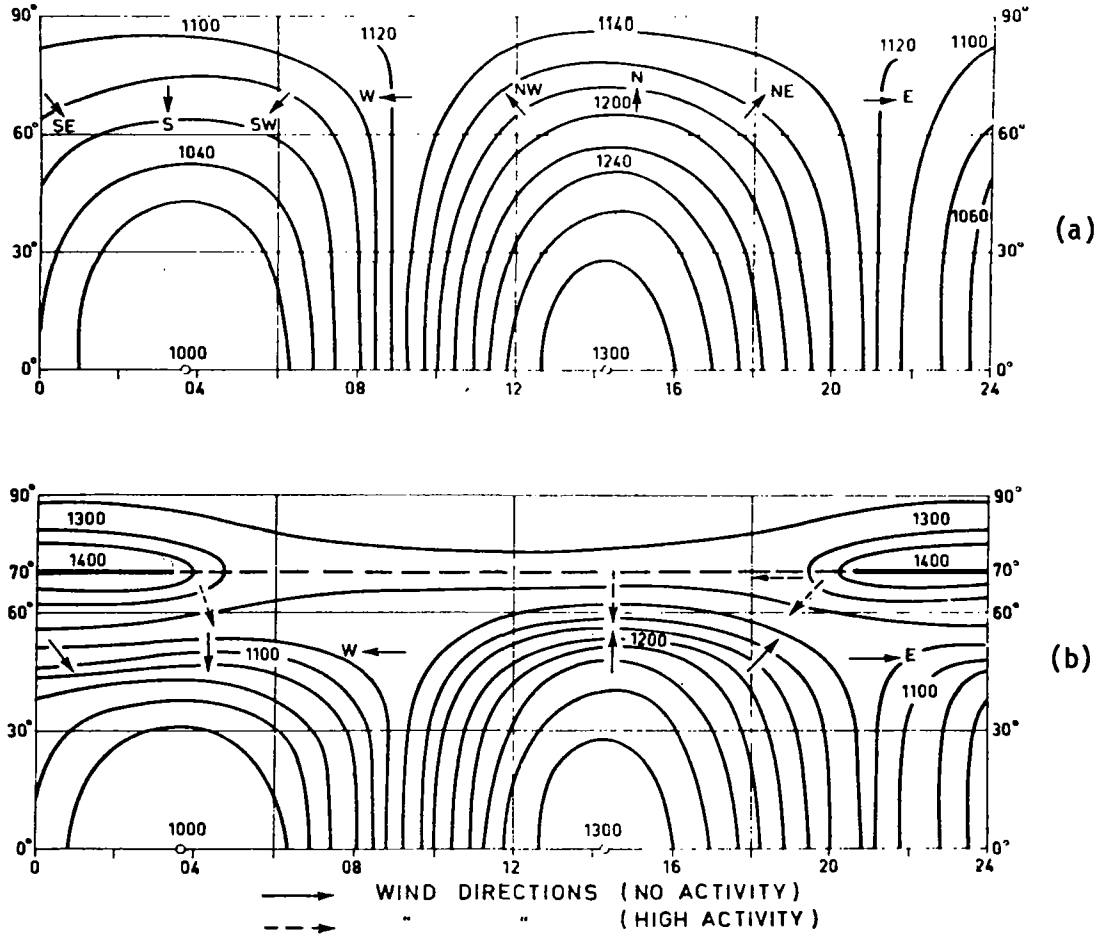

Figure 6-18. SCHEMATIC MODIFICATION OF EXOSPHERIC TEMPERATURE DISTRIBUTION PROPOSED BY STOFFREGEN (1972) TO INCORPORATE AURORAL HEAT SOURCES: (a) ORIGINAL DISTRIBUTION (JACCHIA, 1965); (b) STOFFREGEN'S (1972) MODIFIED DISTRIBUTION

localized sources of Joule and particle heating, it could be complicated, but vertical motions would likely diminish such complexities rapidly.

Despite these disclaimers, however, the temporal structure should not be dismissed entirely because there are physical reasons for expecting it to exist, based on discussions above. If the interpretations made previously are basically correct, Chatanika was more or less surrounded by particle and Joule heating while in the auroral oval. From the variability of the electron densities and electric fields, this heating is evidently highly variable in space and time. Thus, while heating may, for example, occur predominately to the south of Chatanika, sudden localized heating to the north may also occur. Depending on the strength and location of the northern heat source relative to the observation point, the southward pressure gradient could be diminished or even reversed. Hence, rapid changes of neutral wind magnitudes and directions could be a consequence of the sudden development of heat sources in various nearby locations and the resultant fluctuations in pressure gradients.

In this context back pressures must be considered. When a moving gas flows into a stationary gas (or one moving more slowly), density will increase. The localized pressure build up will result in a pressure gradient (back pressure) which opposes the motion of the fast gas but also transmits momentum to the stationary gas causing it to move. As a result, the original fast moving gas will be slowed and probably diverted. The precise role of back pressures in the auroral oval itself is difficult to assess. It is possible that much of the fluctuation in magnitude of the pressure gradients is associated with back pressures. However, conservation of momentum permits a back pressure only to diminish the original pressure gradient, not to reverse its sign. Thus, those frequent fluctuations which involve a reversal of component direction require a different explanation, such as offered previously.

Finally, some idea of the horizontal scale lengths (L) associated with these pressure gradients can be gained from order-of-magnitude estimates. Let Δ denote values of the acceleration due to the weighted altitude average of the pressure gradient, as determined from equations (6-29a, b). The order-of-magnitude is then estimated from

$$\left|\frac{1}{\rho_n} \nabla p\right| \simeq \left|\frac{N_n k T_n}{N_n \bar{m}_n L}\right| \simeq \frac{k T_n}{\bar{m}_n L} \simeq \Delta \quad .$$

When this relation is solved for L, the result is

$$L \simeq \frac{k T_n}{\bar{m}_n \Delta} \quad .$$

Based on T_n = 500°K and $\bar{m}_n$ = 25 AMU, values for L are given in Table 6-3. Thus, scale lengths corresponding to pressure gradients in Figure 6-17 are seen to range generally from a few hundred to a few thousand kilometers, which are not unreasonable.

Table 6-3. HORIZONTAL SCALES ASSOCIATED WITH PRESSURE GRADIENT ESTIMATES

$\left\|\frac{1}{\rho_n} \nabla p\right\|$ (cm s^{-2})	1	10	100
L (km)	2×10^4	2×10^3	2×10^2

6.6 DISCUSSION AND CONCLUSIONS

In recent years several analyses of neutral wind observational data have examined the problem of discrepancies between theoretical winds predicted by global models and those observed under magnetically disturbed conditons. These have considered altitudes above 150 km; however, results obtained here are pertinent to those discussions. Basically the issue comes down to whether ion drag (collisional coupling) or auroral heating (Joule and charged particle precipitation) is primarily responsible for deviations from the models. Stoffregen (1972) and Rothwell, et al. (1974) contend that ion drag cannot account for the observations and that pressure gradients due to heating are the primary driving forces. On the other hand, Rees (1971a) and Meriwether, et al. (1973) favor ion drag, particularly in the evening and midnight sector; and the latter specifically argue against pressure gradients as accounting for discrepancies at other times.

The observations of groups on both sides of the question are based on chemical releases, which are somewhat brief (lasting a few minutes) and are restricted in local time coverage. The arguments are semi-quantitative in nature, relying heavily on the relative directions of the ion and neutral velocities. The more recent papers on both sides cite the results of Fedder and Banks (1972) as indicating that the equilibrium directions for ion and neutral winds are coincident above about 200 km. In this regard the neglect of coriolis effects by Fedder and Banks (1972) is significant. Figure 6-8d shows that a directional difference between ion and neutral velocities is maintained in a steady state, even at higher altitudes, when the coriolis force is taken into account. From the detailed numerical results, at 250 km $\vec{v}_n$ is rotated in a clockwise direction through an angle of 47 degrees from $\vec{v}_i$ in this calculation. This angle develops over a period of time, but even at 3 hours into the calculation this angle has reached a value of about 30 degrees. The time for development and the final equilibrium angle depend on the model values used. At lower altitudes the angles can be somewhat larger (e.g. about 56 degrees for 150 km at 24 hours). Such effects should be considered in future discussions of ion drag.

An additional consideration is the variability of ion velocity. Figures 6-3a, b show that the electric field (hence ion velocity) can change substantially in magnitude and direction while neutral winds at high altitudes are presumably less variable. Thus, observations over relatively short periods of time may be subject to considerable deviation from the general trend over a period of one or more hours. Comparison of ion and neutral velocity directions for brief periods might then be quite misleading.

Results of these calculations indicate that both ion drag and pressure gradients due to auroral heating are important. While heating appears to predominate during this experiment, the effects of ion drag are large enough to modify the winds significantly, even though not decisively. Moreover, it is not obvious that these results apply generally. Both Joule heating and ion drag result from the same physical phenomenon -- ion collisions with neutrals. Joule heating varies with $|\vec{v}_i - \vec{v}_n|^2$ while ion drag varies with $(\vec{v}_i - \vec{v}_n)$.

It therefore appears that as $|\vec{v}_i - \vec{v}_n|$ increases, a transition will occur, below which ion drag will dominate the bulk motion and above which pressure gradients due to Joule heating will assume that role. An important factor in this consideration, however, is the spatial distribution of electric fields, which is the driving function for the ions. This precludes any simple estimate of such a threshold. Furthermore, if particle precipitation heating is larger than Joule heating the question is moot. The point is that under different conditions, also to be found in the high latitude ionosphere, ion drag may predominate.

In summary, the following conclusions are drawn from the calculations. Collisional coupling of neutral particles with ions driven by large electrostatic fields can cause neutral winds of several hundred meters per second, having considerable altitude structure below about 130 km. Coriolis forces have the effect of maintaining ion-neutral velocity differences, even in a steady state for constant electric fields. Attainment of a steady state at low altitudes requires longer times when coriolis forces are taken into account than in their absence.

When observed electric fields and electron number densities are used in a simple collisional coupling calculation, short time variations in these properties are not reflected in the resulting neutral wind at a given altitude. The neutral gas inertia is so large relative to the rate of collisional momentum transfer, that such variations are averaged out. However, when weighted altitude averages of the neutral velocity are computed, short time scale perturbations of up to 50 percent are found to occur, due to fluctuations in the electron density weighting factor.

Comparison of weighted altitude averages of neutral velocities computed by direct numerical integration with those obtained indirectly from similar averages of ion velocities by means of the incoherent scatter radar data analysis procedure reveals: (1) magnitudes are underestimated by up to 40 percent; but (2) temporal structure and general directions are reasonably well reproduced. Magnitudes of velocities determined from the radar data are also

somewhat sensitive to the collision frequencies used, which includes the interaction model, the ion composition model, and the neutral atmosphere model. Some of the temporal structure is associated with variability in ionization density profiles due to the fact that weighted altitude averages of ion velocities are observed. With due recognition of these factors, however, it appears that neutral velocities derived from the incoherent scatter radar observations give a reasonable indication of the time evolution of neutral winds.

From a direct comparison of neutral velocities derived from the incoherent scatter radar observations with the weighted altitude averages of the calculated velocities, it is found that ion drag is inadequate to explain the observations. An equation is derived to compute the pressure gradient required to remove the discrepancies between observed and calculated results. The magnitude of the acceleration associated with this pressure gradient is found to vary from a few centimeters per second per second in quieter periods to a few tens of centimeters per second per second in more active periods. Accelerations due to ion drag are of the same order. These are generally at least an order-of-magnitude larger than those associated with solar heating. Directions of the pressure gradients are consistent with the location of the radar relative to the auroral oval and expected auroral heat sources. Fluctuations in the pressure gradients, to the extent that they are real, are thought to result from shifting balances in highly variable heat sources and from back pressures.

It appears that ion drag and pressure gradients are both required to explain the neutral winds generated in the auroral E region during geomagnetic disturbances.

THIS PAGE INTENTIONALLY LEFT BLANK

Section VII

SUMMATION

7.1 SUMMARY AND CONCLUSIONS

This work is comprised of two basic parts: a formal development of the conservation equations for ionospheric gases, and an application of these equations to ionospheric dynamics, in which the generation of neutral winds during geomagnetic disturbances is investigated. Governing equations for ionospheric gases are developed from kinetic theory, beginning with the Boltzmann equation; and a particle viewpoint is maintained throughout. The final formulation is based on the three-fluid approximation, which requires that the electron, ion, and neutral gases be treated separately, with different temperatures and flow velocities for each. The domain of applicability of the final equations is approximately 90 km to 800 km in altitude for all geographic locations.

Starting from the Boltzmann equation a formal equation of transport for an arbitrary particle property is derived in Section II. This property is successively specified to be mass, momentum, and kinetic energy, resulting in the species conservation equations for these properties. Collision terms are treated separately in Section III in the binary collision formalism of the Boltzmann collision integral. Formal results are extended by approximating the species distribution functions as independent, displaced Maxwellian distributions. In this context a new formalism is developed for the collision terms in the momentum and energy equations; it simplifies calculations for specific interactions, as compared with similar expressions presently in the literature. Explicit evaluations of collision terms are carried out in the Appendix for a sufficient variety of interactions to meet most ionospheric requirements. In addition, proofs of some of the limiting properties of the general expressions are provided there.

In Section IV, the formalism of the species conservation equations is applied to the ionosphere in terms of the three-fluid approximation. This

results in separate sets of conservation equations for electrons, ions, and neutral particles, coupled through the collision terms. Extreme values of ionospheric properties and parameters are considered for the altitude region 90 km to 800 km, for which the three-fluid approximation is assumed to hold. Based on these values, order-of-magnitude estimates are made to determine the range of values possible for each term in the complete set of conservation equations. Those terms which can be clearly identified as negligible under all ionospheric conditions for this altitude region are omitted. The resulting set of equations provides a reasonable starting point for a wide variety of E and F region ionospheric investigations, from purely theoretical model studies to the data analysis of ground-based or *in situ* observations.

In order to close the set of conservation equations, the higher order velocity moments introduced into the equations by the derivation method have to be related to lower order velocity moments, essentially independently of the set of conservation equations. This is accomplished in Section V by means of transport tensors and coefficients. Electron transport is treated in a comprehensive manner by the method of Shkarofsky (1961). In order to take advantage of simplifications in the use of this method when electon-neutral collision frequencies vary with relative velocity as a power law, a new method is derived for approximating an arbitrary collision frequency velocity dependence as a power law. The equations presented represent a condensation of Shkarofsky's procedure, for application to ionospheric calculations. Ion and neutral transport coefficients available from the literature are also provided. Explicit sets of collision frequencies for electron-ion, electron-neutral, and ion-neutral collisions are presented, as computed from results in Section III and the Appendix, or as taken from the literature. Those sets of collision frequencies incorporating the effects of flow velocity differences have not previously been available.

The second basic portion of this work applies the results of the first five Sections to a specific problem in Section VI. In the process, it illustrates the different methods available for modifying the set of initial equations (the products of the first part) so that numerical solutions can be

obtained. These methods include additional approximations based on the physical conditions of the particular problem, use of empirical or analytical models as substitutions for equations or variables, use of observational data in the same manner, and mathematical assumptions required for consistency with these other techniques.

The problem investigated involves neutral winds observed during magnetically disturbed conditions in the auroral E region. One objective of the calculations is to determne the effect of altitude structure in the ion and neutral winds on the determination of neutral winds from incoherent scatter radar observations. A second objective is to determine the relative importance of collisional coupling (ion drag) and auroral heating in the generation of these winds. Observations made by the incoherent scatter radar at Chatanika, Alaska, on 15 May 1974 are used in the calculations and analysis.

Theoretical calculations are based on large auroral electric fields causing ions to move, with collisions between ions and neutrals both modifying the ion flow and causing neutral gas flow. Viscous and coriolis terms modify the neutral gas motion; pressure terms are omitted from the initial phase of the model. Calculations are restricted to altitudes between 90 km and 250 km. To become familiar with the effects of the coriolis term and inertial properties of the neutral gas, model calculations are first carried out with a simple electric field model. From these calculations it is determined that the neutral atmosphere responds much more slowly to ion drag at lower altitudes (<125 km) than at higher altitudes (>150 km). The coriolis term causes a substantial ion-neutral velocity difference to be maintained in a steady-state, resulting from both a smaller neutral velocity magnitude (compared with the ion velocity) and a difference in direction of about 45 degrees. Due to the large inertia of the neutral gas relative to the ion gas at low altitudes, effects of initial conditions can last for many hours at these altitudes, when ion drag is the only driving force.

For the primary calculations, observed electric fields and electron density profiles are employed, providing 6-minute time resolution. Despite

the considerable time variation in these quantities, the neutral gas effectively filters out such variability due to its large inertia relative to the ion gas. Large vertical gradients in horizontal ion and neutral velocity components are found to result from the ion drag model. To make comparisons with observed velocities, weighted altitude averages of the calculated velocities must be taken numerically. By this means it has been possible to assess semiquantitatively the technique for deriving neutral velocities from the incoherent scatter radar observations. It has been found that this data reduction technique systematically underestimates the velocity magnitude by up to 40 percent, but provides a fairly good indication of temporal variation in the weighted altitude average of the neutral velocity. A sensitivity to the collision frequencies used in the data reduction has also been noted. In addition, it has been determined that the process of taking weighted altitude averages itself can introduce fluctuations in magnitude of up to 50 percent in resultant velocities. This is due to variation in the electron density profile part of the weighting factor, together with the altitude structure in the velocity fields.

Comparison of neutral velocities derived from observation with those calculated for E region altitudes shows that the ion drag model used for the calculation is inadequate by itself to account for the observed velocities. An equation is derived to estimate the pressure gradients required to resolve the discrepancy between the calculated and observed velocities. The accelerations resulting from these pressure gradients are generally comparable to those associated with ion drag, but at least an order of magnitude larger than those due to solar heating. Directions of the pressure gradients are consistent with expected locations of auroral heating, relative to the radar location. Since accelerations due to pressure gradients and ion drag are of the same order, it is concluded that both are important in generating and modifying neutral winds in the auroral E region during geomagnetic disturbances.

7.2 RECOMMENDATIONS FOR FUTURE RESEARCH

In the course of preparing a work such as this, certain weak areas in foundations on which sometimes elaborate calculations are based become apparent.

One of these is ion-neutral collision frequencies. The lack of knowledge of ion-neutral interactions at intermediate and close ranges leaves large uncertainties in ion-neutral collision frequencies at temperatures above about 300°K. One consequence of this in the present work was seen to be a significant uncertainty in the absolute magnitude of the neutral velocities derived from observations.

Another weak area, loosely related to the first, is transport properties of ions in a partially ionized gas permeated by a magnetic field of arbitrary strength. A complete theoretical treatment, similar to that presented for electrons, is needed. Because the ion gas undergoes a transition from large ion-neutral collision frequencies to small collision frequencies relative to the ion gyrofrequency, it is clear that transport transverse to the magnetic field is more complex and more significant for ions than for electrons (for which it is largely inhibited). Large ion gas inertia, as compared with the electron gas, and closer collisional coupling to the neutrals result in ions being less mobile than electrons. However, charge neutrality assures that macroscopic densities of ions and electrons are the same. Thus, ionization transport due to mechanical forces are constrained by the ion motion, although electrons play the primary role in responding to electromagnetic forces. At present it is difficult to separate the limitations imposed by lack of a comprehensive theoretical transport treatment from those due to uncertainties in collision frequencies; both require improvement.

With respect to the development of conservation equations for the E and F regions, several modifications could be made to extend the range of applications. These are, for the most part, straightforward, and require only the addition of certain equations. First, problems of ion or neutral composition can be treated by adding the appropriate continuity equations for each ion or neutral species. Second, the set of conservation equations can be augmented by Maxwell's equations in a form appropriate to whatever problem is under study. This would be necessary, for example, in studies involving hydromagnetic waves or self-consistent electric fields resulting from dynamo action. Third, for higher altitudes (>800 km), where light ions are dominant, the three-fluid

approximation may not be reliable. In this case separate sets of conservation equations would be required for each species.

In the study of auroral E region neutral winds, several extensions and improvements are suggested. First, data for a less disturbed case could be used for a case study similar to this one. This could be done rather easily by changing the data input to the computer programs. The primary purpose of such a calculation would be to determine if ion drag is more important than auroral heating under these conditions. Published observations under such conditions indicate that this may be the case. A second addition would be the calculation of electric currents and resulting magnetic field perturbations, and calculation of Joule heating. Both could be accomplished by extending the calculations already made.

Significant improvements in the present neutral wind calculations can be made, but at a significant increase in computational effort. It was demonstrated that pressure gradients due to auroral heating play a dominant role in the generation and modification of neutral winds in the auroral E region during magnetic disturbances. In order to include these pressure gradients in a calculation, horizontal variations would have to be taken into account, requiring at least two spatial dimensions, ideally three. In addition, the neutral continuity and energy equations would be required to replace the static neutral model atmosphere. This would have the added desirable effects of allowing the calculation of vertical velocities (with consequent effects on horizontal velocities) and of permitting inclusion of neutral composition changes, which have been observed during magnetic storms. To accomplish this in the manner of the present study would require observational data from a considerably expanded spatial region. However, initially some of the effects could be profitably explored in more restricted model calculations. Much remains to be done.

Section VIII

REFERENCES

Akasofu, S. I., Polar and Magnetospheric Substorms, Springer-Verlag New York Inc., New York, 1968.

Albares, D. J., "Electron and Ion Momentum Transfer From Plasma Electrical Conductivity in a Magnetic Field", Phys. Flu., Vol. 16, pp. 1252-1259, 1973.

Ashihara, O. and Takayanagi, K., "Velocity Distribution of Ionospheric Low-Energy Electrons", Rep. Ionosph. Space Res. Japan, Vol. 27, pp 65-67, 1973.

Ashihara, O. and Takayanagi, K., "Velocity Distribution of Ionospheric Low-Energy Electrons", Planet. Space Sci., Vol. 22, pp. 1201-1217, 1974.

Banks, P. M., "Collision Frequencies and Energy Transfer - Electrons", Planet. Space Sci., Vol. 14, pp. 1085-1103, 1966a.

Banks, P. M., "Charged Particle Temperatures and Electron Thermal Conductivity in the Upper Atmosphere", Ann. Geophys., Vol. 22, pp. 577-587, 1966b.

Banks, P. M., "Collision Frequencies and Energy Transfer-Ions", Planet. Space Sci., Vol. 14, pp. 1105-1122, 1966c.

Banks, P. M., "The Temperature Coupling of Ions in the Ionosphere", Planet. Space Sci., Vol. 15, pp. 77-93, 1967.

Banks, P. M., "The Thermal Structure of the Ionosphere", Proc. IEEE, Vol. 57, pp. 258-281, 1969.

Banks, P. M. and Doupnik, J. R., "A Review of Auroral Zone Electrodynamics Deduced from Incoherent Scatter Radar Observations", Presented to Solar-Terrestrial Physics Symposium, Sao Paulo, Brazil, June 17-21, 1974.

Banks, P. M., Doupnik, J. R., and Akasofu, S.-I., "Electric Field Observations by Incoherent Scatter Radar in the Auroral Zone", J. Geophys. Res., Vol. 78, pp. 6607-6622, 1973.

Banks, P. M. and Kockarts, G., Aeronomy, Parts A and B, Academic Press, New York, 1973.

Banks, P. M. and Lewak, G. J., "Ion Velocity Distributions in a Partially Ionized Plasma", Phys. Fluids, Vol. 11, pp. 804-810, 1968.

Banks, P. M., Rino, C. L., and Wickwar, V. B., "Incoherent Scatter Radar Observations of Westward Electric Fields and Plasma Densities in the Auroral Ionosphere, I", J. Geophys. Res., Vol. 79, pp. 187-198, 1974.

Blum, P. W. and Harris, I., "Full Non-Linear Treatment of the Global Thermospheric Wind System - I. Mathematical Method and Analysis of Forces", J. Atmosph. Terr. Phys., Vol. 37, pp. 193-212, 1975.

Blum, P. W. and Harris, I., "Full Non-Linear Treatment of the Global Thermospheric Wind System - II. Results and Comparison with Observations", J. Atmosph. Terr. Phys., Vol. 37, pp. 213-235, 1975.

Breig, E. L. and Lin, C. C., "Excitation of the Spin Multiplets of the Ground State of Oxygen by Slow Electrons", Phys. Rev., Vol. 151, pp. 67-79, 1966.

Brekke, A., Doupnik, J. R., and Banks, P. M., "A Preliminary Study of the Neutral Wind in the Auroral E Region", J. Geophys. Res., Vol. 78, pp. 8235-8250, 1973.

Brekke, A., Doupnik, J. R., and Banks, P. M., "Observations of Neutral Winds in the Auroral E Region During the Magnetospheric Storm of August 3-9, 1972", J. Geophys. Res., Vol. 79, pp. 2448-2456, 1974a.

Brekke, A., Doupnik, J. R., and Banks, P. M., "Incoherent Scatter Measurements of E Region Conductivities and Currents in the Auroral Zone", J. Geophys. Res., Vol. 79, pp. 3773-3790, 1974b.

Burgers, J. M., Flow Equations for Composite Gases, Academic Press, New York, 1969.

Carleton, N. P., "Energy Transfer to and Through Ionospheric Electrons", in Physics of the Magnetosphere, edited by Carovillano, R. L., McClay, J. F., and Radoski, H. R., Springer-Verlag New York Inc., New York, pp. 556-562, 1968.

Chan, K. L. and Colin, L., "Global Electron Density Distributions from Topside Soundings", Proc. I.E.E.E., Vol. 57, pp. 990-1004, 1969.

Chandra, S. and Sinha, A. K., "The Diurnal Heat Budget of the Thermosphere", Planet. Space Sci., Vol. 21, pp. 593-604, 1973.

Chapman, S., "The Viscosity and Thermal Conductivity of a Completely Ionized Gas", Astrophys. J., Vol. 120, pp. 151-155, 1954.

Chapman, S. and Cowling, T. G., The Mathematical Theory of Non-Uniform Gases, 3rd Ed., Cambridge University Press, Cambridge, 1970.

Chappel, C. R., Reporting on "Conference on Magnetospheric-Ionospheric Coupling", EOS Trans. Am. Geophys. Union, Vol. 55, pp. 776-795, 1974.

Cicerone, R. J., "Photoelectrons in the Ionosphere: Radar Measurements and Theoretical Computations", Rev. Geophys. Space Phys., Vol. 12, pp. 259-271, 1974.

CIRA (Cospar International Reference Atmosphere) 1972, Akademic-Verlag Berlin, 1972.

Cole, K. D., "Joule Heating of the Upper Atmosphere", Aust. J. Phys., Vol. 15, pp. 223-235, 1962.

Comfort, R. H., "Diurnal Variations of Electron Energy Balance in the Middle Ionosphere", Northrop TR-793-705, 1970.

Comfort, R. H., "Effective Velocity Power Laws for Electron-Neutral Collision Frequencies", Planet. Space Sci., in press, 1975.

Dalgarno, A., "Inelastic Collisions at Low Energies", Can. J. Chem., Vol. 47, pp. 1723-1731, 1969.

Dalgarno, A. and Degges, T. C., "Electron Cooling in the Upper Atmosphere", Planet. Space Sci., Vol. 16, pp. 125-127, 1968.

Dalgarno, A., McDowell, M.R.C., and Williams, A., "The Mobilities of Ions in Unlike Gases", Phil. Trans. Roy. Soc. (London), Vol. A250, pp. 411-425, 1958.

Dalgarno, A., McElroy, M. B., Rees, M. H., and Walker, J.C.G., "The Effect of Oxygen Cooling on Ionospheric Electron Temperatures", Planet. Space Sci., Vol. 16, pp. 1371-1380, 1968.

D'Arcy, R. J. and Sayers, J., "Concerning the Electron Temperature Discrepancy Between In Situ and Remote Probes in the E-Region", Planet. Space Sci., Vol. 22, pp. 961-966, 1974.

DeVries, L. L., "Structure and Motion of the Thermosphere Shown by Density Data from the Low-G Accelerometer Calibration System (LOGACS)", Space Research XII, Akademic-Verlag, Berlin, pp. 867-879, 1972.

Doupnik, J. R., Personal Communication, 1975.

Doupnik, J. R., Banks, P. M., Baron, M. J., Rino, C. L., and Petriceks, J., "Direct Measurements of Plasma Drift Velocities at High Magnetic Latitudes", J. Geophys. Res., Vol. 77, pp. 4268-4279, 1972.

Farley, D. T., "A Theory of Electrostatic Fields in a Horizontally Stratified Ionosphere Subject to a Vertical Magnetic Field", J. Geophys. Res., Vol. 64, pp. 1225-1233, 1959.

Fedder, J. A. and Banks, P. M., "Convection Electric Fields and Polar Thermospheric Winds", J. Geophys. Res., Vol. 77, pp. 2328-2340, 1972.

Feldstein, Y. I. and Starkov, G. V., "Dynamics of Auroral Belt and Polar Geomagnetic Disturbances", Planet. Space Sci., Vol. 15, pp. 209-229, 1967.

Ferguson, E. E., "Laboratory Measurements of Ionospheric Ion-Molecule Reaction Rates", Rev. Geophys. Space Phys., Vol. 12, pp. 703-713, 1974.

Folkestad, K., ed., Magnetosphere-Ionosphere Interactions, Universitetsforlaget, Oslo-Bergen-Tromsö, 1972.

Gautschi, W., "Error Function and Fresnel Integrals", in Handbook of Mathematical Functions, ed. Abramowitz, M. and Stegun, I. A., National Bureau of Standards, pp. 297-329, 1964.

Gradshteyn, I. S. and Ryzhik, I. M., Table of Integrals, Series and Products, Trans. Jeffrey, A., Academic Press, New York, 1965.

Heaps, M. G., "Circulation in the High Latitude Thermosphere Due to Electric Fields and Joule Heating", PhD. Dissertation, Utah State U., 1972.

Heaps, M. G., "The Effects of Including the Coriolis Force on Joule Dissipation in the Upper Atmosphere", Planet, Space Sci., Vol. 22, pp. 1031-1035, 1974.

Heitler, W., The Quantum Theory of Radiation, Oxford University Press, Oxford, 1954.

Heppner, J. P., "High Latitude Electric Fields and the Modulations Related to Interplanetary Magnetic Field Parameters", Radio Sci., Vol. 8, pp. 933-948, 1973.

Hirschfelder, J. O., Curtiss, C. F., and Bird, R. B., Molecular Theory of Gases and Liquids, John Wiley and Sons, Inc., New York, 1954.

Hochstim, A. R. and Massel, G. A., "Calculations of Transport Coefficients in Ionized Gases", in Kinetic Processes in Gases and Plasmas (ed. A. R. Hochstim), Academic Press, New York, 1969.

Horwitz, J. and Banks, P. M., "Ion Momentum and Energy Transfer Rates for Charge Exchange Collisions", Planet. Space Sci., Vol. 21, pp. 1975-1981, 1973.

Huang, K., Statistical Mechanics, John Wiley and Sons, Inc., New York, 1963.

Ingold, J. H., "Energy Exchange Between Non-Equipartition Gases", Plasma Phys., Vol. 10, pp. 203-205, 1968.

Itikawa, Y., "Effective Collision Frequency of Electrons in Atmospheric Gases", Planet. Space Sci., Vol. 19, pp. 993-1007, 1971.

Itikawa, Y., "Momentum Transfer Cross Sections for Electron Collisions on Atoms and Molecules and Their Application to Effective Collision Frequencies", Argonne National Laboratory, ANL-7939, 1972.

Itikawa, Y., "Effective Collision Frequency of Electrons in Gases", Phys. Fluids, Vol. 16, pp. 831-835, 1973.

Jacchia, L. G., "The Temperature Above the Thermopause", Space Research V, North-Holland Publishing Co., Amsterdam, pp. 1152-1174, 1965.

Jacchia, L. G., Slowey, J. W., and Verniani, F., "Geomagnetic Perturbations and Upper Atmosphere Heating", Smithsonian Astrophys. Obs. Spec. Rep. No. 218, 1966.

Jacchia, L. G., "Revised Static Models of the Thermosphere and Exosphere with Empirical Temperature Profiles", Smithsonian Astrophys. Obs. Spec. Rep. No. 332, 1971.

Jelly, D. H. and Petrie, L. E., "The High-Latitude Ionosphere", Proc. I.E.E.E., Vol. 57, pp. 1005-1012, 1969.

Johnson, C. Y., "Ionospheric Composition and Density From 90 to 1200 Kilometers at Solar Minimum", J. Geophys. Res., Vol. 71, pp. 330-332, 1966.

Jones, R. A. and Rees, M. H., "Time Dependent Studies of the Aurora - I. Ion Density and Composition", Planet. Space Sci., Vol. 21, pp. 537-557, 1973.

Kohl, H. and King, J. W., "Atmospheric Winds Between 100 and 700 KM and Their Effects on the Ionosphere", J. Atmosph. Terr. Phys., Vol. 29, pp. 1045-1062, 1967.

Kopp, E., Eberhardt, P., and Geiss, J., "Ion Composition in the E- and Lower F-Region Above Kiruna During Sunset and Sunrise", Planet. Space Sci., Vol. 21, pp. 227-238, 1973.

Leadabrand, R. L., Baron, M. J., Petriceks, J., and Bates, H. F., "Chatanika, Alaska, Auroral-Zone Incoherent-Scatter Facility", Rad. Sci., Vol. 7, pp. 747-756, 1972.

Lincoln, J. V., "Geomagnetic and Solar Data - May 1974", J. Geophys. Res., Vol. 79, p. 3886, 1974.

Mason, E. A., "Estimated Ion Mobilities for Some Air Constituents", Planet. Space Sci., Vol. 18, pp. 137-144, 1970.

Mathews, J. and Walker, R. L., Mathematical Methods of Physics, W. A. Benjamin, Inc., New York, 1965.

Matsushita, S. and Campbell, W. H., ed., Physics of Geomagnetic Phenomena, 2 Vol., Academic Press, New York, 1967.

Matuura, N., "Theoretical Models of Ionospheric Storms", Space Sci. Rev., Vol. 13, pp. 124-189, 1972.

Maynard, N. C., "Electric Fields in the Ionosphere and Magnetosphere", in Magnetosphere-Ionosphere Interactions, ed. K. Folkestad, Universitetsforlaget, Oslo-Bergen-Tromsö, pp. 155-168, 1972.

Meriwether, J. W., Heppner, J. P., Stolarik, J. D., and Wescott, E. M., "Neutral Winds Above 200 KM at High Latitudes", J. Geophys. Res., Vol. 75, pp. 6643-6661, 1973.

Mitchner, M. and Kruger, C. H., Partially Ionized Gases, John Wiley and Sons, Inc., New York, 1973.

Morse, T. F., "Energy and Momentum Exchange Between Non-Equipartition Gases", Phys. Fluids, Vol. 6, pp. 1420-1427, 1963.

National Aeronautics and Space Administration, "The Earth's Ionosphere", NASA SP-8049, March, 1971.

Obayashi, T. and Matuura, N., "Theoretical Model of F-Region Storms", Solar-Terrestrial Physics/1970, ed. E. R. Dyer, D. Reidel Publishing Co., Dordrecht, Holland, Part IV, pp. 199-211, 1972.

Potter, D., Computational Physics, John Wiley & Sons, New York, 1973.

Prasad, S. S. and Furman, D. R., "Electron Cooling by Molecular Oxygen", J. Geophys. Res., Vol. 78, pp. 6701-6707, 1973.

Rees, D., "Vertical Winds in the Lower Ionosphere", J. Brit. Interplan. Soc., Vol. 22, pp. 275-284, 1969.

Rees, D., "Ionospheric Winds in the Auroral Zone", J. Brit. Interplan. Soc., Vol. 24, pp. 233-246, 1971a.

Rees, D., "Upper Atmosphere Neutral Temperature Profiles in the Auroral Zone 1968-1970", Planet. Space Sci., Vol. 19, pp. 233-241, 1971b.

Rees, M. H., and Walker, J.C.G., "Ion and Electron Heating by Auroral Electric Fields", Ann. Géophys., Vol. 24, pp. 193-199, 1968.

Reid, G. C., "Ionospheric Effects of Electrostatic Fields Generated in the Outer Magnetosphere", Rad. Sci., Vol. 69, pp. 827-837, 1965.

Rieger, E., "Neutral Air Motions Deduced from Barium Releases - I. Vertical Winds", J. Atmosph. Terr. Phys., Vol. 36, pp. 1377-1385, 1974.

Rishbeth, H. and Garriott, O. K., Introduction to Ionospheric Physics, Academic Press, New York, 1969.

Rothwell, P., Mountford, R., and Martselli, G., "Neutral Wind Modifications Above 150 KM Altitude Associated with the Polar Substorm", J. Atmosph. Terr. Phys., Vol. 36, pp. 1915-1926, 1974.

Schunk, R. W. and Walker, J.C.G., "Transport Properties of the Ionospheric Electron Gas", Planet. Space Sci., Vol. 18, pp. 1535-1550, 1970.

Schunk, R. W. and Walker, J.C.G., "Transport Processes in the E Region of the Ionosphere", J. Geophys. Res., Vol. 76, pp. 6159-6171, 1971.

Shkarofsky, I. P., "Values of the Transport Coefficients in a Plasma for any Degree of Ionization Based on a Maxwellian Distribution", Can. J. Phys., Vol. 39, pp. 1619-1703, 1961.

Shkarofsky, I. P., Johnston, T. W., and Bachynski, M. P., The Particle Kinetics of Plasmas, Addison-Wesley Publishing Company, Reading, Mass., 1966.

Smith, L. B., "An Observation of Strong Thermospheric Winds During a Geomagnetic Storm", J. Geophys. Res., Vol. 73, pp. 4959-4963, 1968.

Spitzer, L., Physics of Fully Ionized Gases, Interscience Publishers Inc., New York, 1956.

Spitzer, L. and Härm, R., "Transport Phenomena in a Completely Ionized Gas", Phys. Rev., Vol. 89, pp. 977-981, 1953.

Stoffregen, W., "The Anomaly of the Neutral Wind at a Height of ≃ 200 KM at High Latitudes", in Magnetosphere-Ionosphere Interactions, ed. K. Folkestad, Universitetsforlaget, Oslo-Bergen-Tromsø, pp. 83-86, 1972.

Stubbe, P., "Frictional Forces and Collision Frequencies Between Moving Ion and Neutral Gases", J. Atmosph. Terr. Phys., Vol. 30, pp. 1965-1985, 1968.

Stubbe, P. and Varnum, W. S., "Electron Energy Transfer Rates in the Ionosphere", Planet. Space Sci., Vol. 20, pp. 1121-1126, 1972.

Sutton, G. W. and Sherman, A., Engineering Magnetohydrodynamics, McGraw-Hill Book Co., New York, 1965.

Tambe, B. and Henry, R.J.W., "Excitation of Fine Structure Levels of Atomic Oxygen by Electron Impact", Bull. Amer. Phys. Soc., Ser. II, Vol. 18, p. 1531, 1973.

Thomas, G. E. and Ching, B. K., "Upper Atmospheric Response to Transient Heating", J. Geophys. Res., Vol. 74, pp. 1796-1811, 1969.

Victor, G. A., Private Communication, 1974.

Watkins, B. J. and Banks, P. M., "A Preliminary Study of High-Latitude Thermospheric Temperatures From Incoherent Scatter Radar Observations", J. Geophys. Res., Vol. 79, pp. 5307-5310, 1974.

Willmore, A. P., "Electron and Ion Temperatures in the Ionosphere", Space Sci. Rev., Vol. 11, pp. 607-670, 1970.

Wu, T.-Y., Kinetic Equations of Gases and Plasmas, Addison-Wesley, Reading, 1966.

Wu, S. T., "Generalized Ohm's Law in Multifluid Systems", UARI Research Report No. 49, U. of Alabama Research Institute, Huntsville, Ala., May, 1968.

Wu, S. T., "Kinetic Theory of Macroscopic Transport Phenomena in Multifluid Systems", J. Phys. Soc. Japan, Vol. 27, pp. 8-19, 1969.

Wu, S. T., "Conservation Equations for the Non-Equilibrium Radiative Flow", J. Phys. Soc. Japan, Vol. 29, pp. 778-788, 1970.

Wu, S. T., Chang, S. C., and Smith, R. E., "The Dynamical Responses of the Thermosphere due to a Geomagnetic Storm", AIAA Paper No. 74-217, presented to AIAA 12th Aerospace Sciences Meeting, Washington, D.C., January 30-February 1, 1974.

Wu, S. T., Matsushita, S., and DeVries, L. L., "An Analysis of the Upper Atmospheric Wind Observed by LOGACS", Planet. Space Sci., Vol. 22, pp. 1036-1041, 1974.

Zmuda, A. J., Potemra, T. A., and Armstrong, J. C., "Transient Parallel Electric Fields from Electromagnetic Induction Associated with Motion of Field-Aligned Currents", J. Geophys. Res., Vol. 79, pp. 4222-4226, 1974.

Appendix

ANALYTIC EVALUATION OF COLLISION TERMS

A.1 LIMITING FORMS FOR THE COLLISION FREQUENCY AND ITS DERIVATIVE AT COMMON FLOW VELOCITIES

In order for the generalized collision frequency, derived in Section III, to be consistent with previous work, it should reduce to the standard expression in the limit of common flow velocities. In this part of the Appendix this is demonstrated to be the case. It is also shown that in this limit the derivative of the collision frequency with respect to the relative flow velocity vanishes.

From equation (3-35) the effective collision frequency for momentum transfer is given by

$$\nu_{rs}(v_o) = 2\sqrt{\frac{K}{\pi}}\, n_s \frac{\exp(-Kv_o^2)}{v_o^2} \int_o^\infty Q_{rs}(g)\exp(-Kg^2) g^4 d\left[\frac{\sinh(2kgv_o)}{2Kgv_o}\right] \tag{A-1}$$

where

$$\vec{v}_o \equiv \vec{v}_r - \vec{v}_s$$

$$K \equiv \frac{\mu_{rs}}{2kT} = \frac{m_r m_s}{2k(m_r T_s + m_s T_r)} \quad .$$

Clearly, simply setting v_o to zero in equation (A-1) is meaningless. Instead, a series expansion is used for the quantity in brackets:

$$\frac{\sinh(2Kv_o g)}{2Kv_o g} = 1 + \frac{(2Kv_o g)^2}{3!} + \frac{(2Kv_o g)^4}{5!} + \ldots \tag{A-2}$$

Making use of the chain rule and equation (A-2) permits equation (A-1) to be rewritten

$$\nu_{rs}(v_o) = 2n_s\sqrt{\frac{K}{\pi}}\exp(-kv_o^2)(2K)^2 \int_o^\infty Q_{rs}(g)\exp(-Kg^2) g^5 \left[\frac{2}{3!} + \frac{4(2Kv_o g)^2}{5!} + \ldots\right] dg \tag{A-3}$$

In the limit $v_o \to 0$, only the first term of the series contributes, giving

$$\nu_{rs}(0) = n_s \frac{8}{3} \frac{K^{5/2}}{\sqrt{\pi}} \int_o^\infty Q(g)\ \exp(-kg^2)\ g^5\ dg \quad . \tag{A-4}$$

This is the expression derived by Banks (1966a) for two static gases at different temperatures. It is also equivalent to the expression designated by Itikawa (1971) as $\langle \nu_{eff} \rangle$ when applied to electrons.

To evaluate $\partial \nu_{rs} / \partial v_o$, let the integral in equation (A-1) be denoted by J:

$$J \equiv \int_o^\infty Q_{rs}(g)\ \exp(-kg^2)\ g^4\ d\left[\frac{\sinh(2Kv_o g)}{2Kv_o g}\right]. \tag{A-5}$$

Carrying out the differentiation of ν_{rs}, using equation (A-1), gives

$$\frac{\partial \nu_{rs}}{\partial v_o} = 2n_s \sqrt{\frac{K}{\pi}} \left\{ - \frac{2K\ \exp(-Kv_o^2)}{v_o} J - \frac{2\exp(-Kv_o^2)}{v_o^3} J \right.$$

$$+ \frac{\exp(-Kv_o^2)}{v_o^3} \int_o^\infty Q(g)\ \exp(-Kg^2) g^4\ d\left[\cosh(2Kv_o g)\right.$$

$$\left. \left. - \frac{\sinh(2Kgv_o)}{2Kgv_o} \right] \right\} \quad . \tag{A-6}$$

Since the limit of the sum equals the sum of the limits, each term could be examined independently. However, this turns out to be useful only for the first term; the others must be treated collectively because important cancellations take place which must be taken into account before the limiting process.

For notational convenience let the successive terms in equation (A-6) be designated T_1, T_2, T_3, and T_4. From equations (A-1) and (A-5) the first term may be written

$$T_1 = - 2K\ v_o\ \nu_{rs}(v_o). \tag{A-7}$$

Taking the limit as v_o vanishes gives

$$\lim_{v_o \to 0} T_1 = 0 \qquad \text{(A-8)}$$

since, by equation (A-4), ν_{rs} is finite in this limit. From equation (A-5) the fourth term can be written

$$T_4 = -\, 2n_s \sqrt{\frac{K}{\pi}}\, \frac{\exp(-Kv_o^2)}{v_o^3}\, J \qquad \text{(A-9)}$$

The second and fourth terms can be combined immediately resulting in

$$T_2 + T_4 = -\, 6n_s \sqrt{\frac{K}{\pi}}\, \frac{\exp(-Kv_o^2)}{v_o^3}\, J \quad . \qquad \text{(A-10)}$$

Making use of the series expansion (A-2) in J gives

$$T_2 + T_4 = -\, 8n_s\, \frac{K^{5/2}}{\sqrt{\pi}}\, \frac{\exp(-Kv_o^2)}{v_o} \int_0^\infty Q(g)\, \exp(-Kg^2)\, g^5 \cdot \left[1 + \frac{3\cdot 4(2Kv_o g)^2}{5!} + \frac{3\cdot 6(2Kv_o g)^4}{7!} + \ldots\right] dg \quad . \qquad \text{(A-11)}$$

The hyperbolic cosine in the third term of (A-6) is similarly expanded with the result

$$T_3 = 8n_s\, \frac{K^{5/2}}{\sqrt{\pi}}\, \frac{\exp(-Kv_o^2)}{v_o} \int_o^\infty Q(g)\, \exp(-Kg^2)\, g^5 \cdot \left[1 + \frac{(2Kv_o g)^2}{3!} + \frac{(2Kv_o g)^4}{5!} + \ldots\right] dg \qquad \text{(A-12)}$$

Comparison of equations (A-11) and (A-12) shows that the series are both multiplied by the same factors so that they can be combined directly term by term. The result is

$$T_2 + T_3 + T_4 = 8n_s\, \frac{K^{9/2}}{\sqrt{\pi}}\, \exp(-Kv_o^2) v_o \int_o^\infty dg\, Q(g)\, \exp(-Kg^2)\, g^7 \cdot \left[\frac{2}{5\cdot 3!} + \frac{4(2Kv_o g)^2}{7\cdot 5!} + \ldots\right] dg \quad , \qquad \text{(A-13)}$$

where the first terms cancelled completely. From this equation it is clear that

$$\lim_{v_o \to 0} (T_2 + T_3 + T_4) = 0 \quad . \tag{A-14}$$

Combining equations (A-6), (A-8), and (A-14) gives the final result

$$\lim_{v_o \to 0} \frac{\partial \nu_{rs}(v_o)}{\partial v_o} = \lim_{v_o \to 0} (T_1 + T_2 + T_3 + T_4) = 0 \quad . \tag{A-15}$$

A.2 ANALYTIC EVALUATION OF COLLISION FREQUENCIES FOR SPECIFIC FORMS OF INTERACTION

Forms of interaction among charged and neutral particles of the upper atmosphere are varied, and, in some cases, poorly known. In this section, collision frequencies and their relative velocity derivatives are determined analytically from equation (3-35) for those forms likely to be required for most ionospheric applications. Some of these are well known theoretically (e.g., Coulomb and hard sphere interactions), while others are useful for the curve fitting of experimental data (e.g. polynomials or power laws in relative velocity). Specifically, the interactions considered have the forms:

$$Q_{rs}(g) = A_j \, g^j \tag{A-16a}$$

$$Q_{rs}(g) = A_\nu \, g^\nu \tag{A-16b}$$

$$Q_{rs}(g) = A_\beta \exp(-\beta g) \quad , \tag{A-16c}$$

where j is an integer, ν is nonintegral, and β is arbitrary. Since closed-form expressions can be obtained for integral powers, but not for arbitrary nonintegral powers, the distinction between j and ν is useful.

The more familiar interaction laws are usually written as functions of relative distance. When the force between two particles varies inversely as a power of the distance between the particles,

$$\vec{F} = \vec{a}_{12}/r^\mu \quad ,$$

Chapman and Cowling (1970, Chapter 10) demonstrate from classical two-body interaction theory that the momentum transfer cross section (not their terminology) varies with relative velocity as

$$Q_{rs}(g) \propto g^{-4/(\mu-1)}$$

With this expression, the velocity variation of some familiar power law interactions can be identified. Thus, for the inverse square Coulomb force, $\mu = 2$ and $j = -4$. For "Maxwellian molecules", so called because Maxwell first recognized the simplifications resulting from this type of interaction (Chapman and Cowling, 1970, p 173), the force law $\mu = 5$ corresponds to $j = -1$. For the case of hard sphere interactions, $\mu \to \infty$ and $j = 0$ results, so that the momentum transfer cross section is independent of velocity.

For present purposes, the constants of proportionality in equations (A-16) are not of interest; they may be obtained from theory (analytically or numerically) or from experiment. The object here is to evaluate the appropriate integrals. This is done for $-4 \leq j \leq 4$ and for arbitrary ν and β within the mathematical constraints of the integrals.

A.2.1 Integral Power Law Interactions

From equation (3-35) the generalized momentum transfer collision frequency for species r with species s is given by

$$\nu_{rs}(v_o) = 2\sqrt{\frac{K}{\pi}}\, n_s \frac{\exp(-Kv_o^2)}{v_o^2} \int_o^\infty Q_{rs}(g)\, \exp(-Kg^2)\, g^4 \cdot d\left[\frac{\sinh(2Kgv_o)}{2Kgv_o}\right], \qquad \text{(A-17)}$$

where $v_o \equiv |\vec{v}_r - \vec{v}_s|$ is the relative flow velocity. Let J denote the integral in this equation. With the momentum transfer cross section represented by equation (A-16a), J may be written

$$J_j = A_j \int_o^\infty g^{j+4} \exp(-Kg^2)\, d\left[\frac{\sinh(2Kgv_o)}{2Kgv_o}\right]. \qquad \text{(A-18)}$$

Integrating by parts gives

$$J_j = A_j \left\{ \frac{\sinh\,(2Kgv_o)}{2Kgv_o}\, g^{j+4}\, \exp(-Kg^2) \,\Big|_o^\infty - \frac{1}{2Kv_o}\int_o^\infty \sinh\,(2Kgv_o) \right.$$

$$\left. \cdot\, \exp(-Kg^2)\, g^{j+2}\, [(j+4) - 2Kg^2]dg \right\} . \qquad \text{(A-19)}$$

The first term vanishes for $j > -4$. However, the integral is qualitatively different for $j < -2$ than for $j \geq -2$, so the cases $j = -3$, $j = -4$ will be treated separately. For $j < -4$, J_j will not be finite.

First the case of $j \geq -2$ is treated. With the notation $\alpha \equiv \sqrt{K}\, v_o$ and the change of variable $z = \sqrt{K}\, g$, equation (A-19) becomes

$$J_j = \frac{A_j}{2\alpha}\, (K)^{-(j+4)/2} \int_o^\infty \sinh\,(2\alpha z)\, \exp(-z^2) z^{j+2} [2z^2 - (j+4)]dz \qquad \text{(A-20)}$$

Since both terms in brackets are even functions of z the integrand has definite parity. The integrals to be evaluated all have the form

$$\int_o^\infty z^\beta \sinh(2\alpha z)\, \exp(-z^2)dz \quad .$$

If β is an odd integer, then it can be seen that

$$\int_o^\infty z^\beta \sinh\,(2\alpha z)\, \exp(-z^2)dz = \frac{1}{2^\beta}\, \frac{\partial^\beta L_o}{\partial \alpha^\beta} \quad , \qquad \text{(A-21)}$$

where

$$L_o \equiv \int_o^\infty \cosh\,(2\alpha z)\, \exp(-z^2)dz \quad . \qquad \text{(A-22)}$$

Similarly, if β is an even integer, the corresponding result is

$$\int_o^\infty z^\beta \sinh(2\alpha z)\, \exp(-z^2)dz = \frac{1}{2^\beta}\, \frac{\partial^\beta I_o}{\partial \alpha^\beta} \quad , \qquad \text{(A-23)}$$

where

$$I_o \equiv \int_o^\infty \sinh(2\alpha z)\, \exp(-z^2)\, dz \quad . \qquad \text{(A-24)}$$

Thus, once I_o and L_o are evaluated analytically, all results desired for different values of j (β) can be obtained by differentiation with respect to α. It remains only to evaluate L_o and I_o.

Consider L_o first. If the hyperbolic cosine is expanded in terms of exponential functions and the square is completed in the resulting combined exponents, equation (A-22) can be rewritten as

$$L_o = \frac{1}{2} \exp(\alpha^2) \left\{ \int_o^\infty \exp[-(z - \alpha)^2]dz + \int_o^\infty \exp[-(z + \alpha)^2]\, dz \right\} . \tag{A-25}$$

Changing variables to $x = z - \alpha$ in the first integral and $x = z + \alpha$ in the second integral gives

$$L_o = \frac{1}{2} \exp\,(\alpha^2)\left[\int_{-\alpha}^\infty \exp(-x^2)dx + \int_\alpha^\infty \exp(-x^2)dx\right] . \tag{A-26}$$

Since the integrand $\exp(-x^2)$ is an even function of x

$$\int_{-\alpha}^{o} \exp(-x^2)dx = \int_o^\alpha \exp(-x^2)\, dx \quad .$$

Equation (A-25) may then be written

$$L_o = \exp(\alpha^2) \int_o^\infty \exp(-x^2)dx$$

$$= \frac{\sqrt{\pi}}{2} \exp(\alpha^2) \tag{A-27}$$

from standard integral tables.

Following a similar procedure for I_o leads to the equation, analogous to (A-25),

$$I_o = \frac{1}{2} \exp(\alpha^2) \left\{ \int_{-\alpha}^\infty \exp(-x^2)dx - \int_\alpha^\infty \exp(-x^2)dx \right\} . \tag{A-28}$$

The symmetry of the integrand about zero, noted above, allows this equation to be rewritten

$$I_o = \exp(\alpha^2) \int_o^\alpha \exp(-x^2)dx \quad . \tag{A-29}$$

This integral is recognized as the error function, which is conventionally defined as (Gautschi, 1964)

$$\text{erf}(z) \equiv \frac{2}{\sqrt{\pi}} \int_o^z \exp(-t^2)dt \quad . \tag{A-30}$$

With this definition, equation (A-27) is written

$$I_o = \frac{1}{2}\sqrt{\pi}\, \exp(\alpha^2)\, \text{erf}(\alpha) \quad . \tag{A-31}$$

Equation (A-27) can now be used to evaluate equation (A-21) for appropriate (odd) values of β. From equation (A-20) it is seen that if j is in the range $-2 \leq j \leq 4$, β will lie in the range $0 \leq \beta \leq 8$. Carrying out the required differentiation gives the following results:

$$\beta = 1: \int_o^\infty z \sinh(2\alpha z) \exp(-z^2)dz$$

$$= \frac{\sqrt{\pi}}{2} \alpha \exp(\alpha^2) \tag{A-32a}$$

$$\beta = 3: \int_o^\infty z^3 \sinh(2\alpha z) \exp(-z^2)dz$$

$$= \frac{\sqrt{\pi}}{4} \alpha (3 + 2\alpha^2) \exp(\alpha^2) \tag{A-32b}$$

$$\beta = 5: \int_o^\infty z^5 \sinh(2\alpha z) \exp(-z^2)dz$$

$$= \frac{\sqrt{\pi}}{8} \alpha (15 + 20\alpha^2 + 4\alpha^4) \exp(\alpha^2) \tag{A-32c}$$

$$\beta = 7: \int_o^\infty z^7 \sinh(2\alpha z) \exp(-z^2)dz$$

$$= \frac{\sqrt{\pi}}{16} \alpha (105 + 210\alpha^2 + 84\alpha^4 + 8\alpha^6) \exp(\alpha^2) \quad . \tag{A-32d}$$

For even β, equation (A-31) must be used in conjunction with equation (A-23). This requires the derivative of the error function, which is given by (Gautschi, 1964)

$$\frac{d}{dz} \text{erf}(z) = \frac{2}{\sqrt{\pi}} \exp(-z^2) \quad . \tag{A-33}$$

Differentiation then gives the following results:

$$\beta = 0: \int_0^\infty \sinh(2\alpha z)\, \exp(-z^2)\, dz$$

$$= \frac{\sqrt{\pi}}{2} \exp(\alpha^2)\, \mathrm{erf}(\alpha) \qquad \text{(A-34a)}$$

$$\beta = 2: \int_0^\infty z^2 \sinh(2\alpha z)\, \exp(-z^2)\, dz$$

$$= \frac{\alpha}{2} + \frac{\sqrt{\pi}}{4} \exp(\alpha^2)\, \mathrm{erf}(\alpha)\, (1 + 2\alpha^2) \qquad \text{(A-34b)}$$

$$\beta = 4: \int_0^\infty z^4 \sinh(2\alpha z)\, \exp(-z^2)\, dz$$

$$= \frac{\alpha}{4} (5 + 2\alpha^2) + \frac{\sqrt{\pi}}{8} \exp(\alpha^2)\, \mathrm{erf}(\alpha)\, (3 + 12\alpha^2 + 4\alpha^4) \qquad \text{(A-34c)}$$

$$\beta = 6: \int_0^\infty z^6 \sinh(2\alpha z)\, \exp(-z^2)\, dz = \frac{\alpha}{8} (33 + 28\alpha^2 + 4\alpha^4)$$

$$+ \frac{\sqrt{\pi}}{16} \exp(\alpha^2)\, \mathrm{erf}(\alpha)\, (15 + 90\alpha^2 + 60\alpha^4 + 8\alpha^6) \qquad \text{(A-34d)}$$

$$\beta = 8: \int_0^\infty z^8 \sinh(2\alpha z)\, \exp(-z^2)\, dz = \frac{\alpha}{16} (279 + 370\alpha^2 + 108\alpha^4 + 8\alpha^6)$$

$$+ \frac{\sqrt{\pi}}{32} \exp(\alpha^2)\, \mathrm{erf}(\alpha)\, (105 + 840\alpha^2 + 840\alpha^4 + 224\alpha^6 + 16\alpha^8) \qquad \text{(A-34e)}$$

These results, equations (A-32) and (A-34), may now be used as required to evaluate equation (A-20) for different values of j. Beginning with j = -2, the following results are obtained straightforwardly.

$$j = -2: \; J_{-2} = \frac{A_{-2}}{\alpha K} \int_0^\infty (z^2 - 1) \sinh(2\alpha z)\, \exp(-z^2)\, dz$$

$$= \frac{A_{-2}}{4\alpha K} \left[2\alpha + \sqrt{\pi} \exp(\alpha^2)\, \mathrm{erf}(\alpha)\, (2\alpha^2 - 1)\right] \qquad \text{(A-35a)}$$

j = -1: (Maxwellian Molecules)

$$J_{-1} = \frac{A_{-1}}{2\alpha K^{3/2}} \int_o^\infty (2z^3 - 3z) \sinh(2\alpha z) \exp(-z^2) dz$$

$$= \frac{A_{-1} \sqrt{\pi}\, \alpha^2}{2K^{3/2}} \exp(\alpha^2) \qquad \text{(A-35b)}$$

j = 0: (Hard Spheres)

$$J_o = \frac{A_o}{\alpha K^2} \int_o^\infty (z^4 - 2z^2) \sinh(2\alpha z) \exp(-z^2)\, dz$$

$$= \frac{A_o}{8\alpha K^2} [2\alpha(1 + 2\alpha^2)$$

$$+ \sqrt{\pi} \exp(\alpha^2) \operatorname{erf}(\alpha) (-1 + 4\alpha^2 + 4\alpha^4)] \qquad \text{(A-35c)}$$

$$j = 1: \quad J_1 = \frac{A_1}{2\alpha K^{5/2}} \int_o^\infty (2z^5 - 5z^3) \sinh(2\alpha z) \exp(-z^2) dz$$

$$= \frac{A_1\, \alpha^2}{4K^{5/2}} \sqrt{\pi} \exp(\alpha^2) (5 + 2\alpha^2) \qquad \text{(A-35d)}$$

$$j = 2: \quad J_2 = \frac{A_2}{\alpha K^3} \int_o^\infty (z^6 - 3z^4) \sinh(2\alpha z) \exp(-z^2)\, dz$$

$$= \frac{A_2}{16\alpha K^3} [2\alpha(3 + 16\alpha^2 + 4\alpha^4)$$

$$+ \sqrt{\pi} \exp(\alpha^2) \operatorname{erf}(\alpha) (-3 + 18\alpha^2 + 36\alpha^4 + 8\alpha^6)] \qquad \text{(A-35e)}$$

$$j = 3: \quad J_3 = \frac{A_3}{2\alpha K^{7/2}} \int_o^\infty (2z^7 - 7z^5) \sinh(2\alpha z) \exp(-z^2)\, dz$$

$$= \frac{A_3\, \alpha^2}{8K^{7/2}} \sqrt{\pi} \exp(\alpha^2) (35 + 28\alpha^2 + 4\alpha^4) \qquad \text{(A-35f)}$$

$$j = 4: \quad J_4 = \frac{A_4}{\alpha K^4} \int_o^\infty (z^8 - 4z^6) \sinh(2\alpha z) \exp(\alpha^2) dz$$

$$= \frac{A_4}{32\alpha K^4} [2\alpha(15 + 146\alpha^2 + 76\alpha^4 + 8\alpha^6)$$

$$+ \sqrt{\pi} \exp(\alpha^2) \operatorname{erf}(\alpha) (-15 + 120\alpha^2 + 360\alpha^4$$

$$+ 160\alpha^6 + 16\alpha^8)] \quad . \qquad \text{(A-35g)}$$

Clearly this procedure could be used to extend results to higher values of j. However, for the present, these should be sufficient for most curve-fit applications. Lower values of j appear to be limited by properties of the integrand in equation (A-18) to j = -3 and -4; these must be treated individually. For j = -3 equation (A-18) becomes, with the change of variables and notation introduced above,

$$J_{-3} = \frac{A_{-3}}{\sqrt{K}} \int_o^\infty z \exp(-z^2) \, d\left[\frac{\sinh(2\alpha z)}{2\alpha z}\right]$$

$$= \frac{A_{-3}}{\sqrt{K}} \left\{ \frac{\sinh(2\alpha z)}{2\alpha} \exp(-z^2) \Big|_o^\infty \right.$$

$$\left. - \int_o^\infty \frac{\sinh(2\alpha z)}{2\alpha z} (1 - 2z^2) \exp(-z^2) dz \right\}, \qquad \text{(A-36)}$$

where the second equality follows from an integration by parts.

The first term in equation (A-36) vanishes in the limits, leaving two integrals. One may be evaluated from equation (A-32a); the other is

$$-\frac{A_{-3}}{2\alpha\sqrt{K}} \int_o^\infty \frac{\sinh(2\alpha z)}{z} \exp(-z^2) dz \equiv -\frac{A_{-3}}{2\alpha\sqrt{K}} I_{-3}(\alpha) \qquad \text{(A-37)}$$

which defines $I_{-3}(\alpha)$. Differentiating I_{-3} with respect to the parameter α gives

$$\frac{\partial I_{-3}}{\partial \alpha} = 2 \int_o^\infty \cosh\,(2\alpha z)\, \exp(-z^2) dz$$

$$\equiv 2\, L_o = \sqrt{\pi}\, \exp(\alpha^2) \quad , \tag{A-38}$$

where equations (A-22) and (A-27) have been used. Since $I_{-3}(0) = 0$, the differential equation (A-38) can be immediately integrated to obtain

$$I_{-3}(\alpha) = \sqrt{\pi} \int_o^\infty \exp(x^2) dz$$

$$\equiv \frac{\pi}{2i}\, \mathrm{erf}(i\alpha) \tag{A-39}$$

(Gautschi, 1964). The final result is then

$$J_{-3} = \frac{A_{-3}}{2\sqrt{K}} \sqrt{\pi} \left[\exp(\alpha^2) + \frac{i\sqrt{\pi}}{2\alpha}\, \mathrm{erf}(i\alpha) \right] \quad . \tag{A-40}$$

For $j = -4$ a similar procedure is followed. In the new notation equation (A-18) becomes

$$J_{-4} = A_{-4} \int_o^\infty \exp(-z)\, d\left[\frac{\sinh\,(2\alpha z)}{2\alpha z} \right]$$

$$= A_{-4} \left\{ \frac{\sinh\,(2\alpha z)}{2\alpha z}\, \exp(-z^2) \,\Big|_o^\infty \right.$$

$$\left. + \frac{1}{\alpha} \int_o^\infty \sinh\,(2\alpha z)\, \exp(-z^2)\, dz \right\} , \tag{A-41}$$

where an integration by parts has been performed. The first term vanishes at the upper limit, but has a limiting value of 1 at $z = 0$. The integral in the second term is just I_o, equation (A-24). So the desired result can be written immediately

$$J_{-4} = A_{-4} \left[-1 + \frac{\sqrt{\pi}}{2\alpha}\, \exp(\alpha^2)\, \mathrm{erf}(\alpha) \right] \tag{A-42}$$

from equation (A-31).

With equations (A-35), (A-40), and (A-42), collision frequencies can be evaluated from equation (A-17). For notational convenience, the j value is given as a superscript on the collision frequency. Final expressions for the collision frequencies are, in the original notation:

$$j = -4: \nu_{rs}^{-4}(v_o) = \frac{n_s A_{-4}}{v_o^3}\left[\operatorname{erf}(\sqrt{K}\, v_o) - 2v_o\sqrt{\frac{K}{\pi}}\exp(-Kv_o^2)\right] \quad \text{(A-43a)}$$

$$j = -3: \nu_{rs}^{-3}(v_o) = \frac{n_s A_{-3}}{2\, v_o^3}\left[2v_o + i\sqrt{\frac{\pi}{K}}\exp(-Kv_o^2)\operatorname{erf}(i\sqrt{K}\, v_o)\right] \quad \text{(A-43b)}$$

$$j = -2: \nu_{rs}^{-2}(v_o) = \frac{n_s A_{-2}}{2K\, v_o^3}\left[2v_o\sqrt{\frac{K}{\pi}}\exp(-Kv_o^2) + (2Kv_o^2 - 1)\operatorname{erf}(\sqrt{K}\, v_o)\right] \quad \text{(A-43c)}$$

$$j = -1: \nu_{rs}^{-1}(v_o) = n_s A_{-1} \quad \text{(A-43d)}$$

$$j = 0: \nu_{rs}^{o}(v_o) = \frac{n_s A_o}{4K^2 v_o^3}\left[2\sqrt{\frac{K}{\pi}}\, v_o(1 + 2K\, v_o^2)\exp(-Kv_o^2) + (-1 + 4K\, v_o^2 + 4K^2\, v_o^4)\operatorname{erf}(\sqrt{K}\, v_o)\right] \quad \text{(A-43e)}$$

$$j = 1: \nu_{rs}^{1}(v_o) = \frac{n_s A_1}{2K}(5 + 2K\, v_o^2) \quad \text{(A-43f)}$$

$$j = 2: \nu_{rs}^{2}(v_o) = \frac{n_s A_2}{8K^3 v_o^3}\left[2\sqrt{\frac{K}{\pi}}\, v_o(3 + 16Kv_o^2 + 4K^2 v_o^4)\exp(-Kv_o^2) + \operatorname{erf}(\sqrt{K}\, v_o)(-3 + 18Kv_o^2 + 36K^2 v_o^4 + 8K^3 v_o^6)\right] \quad \text{(A-43g)}$$

$$j = 3: \nu_{rs}^{3}(v_o) = \frac{n_s A_3}{4K^2}(35 + 28Kv_o^2 + 4K^2 v_o^4) \quad \text{(A-43h)}$$

$$j = 4: \nu_{rs}^{4}(v_o) = \frac{n_s A_4}{16K^4 v_o^3}\left[2\sqrt{\frac{K}{\pi}}\, v_o(15 + 146Kv_o^2 + 76K^2v_o^4 + 8K^3v_o^6)\exp(-Kv_o^2) + \operatorname{erf}(\sqrt{K}\, v_o)(-15 + 120Kv_o^2 + 360K^2v_o^4 + 160K^3v_o^6 + 16K^4v_o^8)\right] . \quad \text{(A-43i)}$$

For the momentum equation (3-52), collision frequencies as given by these equations represent the entire collisional interaction. However, in the energy equation the derivative of the collision frequency with respect to the relative flow velocity is also required. These expressions are given in the next equations.

$$j = -4: \frac{\partial \nu_{rs}^{-4}}{\partial v_o} = \frac{n_s A_{-4}}{v_o^4}\left[2\, v_o\sqrt{\frac{K}{\pi}}\exp(-Kv_o^2)(3 + 2Kv_o^2) - 3\operatorname{erf}(\sqrt{K}\, v_o)\right] \quad \text{(A-44a)}$$

$$j = -3: \frac{\partial \nu_{rs}^{-3}}{\partial v_o} = -\frac{n_s A_{-3}}{2v_o^4}\left[6v_o + i\sqrt{\frac{\pi}{K}}\exp(-Kv_o^2) \cdot \operatorname{erf}(i\sqrt{K}\, v_o)(3 + 2Kv_o^2)\right] \quad \text{(A-44b)}$$

$$j = -2: \frac{\partial \nu_{rs}^{-2}}{\partial v_o} = \frac{n_s A_{-2}}{2K\, v_o^4}\left[-6v_o\sqrt{\frac{K}{\pi}}\exp(-Kv_o^2) + \operatorname{erf}(\sqrt{K}\, v_o)\,(3 - 2Kv_o^2)\right] \quad \text{(A-44c)}$$

$$j = -1: \frac{\partial \nu_{rs}^{-1}}{\partial v_o} = 0 \quad \text{(A-44d)}$$

$$j = 0: \frac{\partial \nu_{rs}^{o}}{\partial v_o} = \frac{n_s A_o}{4K^2 v_o^4}\left[2\sqrt{\frac{K}{\pi}}\, v_o \exp(-Kv_o^2)(2Kv_o^2 - 3) + \operatorname{erf}(\sqrt{K}\, v_o)(3 - 4Kv_o^2 + 4K^2\, v_o^4)\right] \quad \text{(A-44e)}$$

$$j = 1: \frac{\partial \nu_{rs}^{1}}{\partial v_o} = 2n_s A_1\, v_o \quad \text{(A-44f)}$$

$$j = 2:\frac{\partial \nu_{rs}^{\,2}}{\partial v_o} = \frac{3n_s A_2}{8K^3 v_o^{\,4}}\left[2\sqrt{\frac{K}{\pi}}\, v_o \exp(-Kv_o^{\,2})(-3 + 4Kv_o^{\,2} + 4K^2 v_o^{\,4})\right.$$

$$\left. + \operatorname{erf}(\sqrt{K}\, v_o)(3 - 6Kv_o^{\,2} + 12K^2 v_o^{\,4} + 8K^3 v_o^{\,6})\right] \qquad \text{(A-44g)}$$

$$j = 3:\frac{\partial \nu_{rs}^{\,3}}{\partial v_o} = \frac{2\, n_s A_3\, v_o}{K}(7 + 2Kv_o^{\,2}) \qquad \text{(A-44h)}$$

$$j = 4:\frac{\partial \nu_{rs}^{\,4}}{\partial v_o} = \frac{5n_s A_4}{16K^4 v_o^{\,4}}\left[2\sqrt{\frac{K}{\pi}}\, v_o \exp(-K v_o^{\,2})\ (-9 + 18Kv_o^{\,2}\right.$$

$$+ 44K^2 v_o^{\,4} + 8K^3 v_o^{\,6}) + \operatorname{erf}(\sqrt{K}\, v_o)(9 - 24Kv_o^{\,2} + 72K^2 v_o^{\,4}$$

$$\left. + 96K^3 v_o^{\,6} + 16K^4 v_o^{\,8})\right] \qquad \text{(A-44i)}$$

With these relations and the collision frequencies in equations (A-43), the collisional transfer of energy and momentum can be evaluated for arbitrary temperatures and flow velocities for a variety of interactions.

A.2.2 Nonintegral Power Law Interactions

Experimental data of momentum transfer cross sections or results of numerical calculations may be fit to power law curves of arbitrary power. The appropriate integrals for this case are evaluated here. Because of similarity with the previous case, the analysis is the same through equation (A-20). So here, the starting point is

$$J_\nu = \frac{A_\nu}{2\alpha}(K)^{-(\nu+4)/2}\int_o^\infty \sinh(2\alpha z)\, \exp(-z^2)$$

$$\cdot\, z^{\nu+2}[2z^2 - (\nu + 4)]dz \qquad \text{(A-45)}$$

where ν is nonintegral. As previously, this equation holds only for $\nu > -4$.

Several approaches can be taken for treating this integral; however, all appear to end up in infinite series or in one or more of the less common special functions. For this reason, the most expeditious route

to a series solution is taken, by expanding the hyperbolic sine in a power series:

$$\sinh(2\alpha z) = \sum_{n=0}^{\infty} \frac{(2\alpha z)^{2n+1}}{(2n+1)!} \quad . \tag{A-46}$$

Equation (A-45) can then be rewritten

$$J_\nu = \frac{A_\nu}{2\alpha\, K^{(\nu+4)/2}} \sum_{n=0}^{\infty} \frac{(2\alpha)^{2n+1}}{(2n+1)!} \left\{ 2 \int_o^\infty \exp(-z^2) z^{(2n+\nu+5)} dz \right.$$

$$\left. - (\nu+4) \int_o^\infty \exp(-z^2) z^{(2n+\nu+3)} dz \right\} , \tag{A-47}$$

where now $\nu > -3$ is required for all integrals to be finite. From one of the integral representations of the gamma function, the following result is obtained:

$$\int_o^\infty z^\mu\, e^{-z^2}\, dz = \frac{1}{2}\, \Gamma\left(\frac{\mu+1}{2}\right) \quad , \tag{A-48}$$

which has the form of the integrals in equation (A-47). Use of this equation in (A-47) gives

$$J_\nu = \frac{A_\nu}{K^{(\nu+4)/2}} \sum_{n=0}^{\infty} \frac{(2\alpha)^{2n}}{(2n+1)!}\, n\, \Gamma\left(\frac{2n+\nu+4}{2}\right) , \tag{A-49}$$

where the gamma function property

$$\Gamma(z+1) = z\, \Gamma(z) \tag{A-50}$$

has been used.

For the simple case $\nu = -1$, it can be verified that equation (A-49) is equivalent to equation (A-35b). However, the path is sufficiently devious and tedious that the approach used previously for treating integral power laws appears shorter and less susceptible to error than working back through the power series from the general result given in equation (A-49) for arbitrary ν (restricted only by $\nu > -3$).

The collision frequency is found from equation (A-17) and (A-49) to be given by

$$\nu_{rs}^{\nu}(v_o) = \frac{2n_s A_\nu \exp(-Kv_o^2)}{\sqrt{\pi}\, K^{(\nu+3)/2}\, v_o^2} \sum_{n=1}^{\infty} \frac{(4Kv_o^2)^n}{(2n+1)!}\, n\, \Gamma\left(\frac{2n+\nu+4}{2}\right) . \tag{A-51}$$

Differentiation of equation (A-51) with respect to v_o has the result, after some manipulation of series,

$$\frac{\partial \nu_{rs}^{\nu}}{\partial v_o} = \frac{2n_s A_\nu \exp(-Kv_o^2)}{\sqrt{\pi}\, K^{(\nu+3)/2}\, v_o^3} \sum_{n=2}^{\infty} \frac{(4Kv_o^2)^n (n-1)}{(2n+1)!} \cdot [n(\nu+3)+1]\, \Gamma\left(\frac{2n+\nu+2}{2}\right) . \tag{A-52}$$

With equations (A-51) and (A-52) the collision terms in the momentum and energy equations can be evaluated for the nonintegral power law interaction.

A.2.3 Exponential Law Interaction

The final case to be treated is that in which the momentum transfer cross section varies with velocity according to an exponential law, equation (A-16c). Then the integral in equation (A-17) becomes

$$J_\beta = A_\beta \int_o^\infty \exp(-Kg^2 - \beta g) g^4\, d\left[\frac{\sinh(2Kgv_o)}{2kgv_o}\right] . \tag{A-53}$$

Expanding the differential and changing variables permits equation (A-53) to be rewritten

$$J_\beta = \frac{A_\beta}{2\alpha K^2} \int_o^\infty \exp(-z^2 - \gamma z) \left[z^3 \cosh(2\alpha z) - \frac{z^2}{2\alpha} \sinh(2\alpha z)\right] dz , \tag{A-54}$$

where $z = Kg^2$ and $\gamma = \beta/\sqrt{K}$. The hyperbolic sine and cosine functions can be rewritten in terms of exponentials to obtain

$$J_\beta = \frac{A_\beta}{4\alpha K^2}\left\{\int_o^\infty \exp[-z^2 - (\gamma - 2\alpha)z]\left(z^3 - \frac{z^2}{2\alpha}\right)dz\right.$$

$$\left. + \int_o^\infty \exp[-z^2 - (\gamma + 2\alpha)z]\left(z^3 + \frac{z^2}{2\alpha}\right)dz\right\} . \qquad \text{(A-55)}$$

These integrals all have the form

$$I_n^* = \int_o^\infty \exp(-z^2 - pz)z^n\, dz . \qquad \text{(A-56)}$$

As previously, the integrals for arbitrary n > 0 can be obtained from the integral corresponding to n = 0 by differentiating with respect to the parameter p:

$$I_n^* = (-)^n \frac{\partial^n I_o^*}{\partial p^n} \qquad \text{(A-57)}$$

where

$$I_o^* \equiv \int_o^\infty \exp(-z^2 - pz)dz \quad . \qquad \text{(A-58)}$$

Equation (A-58) can be treated by completing the square in the exponential and changing variables; the result is

$$I_o^* = \frac{\sqrt{\pi}}{2}\exp\left(\frac{1}{4}p^2\right)\left[1 - \text{erf}\left(\frac{p}{2}\right)\right] . \qquad \text{(A-59)}$$

Differentiation with respect to p gives

$$\frac{\partial I_o^*}{\partial p} = \frac{1}{4}\left\{-2 + \sqrt{\pi}\, p\, \exp\left(\frac{1}{4}p^2\right)\left[1 - \text{erf}\left(\frac{p}{2}\right)\right]\right\} \qquad \text{(A-60a)}$$

$$\frac{\partial^2 I_o^*}{\partial p^2} = \frac{1}{8}\left\{-2p + \sqrt{\pi}\exp\left(\frac{p^2}{4}\right)\left[1 - \text{erf}\left(\frac{p}{2}\right)\right]\left[2 + p^2\right]\right\} \qquad \text{(A-60b)}$$

$$\frac{\partial^3 I_o^*}{\partial p^3} = \frac{1}{16}\left\{-2(4 + p^2) + \sqrt{\pi}\, p\, \exp\left(\frac{p^2}{4}\right)\left[1 - \text{erf}\left(\frac{p}{2}\right)\right]\left[6 + p^2\right]\right\} . \qquad \text{(A-60c)}$$

These equations are used together with equations (A-56) and (A-57) to evaluate (A-55) with $p = \gamma - 2\alpha$ in the first integral and $p = \alpha + 2\alpha$ in the second integral, giving the result

$$J_\beta = \frac{A_\beta}{32\alpha K^2}\left\{4\alpha[2 + \gamma^2 + 4\alpha^2]\right.$$

$$- \sqrt{\pi}\exp\left[\left(\frac{\gamma - 2\alpha}{2}\right)^2\right]\left[1 - \operatorname{erf}\left(\frac{\gamma - 2\alpha}{2}\right)\right]$$

$$\cdot\,[2\alpha\gamma - 8\alpha^2 + \gamma^2 + \alpha(\gamma - 2\alpha)^3 + 2]$$

$$- \sqrt{\pi}\exp\left[\left(\frac{\gamma + 2\alpha}{2}\right)^2\right]\left[1 - \operatorname{erf}\left(\frac{\gamma + 2\alpha}{2}\right)\right]$$

$$\left.\cdot\,[2\alpha\gamma + 8\alpha^2 - \gamma^2 + \alpha(\gamma + 2\alpha)^3 - 2]\right\} \quad . \qquad \text{(A-61)}$$

Then in the original notation, the collision frequency, from equation (A-17), is

$$\nu_{rs}^{\beta}(v_o) = \frac{n_s A_\beta \exp(-Kv_o^2)}{16K^2 v_o^3}\left\{4\sqrt{\frac{K}{\pi}}\,v_o\left[2 + \frac{\beta^2}{K} + 4Kv_o^2\right]\right.$$

$$- \exp\left[\frac{(\beta - 2Kv_o)^2}{4K}\right]\left[1 - \operatorname{erf}\left(\frac{\beta - 2Kv_o}{2\sqrt{K}}\right)\right]$$

$$\cdot\left[2\beta\, v_o - 8Kv_o^2 + \frac{\beta^2}{K} + \sqrt{K}\,v_o\left(\frac{\beta - 2Kv_o}{\sqrt{K}}\right)^3 + 2\right]$$

$$- \exp\left[\frac{(\beta + 2Kv_o)^2}{4K}\right]\left[1 - \operatorname{erf}\left(\frac{\beta + 2Kv_o}{2\sqrt{K}}\right)\right]$$

$$\left.\cdot\left[2\,\beta\, v_o + 8Kv_o^2 - \frac{\beta^2}{K} + \sqrt{K}\,v_o\left(\frac{\beta + 2Kv_o}{\sqrt{K}}\right)^3 - 2\right]\right\} . \qquad \text{(A-62)}$$

Since the limit of $\beta = 0$ corresponds to a momentum transfer cross section which is constant (hard sphere), equation (A-62) should reduce to

equation (A-43e) in this limit. A quick check shows that it does, thus verifying all terms except those containing β. Finally the derivative of the collision frequency with respect to v_o is given by

$$\frac{\partial \nu_{rs}^{\beta}}{\partial v_o} = \frac{n_s A_\beta \exp(-Kv_o^2)}{16K^2 v_o^4} \left\{ 4\sqrt{\frac{K}{\pi}}\, v_o \left[4v_o^2(K + \beta^2) - 3\left(\frac{\beta^2}{K} + 2\right)\right] \right.$$

$$- \exp\left[\left(\frac{\beta - 2Kv_o}{2\sqrt{K}}\right)^2\right]\left[1 - \operatorname{erf}\left(\frac{\beta - 2Kv_o}{2\sqrt{K}}\right)\right]$$

$$\cdot \left[\left(\frac{\beta}{K} v_o^2 + \frac{2v_o}{K}\right)(2Kv_o - \beta)^3 - 24K^2 v_o^4 + 32\beta\, Kv_o^3\right.$$

$$\left. + 8v_o^2(K - \beta^2) - \beta v_o\left(6 + \frac{\beta^2}{K}\right) - 3\left(2 + \frac{\beta^2}{K}\right)\right]$$

$$- \exp\left[\left(\frac{\beta + 2Kv_o}{2\sqrt{K}}\right)^2\right]\left[1 - \operatorname{erf}\left(\frac{\beta + 2Kv_o}{2\sqrt{K}}\right)\right]$$

$$\cdot \left[\left(\frac{\beta}{K} v_o^2 - \frac{2v_o}{K}\right)(2Kv_o + \beta)^3 + 24K^2 v_o^4 + 16\beta\, Kv_o^3\right.$$

$$\left.\left. + 4v_o^2(\beta^2 - 2K) + \beta v_o\left(\frac{\beta^2}{K} - 2\right) + 3\left(\frac{\beta^2}{K} + 2\right)\right]\right\} . \quad \text{(A-63)}$$

Comparisons of this equation in the limit $\beta \to 0$ with equation (A-44e) verifies the terms not containing β.

This concludes the analytic calculation of collision frequencies for nonequilibrium gases moving relative to one another. Results presented here should be adequate for most ionospheric applications.

*U.S. GOVERNMENT PRINTING OFFICE: 1975 - 635-275/6